APPENDIX A

LISTING OF KRIEG CPG

PATENTS AND APPLICATIONS

US PATENT & TRADEMARK OFFICE

PATENT APPLICATION FULL TEXT AND IMAGE DATABASE

Searching PGPUB Production Database...

Results of Search in PGPUB Production Database for:
IN/krieg AND cpg: 92 applications.
*Hits **1** through **50** out of **92***

Final 42 Hits

Jump To

Refine Search IN/krieg AND cpg

	PUB. APP. NO.	Title
1	20070078104	Immunostimulatory nucleic acid molecules
2	20070066554	Immunostimulatory nucleic acids
3	20070066553	Immunostimulatory nucleic acid molecules
4	20070065467	Immunostimulatory nucleic acid molecules for activating dendritic cells
5	20070010470	Immunomodulatory oligonucleotides
6	20070009482	Immunomodulatory oligonucleotides
7	20060286070	Methods related to immunostimulatory nucleic acid-induced interferon
8	20060241076	Modified oligoribonucleotide analogs with enhanced immunostimulatory activity
9	20060229271	Methods for treating infectious disease exacerbated asthma
10	20060211644	Immunostimulatory oligonucleotides
11	20060188913	Methods and products for enhancing immune responses using imidazoquinoline compounds
12	20060140875	Semi-soft C-class immunostimulatory oligonucleotides
13	20060094683	Immunomodulatory oligonucleotides
14	20060089326	Immunostimulatory nucleic acid molecules
15	20060058251	Methods for treating and preventing infectious disease
16	20060019916	Immunostimulatory nucleic acids for inducing IL-10 responses
17	20060003955	Immunostimulatory nucleic acid molecules
18	20050277609	Immunostimulatory nucleic acid molecules
19	20050277604	Immunostimulatory nucleic acid molecules
20	20050267064	Immunostimulatory nucleic acid molecules
21	20050267057	Immunostimulatory nucleic acid molecules

22	20050250726	Immunostimulatory nucleic acid for treatment of non-allergic inflammatory diseases
23	20050245477	Immunomodulatory oligonucleotides
24	20050244380	Immunomodulatory oligonucleotides
25	20050244379	Immunomodulatory oligonucleotides
26	20050239736	Immunomodulatory oligonucleotides
27	20050239734	C-class oligonucleotide analogs with enhanced immunostimulatory potency
28	20050239733	Sequence requirements for inhibitory oligonucleotides
29	20050239732	Immunostimulatory nucleic acid molecules
30	20050233999	Immunostimulatory nucleic acid molecules
31	20050233995	Immunostimulatory nucleic acid molecules
32	20050215500	Immunostimulatory nucleic acid molecules
33	20050197314	Methods and products for stimulating the immune system using immunotherapeutic oligonucleotides and cytokines
34	20050182017	Immunostimulatory nucleic acid molecules
35	20050171047	Immunostimulatory nucleic acid molecules
36	20050169888	Methods related to immunostimulatory nucleic acid-induced interferon
37	20050148537	Immunostimulatory nucleic acid molecules
38	20050130911	Nucleic acid-lipophilic conjugates
39	20050123523	Immunostimulatory nucleic acid molecules
40	20050101557	Immunostimulatory nucleic acid molecules
41	20050101554	Methods for treating and preventing infectious disease
42	20050070491	Immunostimulatory nucleic acid molecules
43	20050059625	Immunostimulatory nucleic acid molecules
44	20050059619	Immunostimulatory nucleic acids
45	20050054602	Immunostimulatory nucleic acid molecules
46	20050049216	Immunostimulatory nucleic acid molecules
47	20050049215	Immunostimulatory nucleic acid molecules
48	20050043529	Use of nucleic acids containing unmethylated CpG dinucleotide as an adjuvant
49	20050037985	Methods and products for treating HIV infection
50	20050037403	Immunomodulatory oligonucleotides

Next List | Top | View Shopping Cart
Help | Home | Boolean | Manual | Number | PTDLs

USPTO Patent Full-Text and Image Database

Searching US Patent Collection...

Results of Search in US Patent Collection db for:
IN/krieg AND cpg: 12 patents.
*Hits **1** through **12** out of **12***

Jump To

Refine Search IN/krieg AND cpg

	PAT. NO.		Title
1	7,223,741	T	Immunostimulatory nucleic acid molecules
2	6,949,520	T	Methods related to immunostimulatory nucleic acid-induced interferon
3	6,821,957	T	Vectors and methods for immunization or therapeutic protocols
4	6,653,292	T	Method of treating cancer using immunostimulatory oligonucleotides
5	6,429,199	T	Immunostimulatory nucleic acid molecules for activating dendritic cells
6	6,406,705	T	Use of nucleic acids containing unmethylated CpG dinucleotide as an adjuvant
7	6,339,068	T	Vectors and methods for immunization or therapeutic protocols
8	6,239,116	T	Immunostimulatory nucleic acid molecules
9	6,218,371	T	Methods and products for stimulating the immune system using immunotherapeutic oligonucleotides and cytokines
10	6,214,806	T	Use of nucleic acids containing unmethylated CPC dinucleotide in the treatment of LPS-associated disorders
11	6,207,646	T	Immunostimulatory nucleic acid molecules
12	6,194,388	T	Immunomodulatory oligonucleotides

- APPENDIX B
- REFERENCES CITING AHONEN ET AL., J. Exp. Med. 199(6) March 15, 2004 as first teaching in vivo immune synergy achieved by co-administration of TLR/CD40 agonist immunostimulatory combinations.
-
- Habib, M., Rivas, M. N., Chamekh, M., Wieckowski, S., Sun, W., Bianco, A., Trouche, N., Chaloin, O., Dumortier, H., Goldman, M., Guichard, G., Fournel, S., Vray, B. (2007). Cutting Edge: Small Molecule CD40 Ligand Mimetics Promote Control of Parasitemia and Enhance T Cells Producing IFN-{gamma} during Experimental Trypanosoma cruzi Infection. *J. Immunol.* 178: 6700-6704 [Abstract] [Full Text]
- Soares, H., Waechter, H., Glaichenhaus, N., Mougneau, E., Yagita, H., Mizenina, O., Dudziak, D., Nussenzweig, M. C., Steinman, R. M. (2007). A subset of dendritic cells induces CD4+ T cells to produce IFN-{gamma} by an IL-12-independent but CD70-dependent mechanism in vivo. *J. Exp. Med.* 204: 1095-1106 [Abstract] [Full Text]
- Erlebacher, A., Vencato, D., Price, K. A., Zhang, D., Glimcher, L. H. (2007). Constraints in antigen presentation severely restrict T cell recognition of the allogeneic fetus.. *J. Clin. Invest.* 117: 1399-1411 [Abstract] [Full Text]
- den Haan, J. M. M., Kraal, G., Bevan, M. J. (2007). Cutting Edge: Lipopolysaccharide Induces IL-10-Producing Regulatory CD4+ T Cells That Suppress the CD8+ T Cell Response. *J. Immunol.* 178: 5429-5433 [Abstract] [Full Text]
- Rus, V., Nguyen, V., Puliaev, R., Puliaeva, I., Zernetkina, V., Luzina, I., Papadimitriou, J. C., Via, C. S. (2007). T Cell TRAIL Promotes Murine Lupus by Sustaining Effector CD4 Th Cell Numbers and by Inhibiting CD8 CTL Activity. *J. Immunol.* 178: 3962-3972 [Abstract] [Full Text]
- Hernandez, M. G. H., Shen, L., Rock, K. L. (2007). CD40-CD40 Ligand Interaction between Dendritic Cells and CD8+ T Cells Is Needed to Stimulate Maximal T Cell Responses in the Absence of CD4+ T Cell Help. *J. Immunol.* 178: 2844-2852 [Abstract] [Full Text]
- Vonderheide, R. H. (2007). Prospect of Targeting the CD40 Pathway for Cancer Therapy. *Clin. Cancer Res.* 13: 1083-1088 [Abstract] [Full Text]
- Kochenderfer, J. N., Chien, C. D., Simpson, J. L., Gress, R. E. (2006). Synergism between CpG-Containing Oligodeoxynucleotides and IL-2 Causes Dramatic Enhancement of Vaccine-Elicited CD8+ T Cell Responses. *J. Immunol.* 177: 8860-8873 [Abstract] [Full Text]
- Kornbluth, R. S., Stone, G. W. (2006). Immunostimulatory combinations: designing the next generation of vaccine adjuvants. *J. Leukoc. Biol.* 80: 1084-1102 [Abstract] [Full Text]
- Sanchez-Perez, L., Kottke, T., Daniels, G. A., Diaz, R. M., Thompson, J., Pulido, J., Melcher, A., Vile, R. G. (2006). Killing of Normal Melanocytes, Combined with Heat Shock Protein 70 and CD40L Expression, Cures Large Established Melanomas. *J. Immunol.* 177: 4168-4177 [Abstract] [Full Text]
- Chen, L., Arora, M., Yarlagadda, M., Oriss, T. B., Krishnamoorthy, N., Ray, A., Ray, P. (2006). Distinct Responses of Lung and Spleen Dendritic Cells to the

TLR9 Agonist CpG Oligodeoxynucleotide. *J. Immunol.* 177: 2373-2383 [Abstract] [Full Text]

- Overwijk, W. W., de Visser, K. E., Tirion, F. H., de Jong, L. A., Pols, T. W. H., van der Velden, Y. U., van den Boorn, J. G., Keller, A. M., Buurman, W. A., Theoret, M. R., Blom, B., Restifo, N. P., Kruisbeek, A. M., Kastelein, R. A., Haanen, J. B. A. G. (2006). Immunological and Antitumor Effects of IL-23 as a Cancer Vaccine Adjuvant. *J. Immunol.* 176: 5213-5222 [Abstract] [Full Text]
- Trumpfheller, C., Finke, J. S., Lopez, C. B., Moran, T. M., Moltedo, B., Soares, H., Huang, Y., Schlesinger, S. J., Park, C. G., Nussenzweig, M. C., Granelli-Piperno, A., Steinman, R. M. (2006). Intensified and protective CD4+ T cell immunity in mice with anti-dendritic cell HIV gag fusion antibody vaccine. *J. Exp. Med.* 203: 607-617 [Abstract] [Full Text]
- Wakita, D., Chamoto, K., Zhang, Y., Narita, Y., Noguchi, D., Ohnishi, H., Iguchi, T., Sakai, T., Ikeda, H., Nishimura, T. (2006). An indispensable role of type-1 IFNs for inducing CTL-mediated complete eradication of established tumor tissue by CpG-liposome co-encapsulated with model tumor antigen. *Int Immunol* 18: 425-434 [Abstract] [Full Text]
- Stone, G. W., Barzee, S., Snarsky, V., Kee, K., Spina, C. A., Yu, X.-F., Kornbluth, R. S. (2006). Multimeric Soluble CD40 Ligand and GITR Ligand as Adjuvants for Human Immunodeficiency Virus DNA Vaccines. *J. Virol.* 80: 1762-1772 [Abstract] [Full Text]
- Errington, F., Bateman, A., Kottke, T., Thompson, J., Harrington, K., Merrick, A., Hatfield, P., Selby, P., Vile, R., Melcher, A. (2006). Allogeneic Tumor Cells Expressing Fusogenic Membrane Glycoproteins as a Platform for Clinical Cancer Immunotherapy. *Clin. Cancer Res.* 12: 1333-1341 [Abstract] [Full Text]
- Harada, K, Isse, K, Nakanuma, Y (2006). Interferon {gamma} accelerates NF-{kappa}B activation of biliary epithelial cells induced by Toll-like receptor and ligand interaction. *J. Clin. Pathol.* 59: 184-190 [Abstract] [Full Text]
- Seyler, T. M., Park, Y. W., Takemura, S., Bram, R. J., Kurtin, P. J., Goronzy, J. J., Weyand, C. M. (2005). BLyS and APRIL in rheumatoid arthritis. *J. Clin. Invest.* 115: 3083-3092 [Abstract] [Full Text]
- Honda, K., Yanai, H., Takaoka, A., Taniguchi, T. (2005). Regulation of the type I IFN induction: a current view. *Int Immunol* 17: 1367-1378 [Abstract] [Full Text]
- Bendriss-Vermare, N., Burg, S., Kanzler, H., Chaperot, L., Duhen, T., de Bouteiller, O., D'agostini, M., Bridon, J.-M., Durand, I., Sederstrom, J. M., Chen, W., Plumas, J., Jacob, M.-C., Liu, Y.-J., Garrone, P., Trinchieri, G., Caux, C., Briere, F. (2005). Virus overrides the propensity of human CD40L-activated plasmacytoid dendritic cells to produce Th2 mediators through synergistic induction of IFN-{gamma} and Th1 chemokine production. *J. Leukoc. Biol.* 78: 954-966 [Abstract] [Full Text]
- Gunzer, M., Riemann, H., Basoglu, Y., Hillmer, A., Weishaupt, C., Balkow, S., Benninghoff, B., Ernst, B., Steinert, M., Scholzen, T., Sunderkotter, C., Grabbe, S. (2005). Systemic administration of a TLR7 ligand leads to transient immune incompetence due to peripheral-blood leukocyte depletion. *Blood* 106: 2424-2432 [Abstract] [Full Text]
- Ernstoff, M. S. (2005). Self-Recognition and Tumor Response to Immunotherapy.

JCO 23: 5875-5877 [Full Text]

- Radhakrishnan, S., Celis, E., Pease, L. R. (2005). B7-DC cross-linking restores antigen uptake and augments antigen-presenting cell function by matured dendritic cells. *Proc. Natl. Acad. Sci. USA* 102: 11438-11443 [Abstract] [Full Text]
- Craft, N., Bruhn, K. W., Nguyen, B. D., Prins, R., Lin, J. W., Liau, L. M., Miller, J. F. (2005). The TLR7 Agonist Imiquimod Enhances the Anti-Melanoma Effects of a Recombinant Listeria monocytogenes Vaccine. *J. Immunol.* 175: 1983-1990 [Abstract] [Full Text]
- Orinska, Z., Bulanova, E., Budagian, V., Metz, M., Maurer, M., Bulfone-Paus, S. (2005). TLR3-induced activation of mast cells modulates CD8+ T-cell recruitment. *Blood* 106: 978-987 [Abstract] [Full Text]
- Honda K, Yanai H, Negishi H, Asagiri M, Sato M, Mizutani T, Shimada N, Ohba Y, Takaoka A, Yoshida N, Taniguchi T.
  IRF-7 is the master regulator of type-I interferon-dependent immune responses. Nature. 2005 Apr 7;434(7034):772-7. Epub 2005 Mar 30.

The Journal of Experimental Medicine

Combined TLR and CD40 Triggering Induces Potent CD8$^+$ T Cell Expansion with Variable Dependence on Type I IFN

Cory L. Ahonen,[1] Christie L. Doxsee,[3] Sean M. McGurran,[3] Tony R. Riter,[3] William F. Wade,[1] Richard J. Barth,[2] John P. Vasilakos,[3] Randolph J. Noelle,[1] and Ross M. Kedl[3]

[1]*Department of Microbiology and Immunology, and* [2]*Department of Surgery, Dartmouth Medical School, Lebanon, NH 03756*

[3]*Department of Pharmacology, 3M Pharmaceuticals, St. Paul, MN 55144*

Abstract

Toll-like receptors are important in the activation of innate immunity, and CD40 is a molecule critical for many T and B cell responses. Whereas agonists for either pathway have been used as vaccine adjuvants, we show that a combination of Toll-like receptor (TLR)7 and CD40 agonists synergize to stimulate CD8$^+$ T cell responses 10–20-fold greater than the use of either agonist alone. Antigen-specific CD8$^+$ T cells elicited from combination CD40/TLR7 treatment demonstrated both lytic activities and interferon (IFN)γ production and an enhanced secondary response to antigenic challenge. Agonists for TLRs 2/6, 3, 4, and 9 also synergized with CD40 stimulation, demonstrating that synergy with the CD40 pathway is a property of TLR-derived stimuli in general. The CD8$^+$ T cell expansion induced by CD40/TLR7 triggering was independent of CD4$^+$ T cells, IFNγ, and IL-12 but dependent on B7-mediated costimulation and surprisingly on type I IFN. These studies provide the rational basis for the use of TLR and CD40 agonists together as essential adjuvants to optimize vaccines designed to elicit protective or therapeutic immunity.

Key words: Toll like receptor • TLR7 • CD40 • CD8 • T cell

Introduction

The magnitude and quality of the innate immune response exerts a profound impact on the ensuing adaptive immune response. Inflammatory cells and mediators generated as a result of initial tissue injury, infection, or necrotic death serve as initiators of a cascade of events that, when successful, culminates in the generation of productive T and B cell responses and long-term immunity. A family of receptors known as the Toll-like receptors (TLRs), named for their homology to molecules in *Drosophila* that serve functions in development and antimicrobial immunity (1), are critical to the ability of the cells of the innate immune system to respond to microbial and viral infections. Over the past few years, the macromolecules recognized by TLRs have been identified. Agonists for TLRs include the inflammatory mediators tri-acyl lipopeptides (TLR1), lipoteichoic acid (TLR2), dsRNA (TLR3), LPS (TLR4), flagellin (TLR5), diacyl lipopeptides (TLR6), imidazoquinolines (TLR7, TLR8), and CpGs (TLR9) (2). Activation of cells through TLRs elicits a variety of inflammatory cytokines and chemokines depending on the cell type and specific TLR being stimulated. As a testament to the importance of TLRs in immunity, TLR knockouts and knockouts of molecules critical to TLR signaling, such as MyD88 and TIRAP, result in the elimination of the majority of innate inflammatory mediators and a dramatic reduction in T and B cell responses (3–8).

The low molecular weight molecules known as imidazoquinolines or immune response modifiers (IRMs) have significant immunomodulatory capabilities and have been shown recently to be agonists for TLR7 in mouse and TLR7 and 8 in humans (9–11). Similar to other TLR agonists, IRMs such as imiquimod, resiquimod (R-848), and S-27609 (27609) induce a variety of cellular effects such as DC cytokine production, migration, and activation marker up-regulation, and B cell activation (12–15). Furthermore, IRMs induce significant amounts of type 1 IFN from the plasmacytoid DCs (9, 10, 16) in several species (15, 17, 18).

C.L. Ahonen and C.L. Doxsee contributed equally to this work.

Address correspondence to Ross M. Kedl, 3M Pharmaceuticals, 3M Center, Bldg. 270-02-S-06, St. Paul, MN 55144. Phone: (651) 733-4821; Fax: (651) 737-5886; email: rmkedl@mmm.com

Abbreviations used in this paper: IRM, immune response modifier; TLR, Toll-like receptor.

 J. Exp. Med. © The Rockefeller University Press • 0022-1007/2004/03/775/10 $8.00
Volume 199, Number 6, March 15, 2004 775–784
http://www.jem.org/cgi/doi/10.1084/jem.20031591

The central role played by TLRs in triggering innate immunity is mirrored by CD40 in controlling acquired immune responses. CD40, a TNFR superfamily member, is essential for a spectrum of cell-mediated immune responses and required for the development of T cell–dependent humoral immunity (19–21). The expression of CD40 on APCs (DCs, macrophages) and on B cells (19–23) provides an understanding for its profound impact on both arms of the acquired immune response. Stimulation through CD40 has been shown to induce the generation of CD4-independent $CD8^+$ T cell responses (24–27). These reports speculated that CD40 agonists could potentially rescue failing CD4-dependent $CD8^+$ T cell responses in some disease settings. Although data has supported the observation that CD40 has effects on long-term T cell survival (24, 28, 29), other data demonstrated that CD40 agonists alone are not sufficient to generate protective antitumor immunity or long-term immunity (30–32). In these cases, CD40 agonists used as a monotherapy have been shown to induce the deletion of antigen-specific T cells and cause the premature termination of humoral (32) and cellular (30, 31) immunity.

In the present study, we asked how the concomitant delivery of TLR and CD40 agonists enhanced antigen-specific, acquired immune responses. Although antigenic challenge in conjunction with either CD40 or TLR7 agonists alone elicited a minimal, though detectable, primary $CD8^+$ T cell response, the combination of both agonists induced an exponential expansion of antigen-specific T cells. The combination of agonists induced heightened T cell expansion, high levels of lytic activity and cytokine production, and the development of a functional memory T cell pool. Interestingly, this synergy was a property of multiple TLR agonists including TLRs 2/6, 3, 4, and 9. Although the T cell expansion was not dependent on $CD4^+$ cells or IL-12, IL-23, or IFNγ, synergy resulting from most, though not all, TLR agonists was dependent on type I IFN. Hence, the use of a CD40 agonistic antibody in conjunction with a low molecular weight TLR7 agonist can reconstitute all of the signals required to elicit profound acquired cell-mediated immunity.

Materials and Methods

Mice. C57BL/6 (Ly5.1) mice were purchased from National Cancer Institute and Charles River Laboratories and housed under specific pathogen-free conditions. B6.129S1-*Il12a*^{tm1Jm}, B6.129S1-*Il12b*^{tm1Jm}, B6.129P2-*Tnfrsf5*^{tm1Kik}, B6.129S4-*CD80*^{tm1Shr}*CD86*^{tm1Shr}, B6.129S7-*Ifng*^{tm1Ts}, and B6.129S2-*CD4*^{tm1Mak} mice were purchased from The Jackson Laboratory. B6.129-*Abb*^{Tm1}N5 and B6/129 F1 mice were purchased from Taconic Farms Inc. MyD88 KO mice were a gift from Dr. Douglas T. Golenbock (University of Massachusetts Medical School, Worcester, MA) and were bred at Dartmouth College. IFNαβR KO mice were a gift from Dr. Philippa Marrack (National Jewish Medical and Research Center, Denver, CO) and were bred on site at 3M Pharmaceuticals.

Monoclonal Antibodies. The following antibodies were purchased from BD Biosciences: anti–mouse CD8-APC (Ly-2), anti–mouse CD44-FITC (Pgp-1, Ly-24), and B220-Cy (RA3–6B2). CD40 (1C10 or FGK45) were produced by hybridomas that were grown in serum-free conditions. Ova-specific CD8 T cells were detected by H-$2K^b$–specific tetramers containing the SIINFEKL peptide, either made as described previously (33) (a gift from Dr. Lefrancois, University of Connecticut Health Center, Farmington, CT) or purchased from Beckman Coulter.

TLR Agonists. The IRM 1-(4-amino-2-methyl-1*H*-imidazo[4,5-c]quinolin-1-yl)-2-methylpropan-2-ol hydrochloride (S-27609) was synthesized as described previously (15). It was reconstituted in water at 10 mg/ml and diluted in PBS for injection into mice. Other TLR agonists used were CpG 1826 (Invitrogen Life Technologies), LPS (Sigma-Aldrich), polyinosinic-polycytidylic acid (polyI:C) (Amersham Biosciences), Malp-2 (Alexis Biochemicals), and S-27609 (3M Pharmaceuticals).

Immunization. 6–12-wk-old female C57BL/6J mice were injected i.p., unless otherwise noted, with 0.5 mg whole ovalbumin (Sigma-Aldrich) with or without varying amounts of TLR agonists and/or 50 μg of 1C10 or FGK45 (anti-CD40). Where peptide injections are noted, mice were injected with anti-CD40 i.p. and then 4–6 h later injected i.v. with 100 mg SIINFEKL peptide and a given TLR agonist. Anti-CD40 was used at 50 μg per injection. Mice were immunized with a single injection i.p. and killed 6 d later unless otherwise noted.

Cell Preparation. 6 d after i.p. injections, spleens were removed and homogenized into single cell suspensions. RBCs were lysed using an ammonium chloride buffer followed by washing. Cells were resuspended in complete medium (SMEM [Biosource International], 10% heat-inactivated FBS [Hyclone], 1 mM sodium pyruvate, 0.1 mM nonessential amino acids, 1% PenStrep, and 1% L-glutamine [Sigma-Aldrich]). Cells were resuspended at 2–4 × 10^7 cells/ml.

Analysis of MHC Tetramer by Extracellular Staining and Flow Cytometry. Cells were plated in duplicate in 96-well round-bottomed plates and stained with K^b/ovalbumin tetramer (33) for 1–2 h at room temperature (RT) or 37°C. Multiparameter analysis of tetramer-positive cells was afforded by staining cells (30 min at 37°C or RT) with anti-CD44–FITC, anti-Y3P–TNP, anti-B220–cychrome, and anti-CD8–APC. Cells were then washed in FACS® buffer, and four-color FACS® data was collected on a BD FACSCalibur flow cytometer and analyzed using CELLQUEST software. Analysis typically gated on $CD8^+$, MHC class II^- cells to assess tetramer staining.

Analysis of IFN-γ by Intracellular Staining and Flow Cytometry. Cells were plated in 96-well round-bottomed plates and pulsed with SIINFEKL peptide as antigen (or without antigen as a control) in the presence of Golgi-plug (BD Biosciences) (brefeldin A) for 4–6 h in complete media at 37°C. Cells were stained using anti-CD4–cychrome and anti-CD8–FITC. After washing, cells were fixed using Cytofix (BD Biosciences) for ~15 min. Cells were then washed and permeabilized using Perm/Wash (BD Biosciences). Intracellular staining for IFN-γ–APC was then performed according to the BD Biosciences protocol. Four-color FACS® data was collected on a BD FACSCalibur flow cytometer and analyzed using CELLQUEST software to quantify $CD8^+$ T cells producing IFN.

In Vivo Cytotoxicity Assay. Syngeneic splenocytes were labeled with either 0.5 or 5 μM CFSE for 15 min at 37°C and washed twice. $CFSE^{high}$ cells were subsequently pulsed with 50 μg/ml SIINFEKL peptide for 60 min at 37°C. $CFSE^{low}$ cells served as an internal control and therefore were not pulsed with peptide. Cells were mixed at a 1:1 ratio, and then 5 × 10^6 total cells were injected i.v. into mice challenged previously with combinations of antigen, TLR agonist, and CD40 as described above.

12–18 h later, splenocytes from each mouse were analyzed by FACS® to detect the presence of CFSE-labeled cells. The ratio of antigen-unpulsed, low CFSE cells to pulsed, high CFSE labeled cells was calculated as an indication of antigen-specific lytic activity.

Results

Concomitant Administration of TLR and CD40 Agonists Induce the Synergistic Expansion of Antigen-specific CD8$^+$ T Cells. Previous studies have shown that CD40 triggering of DCs can enhance CTL activation and replace the need for T cell help (24–27). However, emerging data suggest that TLR triggering may be critical at optimizing CD40-induced maturation of DCs (34, 35). No studies thus far have exhaustively evaluated the impact of combined TLR and CD40 engagement on the CD8$^+$-acquired immune response. To this end, mice were immunized with 500 μg soluble OVA protein combined with an agonistic anti-CD40 mAb and/or the TLR7 agonist, S-27609 (27609) (13) (Fig. 1 A). Expansion of antigen-specific CD8$^+$ T cells in vivo was quantified by staining with an OVA H-2 K^b tetramer 6 d after immunization. As has been shown previously by Lefrancois et al., the administration of anti-CD40 and OVA can enhance the accumulation of tetramer-positive cells (24). Compared with the soluble OVA alone, modest enhancements in tetramer-positive CD8$^+$ T cells appeared with OVA and anti-CD40 or S-27609 (Fig. 1 A). However, combined administration of OVA, anti-CD40, and S-27609 induced a synergistic accumulation of tetramer-positive cells. To determine whether the synergy between the TLR7 and CD40 would enhance CD8$^+$ T cell responses at more limiting antigen doses as well, we immunized mice with decreasing amounts of ovalbumin peptide (Fig. 2 B) or protein (Fig. 2 C), and the CD8$^+$ T cell response was assessed as before. As expected, cotriggering of CD40 and TLR7 induced a significant expansion of antigen-specific CD8$^+$ T cells well above that (>10-fold) seen with antigen and CD40 alone even down to as little as 5 μg of peptide or 100 μg of protein.

The kinetics and antigen dose response of the OVA-specific CD8$^+$ T cell responses to combined CD40/TLR administration was evaluated. As seen in Fig. 1 D, combined TLR and CD40 triggering induces a rapid expan-

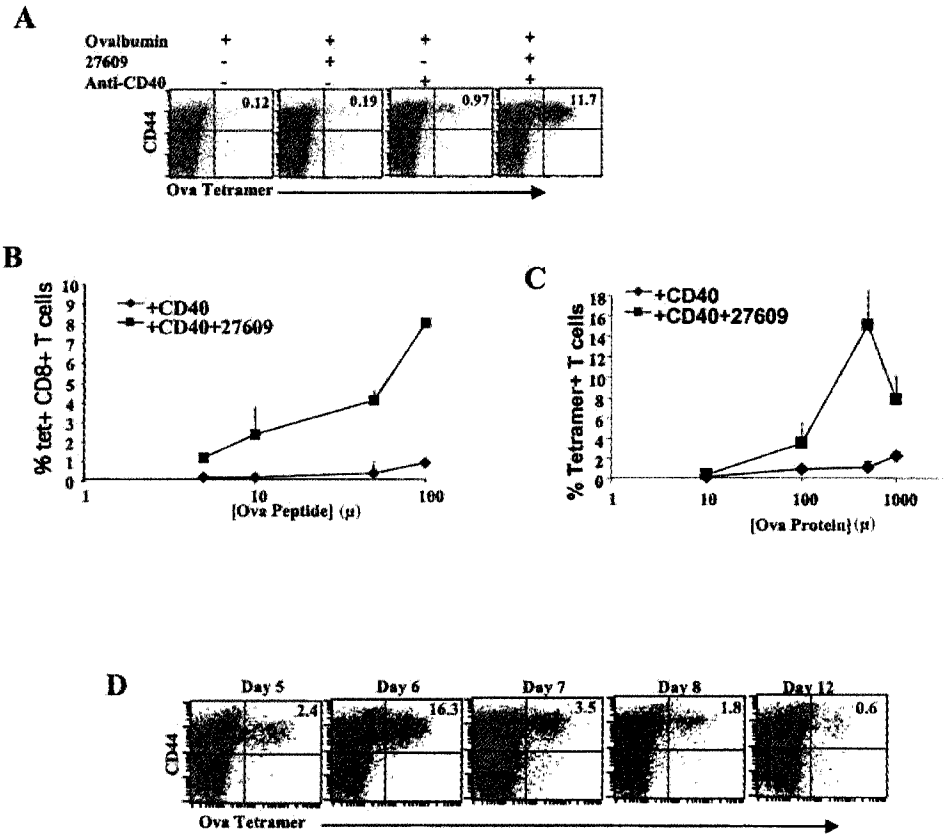

Figure 1. Anti-CD40 and the TLR7 agonist 27609 synergize to induce enhanced CD8$^+$ T cell expansion. (A) C57BL/6 mice were immunized i.p. with 500 μg of whole ovalbumin protein, 50 μg of the anti-CD40 antibody FGK45, and 100 μg of 27609 in the combinations indicated above. Mice were killed 6 d after immunization, and spleen cells were isolated and stained with tetramer as described in Materials and Methods to identify ovalbumin-specific T cells. The data shown has been gated on all CD8$^+$, B220$^-$ events. The percentages given in the top right quadrant are the percentage of tetramer staining cells out of total CD8$^+$ T cells. (B and C) Mice were immunized as in A with increasing amounts of peptide i.v. (B) or whole ovalbumin (C) and anti-CD40 ± 27609 i.p. 6 d after priming, the spleen cells were stained and analyzed as in A for ovalbumin-specific T cells. Percentages given are tetramer staining cells out of total CD8$^+$ T cells. Error bars represent SD of three mice per group. (D) Mice were immunized as in A with whole ovalbumin, anti-CD40, and 27609, and at the times indicated after priming, the spleen cells were removed and analyzed as in A. The data shown was gated on all live, CD8$^+$, B220$^-$ events. The percentages given in the top right quadrant are the percentage of tetramer staining cells out of total CD8$^+$ T cells.

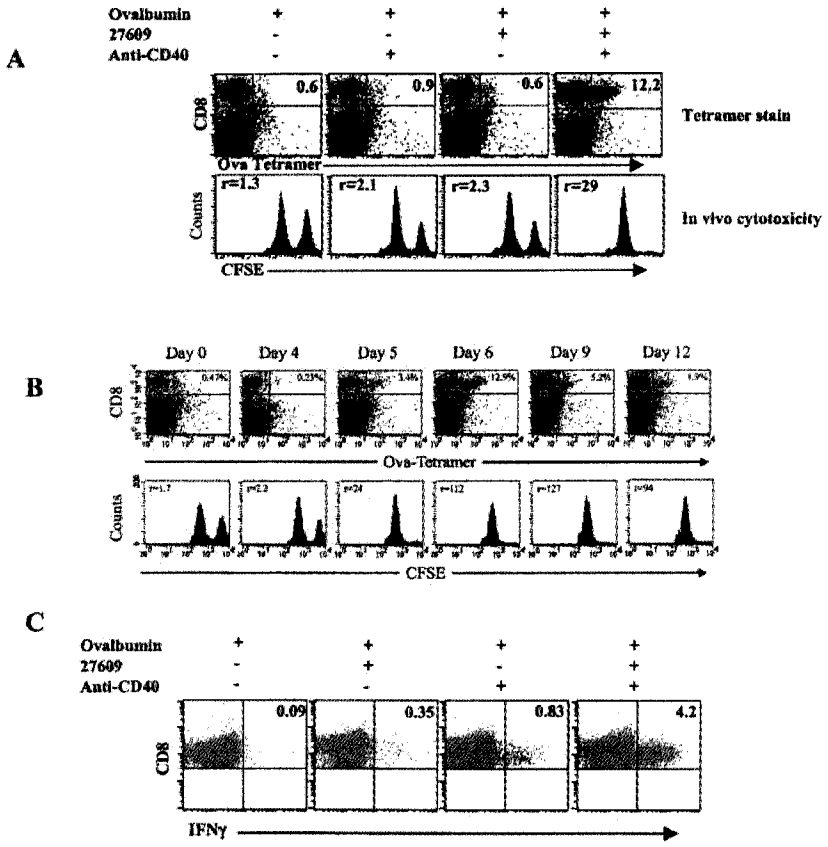

Figure 2. CD40/TLR7 triggering induces functional CTL. (A) Mice primed with 500 μg whole ovalbumin ± CD40 and/or S-27609 were assessed by using an in vivo cytotoxicity assay as described in Materials and Methods. The number in the top left of the histograms indicates the ratio of nonantigen pulsed, low CFSE-labeled spleen cells to antigen pulsed, high CFSE-labeled spleen cells. (B) As in A, mice were immunized and analyzed by tetramer staining and in vivo cytotoxic activity at the time points indicated. (C) Cells from mice treated as in A (day 7 after priming) were incubated in the presence of brefeldin A with or without SIINFEKL peptide for 6 h at 37°. The cells were then stained for CD8, fixed, permeabilized, and stained for intracellular IFNγ as described in Materials and Methods. The data shown is gated on all $CD8^+$ events. Numbers in the top right quadrant indicate the percentage of $IFN\gamma^+$ cells out of the total $CD8^+$ cells.

sion in response to protein immunization followed by a contraction of antigen-specific $CD8^+$ T cells. The peak accumulation of antigen-specific $CD8^+$ T cells was observed on day 6 postadministration of antigen, TLR, and CD40 agonists. After the day 6 peak, a rapid contraction in $CD8^+$ T cell numbers was observed by day 9. The magnitude of the CD8 response elicited by the combined triggering of CD40 and TLR is similar to that seen in antiviral responses, such as responses against LCMV (36). The time course of the response after peptide immunization was essentially indistinguishable from protein immunization (not depicted).

TLR7/CD40 Synergy Induces Functional CTL. In addition to $CD8^+$ T cell expansion, CTL killing activity and expression of IFNγ were evaluated. On days after immunization, in vivo CTL activity was measured (37–40). The in vivo CTL assay showed that cotriggering of CD40 and TLR7 induced significant lytic activity (Fig. 2 A). Detectable lytic activity was present in the immunized mice from day 5 through 12 (Fig. 2 B). Cotriggering of CD40/TLR7 also elicited intracellular expression of IFNγ (Fig. 2 C), though CD40 stimulation alone also induced detectable IFNγ production (Fig. 2 C) from the cells from this time point. IFNγ production was first detected on day 6 after priming (5–20% of Ag-specific T cells) and peaked by day 7–8 (60–90% of Ag-specific T cells) (not depicted and Fig. 1 C). Therefore, the data show that the combined actions of CD40 and TLR7 agonists resulted in antigen-specific T cell expansion and differentiation.

TLR/CD40 Triggering Elicits Long-Term, Antigen-specific $CD8^+$ T Cell Immunity. The fate of the TLR/CD40-induced T cells was evaluated to determine if the initial expansion and contraction of the tetramer-positive T cells lead to anergy or memory. Numerous models exist whereby dramatic T cell expansion is followed by an equally dramatic demise in T cell numbers and function, leaving any remaining cells in a hyporesponsive state of tolerance (30, 36, 41–44). Alternatively, productive responses present the same patterns of expansion and contraction, yet upon rechallenge, secondary expansion can be observed. Mice initially immunized with OVA, anti-CD40, and S-27609 were rechallenged 30 d after initial priming with combinations or CD40 and TLR7 agonists and either peptide (Fig. 3, top) or protein (Fig. 3, bottom). The secondary response was less reliant on costimulatory signals than the primary response, demonstrating a detectable increase in tetramer-staining cells in response to protein or peptide rechallenge alone. The addition of the TLR7 agonist to peptide rechallenge elicited a better (enhanced) response compared with peptide alone, which peaked on day 3 after rechallenge. In contrast, rechallenge with protein was enhanced when CD40 was added and the response peaked on day 5 after rechallenge. This difference between peptide and protein rechallenge in the time of the peak of the response likely reflects the additional time neces-

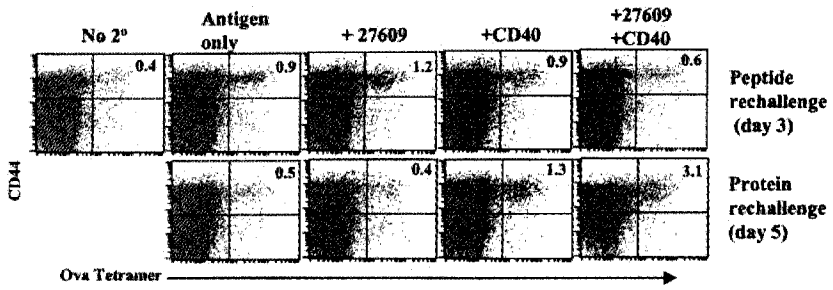

Figure 3. TLR/CD40 triggering produces long-term T cell immunity. (A) Mice were immunized i.p. with ovalbumin, anti-CD40, and S-27609 as in Fig. 1. 30 d later, the mice were rechallenged i.p. with either 100 μg SIINFEKL peptide or 500 μg ovalbumin protein ± 27609/CD40 as indicated. At days 3 and 5 after rechallenge, spleen cells were isolated and stained with tetramer as described in Materials and Methods. Peak responses for peptide or protein responses are shown (day 3 for peptide rechallenge and day 5 for protein rechallenge). The data shown was gated and analyzed as in Fig. 1 A. The data is representative of three experiments performed.

sary for processing and presentation of the protein. The enhancement of the protein response with anti-CD40 is also consistent with the role of CD40 in augmenting crosspriming. CD40 did enhance the peptide response compared with peptide alone, but for reasons that are not clear, this response peaked on day 5 and was not any greater than the day 3 response to peptide and the TLR7 agonist (not depicted). In all cases, the secondary response was more rapid but lower than the peak of the primary response. This has been is seen in other experimental systems (41, 45, 46) and is probably due to the rapid clearance of the antigen by the high frequency of functional memory cells. In general, the data demonstrate that the primary response generated by immunization in the combined presence of CD40 and TLR7 agonists leads to the generation of functional memory CTLs.

Synergy with CD40 in the Induction of CD8⁺ T Cell Proliferation and Differentiation Is a Property of Multiple TLR Agonists. CD40 has been used in combination with a variety of stimuli and has been shown to enhance immune responses (28, 33, 47). We considered the possibility that the synergy we observed between TLR7 and CD40 was a property of TLR agonists in general and not necessarily of only TLR7 agonists. Mice were immunized with anti-CD40, ovalbumin protein (Fig. 4, A and B), or peptide (Fig. 4 C) and agonists for TLR 2/6, 3, 4, 7, or 9. 6 d after the administration of these agents, the frequency of OVA-

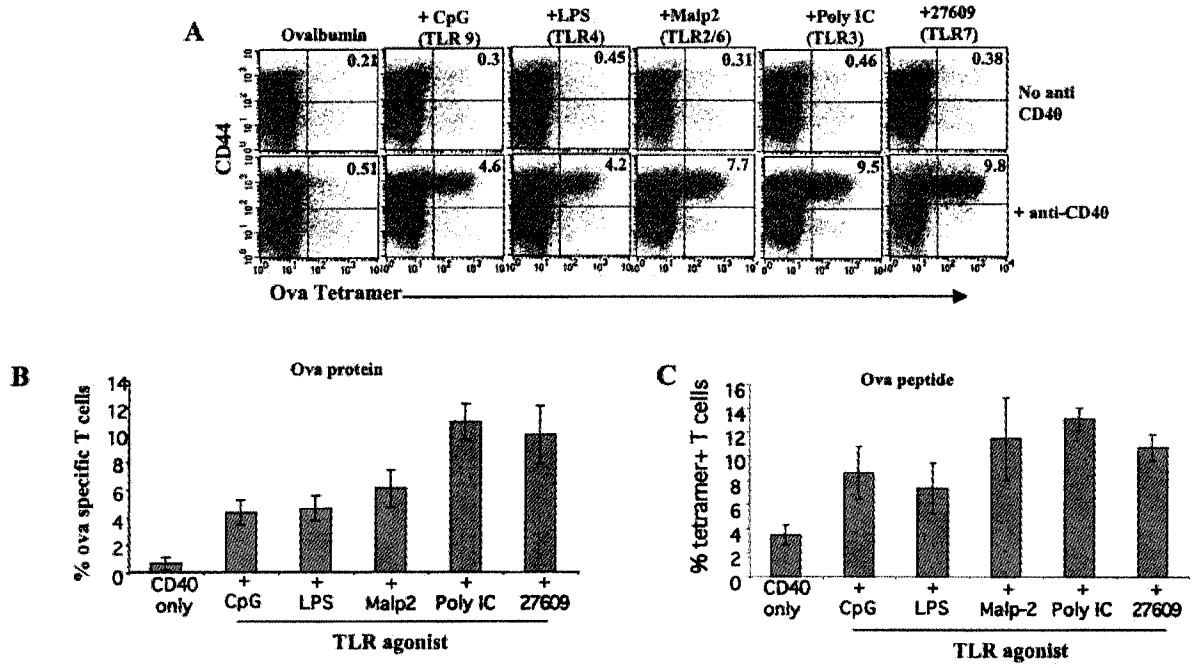

Figure 4. Synergy with CD40 in the induction of CD8⁺ T cell proliferation and differentiation is a property of multiple TLR agonists. (A) Mice were challenged i.p. with ovalbumin and the indicated TLR agonists (30 μg LPS as a TLR4 agonist, 100 μg CpG 1826 as a TLR9 agonist, 25 μg Malp-2 as a TLR2/6 agonist, 50 μg poly IC as a TLR3 agonist, and 100 μg 27609 as the TLR7 agonist), with or without anti-CD40. 6 d after challenge, spleens cells were isolated and stained with tetramer as described in Fig. 1. The data shown was gated and analyzed as in Fig. 1 A. (B and C) The average percentage of tetramer staining T cells and their SDs from three mice per treatment primed with whole protein (B) or peptide (C) were analyzed and calculated. The data shown is representative of three to eight experiments performed, depending on the TLR agonist.

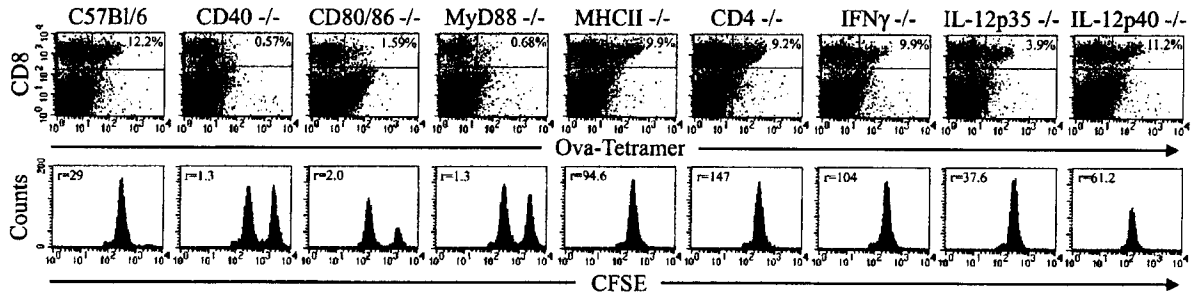

Figure 5. TLR/CD40 triggering of $CD8^+$ T cell expansion and effector function is largely dependent on costimulation via CD80/86 but independent of CD4 cells, IFNγ, IL-12, or IL-23. The indicated genetically deficient mice were immunized with 500 μg ovalbumin plus 50 μg anti-CD40 and 200 μg 27609 by i.p. injection. On day 6 postimmunization, in vivo lytic activity was measured as in Fig. 2 A, and splenocytes were isolated and analyzed as in Fig. 1 but using anti-CD8α PE and APC-labeled SIINFEKL/H-$2K^b$ tetramers. Data is representative of at least three mice per group. Numbers in the top right quadrant of the dotplots indicates the percentage of $tetramer^+$ CD8 T cells out of total CD8 T cells. The number in the top left of the histograms indicates the ratio of nonantigen pulsed, low CFSE-labeled spleen cells to antigen pulsed, high CFSE-labeled spleen cells.

specific T cells was determined as before. With respect to OVA-specific tetramer-positive CTL expansion, all TLR agonists demonstrated synergy with the CD40 agonist (Fig. 4 A), though each TLR agonists synergized to varying degrees with CD40 (Fig. 4, B and C). As with the TLR7 agonist, all of the TLR agonists elicited IFNγ production from the T cells as well (not depicted). Therefore, signals derived from a variety of TLRs are able to synergize with CD40 signaling to induce T cell expansion and differentiation.

TLR7/CD40 Triggering of $CD8^+$ T Cell Expansion Is Independent of CD4 Cells, IFNγ, IL-12, or IL-23. $CD8^+$ T cell responses have been shown to be either dependent or independent of $CD4^+$ T cells or cytokine-mediated help (48). To determine which cellular and molecular components influenced the magnitude of the $CD8^+$ T cell response induced by CD40 and TLR7 agonists and antigen, a series of studies in genetically deficient mice were performed (Fig. 5). The magnitude of the $CD8^+$ expansion or differentiation to lytic function induced by immunization with OVA and CD40 and TLR7 agonists was not diminished in either $CD4^{-/-}$ or class II $MHC^{-/-}$ mice, demonstrating the helper independent nature of this form of priming. Additionally, neither IL-12, IL-23, nor IFNγ were required, as expansion in IL-$12p35^{-/-}$, IL-$12p40^{-/-}$, and $IFN\gamma^{-/-}$ mice, respectively, were similar to WT mice. Costimulation via CD28 was deemed critical as expansion in the CD80/$CD86^{-/-}$ mice was ablated. Reaffirmation of the functional importance of CD40 and the TLR signaling pathway (2) was demonstrated by the lack of expansion of tetramer-positive cells in $CD40^{-/-}$ and $MyD88^{-/-}$ mice. Thus, other than classical B7-mediated costimulation, which is a property of T cell responses in general, the induction of primary immunity by TLR/CD40 cotriggering is independent of IL-12, IL-23 (49), IFNγ, and the presence of CD4 helper cells.

Dependence on Type I IFN Varies with the Specific TLR Agonist Employed. In previous experiments, it was observed that the TLR agonists that synergized with CD40 to produce the highest level of $CD8^+$ T cell expansion (poly IC and 27609) were also potent inducers of type I IFN (IFNα/β) (Fig. 3). We sought to determine whether IFNα/β contributed to $CD8^+$ T cell expansion by performing experiments in IFNα/β receptor knockout mice (IFNα/βR KO). Surprisingly, the synergy between CD40 and TLR7 was essentially abrogated in IFNα/βR KO mice with the $CD8^+$ T cell expansion being reduced down to that seen in the presence of anti-CD40 alone (Fig. 6 A). However, the TLR agonists that induced the least IFNαβ appeared to induce synergy that was least affected by the loss of type I IFN signaling (Fig. 6, A–C). For example, in response to peptide immunization (Fig. 6, A and B) Malp-2 (TLR2/6 agonist) synergy with CD40 was only modestly affected in the IFNαβR KOs (60–90% of max), whereas LPS, CpG, polyI:C, and 27609 were increasingly affected (respectively) in the absence of the IFNαβ receptor. In contrast, synergy with all TLR agonists was all but abrogated when the mice were challenged with protein instead of peptide (Fig. 6 C). This is consistent with recent literature reporting that type I IFN facilitates crosspriming in APC (50, 51). However, the loss of synergy in response to priming with peptide (Fig. 6, A and B) demonstrates that for all TLR agonists but Malp-2, type I IFN plays a larger role than just enabling crosspriming. Thus, the data suggests that synergy between the TLR pathway and the CD40 pathway is best observed under conditions where the TLR agonist induces type I IFN and further that the $CD8^+$ T cell expansion seen under these conditions is dependent on some aspect of type I IFN signaling.

Discussion

The work presented here demonstrates that the concomitant signaling via TLR and CD40 results in a synergistic increase in expansion of antigen-specific CTL and their differentiation to effector cells. The combination of TLR7 and CD40 agonists synergized to stimulate heightened CTL proliferation and function with respect to IFNγ production and lytic activity. The high level of $CD8^+$ T cell proliferation seen was neither abortive nor exhaustive (30, 36, 42, 43), since the mice generated secondary T cell ex-

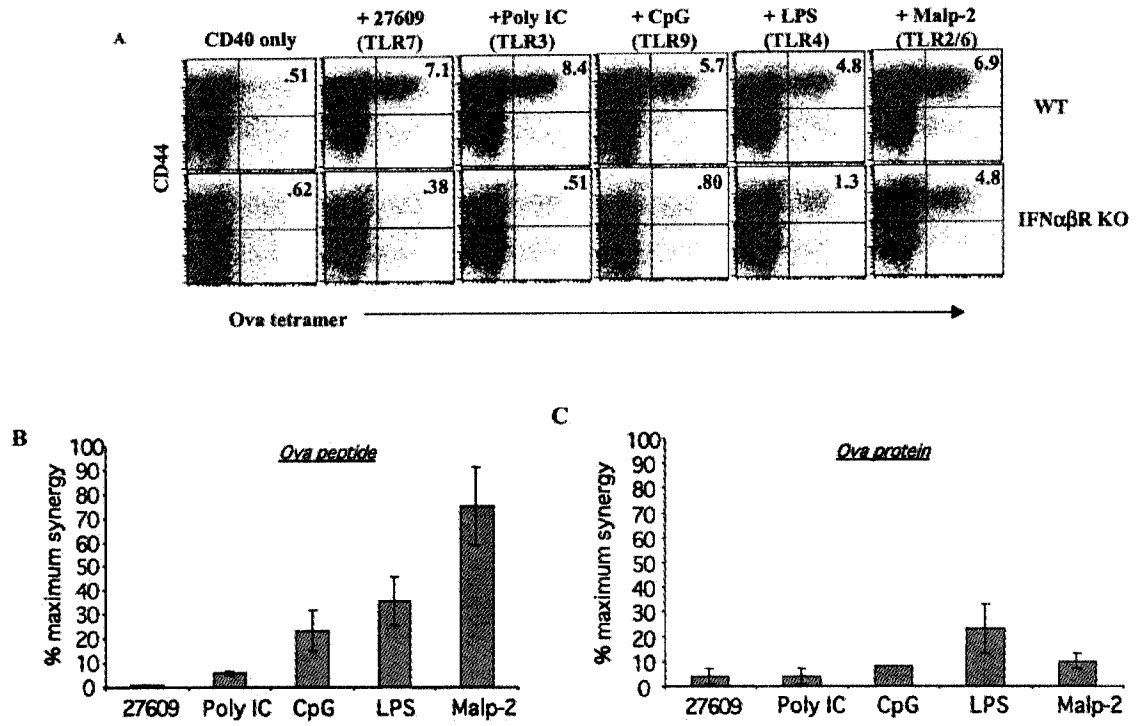

Figure 6. CD40 synergy with IFNα/β-inducing TLR agonists is critically dependent on type I IFN. Either wt control B6/129 F1 or IFNαβR KO mice were immunized with 100 μg of SIINFEKL peptide (A and B) or 500 μg ovalbumin protein (C), 50 μg anti CD40, and the indicated TLR agonist (30 μg LPS as a TLR4 agonist, 100 μg CpG 1826 as a TLR9 agonist, 25 μg Malp-2 as a TLR2/6 agonist, 50 μg poly IC as a TLR3 agonist, and 100 μg 27609 as the TLR7 agonist) as in Fig. 3. On day 6, spleen cells were stained with tetramer and analyzed as in Fig. 1 A. The legend above the figure indicates the TLR agonist used. (B and C) The percentage of tetramer staining cells in the mice from A after either peptide (B) or whole protein (C) challenge were calculated as the percentage of tetramer staining cells out of total $CD8^+$ T cells. This percentage was then divided by the percentage of tetramer staining cells from wild-type mice challenged with the same TLR agonist. The data is expressed as the percentage of maximum synergy seen in the IFNαβR KO mice compared with the wild type for the given TLR agonist. The data shown is an average from three mice per treatment group, and error bars indicate the calculated SD. The data represents three experiments performed.

pansion upon rechallenge with antigen with or without TLR7/CD40 agonists. These memory T cells expressed all of the hallmarks of a functional secondary response, i.e., responding more rapidly and with a reduced dependency on adjuvant compared with the primary response (46, 52–55). Of particular interest was the fact that TLR 2/6, 3, 4, and 9 agonists also were capable of synergizing with anti-CD40 to induce the expansion of OVA-specific $CD8^+$ T cells, with the TLR agonists that generated higher levels of type I IFN tending to produce the highest levels of T cell expansion. Thus, some aspect of TLR and CD40 signaling must have a general point of intersection, an observation that is consistent with the biology of the receptors, i.e., APC could receive an initial activation stimulus through a TLR at the site of infection and after migration to the T cell zones of the lymphoid tissue receive a CD40 stimulus from antigen-specific T cells, effectively "confirming" the APC's activation and further reinforcing T cell expansion.

Previous studies have suggested that, at least in certain circumstances, CD40 stimulation could rescue defective or abortive $CD8^+$ T cell proliferation and effector cell function. Indeed, these reports demonstrated that CD40 stimulation alone allowed normally CD4-dependent $CD8^+$ T cell responses to proceed in the absence of CD4 help (24–27), implicating CD40 signaling as the primary mechanism of CD4 help for CTL proliferation. More recent reports have further suggested that at least in some disease and experimental models CD40 stimulation alone was necessary and sufficient to initiate long-lived CTL expansion and effector function (24, 28, 29). However, this is not the case in all systems and models tested. Both IL-12 production (34) and antitumor CTL responses (30) have been shown to be dependent on CD40 in combination with other bacterial/viral-derived stimuli. Indeed, some studies have demonstrated that CD40 stimulation alone resulted not in immunity but in deletion of antigen-specific T cells (30, 31) and termination of humoral responses (32). Our data demonstrates that although CD40 is able to induce $CD8^+$ T cell immunity to a limited degree, this can be exponentially enhanced by the addition of a TLR agonist. Therefore, we would predict that the clinical efficacy of CD40 agonists could be dramatically improved if provided in conjunction with an appropriate antigen and TLR agonist, specifically a TLR7 agonist, as our data demonstrates.

CD40 is expressed on APCs (DCs, macrophages, B cells), and it is generally agreed that stimulation through

CD40 plays a role in the activation of APCs to become competent to initiate $CD8^+$ T cell proliferation. In contrast, a report from Bourgeois et al. has demonstrated that $CD8^+$ T cells can express CD40 after activation and that this expression of CD40 on the T cells may play a greater role in $CD8^+$ T cell proliferation than CD40 expression on the APC (56). Given this observation, it is possible that the synergy we demonstrate between TLR and CD40 agonists is due to direct stimulation of CD40 on the antigen-specific T cells themselves and not on the APC. However, a recent report from Lee et al. shows that CD8 responses to influenza are dependent on CD40 expression on the APC and that neither the APC nor the CD4 T cells directly stimulate CD8 T cells through CD40–CD40L interactions (57). This study showed through various bone marrow chimeras that $CD40^{-/-}$ CD8 T cells expanded as well as $CD40^{+/+}$ CD8 cells in host, strongly arguing against a functional role for CD40 expression on the CD8 T cells. However, we cannot as of yet rule out a role for direct stimulation of CD40 on the T cells in the $CD8^+$ T cell expansion seen in our model system. Experiments are in progress to determine whether CD40 expression on APC or T cells is necessary for this synergistic induction of T cell expansion by the cotriggering of TLR/CD40.

Perhaps the most interesting feature of the observed synergy is its variable dependence on type I IFN. In general, the data is consistent with the interpretation that the degree of synergy is related to and dependent on the level of IFN induced by the TLR agonists. However, the TLR2/6 agonist Malp-2 (58, 59) appears to be somewhat of an exception to that rule. TLR2 agonists have been shown to induce little to no type I IFN (3, 60, 61), but Malp-2 demonstrated significant levels of synergy with CD40 nonetheless. Therefore, the data suggest that there are at least two ways that TLRs synergize with CD40: one mediated through type I IFN signaling and the other mediated through some aspect of Malp-2 signaling. We have demonstrated that for those TLR agonists that induce either IFNα or β, synergy with CD40 is increasingly dependent on type I IFN. However, it is currently unclear given the almost ubiquitous expression of the IFN$\alpha\beta$ receptor, in which cell type(s) IFN signaling is necessary for producing this synergy. Interestingly the TLR/CD40-triggered $CD8^+$ T cell expansion in the IFN-$\alpha\beta$R KO mice was reduced to a greater extent in response to whole protein antigen challenge, even when using Malp-2 as the TLR agonist. This further supports the identified role of type I IFN in crosspriming (50, 51) and demonstrates that at least some, though not all, aspects of TLR/CD40-induced synergy are mediated by the effects of IFN on antigen processing and presentation.

In conclusion, these studies underscore the powerful immune synergy that exists when receptors from both innate and acquired immunity are triggered. It is tempting to speculate that the TLR and CD40 signaling cascades evolved the means for cross talk and integration so as to control the magnitude, duration, and quality of the immune response. At this time, the basis for TLR/CD40 cross talk is not known. Studies are underway to determine if signaling derived from TLR and CD40 agonists are directed at the same or different cellular targets and whether signaling elements common to both cascades may play a role in communications between these two receptor systems.

The authors would like to thank Jody Lutterman and Dave Johnson for breeding and maintaining the mouse color, and John Vasilakos and W. Chad Kieper for help in reviewing the manuscript.

Submitted: 15 September 2003
Accepted: 21 January 2004

References

1. Medzhitov, R., P. Preston-Hurlburt, and C.A. Janeway, Jr. 1997. A human homologue of the *Drosophila* Toll protein signals activation of adaptive immunity. *Nature.* 388:394–397.
2. Akira, S. 2003. Mammalian Toll-like receptors. *Curr. Opin. Immunol.* 15:5–11.
3. Kawai, T., O. Adachi, T. Ogawa, K. Takeda, and S. Akira. 1999. Unresponsiveness of MyD88-deficient mice to endotoxin. *Immunity.* 11:115–122.
4. Yamamoto, M., S. Sato, H. Hemmi, H. Sanjo, S. Uematsu, T. Kaisho, K. Hoshino, O. Takeuchi, M. Kobayashi, T. Fujita, et al. 2002. Essential role for TIRAP in activation of the signalling cascade shared by TLR2 and TLR4. *Nature.* 420:324–329.
5. Alexopoulou, L., V. Thomas, M. Schnare, Y. Lobet, J. Anguita, R.T. Schoen, R. Medzhitov, E. Fikrig, and R.A. Flavell. 2002. Hyporesponsiveness to vaccination with *Borrelia burgdorferi* OspA in humans and in TLR1- and TLR2-deficient mice. *Nat. Med.* 8:878–884.
6. Hemmi, H., T. Kaisho, O. Takeuchi, S. Sato, H. Sanjo, K. Hoshino, T. Horiuchi, H. Tomizawa, K. Takeda, and S. Akira. 2002. Small anti-viral compounds activate immune cells via the TLR7 MyD88-dependent signaling pathway. *Nat. Immunol.* 3:196–200.
7. Horng, T., G.M. Barton, R.A. Flavell, and R. Medzhitov. 2002. The adaptor molecule TIRAP provides signalling specificity for Toll-like receptors. *Nature.* 420:329–333.
8. Adachi, O., T. Kawai, K. Takeda, M. Matsumoto, H. Tsutsui, M. Sakagami, K. Nakanishi, and S. Akira. 1998. Targeted disruption of the MyD88 gene results in loss of IL-1- and IL-18-mediated function. *Immunity.* 9:143–150.
9. Gibson, S.J., J.M. Lindh, T.R. Riter, R.M. Gleason, L.M. Rogers, A.E. Fuller, J.L. Oesterich, K.B. Gorden, X. Qiu, and S.W. McKane. 2002. Plasmacytoid dendritic cells produce cytokines and mature in response to the TLR7 agonists, imiquimod and resiquimod. *Cell. Immunol.* 218:74–86.
10. Hemmi, H., T. Kaisho, O. Takeuchi, S. Sato, H. Sanjo, K. Hoshino, T. Horiuchi, H. Tomizawa, K. Takeda, and S. Akira. 2002. Small anti-viral compounds activate immune cells via the TLR7 MyD88-dependent signaling pathway. *Nat Immunol.* 3:196–200.
11. Jurk, M., F. Heil, J. Vollmer, C. Schetter, A.M. Krieg, H. Wagner, G. Lipford, and S. Bauer. 2002. Human TLR7 or TLR8 independently confer responsiveness to the antiviral compound R-848. *Nat. Immunol.* 3:499.
12. Bishop, G.A., Y. Hsing, B.S. Hostager, S.V. Jalukar, L.M. Ramirez, and M.A. Tomai. 2000. Molecular mechanisms of B lymphocyte activation by the immune response modifier

R-848. *J. Immunol.* 165:5552–5557.
13. Doxsee, C.L., T.R. Riter, M.J. Reiter, S.J. Gibson, J.P. Vasilakos, and R.M. Kedl. 2003. The immune response modifier and TLR7 agonist S-27609 selectively induces IL-12 and TNFα production in CD11c+CD11b+CD8− dendritic cells. *J. Immunol.* 171:1156–1163.
14. Ahonen, C.L., S.J. Gibson, R.M. Smith, L.K. Pederson, J.M. Lindh, M.A. Tomai, and J.P. Vasilakos. 1999. Dendritic cell maturation and subsequent enhanced T-cell stimulation induced with the novel synthetic immune response modifier R-848. *Cell. Immunol.* 197:62–72.
15. Testerman, T.L., J.F. Gerster, L.M. Imbertson, M.J. Reiter, R.L. Miller, S.J. Gibson, T.L. Wagner, and M.A. Tomai. 1995. Cytokine induction by the immunomodulators imiquimod and S-27609. *J. Leukoc. Biol.* 58:365–372.
16. Ito, T., R. Amakawa, T. Kaisho, H. Hemmi, K. Tajima, K. Uehira, Y. Ozaki, H. Tomizawa, S. Akira, and S. Fukuhara. 2002. Interferon-{alpha} and interleukin-12 are induced differentially by Toll-like receptor 7 ligands in human blood dendritic cell subsets. *J. Exp. Med.* 195:1507–1512.
17. Karaca, K., J.M. Sharma, M.A. Tomai, and R.L. Miller. 1996. In vivo and in vitro interferon induction in chickens by S-28828, an imidazoquinolinamine immunoenhancer. *J. Interferon Cytokine Res.* 16:327–332.
18. Tomai, M.A., S.J. Gibson, L.M. Imbertson, R.L. Miller, P.E. Myhre, M.J. Reiter, T.L. Wagner, C.B. Tamulinas, J.M. Beaurline, J.F. Gerster, et al. 1995. Immunomodulating and antiviral activities of the imidazoquinoline S-28463. *Antiviral Res.* 28:253–264.
19. Aruffo, A., M. Farrington, D. Hollenbaugh, X. Li, A. Milatovich, S. Nonoyama, J. Bajorath, L.S. Grosmaire, R. Stenkamp, M. Neubauer, et al. 1993. The CD40 ligand, gp39, is defective in activated T cells from patients with X-linked hyper-IgM syndrome. *Cell.* 72:291–300.
20. Farrington, M., L.S. Grosmaire, S. Nonoyama, S.H. Fischer, D. Hollenbaugh, J.A. Ledbetter, R.J. Noelle, A. Aruffo, and H.D. Ochs. 1994. CD40 ligand expression is defective in a subset of patients with common variable immunodeficiency. *Proc. Natl. Acad. Sci. USA.* 91:1099–1103.
21. Renshaw, B.R., W.C. Fanslow, III, R.J. Armitage, K.A. Campbell, D. Liggitt, B. Wright, B.L. Davison, and C.R. Maliszewski. 1994. Humoral immune responses in CD40 ligand-deficient mice. *J. Exp. Med.* 180:1889–1900.
22. Alderson, M.R., R.J. Armitage, T.W. Tough, L. Strockbine, W.C. Fanslow, and M.K. Spriggs. 1993. CD40 expression by human monocytes: regulation by cytokines and activation of monocytes by the ligand for CD40. *J. Exp. Med.* 178:669–674.
23. Caux, C., C. Massacrier, B. Vanbervliet, B. Dubois, C. Van Kooten, I. Durand, and J. Banchereau. 1994. Activation of human dendritic cells through CD40 cross-linking. *J. Exp. Med.* 180:1263–1272.
24. Lefrancois, L., J.D. Altman, K. Williams, and S. Olson. 2000. Soluble antigen and CD40 triggering are sufficient to induce primary and memory cytotoxic T cells. *J. Immunol.* 164:725–732.
25. Bennett, S.R., F.R. Carbone, F. Karamalis, R.A. Flavell, J.F. Miller, and W.R. Heath. 1998. Help for cytotoxic-T-cell responses is mediated by CD40 signalling. *Nature.* 393:478–480.
26. Ridge, J.P., F. Di Rosa, and P. Matzinger. 1998. A conditioned dendritic cell can be a temporal bridge between a CD4+ T-helper and a T-killer cell. *Nature.* 393:474–478.
27. Schoenberger, S.P., R.E. Toes, E.I. van der Voort, R. Offringa, and C.J. Melief. 1998. T-cell help for cytotoxic T lymphocytes is mediated by CD40-CD40L interactions. *Nature.* 393:480–483.
28. Sotomayor, E.M., I. Borrello, E. Tubb, F.M. Rattis, H. Bien, Z. Lu, S. Fein, S. Schoenberger, and H.I. Levitsky. 1999. Conversion of tumor-specific CD4+ T-cell tolerance to T-cell priming through in vivo ligation of CD40. *Nat. Med.* 5:780–787.
29. Diehl, L., A.T. den Boer, S.P. Schoenberger, E.I. van der Voort, T.N. Schumacher, C.J. Melief, R. Offringa, and R.E. Toes. 1999. CD40 activation in vivo overcomes peptide-induced peripheral cytotoxic T-lymphocyte tolerance and augments anti-tumor vaccine efficacy. *Nat. Med.* 5:774–779.
30. Kedl, R.M., M. Jordan, T. Potter, J. Kappler, P. Marrack, and S. Dow. 2001. CD40 stimulation accelerates deletion of tumor-specific CD8(+) T cells in the absence of tumor-antigen vaccination. *Proc. Natl. Acad. Sci. USA.* 98:10811–10816.
31. Mauri, C., L.T. Mars, and M. Londei. 2000. Therapeutic activity of agonistic monoclonal antibodies against CD40 in a chronic autoimmune inflammatory process. *Nat. Med.* 6:673–679.
32. Erickson, L.D., B.G. Durell, L.A. Vogel, B.P. O'Connor, M. Cascalho, T. Yasui, H. Kikutani, and R.J. Noelle. 2002. Short-circuiting long-lived humoral immunity by the heightened engagement of CD40. *J. Clin. Invest.* 109:613–620.
33. Kedl, R.M., W.A. Rees, D.A. Hildeman, B. Schaefer, T. Mitchell, J. Kappler, and P. Marrack. 2000. T cells compete for access to antigen-bearing antigen-presenting cells. *J. Exp. Med.* 192:1105–1114.
34. Schulz, O., A.D. Edwards, M. Schito, J. Aliberti, S. Manickasingham, A. Sher, and C. Reis e Sousa. 2000. CD40 triggering of heterodimeric IL-12 p70 production by dendritic cells in vivo requires a microbial priming signal. *Immunity.* 13: 453–462.
35. Reis e Sousa, C., S. Hieny, T. Scharton-Kersten, D. Jankovic, H. Charest, R.N. Germain, and A. Sher. 1997. In vivo microbial stimulation induces rapid CD40 ligand-independent production of interleukin 12 by dendritic cells and their redistribution to T cell areas. *J. Exp. Med.* 186:1819–1829.
36. Moskophidis, D., F. Lechner, H. Pircher, and R.M. Zinkernagel. 1993. Virus persistence in acutely infected immunocompetent mice by exhaustion of antiviral cytotoxic effector T cells. *Nature.* 362:758–761.
37. Barber, D.L., E.J. Wherry, and R. Ahmed. 2003. Cutting edge: rapid in vivo killing by memory CD8 T cells. *J. Immunol.* 171:27–31.
38. Byers, A.M., C.C. Kemball, J.M. Moser, and A.E. Lukacher. 2003. Cutting edge: rapid in vivo CTL activity by polyoma virus-specific effector and memory CD8+ T cells. *J. Immunol.* 171:17–21.
39. Coles, R.M., S.N. Mueller, W.R. Heath, F.R. Carbone, and A.G. Brooks. 2002. Progression of armed CTL from draining lymph node to spleen shortly after localized infection with herpes simplex virus 1. *J. Immunol.* 168:834–838.
40. Hernandez, J., S. Aung, W.L. Redmond, and L.A. Sherman. 2001. Phenotypic and functional analysis of CD8(+) T cells undergoing peripheral deletion in response to cross-presentation of self-antigen. *J. Exp. Med.* 194:707–717.
41. Schmidt, C.S., and M.F. Mescher. 1999. Adjuvant effect of IL-12: conversion of peptide antigen administration from tolerizing to immunizing for CD8+ T cells in vivo. *J. Immunol.* 163:2561–2567.
42. Kearney, E.R., K.A. Pape, D.Y. Loh, and M.K. Jenkins. 1994. Visualization of peptide-specific T cell immunity and

peripheral tolerance induction in vivo. *Immunity*. 1:327–339.
43. Pape, K.A., R. Merica, A. Mondino, A. Khoruts, and M.K. Jenkins. 1998. Direct evidence that functionally impaired CD4+ T cells persist in vivo following induction of peripheral tolerance. *J. Immunol.* 160:4719–4729.
44. Shrikant, P., A. Khoruts, and M.F. Mescher. 1999. CTLA-4 blockade reverses CD8+ T cell tolerance to tumor by a CD4+ T cell- and IL-2-dependent mechanism. *Immunity*. 11:483–493.
45. Reinhardt, R.L., A. Khoruts, R. Merica, T. Zell, and M.K. Jenkins. 2001. Visualizing the generation of memory CD4 T cells in the whole body. *Nature*. 410:101–105.
46. Kedl, R.M., and M.F. Mescher. 1998. Qualitative differences between naive and memory T cells make a major contribution to the more rapid and efficient memory CD8+ T cell response. *J. Immunol.* 161:674–683.
47. Maxwell, J.R., J.D. Campbell, C.H. Kim, and A.T. Vella. 1999. CD40 activation boosts T cell immunity in vivo by enhancing T cell clonal expansion and delaying peripheral T cell deletion. *J. Immunol.* 162:2024–2034.
48. Sprent, J., and M. Schaefer. 1990. Antigen-presenting cells for CD8+ T cells. *Immunol. Rev.* 117:213–234.
49. Oppmann, B., R. Lesley, B. Blom, J.C. Timans, Y. Xu, B. Hunte, F. Vega, N. Yu, J. Wang, K. Singh, et al. 2000. Novel p19 protein engages IL-12p40 to form a cytokine, IL-23, with biological activities similar as well as distinct from IL-12. *Immunity*. 13:715–725.
50. Le Bon, A., N. Etchart, C. Rossmann, M. Ashton, S. Hou, D. Gewert, P. Borrow, and D.F. Tough. 2003. Cross-priming of CD8+ T cells stimulated by virus-induced type I interferon. *Nat. Immunol.* 4:1009–1015.
51. Cho, H.J., T. Hayashi, S.K. Datta, K. Takabayashi, J.H. Van Uden, A. Horner, M. Corr, and E. Raz. 2002. IFN-alpha beta promote priming of antigen-specific CD8+ and CD4+ T lymphocytes by immunostimulatory DNA-based vaccines. *J. Immunol.* 168:4907–4913.
52. Pihlgren, M., P.M. Dubois, M. Tomkowiak, T. Sjogren, and J. Marvel. 1996. Resting memory CD8+ T cells are hyperreactive to antigenic challenge in vitro. *J. Exp. Med.* 184: 2141–2151.
53. Dubey, C., M. Croft, and S.L. Swain. 1996. Naive and effector CD4 T cells differ in their requirements for T cell receptor versus costimulatory signals. *J. Immunol.* 157:3280–3289.
54. Byrne, J.A., J.L. Butler, and M.D. Cooper. 1988. Differential activation requirements for virgin and memory T cells. *J. Immunol.* 141:3249–3257.
55. Croft, M., L.M. Bradley, and S.L. Swain. 1994. Naive versus memory CD4 T cell response to antigen. Memory cells are less dependent on accessory cell costimulation and can respond to many antigen-presenting cell types including resting B cells. *J. Immunol.* 152:2675–2685.
56. Bourgeois, C., B. Rocha, and C. Tanchot. 2002. A role for CD40 expression on CD8+ T cells in the generation of CD8+ T cell memory. *Science*. 297:2060–2063.
57. Lee, B.O., L. Hartson, and T.D. Randall. 2003. CD40-deficient, influenza-specific CD8 memory T cells develop and function normally in a CD40-sufficient environment. *J. Exp. Med.* 198:1759–1764.
58. Takeuchi, O., K. Hoshino, and S. Akira. 2000. Cutting edge: TLR2-deficient and MyD88-deficient mice are highly susceptible to *Staphylococcus aureus* infection. *J. Immunol.* 165: 5392–5396.
59. Takeuchi, O., K. Hoshino, T. Kawai, H. Sanjo, H. Takada, T. Ogawa, K. Takeda, and S. Akira. 1999. Differential roles of TLR2 and TLR4 in recognition of gram-negative and gram-positive bacterial cell wall components. *Immunity*. 11:443–451.
60. Toshchakov, V., B.W. Jones, P.Y. Perera, K. Thomas, M.J. Cody, S. Zhang, B.R. Williams, J. Major, T.A. Hamilton, M.J. Fenton, and S.N. Vogel. 2002. TLR4, but not TLR2, mediates IFN-beta-induced STAT1alpha/beta-dependent gene expression in macrophages. *Nat. Immunol.* 3:392–398.
61. Doyle, S., S. Vaidya, R. O'Connell, H. Dadgostar, P. Dempsey, T. Wu, G. Rao, R. Sun, M. Haberland, R. Modlin, and G. Cheng. 2002. IRF3 mediates a TLR3/TLR4-specific antiviral gene program. *Immunity*. 17:251–263.

APPENDIX C

TOXICITY OF CDYOL OR CPG ALONE VERSUS SUBJECT SYNERGISTIC COMBINATIONS AND SUPPORTING REFERENCES

1. Background/Significance

1.a. Overview.

While the past 10 years have witnessed an exponential growth in the identification of cancer target antigens, a similar pace for the development of human adjuvants to effectively immunize against these targets has lagged. The molecular identification of Toll-like Receptors and their ligands, and receptor-ligands that control adaptive immunity have provided the first logical, hypothesis-based strategies to molecularly concoct adjuvants so as to elicit protective immune responses to cancer. Parallel to the importance of TLRs in mobilizing the innate immune response, CD40 and its ligand are the central activators for the development of the adaptive immune responses. Our data show that the use of well-defined agonists that activate specific TLRs, combined with the use of agonists for CD40, elicit profound cell-mediated immune responses to defined peptides that meet or exceed that which is seen with the most potent viral vectors. Based on these observations, we have used this CD40/TLR platform and have shown that it can be therapeutically effective in the treatment of melanoma. We hypothesize that these two agonists impinge on the dendritic cell (DC) as a target, and induce functional features which uniquely empower the DC to drive profound CMI responses. While we do not fully understand why these DCs are so effective in inducing CMI, we show that the molecular signature of DCs triggered with TLR* and αCD40 is distinctive from DCs triggered with either agent alone *in vivo*.

1.b. Adjuvants.

Perhaps one of the weakest aspects of our approach to fight cancer, is the lack of adjuvants that can elicit robust, long-lasting immunity to cancer-related antigens. In the past, we have relied on the use of agents that appeared to induce inflammation. Alum is salts of aluminum hydroxide and phosphate and primarly elicits humoral-mediated immune responses. This adjuvant was first employed in 1926 and was effectively grandfathered in when the FDA first assumed new drug approval authority in 1938. Alum is the only FDA approved adjuvant, and is a component of a number of our commonly used vaccines, like tentanus toxoid. There are many other adjuvants (non-cytokine) that have been employed in cancer clinical trials like Bacille Calmette-Guérin (BCG), keyhole limpet hemocyanin (KLH), incomplete Freund's adjuvant (IFA), all which have poorly understood mechanisms of action and modest adjuvant activities. Not until 1999 (1), when the first studies elucidating the receptors for immune adjuvants (Toll-like receptors) emerged on the horizon, did a molecular understanding of how these "non-specific" activators of the immune system trigger innate immunity.

1.c. The Toll-like receptors (TLRs). TLRs are type 1 membrane proteins that are expressed on hematopoietic and non-hematopoietic cells. Currently, there are 11 members in the TLR family. These receptors are characterized by their capacity to recognize pathogen-associated molecular patterns (PAMP) expressed by pathogenic organisms. Typical PAMPS include LPS, DNA (CpG), lipoproteins, ssRNA, and glycolipids, as detailed in the Table I below. Whether there are true endogenous ligands for TLRs is still controversial, although it has been reported that TLR2 and TLR4 are able to recognize several self-proteins including members of heat shock protein family hsp60 and hsp70 (2-4).

In general, triggering of TLR elicits profound inflammatory responses through enhanced cytokine production (IL12, IL18, etc), chemokine receptor expression (CCR2, CCR5 and CCR7), and costimulatory molecule expression. As such, these receptors in the innate immune systems exert control over the polarity of the ensuing acquired immune response.

CD154 and its receptor, CD40: CD154, the ligand for CD40 (CD40L, gp39) is a 32-39 kD member of the Tumor Necrosis Factor Family, which includes TNF-α,

lymphotoxin, FasL, CD30L, CD27L, 4-1BBL, and OX-40L. Activated CD4 T-cells are the predominant cell type responsible for CD154 expression. Expression of CD154 on $CD8^+$ T-cells, eosinophils, mast cells and basophils, NK cells, and DCs has also been described. The receptor for CD154, CD40 is a member of the tumor necrosis factor receptor (TNF-R) superfamily that includes TNF-RI (p55), TNF-RII (p75), p75 neurotrophin receptor, fas, CD30, CD27, 4-1BB, and OX-40. It is a 50-kDa membrane protein whose tissue distribution was originally thought to be restricted to B cells, DCs (DC's) and basal epithelial cells however, later studies have shown functional expression of CD40 on monocytes/macrophages, microglial cells and endothelial cells, as reviewed in (26-29).

The function of CD154 in regulating cell-mediated immunity (CMI): In vitro studies on isolated DCs have shown that CD40 triggering alters the expression of cytokines (IL12, IL15) (30-32), chemokines (IP10, MIP-1α MIP-1β and IL-8)(33, 34) co-stimulatory molecule expression (CD80, CD86) and chemokine receptors (34, 35). All of these effects culminate in the ability of CD40-activated DCs to stimulate enhanced T cell proliferation and differentiation (36). Our own data shows that CD154 exerts far more profound effects on the early signaling, cytokine production and chemokine production compared to TNFα and RANKL. One other critical impact of CD40 triggering of DCs is the change in the turnover of peptide-MHCII. Lanzavecchia has shown using LPS (37), and we have shown using sCD154(38), that maturation of DCs with a CD40 agonist facilitates the accumulation of MHCII-peptide complexes on the surface of DCs. Studies from our lab (38) and others (39), indicate that CD40 appears to be a critical longevity signal for DCs *in vivo*. We have hypothesized that DC longevity is essential for the prolonged clonal expansion of $CD4^+$ T cell responses (38). The impact of CD40 signaling on DC longevity, we feel is a critical feature of the synergy that is observed when TLR and CD40 agonists are used in combination and will be discussed below. In summary, there is no doubt that CD40 agonists induce profound biologic changes in DCs *in vitro* and *in vivo*. However, we hypothesize that these changes are not sustained, ineffective and inadequate to "license" the DC to truly trigger effective CMI responses.

CD40 agonists to induce tumor immunity. The success of CD40 agonists to elicit CMI in the absence of $CD4^+$ T cells generated substantial enthusiasm to use CD40 agonists as adjuvants for cancer vaccines. A series of studies by Glennie and co-workers (44-46) showed that one can achieve tumor regression of $CD40^+$ lymphoma using αCD40, but the doses of αCD40 were very high (250ug/day, days 2-5), and oddly, the tumor inoculum needed for immunization was very high ($5x10^7$/mouse). Nonetheless, clinical remission of these $CD40^+$ lymphoma was impressive. Less impressive were studies on hematopoietic tumors which were $CD40^-$. It is likely that the successes with $CD40^+$ lymphomas and leukemias were due to direct effects of CD40 agonists on the tumor. For lymphomas and leukemias, αCD40 may also enhance their APC activities, and at the same time enhance their apoptosis. Later studies by this same group, however, did demonstrate that CD40 agonists could exert beneficial therapeutic effects on solid tumors. (44). With solid tumors, a number of studies have shown that CD40 activation promotes apoptotic death and that CD40 expression is an important factor in the generation of tumor-specific T-cell responses that contribute to tumor cell elimination. Other groups, like that of Meleif and co-workers have shown that CD40 agonists alone *or* TLR agonists alone could elicit effective therapeutic on Ad5E1Aexpressing (CD40-) tumors *in vivo* (tumor type not described) (47). Using a renal cell carcinoma model, Murphy and co-workers have shown that only the combination of an agonist αCD40 and IL-2, but neither agent administered alone, induced complete regression of metastatic tumor and specific immunity to subsequent rechallenge in the

majority of treated mice (48). At this time efficacy with CD40 agonists alone is unpredictable. It is not clear if CD40 expression on the tumor is important, if tumor burden is important, if CD40 alone is adequate and if there is a distinctive difference in the efficacy of αCD40 therapy in liquid or solid tumors. We would contend that when used with a TLR agonist, CD40 agonists will induce high levels of tumor-specific immunity, and avoid the idiosyncracies seen in different tumor models with αCD40 monotherapy.

The basic immunology of CD40 agonists and their synergy with TLR agonists. CD40 is a reasonable target for inducing heightened CMI responses for the purposes of tumor protection, yet the data in the literature suggested that it was not applicable in a wide range of tumors. My laboratory has worked intensively for a number of years to try to develop a general method to enhance protective tumor immunity using αCD40 as a monotherapy, and failed. Any and all parameters of dose of antibody, timing, route of inoculation, tumor type, different mabs, etc were extensively tested yet these efforts proved futile, except in B lymphoma and leukemia models, as reported by Glennie. A recent study from Kedl and co-workers (49) has shed much light on some of the important parameters that may influence the generation of protective CTL when using CD40 agonists. Using tetramer staining for SIINFYKL-specific CTL, and OVA-transduced B16, they showed that αCD40 agonists actually *accelerated the loss* of SIINFYKL-specific CTL. However, if immunization were done with a vaccinia virus carrying a SIINFYKL minigene, enhanced CTL expansion was observed using αCD40 agonists. It was concluded that long-term immunization to tumor antigens are only enhanced by CD40 agonists if those tumor antigens are delivered in viral vectors or in the context of inflammation. Hence, the great disparities in the outcome of innumerable tumor models may be due to the inadvertent addition of co-inflammatory mediators that synergize with the αCD40 agonist.

Such *in vivo* studies led to a number of recent reports on the requirements of co-signals for the activation of DCs by CD40 agonists. Published studies, as well as those to be presented in the Preliminary Data section, show that CD40 engagement *alone* is insufficient to induce IL12p70 production by DCs *in vitro* and *in vivo* (50). By evaluating mRNA for p40 and p35, the authors show that co-engagement via TLR (STAg, an extract from *Toxoplasma* gondi) and CD40 is critical for enhanced p35 mRNA expression and the production of IL12p70. This study was followed by an investigation using human DCs where it was shown that CpG DNA was a critical co-stimulus with CD40 signaling for IL12p70 production *in vitro* (51). Taken together, these were the first studies to document that CD40 was necessary but not sufficient to drive DC certain aspects of DC maturation. However, they did not provide compelling evidence that the combined actions of CD40 and TLR agonism was essential to fulminately elicit CMI.

The question of synergy between CD40 and TLR agonism was approached directly by quantifying the impact of either TLR or CD40 engagement or TLR/CD40 engagement on the expansion of OVA-specific tetramer$^+$ cells *in vivo*. We have shown (52) that the administration of αCD40, a TLR7 agonist (S27609) and OVA (protein or peptide) can induce the generation of OVA-specific CD8$^+$ T cells (see examples in Preliminary data section). By day 6, the antigen-specific T cells can represent over 25% of the entire CD8$^+$ T cell population. All TLR agonists tested synergize with αCD40 and induce potent antigen-specific CTL activities. These findings supported the hypothesis that the combined triggering of innate and acquired immunity maximized the capacity to induce potent effector T cells and set the stage for the use of this technology as a vaccine platform in cancer immunotherapy.

CD40 associated toxicity. Studies in both mouse and human have shown that the administration of CD40 agonists alone induce toxicity. In intact mice, it has been shown that CD40 agonists induce liver toxicity. In immune deficient mice and non-lethally-irradiated mice, the administration of CD40 agonists induce lethality. During the course of our studies with combined administration of αCD40 and TLR agonists (or IFNa) we discovered that the addition of either a TLR agonist or IFNa *in vivo* to mice treated with αCD40 resolved toxicity. Thus the co-adminstration of IFNa or TLR agonist with a CD40 agonist should resolve the toxicity observed in the clinical use of CD40 agonists.

Combination therapy with TLR agonist or IFNα abrogates toxicity seen with anti-CD40 based monotherapy in intact C57BL/6 mice

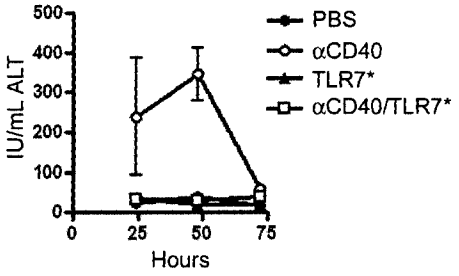

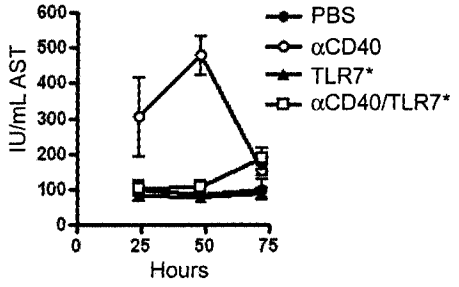

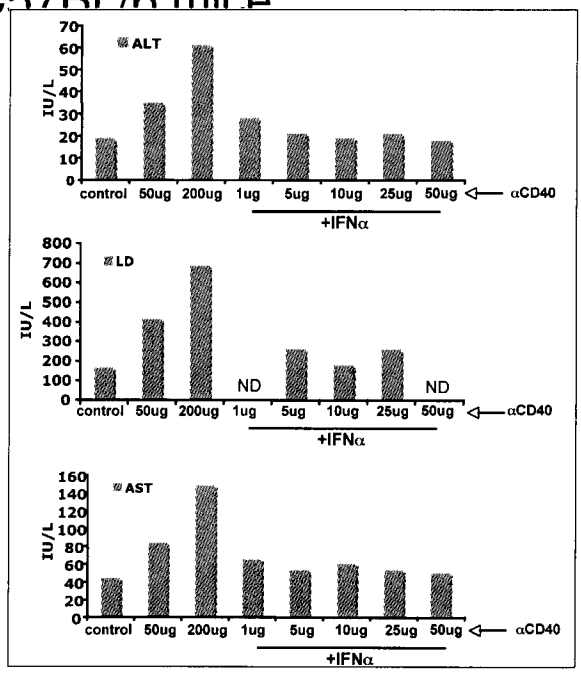

Abatement of Liver toxicity by co-administration of TLR agonist or IFNa with a CD40 agonist.

Hepatocellular injury was biochemically assessed by measuring serum liver enzyme activity. Specifically, mice received 100μg anti-CD40, 100μg S-27609 or both i.v. In some cases, mice also received graded doses of recombinant Interferon-alpha (normally, one million international units per mouse). Serum was harvested 24-72 hours later and sent to Charles River Laboratories (Worcester, MA) for liver chemistry profile analysis. Alternatively, serum samples were analyzed by the National Jewish Medical Center Core Lab (Denver, CO).

IFN/CD40 combination has low hepatic toxicity

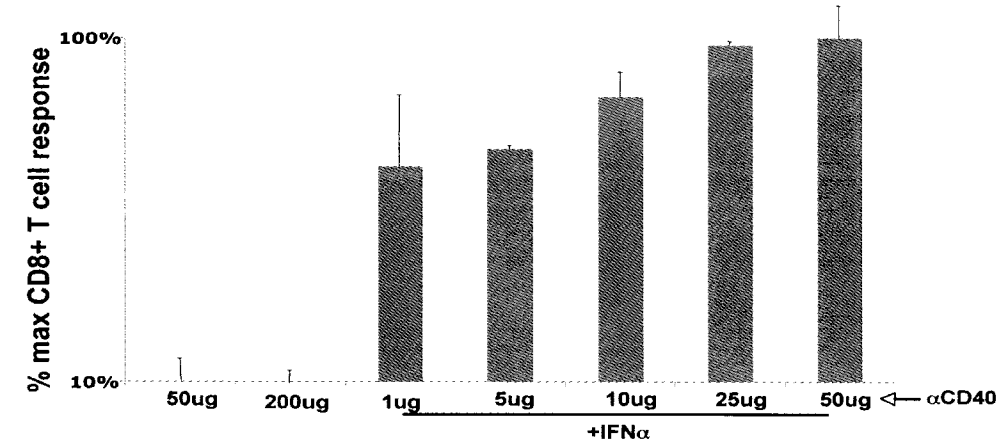

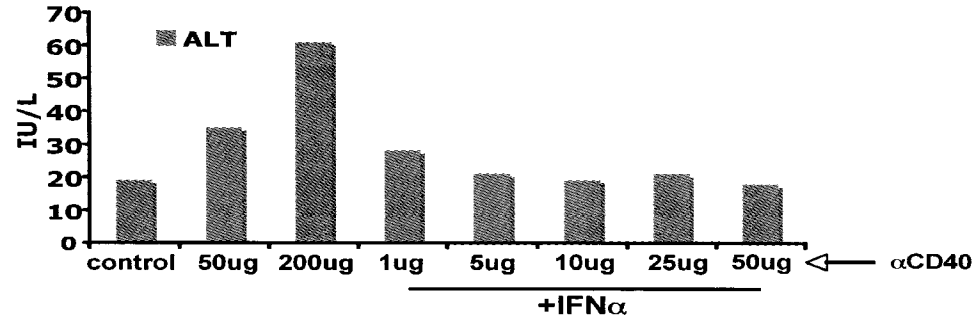

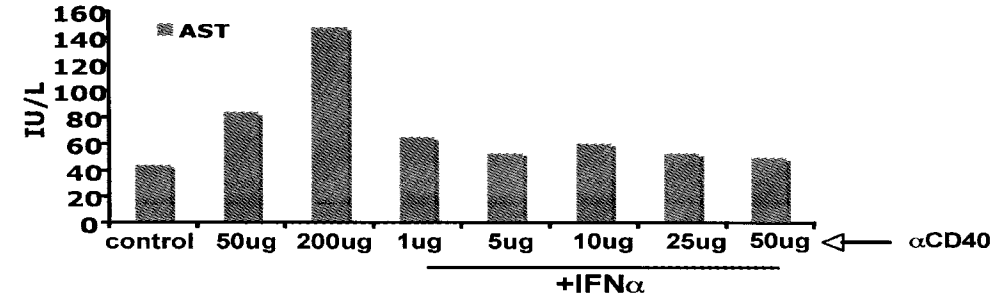

Toxicity

ImmuRx

Confidential

TLR/CD40 combination has low hepatic toxicity

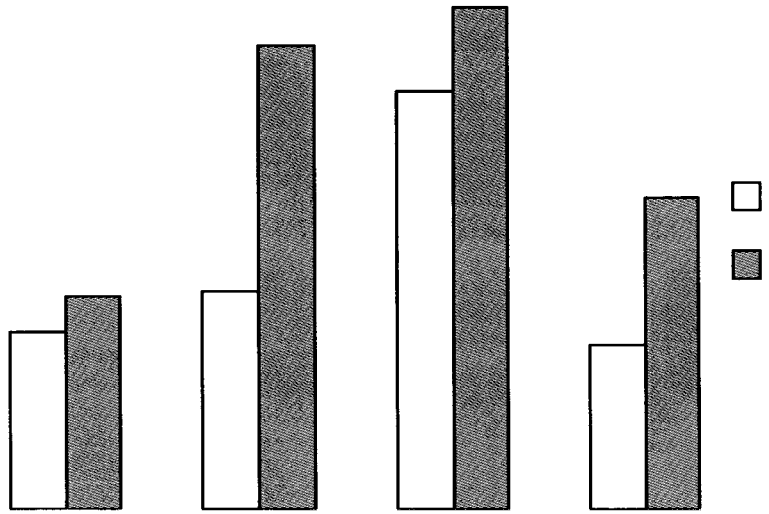

Toxicity

TLR7 Agonists Rescue αCD40 mAb Toxicity in Rag -/- mice

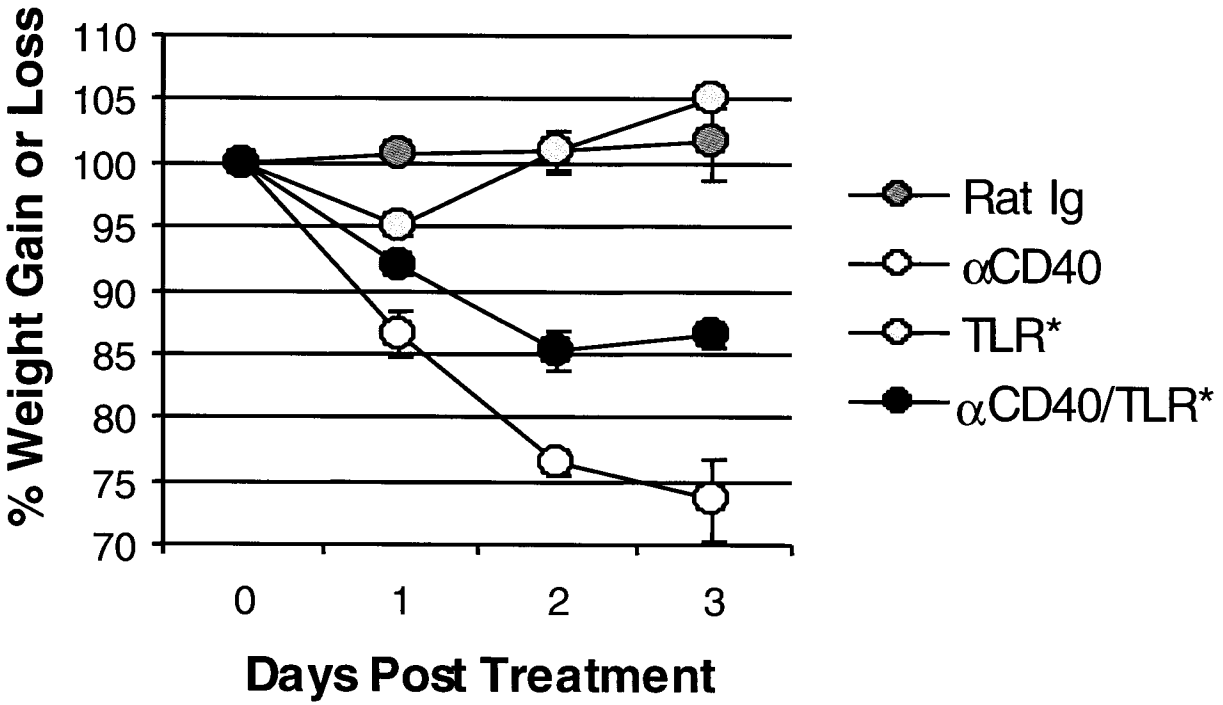

Toxicity

Mitigation of Hepatic Toxicity

Dose dependent hepatotoxicity in humans*

ALT

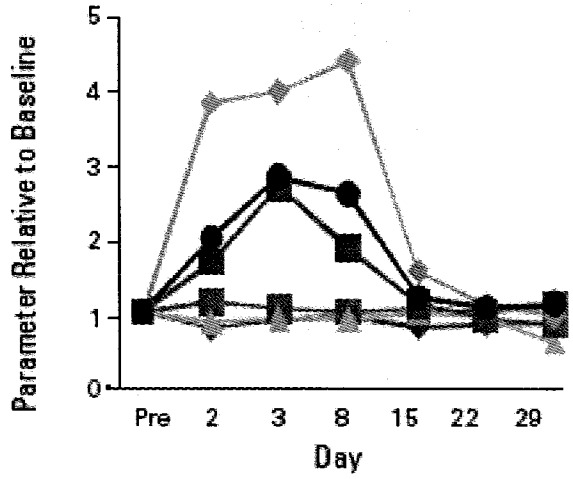

AST

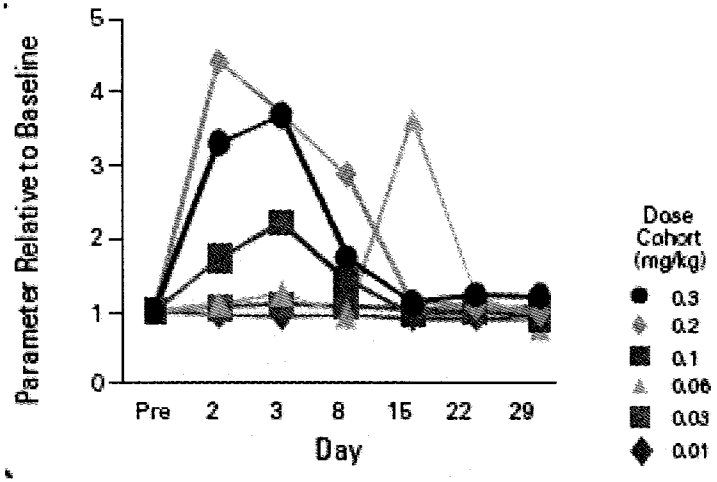

*Pfizer Phase I trial

Mitigation by Combination

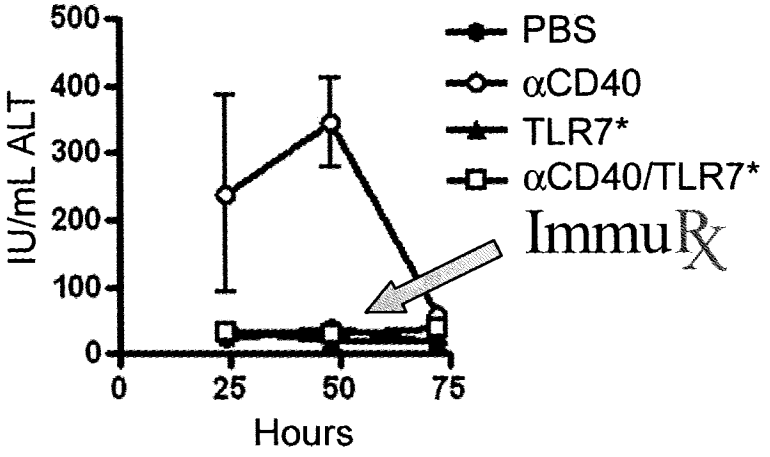

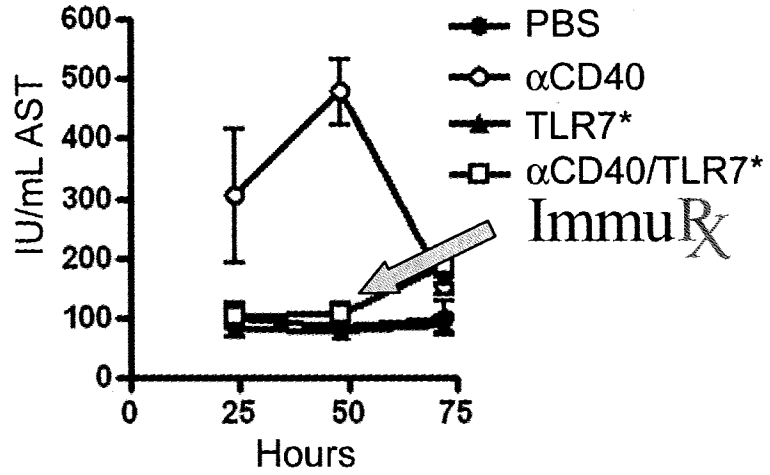

ImmuRx

Low Hepatic Toxicity

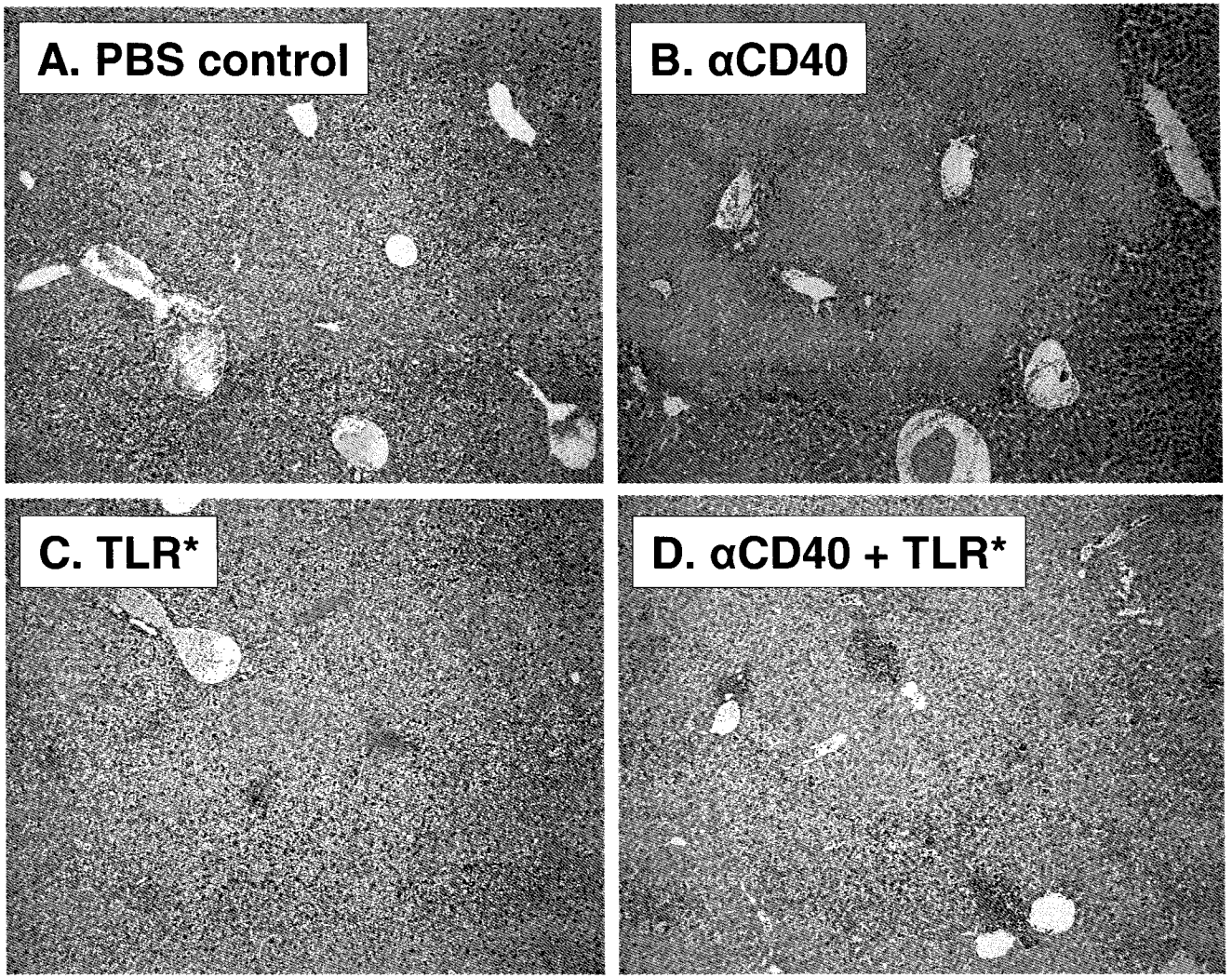

Higher Immunity, Lower Toxicity

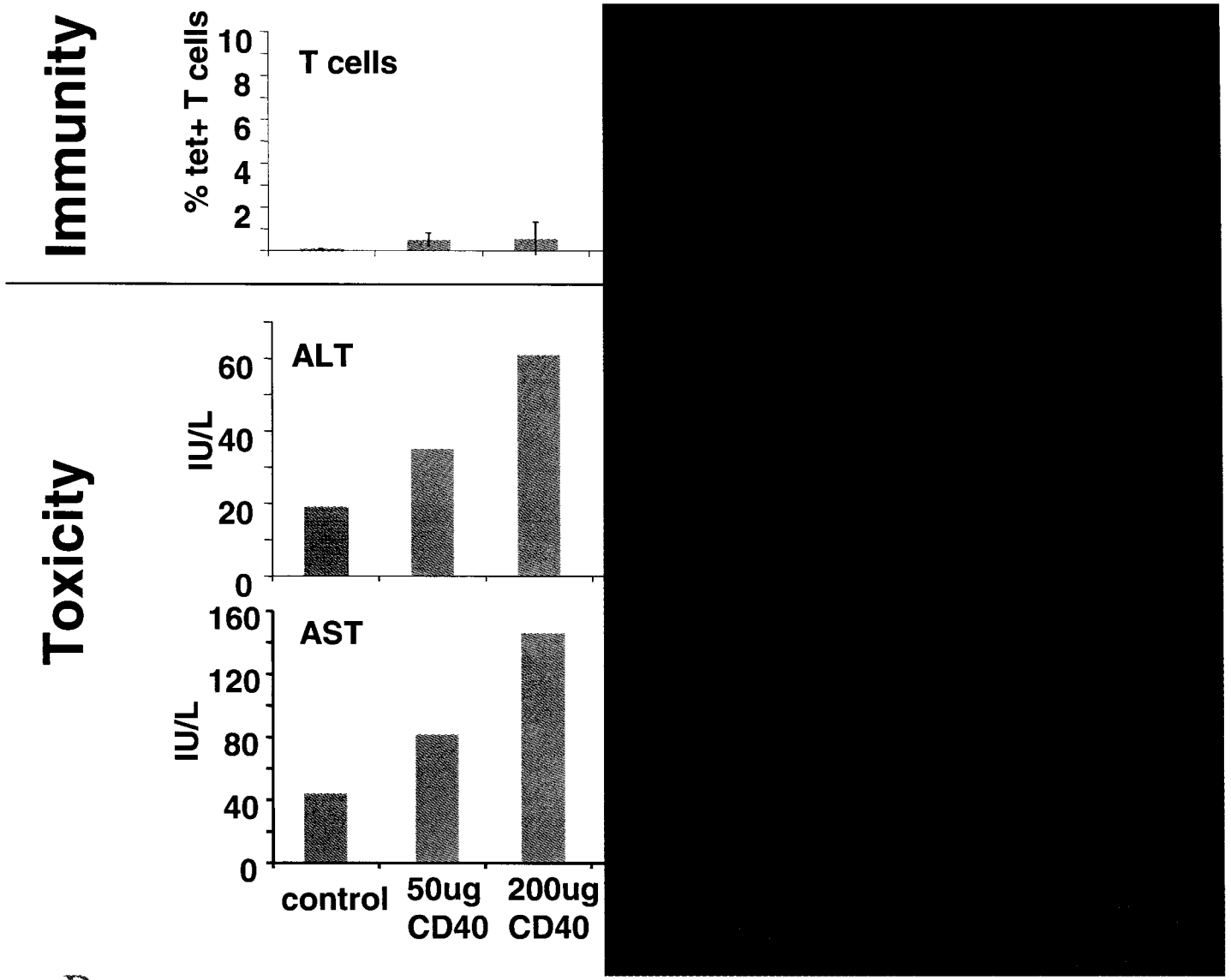

CD40 stimulation accelerates deletion of tumor-specific CD8$^+$ T cells in the absence of tumor-antigen vaccination

Ross M. Kedl*†‡, Michael Jordan†, Terence Potter†§, John Kappler†¶‖, Philippa Marrack†¶**††, and Steven Dow†§**

*Cancer Research Institute, ¶Howard Hughes Medical Institute, †Department of Immunology, National Jewish Medical and Research Center, and Departments of ††Biochemistry and Molecular Genetics, ‖Pharmacology, and **Medicine, §Cancer Center, University of Colorado Health Sciences Center, Denver, CO 80206

Contributed by Philippa Marrack, July 19, 2001

Previous work has established a role for CD40-mediated signals in eliciting helper-dependent CD8$^+$ T cell responses. Here we investigated the effects of *in vivo* CD40 stimulation on the survival and function of tumor-specific CD8$^+$ T cells in a mouse melanoma model system. We found that agonistic anti-CD40 antibody treatment alone of tumor-bearing mice accelerated the deletion of tumor-antigen-specific T cells. However, long-term survival and function of tumor-antigen-specific T cells could be achieved when viral immunization with tumor antigen and anti-CD40 treatment were combined. This rescue of CD8$^+$ T cells could not be easily replicated by inflammatory or antigen-specific stimuli alone, demonstrating the specificity of signals that regulate the deletion or survival of tumor-specific T cells. These results demonstrate that opposing effects can be elicited by CD40 stimulation *in vivo* and suggest the need for caution in using this treatment for cancer patients.

melanoma | MHC tetramer

T cells play an important role in immunity to tumors, particularly melanomas. T cells specific for melanoma antigens can often be isolated from the tumor site, lymphoid tissue, or the blood of melanoma patients (1–3). These T cells have various ranges of functional activity, but in some cases their presence correlates with a better clinical prognosis for the patient (4–7). For example, melanoma patients who develop vitiligo, a T cell-mediated autoimmune destruction of normal melanocytes, demonstrate a greater ability to control their tumor growth (8–11).

Despite the importance of T cells in tumor immunity, we still know very little about the induction of tumor-specific T cells and the signals that are necessary to sustain their activation and effector function. Melanoma-specific T cells are frequently isolated from patients but are often functionally unresponsive (12–16). In humans, where we are unable to follow the progression of the disease from its earliest stages of development, it is difficult to determine either the causes of this functional inactivation or the intervention(s) necessary to prevent it.

The activation state of the antigen-presenting cell (APC) has been shown to have a dramatic effect on CD8$^+$ T cell responses. Three groups simultaneously demonstrated that a helper-dependent CD8$^+$ T cell response could be converted to a helper-independent response simply by activating the APC with antibodies against CD40 (17–19). Because suboptimal tumor antigen presentation is speculated to be a problem in tumor-bearing hosts, several groups have used CD40 stimulation in tumor model systems in an attempt to augment failed or weak CD8$^+$ T cell responses (20–22). While CD40 stimulation has shown some promise, the precise conditions under which this approach is most effective have not been fully defined. Indeed, a recent report suggests that agonistic anti-CD40 antibodies can be immunosuppressive (23), exemplifying the need for careful assessment of this therapeutic intervention, particularly in the case of a tumor-bearing host where the immune response against the tumor may be minimal to begin with.

We have developed a melanoma model system that allows the tracking of endogenously generated tumor-specific T cells *in vivo* during the course of tumor growth. Mice were challenged with the murine melanoma tumor line B16 transfected with the gene for ovalbumin (B16ova). The CD8$^+$ T cell responses to the dominant ovalbumin epitope SIINFEKL (ova8) were followed with the use of a class I K^b/ova8 tetrameric staining reagent. In these studies we demonstrated that tumor-specific T cells expanded and migrated to tumor tissues. We further demonstrated that agonistic antibodies against CD40 actually enhanced the deletion of antigen-specific CD8$^+$ T cells, and this deletion could be prevented by vaccination with tumor antigen.

IMMUNOLOGY

Materials and Methods

Tumor Cell Lines and Mouse Injections. The B16-ovalbumin (B16ova) and B16-neomycin (B16neo) cell lines were kindly provided by Richard Duke (University of Colorado Health Sciences Center, Denver). These cell lines were made by lipofection of the B16-F10 cell line with constructs encoding the full-length ovalbumin gene with the neomycin-resistance selection gene (B16ova) or with the neomycin-resistance selection gene alone (B16neo) under the control of the cytomegalovirus long terminal repeat promoter. These tumor cells were cultured in complete media containing 750 μg/ml G418. Before injection into mice, the cells were trypsinized for 5 min at 37°C, washed with complete media and balanced salt solution (Earle's BSS), and resuspended in BSS at 1×10^6 cells per milliliter. Six- to 12-week-old C57BL/6J (B6) female mice from the Jackson Laboratory were anesthetized with Avertin, their rear flanks were shaved, and they were injected with 1×10^5 tumor cells intradermally.

Virus and DNA Vaccination. Vaccinia virus (VV) (kindly provided by Tom Mitchell, University of Louisville, Louisville, KY) was propagated in and titrated by plaque assay on cultured 143B osteosarcoma cells as described (24). Mice were challenged i.v. with $2–4 \times 10^6$ plaque-forming units of VV encoding ovalbumin (VVova) (25) or influenza virus nucleoprotein (VV-NP) (25).

The ovalbumin gene was subcloned into an expression vector containing the tissue plasminogen activator leader sequence for secretion, along with a cytomegalovirus promoter and the bovine growth hormone polyadenylation sequence (a kind gift from

Abbreviations: APC, antigen-presenting cell; B16ova, murine melanoma tumor line B16 transfected with the gene for ovalbumin; B16neo, B16-neomycin; VV, vaccinia virus; VVova, VV encoding ovalbumin; VV-NP, VV encoding influenza virus nucleoprotein.

‡To whom reprint requests should be sent at the present address: 3M Pharmaceuticals, 3M Center, Building 270-2S-06, St. Paul, MN 55144-1000. E-mail: rmkedl@mmm.com.

The publication costs of this article were defrayed in part by page charge payment. This article must therefore be hereby marked "*advertisement*" in accordance with 18 U.S.C. §1734 solely to indicate this fact.

Keith Rushlow, Heska Corp., Fort Collins, CO). Plasmid DNA was prepared by a modified alkaline lysis procedure followed by glycol precipitation as described (26). Mice were injected with 50 μg of total plasmid DNA in a total volume of 200 μl. Equal amounts of DNA were injected bilaterally into the quadriceps muscles of mice anesthetized with Avertin.

Monoclonal Antibodies. The antibodies used in these studies were 1C10 (anti-CD40), XMG1.2 (anti-IFNγ), GK1.5 (anti-CD4), and 20LC-11.1 (anti-DR1 used as a control rat antibody). The respective hybridomas were grown in serum-free conditions, and each antibody was purified on a protein G column. After elution in a glycine·HCl buffer and neutralization with a Tris buffer, the purified antibodies were dialyzed into PBS and injected i.p. into tumor-bearing hosts. Two hundred micrograms of anti-CD40 antibody (27) was injected 7–10 days after initial tumor challenge and, in the cases where noted, every 7 days thereafter. *In vivo* depletion of CD4$^+$ T cells was performed by the weekly injection of 500 μg of anti-CD4 (28). *In vivo* blocking of IFNγ was performed by the weekly injection of 2–3 mg XMG1.2. This treatment was shown to be effective in blocking the effect of IFNγ *in vivo* in previous studies (29, 30).

Cell Preparation, Tetramers, and Cell Staining. After sacrifice of the animals at various times, the draining nodes (periaortic, inguinal, axillary, and brachial), spleen, and tumor tissues were removed and homogenized into single-cell suspensions. In the case of spleen and tumor, the red blood cells were lysed by brief treatment with ammonium chloride buffer followed by washing with BSS. All cells were finally suspended in complete SMEM, and total cell numbers were determined with a Coulter Counter.

Anti-CD8-APC, CD44-FITC, B220-Cychrome, IA^b-biotin, and streptavidin-Cychrome were all purchased from PharMingen. K^b covalently linked by the C terminus to a peptide tag which is a substrate for BirA was produced in insect cells, biotinylated, and bound to phycoerythrin-streptavidin as described (31, 32). A 5–10 M excess of SIINFEKL peptide (ova8, ovalbumin residues 257–264) or SIYRYYGL peptide (which, in the context of K^b class I, activates T cells bearing the 2C T cell antigen receptor) was added directly to newly constructed K^b–phycoerythrin-streptavidin tetramer for at least 30 min at 4°C. Tetramer staining was performed as described (32). The K^b/SIYRYYGL tetramer (i.e., same MHC, wrong peptide) and/or K^b/ova8 staining of cells from mice bearing a non-ovalbumin-expressing tumor (B16neo) was used to establish the background tetramer staining of experimental samples. Each batch of K^b/ova8 tetramer was tested and normalized for binding to naive OT1 transgenic T cells, which are specific for K^b/ova8, before use in experiments (32).

Cells were stained with tetramer for 1 h and then treated with GolgiStop (brefeldin A) in the presence of ovalbumin peptide for 4–6 h in complete medium at 37°C. The cells were then stained for CD8 and IFNγ according to the Becton Dickinson protocol for intracellular cytokine staining.

Four-color fluorescence-activated cell sorter data were collected on a Becton Dickinson FACSCalibur flow cytometer and analyzed with CELLQUEST software.

***In Vitro* Restimulation and ^{51}Cr Release Lytic Assays.** Single-cell suspensions were made from the spleens of experimental mice, placed at 3–4 $\times$ 10^6 cells per milliliter in 12-well plates, and incubated in the presence of peptide and 10% Rat Con-A supernatant in complete minimal essential medium (MEM) for 5 days. The cells were then washed and plated at increasing cell densities in 96-well plates. ^{51}Cr lytic assays were performed as described (33) with the use of EL4 tumor cells (H-2^b) as targets ± the ova8 peptide.

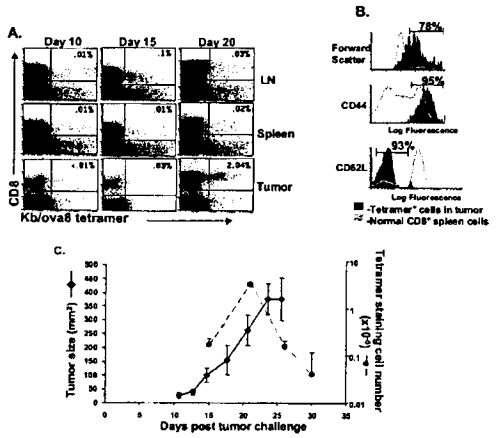

Fig. 1. ova8-specific T cells are detectable by tetramer staining in B16ova-bearing mice. B6 mice were injected intradermally with 1 $\times$ 10^5 B16ova cells. At the times indicated in *A*, mice were killed and the cells were isolated from lymph nodes, spleen, and tumor. (*A* and *B*) The cells were stained with anti-CD8, anti-IA^b, and either K^b/ova8-tetramer or control K^b-tetramer. Plots shown were gated on all live, IAb$^-$ events, and the percentages given in the upper right quadrant are of the total CD8$^+$ T cells. The settings for determining K^b/ova8-tetramer staining were obtained by staining cells with control tetramer (not shown). Results are representative of five separate experiments. (*B*) All histograms are gated on K^b/ova8-tetramer$^+$ events from tumor tissue 20 days after initial tumor challenge, stained as described in *A*. (*C*) Data from two separate experiments were plotted for tumor size (◆, left axis) vs. number of tetramer-staining CD8$^+$ T cells (●, right axis). Tumor size was measured in two dimensions with a caliper; error bars represent the standard error between six individual mice. The numbers of tetramer-staining T cells were calculated from the percentage of tetramer-staining cells, as shown in the upper right quadrant in *A* and the total cell number as determined with a Coulter Counter.

Results

T Cell Responses in Tumor-Bearing Hosts Are Detectable but Transient and Nonfunctional. Many human tumors express mutated gene products or gene products that are normally expressed only within a developing embryo (34–38). Because of a lack of central tolerance of these so-called tumor neo-antigens, epitopes from these gene products can serve as tumor rejection antigens. In an effort to approximate this kind of tumor rejection antigen, we used the B16 melanoma cell line transfected with the gene for ovalbumin (B16ova) as a representative tumor neo-antigen.

Mice were injected with B16ova intradermally, and at various times thereafter spleen, lymph nodes, and tumor tissue were removed, and the cells were stained with the K^b/ova8 tetramer to identify all T cells directed against the dominant epitope of the ovalbumin tumor neo-antigen. Despite the development of palpable tumors by day 7–10, tumor-specific T cells were not detectable until about day 15 (Fig. 1*A*). This population of CD8$^+$ T cells was usually very small and was seen in either the lymph nodes or spleen. Tumor-specific T cells were more readily detectable within the tumor itself, but usually not until after day 20. Forty to eighty percent of the ova8-specific T cells in the tumor were blasts (high forward scatter) at this time point, suggesting that clonal expansion occurred within the tumor tissue (Fig. 1*B*). These cells demonstrated an activated phenotype of high CD44 and low L-selectin expression (Fig. 1*B*). Despite this activated phenotype, little if any ova8-specific lytic activity could be detected either directly *ex vivo* (data not shown) or after *in vitro* restimulation (see Fig. 4*A*).

The number of ova8-specific T cells within the tumor declined over time as the tumor increased in size until the animal was

killed, suggesting that the process of deletion of this T cell population was limited only by the life span of the host (Fig. 1*C*). The growing tumor still expressed ovalbumin, based on the ability of naive OT1 transgenic T cells (specific for the K^b/ova8 epitope) to proliferate within the tumor when transferred into tumor-bearing hosts at late time points (data not shown), which suggested that the loss of K^b/ova8-specific T cells at late time points was not due to the outgrowth of a tumor-antigen-loss variant. In addition, the decline in T cells within the tumor was not caused by their migration to other sites such as lung and liver; although tumor-specific T cells could be detected in these peripheral tissues (data not shown) they were only detectable at such sites at times when they were also detectable in the tumor. Therefore the data suggest that initial T cell activation occurred at early time points within the lymphoid tissue (Fig. 1*A*) followed by a trafficking to and clonal expansion of the cells within the peripheral tumor compartment (Fig. 1*B*). Despite this clonal expansion, the tumor-specific T cells were nonfunctional, and their decline in number indicated their progressive deletion (Fig. 1*C*).

This model system is remarkably consistent with what little is known about tumor-specific T cell responses from human patient samples. Similar to our model system, the melanoma-specific T cells detectable by tetramer staining in blood or tissue samples from patients often show an activated phenotype but no functional response when assessed for lytic activity or cytokine production (12–16). In addition, whereas we originally designed these experiments to assess the activity of T cells directed against a representative tumor neo-antigen (ovalbumin), we were also recently able to confirm these findings for T cells directed against the endogenous B16 tumor antigen TRP2. The kinetics of the response of TRP2-specific T cells, as assessed by tetramer staining in B16 tumor-bearing mice, is remarkably similar to the ovalbumin-specific response in terms of expansion and deletion (data not shown) and further supports the physiological relevance of this model system (R.M.K. and S.D., unpublished results).

Agonistic Anti-CD40 Antibody Treatment Accelerates the Deletion of Tumor-Specific $CD8^+$ T Cells. CD40 is a molecule expressed on APCs which, when stimulated with agonistic antibodies, can dramatically affect $CD8^+$ T cell responses (17–19). A number of groups have used anti-CD40 treatment in studies of tumor growth and rejection and have reported significant benefits from this treatment, particularly with respect to inhibiting the long-term deletion of tumor-antigen-specific T cells (21, 22). In those studies, anti-CD40 treatment was accompanied by some form of tumor-antigen immunization in the presence of adjuvant (e.g., peptide in complete Freund's adjuvant or virus), to enhance tumor-antigen expression and presentation to a level that was detectable by the specific T cells.

Using MHC tetrameric reagents, we were able to detect an ovalbumin T cell response in tumor-bearing mice, suggesting that ova8 antigen presentation was occurring to a significant extent in mice challenged with tumor alone. It therefore seemed possible that tumor-antigen immunization was unnecessary and that anti-CD40 treatment alone of tumor-bearing mice might prevent the deletion and/or rescue the function of the tumor-specific T cell response. If true, this treatment with anti-CD40 alone might be of significant clinical benefit, alleviating the need to determine *a priori* the primary tumor-antigen candidates in any given patient and essentially allowing the host to focus its responses on whatever tumor antigens it is already presenting. We therefore treated mice with anti-CD40 alone 7 days after initial tumor challenge and assessed the T cell response as before.

Shortly after the anti-CD40 treatment, we observed an increase in the numbers of K^b/ova8-specific T cells within the tumor by comparison with controls (Fig. 2*A*), indicating that this treatment did have an effect on the developing T cell response. However, in the long term, the anti-CD40 treatment actually accelerated deletion of the K^b/ova8-specific T cells (Fig. 2 *A* and *C*). Moreover, even the T cells present during the early expansion immediately after anti-CD40 treatment did not demonstrate significant IFNγ production (Fig. 2*D*) or lytic activity (data not shown and see Fig. 4*A*), a result that was consistent with the continued growth of the tumor (Fig. 2*B*) and further indicated that anti-CD40 stimulation alone was deficient for signals necessary for a functional T cell response.

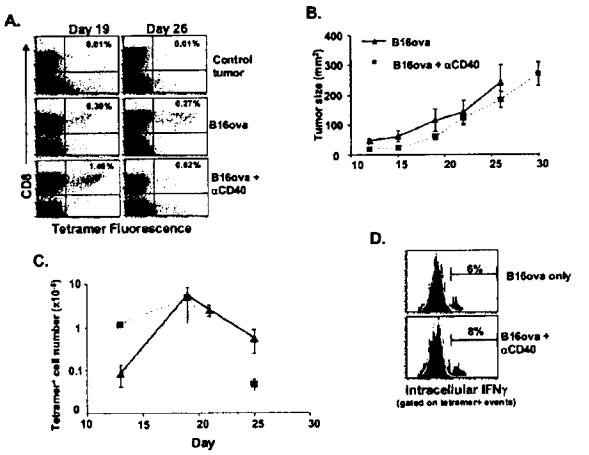

Fig. 2. Anti-CD40 treatment accelerates the deletion of tumor-specific T cells. Mice were challenged with 1×10^5 B16ova cells intradermally. Seven days later, when the tumor was palpable, mice were injected with 200 μg of either anti-CD40 or control antibody i.p. (*A*) At the times indicated, the tumor was removed, stained, and analyzed as described in the legend of Fig. 1. (*B* and *C*) Tumor-bearing mice were injected with 200 μg of anti-CD40 i.p. on day 7 after initial tumor challenge and every 7 days thereafter (i.e., days 14 and 21). The data were analyzed as described in the legend of Fig. 1*C*. (*D*) Fifteen days after initial tumor challenge and 8 days after anti-CD40 treatment, cells from the tumors of control and anti-CD40-treated mice were stained as described in *Materials and Methods* for intracellular IFNγ. The data shown (solid histograms) have been gated on all class II^-, $CD8^+$, $tetramer^+$ events. The background (open histogram) is from gating on all non-tetramer-staining $CD8^+$ T cells in the tumor. These results are representative of three separate experiments.

T Cell Deletion Is Prevented by Coimmunization with Anti-CD40 and Ovalbumin-Expressing VV. As mentioned, other groups have demonstrated that anti-CD40 treatment of tumor-bearing hosts significantly augments a tumor-specific T cell response when the host is coimmunized in some fashion with tumor antigen (21, 22). By using VVova, we determined whether tumor-antigen immunization in our model system would similarly prevent the deletion of tumor-specific T cells. B16ova tumor-bearing mice were injected on day 7 with VVova with or without the addition of anti-CD40 antibody treatment. Control VV-immunized mice showed little difference from nonimmunized (control) mice with respect to tumor growth and expansion of K^b/ova8-specific T cells (Fig. 3*A*). Interestingly, immunization of mice with control virus and anti-CD40 showed little difference from mice treated with anti-CD40 only, demonstrating that the inflammatory signals induced by the viral infection were not sufficient to prevent the anti-CD40-enhanced deletion of ova8-specific T cells. Immunization of a tumor-bearing host with VVova alone resulted in a significant expansion of ova8-specific T cells in both the spleen and tumor (Fig. 3 *A* and *C*). Initially the expansion of T cells in VVova-immunized hosts correlated with a dramatic

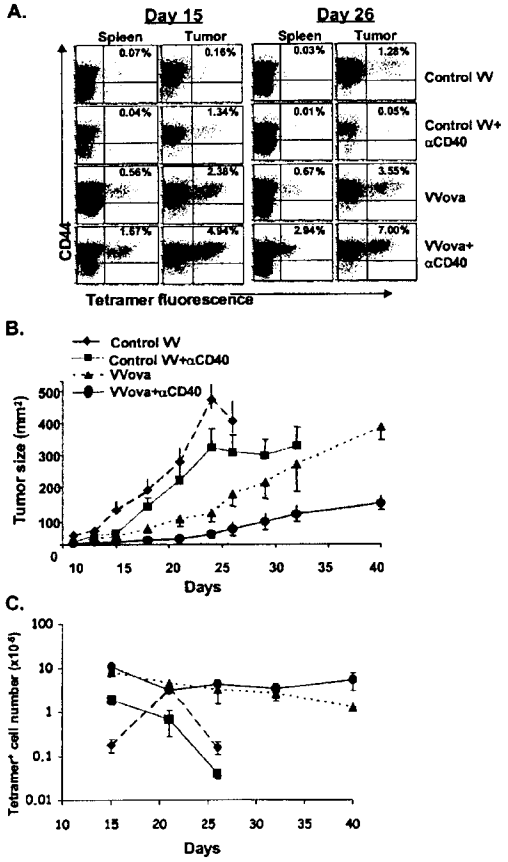

Fig. 3. Virus immunization with tumor antigen inhibits anti-CD40-mediated deletion of tumor-specific T cells and elicits effective tumor growth control. B6 mice were injected with 1×10^5 B16ova cells intradermally. Seven days later mice were injected with the indicated combinations of anti-CD40 (i.p.), the control virus VV-NP (i.v.), and VVova (i.v.). (*A*) Cells were isolated from spleen and tumor on the days given and stained and analyzed as in Fig. 1. (*B*) Tumor sizes were measured by caliper on four to six mice per group. The error bars represent the calculated standard error between at least four mice per group. (*C*) The total number of tetramer-staining cells was calculated as in Fig. 1. Error bars represent the standard error between four and six mice per time point per group. The results are representative of three separate experiments.

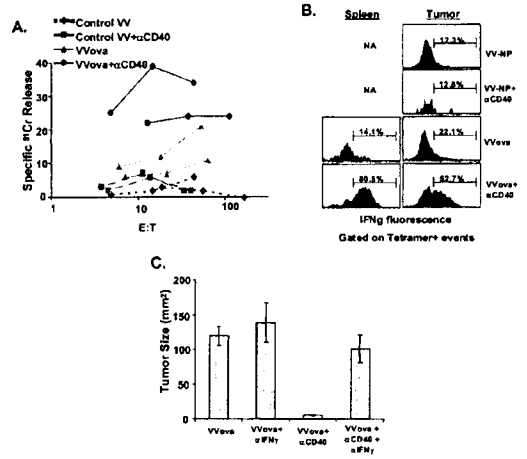

Fig. 4. VVova and anti-CD40 treatment results in enhanced lytic activity and IFNγ production from tumor-specific $CD8^+$ T cells. Mice were challenged with tumor and treated with VVova and/or anti-CD40 as in Fig. 3. (*A*) Twenty-five days after initial tumor challenge, spleens were removed from the different treated groups and restimulated with 5 μg/ml ovalbumin peptide *in vitro* for 5 days. The cells were washed, and ^{51}Cr release lytic assays were performed as described in *Materials and Methods*. Cells from two mice per treatment group are shown and are representative of two separate experiments performed. (*B*) Twenty-five days after initial tumor challenge, spleen and tumor tissue were removed from the different groups, and the cells were stained and analyzed for the expression of intracellular IFNγ in tetramer-staining cells as described for Fig. 2. The results are representative of four independent experiments. (*C*) Blocking IFNγ in VVova + anti-CD40-treated tumor-bearing mice eliminates the inhibition of tumor growth normally seen with this treatment. Tumor-bearing mice were treated with anti-CD40 and/or VVova as in Fig. 3. Seven days after VVova immunization, mice were injected with 3 mg of XMG1.2 (anti-IFNγ) or control anti-DR4 i.p. every 7 days. Twenty-five days after initial tumor challenge, tumors from two to three mice per group were measured by caliper. The error bars indicate the standard error of tumor size within a given treatment group. The data are representative of three experiments performed.

reduction in tumor size compared with control virus-immunized hosts (Fig. 3*B*). Despite this initial expansion of T cells, however, the ova8-specific T cell number gradually declined (Fig. 3 *A* and *C*; note the logarithmic scale), and the tumor resumed growth (Fig. 3*B*) until sacrifice of the host was necessary.

In contrast, the combination of anti-CD40 treatment and VVova immunization resulted in an increase in the percentage of tumor-antigen-specific T cells over VVova infection alone (Fig. 3*A*). Moreover, no discernible decrease in ova8-specific T cell number occurred over 5 weeks after immunization (Fig. 3*C*). Anti-CD40 treatment of VVova-immunized mice also resulted in long-term inhibition of tumor growth (Fig. 2*B*). Consistent with data from previous reports (21, 22), this treatment induced significant lytic activity (Fig. 4*A*) and IFNγ production by the tumor-specific T cells (Fig. 4*B*). The IFNγ production appeared to be the primary cause of the tumor growth inhibition observed, as demonstrated by *in vivo* anti-IFNγ antibody blocking experiments (Fig. 4*C*). Thus our model system is consistent with other experimental model systems (21, 22) as well as with observed clinical data on the progression of tumor-specific T cell responses in patients (12–16).

Antigenic Immunization or Inflammation Alone Is Not Sufficient to Rescue T Cell Function. Because it was apparent that anti-CD40 treatment during challenge with VVova was capable of rescuing both T cell survival and function (Fig. 3), we attempted to determine what cellular, inflammatory, and antigenic factors played a role in this rescue. $CD4^+$ T cells have been shown to be necessary for enhancing the survival and function of $CD8^+$ T cells and/or the host, particularly after vaccination in tumor model systems (39–41). However, CD4 cells did not appear to play a significant role in mediating the rescue seen by VVova and anti-CD40 treatment, as CD4 depletion of these tumor-bearing hosts demonstrated T cell function (Fig. 5*A*) and tumor growth control (data not shown) comparable to those of the non-CD4-depleted controls. It therefore appeared that some combination of antigenic and inflammatory stimuli may have acted directly upon the $CD8^+$ T cells. Neither a control virus infection alone, to provide non-antigen-specific inflammatory conditions as in Fig. 3, nor an increased antigen load alone, in the form of ovalbumin DNA immunization, was able to replicate the ability of VVova and anti-CD40 treatment to rescue T cell function (Fig. 5*B*). Only when tumor-bearing mice were treated with a combination of ovalbumin DNA immunization, control virus, and anti-CD40, a situation that essentially recapitulates VVova and anti-CD40 treatment, was T cell function rescued (Fig. 5*B*). Therefore, the accelerated tolerance and deletion brought on by anti-CD40 treatment alone appeared to be dominant in most cases, whereas preventing this deletion was accomplished solely

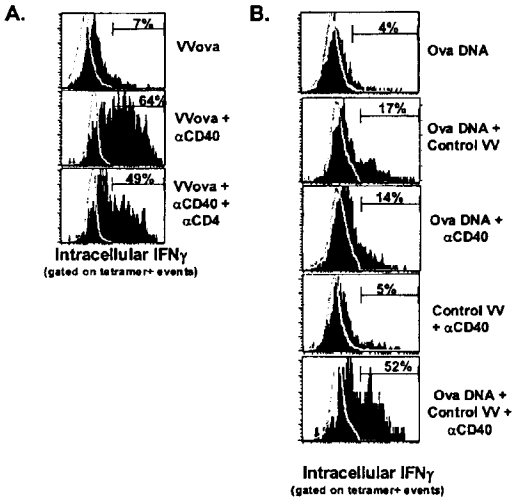

Fig. 5. Rescue of tumor-specific $CD8^+$ T cell function is $CD4^+$ T cell-independent and requires both antigenic immunization and virally mediated inflammation. (*A*) Mice were injected with 500 μg of anti-CD4 antibody (GK1.5) i.p. 1 day before B16ova tumor challenge and every 7 days thereafter. Mice were then immunized as in Fig. 3 with VVova and anti-CD40, and the IFNγ production of ova8-specific T cells in the tumor was assessed 25 days after initial tumor challenge as described in Fig. 2. Staining spleen cells with anti-CD4 (RM4-4) indicated that CD4 cells had been depleted (less than 0.2% staining; data not shown). Open histograms are of total $CD8^+$ T cells from within the tumor, and closed histograms are of $tetramer^+$, $CD8^+$ cells. (*B*) Seven days after B16ova challenge, mice were treated with combinations of control VV, intramuscular ovalbumin DNA immunization, and/or anti-CD40. Eighteen days later, tumor tissue was removed, and the IFNγ production of tetramer-staining $CD8^+$ T cells was assessed as in Fig. 2. The results are representative of two independent experiments.

by the expression of specific antigen in the context of a viral infection.

Discussion

It is well known that the activation state of the APC significantly affects the success of a T cell response. Our data suggest, however, that the success of a T cell response may depend upon more than simple activation of antigen-bearing APC. Stimulation of APC via CD40 has been shown to have a positive effect upon the activation of APC and, as a result, on the development and effector function of $CD8^+$ T cells in a variety of model systems (17–19). These effects on the generation of $CD8^+$ T cells have made anti-CD40 treatment seem particularly useful for tumor immunotherapy. Indeed, we (Fig. 2) and others (21, 22) have found that in the appropriate immunization context, agonistic CD40 antibody treatment can induce tumor regression and activation of tumor-specific T cells in tumor-bearing hosts. However, CD40 stimulation alone in B16ova-bearing mice unexpectedly resulted in a more rapid deletion of the tumor-specific T cells. This finding demonstrated that, rather than immunity, anti-CD40 stimulation in this context enhanced systemic tolerance of a tumor-specific antigen.

Whereas we have demonstrated this effect of CD40 treatment in a tumor model system, another group has documented the ability of an agonistic anti-CD40 antibody to mediate T cell deletion in an autoimmunity model system (23), suggesting that this effect of agonistic CD40-mediated stimulation is not limited to our experimental protocol. It is worth noting that we used a rather late time point of anti-CD40 treatment compared with that of other reports (21, 22), so possibly the anti-CD40 was administered too late to prevent the death of the tumor-reactive cells. However, the anti-CD40 in our protocol did initially increase the numbers of tumor-specific T cells for 7–10 days after treatment, so this seems unlikely.

It is not clear what signals are responsible, in the cascade of signals that a virus such as vaccinia induces, for synergizing with anti-CD40 to supply the T cells with the proper stimuli for long-term survival and IFNγ production. It is likely that proinflammatory cytokines such as IL-12 (42–44), tumor necrosis factor-γ (45–48), or the recently described IL-23 (49) may be involved, and they may not be elicited by anti-CD40 treatment alone. This hypothesis is supported by a recent report demonstrating that whereas anti-CD40 treatment of dendritic cells *in vitro* elicits IL-12 production, anti-CD40 treatment alone *in vivo* does not (50). However, it is unlikely that the expression of a single cytokine such as IL-12 will make up the entire difference between a functional or nonfunctional T cell response. For example, preliminary experiments using intramuscular IL-12 DNA injections to provide long-term IL-12 expression *in vivo* in tumor-bearing hosts has demonstrated that although this treatment does promote the survival and/or expansion of tumor-specific T cells, it has little effect on promoting their ability to produce IFNγ (R.K. and S.D., unpublished results). It is likely that an integration of the type, quantity, and timing of cytokine(s) expression during antigen presentation is necessary for inducing a long-lived, functional T cell response.

In conclusion, our results demonstrate that the activation of APC through CD40 alone is not sufficient to elicit a long-lived T cell response in a tumor-bearing host unless it is coupled to a tumor antigen/inflammatory/adjuvant immunization. Clinical trials evaluating anti-CD40 treatment have been proposed for a number of different cancer types. Our data suggest that caution must be used in treating these patients with anti-CD40 and that continuing research must focus on understanding what other stimuli act in concert with this APC stimulatory pathway to promote either tolerance or immunity.

We thank Fran Crawford, Chris Wagner, and Tracy DeBlieck for technical assistance and Brian Schaefer for assistance in reviewing the manuscript. This work was supported by a Postdoctoral Fellowship Grant from the Cancer Research Institute (R.M.K.) and U.S. Public Health Service Grants AI-17134, AI-18785, AI-22295, and CA86224-01.

1. thor Straten, P., Becker, J. C., Guldberg, P. & Zeuthen, J. (1999) *Cancer Immunol. Immunother.* **48,** 386–395.
2. thor Straten, P., Guldberg, P., Gronbaek, K., Hansen, M. R., Kirkin, A. F., Seremet, T., Zeuthen, J. & Becker, J. C. (1999) *J. Immunol.* **163,** 443–447.
3. Clark, W. H. (1991) *Br. J. Cancer.* **64,** 631–644.
4. Mihm, M. C., Jr., Clemente, C. G. & Cascinelli, N. (1996) *Lab. Invest.* **74,** 43–47.
5. Bartoli, C., Bono, A., Clemente, C., Del Prato, I. D., Zurrida, S. & Cascinelli, N. (1996) *Cancer (Philadelphia)* **77,** 888–892.
6. Clemente, C. G., Mihm, M. C., Jr., Bufalino, R., Zurrida, S., Collini, P. & Cascinelli, N. (1996) *Cancer (Philadelphia)* **77,** 1303–1310.
7. Halliday, G. M., Patel, A., Hunt, M. J., Tefany, F. J. & Barnetson, R. S. (1995) *World J. Surg.* **19,** 352–358.
8. Becker, J. C., Guldberg, P., Zeuthen, J., Brocker, E. B. & Straten, P. T. (1999) *J. Invest. Dermatol.* **113,** 1033–1038.
9. Ho, R. C. (1995) *Cancer (Philadelphia)* **75,** 735–741.
10. Kawakami, Y. & Rosenberg, S. A. (1996) *Immunol. Res.* **15,** 179–190.
11. Yee, C., Thompson, J. A., Roche, P., Byrd, D. R., Lee, P. P., Piepkorn, M., Kenyon, K., Davis, M. M., Riddell, S. R. & Greenberg, P. D. (2000) *J. Exp. Med.* **192,** 1637–1644.
12. Romero, P., Dunbar, P. R., Valmori, D., Pittet, M., Ogg, G. S., Rimoldi, D., Chen, J. L., Lienard, D., Cerottini, J. C. & Cerundolo, V. (1998) *J. Exp. Med.* **188,** 1641–1650.
13. Anichini, A., Molla, A., Mortarini, R., Tragni, G., Bersani, I., Di Nicola, M., Gianni, A. M., Pilotti, S., Dunbar, R., Cerundolo, V., *et al.* (1999) *J. Exp. Med.* **190,** 651–667.

14. Lee, P. P., Yee, C., Savage, P. A., Fong, L., Brockstedt, D., Weber, J. S., Johnson, D., Swetter, S., Thompson, J., Greenberg, P. D., *et al.* (1999) *Nat. Med.* **5,** 677–685.
15. Pittet, M. J., Valmori, D., Dunbar, P. R., Speiser, D. E., Lienard, D., Lejeune, F., Fleischhauer, K., Cerundolo, V., Cerottini, J. C. & Romero, P. (1999) *J. Exp. Med.* **190,** 705–715.
16. Yee, C., Savage, P. A., Lee, P. P., Davis, M. M. & Greenberg, P. D. (1999) *J. Immunol.* **162,** 2227–2234.
17. Schoenberger, S. P., Toes, R. E., van der Voort, E. I., Offringa, R. & Melief, C. J. (1998) *Nature (London)* **393,** 480–483.
18. Ridge, J. P., Di Rosa, F. & Matzinger, P. (1998) *Nature (London)* **393,** 474–478.
19. Bennett, S. R., Carbone, F. R., Karamalis, F., Flavell, R. A., Miller, J. F. & Heath, W. R. (1998) *Nature (London)* **393,** 478–480.
20. Schultze, J. L., Gribben, J. G. & Nadler, L. M. (1998) *Curr. Opin. Oncol.* **10,** 542–547.
21. Diehl, L., den Boer, A. T., Schoenberger, S. P., van der Voort, E. I., Schumacher, T. N., Melief, C. J., Offringa, R. & Toes, R. E. (1999) *Nat. Med.* **5,** 774–779.
22. Sotomayor, E. M., Borrello, I., Tubb, E., Rattis, F. M., Bien, H., Lu, Z., Fein, S., Schoenberger, S. & Levitsky, H. I. (1999) *Nat. Med.* **5,** 780–787.
23. Mauri, C., Mars, L. T. & Londei, M. (2000) *Nat. Med.* **6,** 673–679.
24. Mitchell, T., Kappler, J. & Marrack, P. (1999) *J. Immunol.* **162,** 4527–4535.
25. Restifo, N. P., Bacik, I., Irvine, K. R., Yewdell, J. W., McCabe, B. J., Anderson, R. W., Eisenlohr, L. C., Rosenberg, S. A. & Bennink, J. R. (1995) *J. Immunol.* **154,** 4414–4422.
26. Liu, Y., Liggitt, D., Zhong, W., Tu, G., Gaensler, K. & Debs, R. (1995) *J. Biol. Chem.* **270,** 24864–24870.
27. Heath, A. W., Wu, W. W. & Howard, M. C. (1994) *Eur. J. Immunol.* **24,** 1828–1834.
28. Mielke, M. E., Ehlers, S. & Hahn, H. (1988) *Infect. Immun.* **56,** 1920–1925.
29. Smith, D., Hansch, H., Bancroft, G. & Ehlers, S. (1997) *Immunology* **92,** 413–421.
30. Appelberg, R., Castro, A. G., Pedrosa, J., Silva, R. A., Orme, I. M. & Minoprio, P. (1994) *Infect. Immun.* **62,** 3962–3971.
31. Crawford, F., Kozono, H., White, J., Marrack, P. & Kappler, J. (1998) *Immunity* **8,** 675–682.
32. Kedl, R. M., Rees, W. A., Hildeman, D. A., Schaefer, B., Mitchell, T., Kappler, J. & Marrack, P. (2000) *J. Exp. Med.* **192,** 1105–1114.
33. Kedl, R. M. & Mescher, M. F. (1997) *J. Immunol.* **159,** 650–663.
34. Sahin, U., Tureci, O. & Pfreundschuh, M. (1997) *Curr. Opin. Immunol.* **9,** 709–716.
35. Tureci, O., Sahin, U. & Pfreundschuh, M. (1997) *Mol. Med. Today* **3,** 342–349.
36. Pinilla-Ibarz, J., Cathcart, K. & Scheinberg, D. A. (2000) *Blood Rev.* **14,** 111–120.
37. Offringa, R., Vierboom, M. P., van der Burg, S. H., Erdile, L. & Melief, C. J. (2000) *Ann. N.Y. Acad. Sci.* **910,** 223–236.
38. Abrams, S. I., Hand, P. H., Tsang, K. Y. & Schlom, J. (1996) *Semin. Oncol.* **23,** 118–134.
39. Hung, K., Hayashi, R., Lafond-Walker, A., Lowenstein, C., Pardoll, D. & Levitsky, H. (1998) *J. Exp. Med.* **188,** 2357–2368.
40. Overwijk, W. W., Lee, D. S., Surman, D. R., Irvine, K. R., Touloukian, C. E., Chan, C. C., Carroll, M. W., Moss, B., Rosenberg, S. A. & Restifo, N. P. (1999) *Proc. Natl. Acad. Sci. USA* **96,** 2982–2987.
41. Toes, R. E., Ossendorp, F., Offringa, R. & Melief, C. J. (1999) *J. Exp. Med.* **189,** 753–756.
42. Schmidt, C. S. & Mescher, M. F. (1999) *J. Immunol.* **163,** 2561–2567.
43. Parmiani, G., Rivoltini, L., Andreola, G. & Carrabba, M. (2000) *Immunol. Lett.* **74,** 41–44.
44. Becker, J. C. & Brocker, E. B. (1994) *Exp. Dermatol.* **3,** 283–289.
45. Pape, K. A., Kearney, E. R., Khoruts, A., Mondino, A., Merica, R., Chen, Z. M., Ingulli, E., White, J., Johnson, J. G. & Jenkins, M. K. (1997) *Immunol. Rev.* **156,** 67–78.
46. Pape, K. A., Khoruts, A., Mondino, A. & Jenkins, M. K. (1997) *J. Immunol.* **159,** 591–598.
47. Vella, A. T., McCormack, J. E., Linsley, P. S., Kappler, J. W. & Marrack, P. (1995) *Immunity* **2,** 261–270.
48. Gorelik, L., Bar-Dagan, Y. & Mokyr, M. B. (1996) *J. Immunol.* **156,** 4298–4308.
49. Oppmann, B., Lesley, R., Blom, B., Timans, J. C., Xu, Y., Hunte, B., Vega, F., Yu, N., Wang, J., Singh, K., *et al.* (2000) *Immunity* **13,** 715–725.
50. Schulz, O., Edwards, D. A., Schito, M., Aliberti, J., Manickasingham, S., Sher, A. & Reise, S. (2000) *Immunity* **13,** 453–462.

Microbial Recognition Via Toll-Like Receptor-Dependent and -Independent Pathways Determines the Cytokine Response of Murine Dendritic Cell Subsets to CD40 Triggering[1]

Alexander D. Edwards,* Shivanthi P. Manickasingham,* Roman Spörri,* Sandra S. Diebold,* Oliver Schulz,* Alan Sher,† Tsuneyasu Kaisho,‡§ Shizuo Akira,‡ and Caetano Reis e Sousa[2]*

Dendritic cells (DC) can produce Th-polarizing cytokines and direct the class of the adaptive immune response. Microbial stimuli, cytokines, chemokines, and T cell-derived signals all have been shown to trigger cytokine synthesis by DC, but it remains unclear whether these signals are functionally equivalent and whether they determine the nature of the cytokine produced or simply initiate a preprogrammed pattern of cytokine production, which may be DC subtype specific. Here, we demonstrate that microbial and T cell-derived stimuli can synergize to induce production of high levels of IL-12 p70 or IL-10 by individual murine DC subsets but that the choice of cytokine is dictated by the microbial pattern recognition receptor engaged. We show that bacterial components such as CpG-containing DNA or extracts from *Mycobacterium tuberculosis* predispose CD8α^+ and CD8α^-CD4$^-$ DC to make IL-12 p70. In contrast, exposure of CD8α^+, CD4$^+$ and CD8α^-CD4$^-$ DC to heat-killed yeasts leads to production of IL-10. In both cases, secretion of high levels of cytokine requires a second signal from T cells, which can be replaced by CD40 ligand. Consistent with their differential effects on cytokine production, extracts from *M. tuberculosis* promote IL-12 production primarily via Toll-like receptor 2 and an MyD88-dependent pathway, whereas heat-killed yeasts activate DC via a Toll-like receptor 2-, MyD88-, and Toll/IL-1R domain containing protein-independent pathway. These results show that T cell feedback amplifies innate signals for cytokine production by DC and suggest that pattern recognition rather than ontogeny determines the production of cytokines by individual DC subsets. *The Journal of Immunology,* 2002, 169: 3652–3660.

Induction of an appropriate class of adaptive immune response is essential for protection from many infections and APCs play a critical role in this process. APC function is largely regulated by direct recognition of pathogens or indirect sensing of correlates of infection such as cell damage or inflammation (1). Direct recognition involves APC-expressed pattern recognition receptors (PRRs),[3] such as members of the Toll-like receptor (TLR) family (2, 3). Many of the microbial ligands for TLRs have remarkably similar effects on APC, generally characterized by the induction of proinflammatory cytokines and IL-12 (2, 3). This suggests that TLR recognition may be primarily involved in the generation of inflammatory immune responses and that other classes of PRR involved in the generation of noninflammatory adaptive immunity await identification. This is further supported by the observation that mice deficient for MyD88, a critical adapter in TLR signaling for cytokine production, mount defective Th1-type responses but have normal type 2 immune responses (4).

Dendritic cells (DC) are the major APC in the initiation of adaptive immune responses. DC can produce Th-polarizing cytokines, but it is still unclear how cytokine production by DC is regulated and matched to pathogen recognition (1, 5, 6). Given the existence of multiple DC subsets, it has been argued that some may be specialized to produce IL-12 and drive Th1 responses whereas others induce Th2 immunity. In this model, such DC1 and DC2 subsets possess mutually exclusive sets of PRR and respond to distinct groups of pathogens (7). This has been shown for human monocyte-derived vs plasmacytoid DC (8–10), although at present no publications have addressed whether mouse DC subsets also differ in PRR expression. An alternative model is that individual DC subsets are not necessarily preexisting DC1 or DC2 but respond in a flexible manner to distinct pathogens and make distinct cytokines depending on which PRR are triggered (1, 6, 11).

We have previously concentrated on the mechanisms leading to IL-12 production by DC (12, 13). Here, we focus on the roles of microbial stimulation and T cell feedback on production of two opposing cytokines, IL-12 and IL-10, by distinct DC subsets. We demonstrate that production of high levels of either IL-12 or IL-10 by murine splenic DC requires two signals, one from a microbe and the other from T cells. Microbial stimuli can act directly on DC via TLR and non-TLR PRRs, whereas T cell signals can be replaced by CD40 ligand (CD40L), but the microbial stimulus and not the T cell signal dictates which cytokine is produced. Importantly, we demonstrate that differential IL-10 and IL-12 production by DC is not attributable to the activity of specialized IL-12- or IL-10-producing DC subsets. Our results support the notion that DC subsets possess significant plasticity in their cytokine response and show that T cell feedback signals amplify a program established by pattern recognition.

*Immunobiology Laboratory, Cancer Research U.K., London Research Institute, London, United Kingdom; †Immunobiology Section, Laboratory of Parasitic Diseases, National Institute of Allergy and Infectious Diseases, National Institutes of Health, Bethesda, MD 20892; ‡Department of Host Defense, Research Institute for Microbial Diseases, Osaka University, Suita City, Osaka, Japan; and §RIKEN Research Center for Allergy and Immunology, Yokohama City, Japan

Received for publication April 18, 2002. Accepted for publication July 26, 2002.

The costs of publication of this article were defrayed in part by the payment of page charges. This article must therefore be hereby marked *advertisement* in accordance with 18 U.S.C. Section 1734 solely to indicate this fact.

[1] This work was supported by Cancer Research U.K.

[2] Address correspondence and reprint requests to Dr. Caetano Reis e Sousa, Immunobiology Laboratory, Cancer Research U.K., London Research Institute, Lincoln's Inn Fields Laboratories, 44 Lincoln's Inn Fields, London WC2A 3PX, U.K. E-mail address: caetano@cancer.org.uk

[3] Abbreviations used in this paper: PRR, pattern recognition receptor; PPD, purified protein derivative of *Mycobacterium tuberculosis*; DC, dendritic cells; STAg, soluble tachyzoite Ag; TLR, Toll-like receptor; CD40L, CD40 ligand; DN, double negative; TIRAP, Toll/IL-1R domain containing protein.

0022-1767/02/$02.00

Materials and Methods

Animals

Male and female 6- to 10-wk-old mice were obtained from Charles River (Margate, U.K.), Harlan U.K. (Bicester, Oxon, U.K.) or from the breeding unit of Cancer Research U.K. (Clare Hall, South Mimms, U.K.). C57BL/6 (B6), B10.BR, BALB/c, C3H/HeN, and C3H/HeJ mice were used interchangeably, after determining that the responses studied were strain independent (not shown). The strain used for each experiment is indicated in each figure legend. DO11.10 mice (14) on a BALB/c-*scid* background were bred at Cancer Research U.K.

To analyze DC genetically deficient for MyD88 or TLR2, bone marrow chimeras were made by reconstituting lethally irradiated CD45.1 B6.SJL mice with congenic bone marrow from CD45.2 TLR2$^{-/-}$ or MyD88$^{-/-}$ mice on a C57BL/6 × 129 background (15, 16). Control chimeras were made with bone marrow taken from control C57BL/6 mice. DC were purified from the spleens of recipients 5–8 wk after reconstitution (17).

Reagents

Soluble tachyzoite Ag (STAg) was prepared from tachyzoites of the RH 88 strain of *Toxoplasma gondii* (12). Zymosan (Sigma, Poole, U.K.) was boiled for 30 min and washed twice in PBS. Laboratory cultures of *Saccharomyces cerevisiae* (strain K700) and *Schizosaccharomyces pombe* (strain 513) were autoclaved and washed twice in PBS. *Escherichia coli* LPS was a gift from Dr. S. Vogel (Uniformed Services University of the Health Sciences, Bethesda, MD). CpG-containing DNA was a phosphorothioate-linked oligonucleotide with the sequence TCC ATG ACG TTC CTG ATG CT (18). Purified protein derivative (PPD) of *Mycobacterium tuberculosis* was obtained from Statens Serum Institut (Copenhagen, Denmark). All microbial stimuli were used at saturation unless otherwise indicated. The OVA peptide 323–339 (OVA peptide; ISQAVHAAH AEINEAGR), Toll/IL-1R domain containing protein TIRAP peptide, and control peptide (19) were made by the Cancer Research U.K. peptide synthesis service. Endotoxin levels in all reagents were significantly lower than the minimum required for DC activation.

Cells

The cell lines 3T3-CD40L and 3T3-SAMEN (control) were a gift from Dr. P. Hwu (National Cancer Institute, Bethesda, MD) and were derived from NIH 3T3 by stable transduction with murine CD40L or empty vector.

Spleen cell suspensions were prepared by Liberase CI (Roche Diagnostics, Lewes, U.K.) and Dnase I digestion (13). DC-enriched fractions were prepared by labeling splenocytes with anti-CD11c MACS beads (Miltenyi, Bisley, U.K.) for 10 min at 4°C, followed by washing and positive selection using LS magnetic columns (Miltenyi Biotec), as described (13). Resulting preparations contained 70–95% CD11c^{bright} DC. To obtain DC subsets, CD11c-enriched preparations were further stained with PE-anti-CD11c, FITC-anti-CD4, and TriColor-anti-CD8α (Caltag, Burlingame, CA) and sorted on a MoFlo cytometer (Cytomation, Fort Collins, CO). To obtain pure CD45.2$^+$ DC from bone marrow chimeras, CD11c-enriched splenocytes were stained with PE-anti-CD11c and FITC-anti-CD45.1 and sorted for CD11c^{bright}CD45.1$^-$ cells, as described (17).

T cells were purified from the lymph nodes of DO-11.10/*scid* mice by negative selection of contaminating cells.

DC cultures and cytokine assays

For in vitro stimulation, MACS-enriched or FACS-sorted DC were cultured in 96-well flat-bottom plates alone or on a monolayer of CD40L-expressing or control fibroblasts. Cultures were incubated in the presence or absence of different stimuli in RPMI 1640 supplemented with 10% FCS, penicillin (100 U/ml), streptomycin (100 μg/ml), glutamine (2 mM), and 2-ME (5 × 10^{-7} M). Culture supernatants were collected at 18–24 h and assayed for the presence of cytokines by sandwich ELISA. Ab pairs were (capture, detection): 9A5, C17.8 (biotinylated) for IL-12 p70; JES5-2A5, SXC-1 (biotinylated) for IL-10. Cells were recovered in PBS plus 5 mM EDTA for FACS analysis.

Antibody staining

For analysis of DC maturation, cells were washed and stained in PBS containing 5 mM EDTA, 1% FCS, and 0.02% sodium azide (FACS wash). Cells were stained with FITC-conjugated anti-CD40 or anti-CD86 plus PE-conjugated anti-CD11c in the presence of 5 μg/ml anti-FcγRII/III. In some experiments, biotinylated anti-CD40 was used, followed by streptavidin conjugated to an appropriate fluorophore. The mAbs used were: HL3 and 16-10A1, hamster IgG mAbs against CD11c and CD80, respectively; NLDC-145, RM4-5, 53-6.7, 3/23, and GL1, rat IgG2a mAbs against DEC-205, CD4, CD8α, CD40, and CD86, respectively; JES5-2A5, rat IgG1 neutralizing mAb against IL-10; A20, mouse IgG2a mAb against CD45.1. All mAbs were from BD PharMingen (San Diego, CA) or produced in house.

Single cell staining for IL-10 was performed using the mouse IL-10 secretion assay kit (Miltenyi Biotec). CD11c-enriched spleen cells were divided into two fractions. One half was stained with FITC-anti-CD11c and kept live; the remainder was stained with TriColor-anti-CD11c and then fixed by treating with 1% paraformaldehyde in PBS for 10 min at room temperature, followed by quenching with 1 mM glycine in PBS. A 1:1 mixture of live and fixed cells in medium was then cultured with control fibroblasts or with zymosan (50 μg/ml) plus CD40L-expressing fibroblasts for 4 h in 24-well plates. Cells were harvested and coated with anti-IL-10 capture reagent, then recultured at 2.5 × 10^5 DC/well in six-well plates with fresh fibroblasts ± zymosan stimulation as above. After 60–100 min, cells were harvested once more, washed in PBS containing 2 mM EDTA plus 1% FCS, and stained with PE-conjugated anti-IL-10 (Miltenyi Biotec) and APC-anti-CD8α.

Intracellular staining for IL-12 was performed as described (13) using anti-IL-12 p40 (clone C17.15.10), anti-IL-12 p70 (clone 9A5) or a mixture of isotype-matched RtIgG2a and RtIgG2b irrelevant control Abs, followed by biotinylated mouse anti-rat (Jackson ImmunoResearch Laboratories, West Grove, PA) and PE- or APC-streptavidin (BD PharMingen).

Cell acquisition was performed on a FACSCalibur flow cytometer (BD Biosciences, San Jose, CA), and data were analyzed using FlowJo software (Tree Star, San Carlos, CA).

Results

Activation of DC by microbial stimuli

Several microbial stimuli were tested for their ability to act as activators of primary mouse DC in vitro. DC-enriched spleen cells were plated with or without test stimuli, and expression of the activation markers CD40, CD80, and CD86 was measured on CD11c^{bright} cells after overnight culture. Culture alone was sufficient to induce up-regulation of CD40, CD80, and CD86 (not shown). Nevertheless, a wide range of products from bacteria, fungi, or protozoa were able to increase CD40, CD80, and CD86 expression further (Fig. 1). They included mycobacterial PPD, heat-inactivated yeasts (*Saccharomyces cerevisiae, S. pombe*) and zymosan (yeast cell walls), as well as established murine DC activators such as STAg (12) and CpG-containing DNA oligonucleotides (CpG DNA) (Fig. 1). All test agents induced CD40, CD80, and CD86 up-regulation to a similar extent in DC from control C3H/HeN- and TLR4-deficient C3H/HeJ mice, demonstrating that they did not contain endotoxin (data not shown).

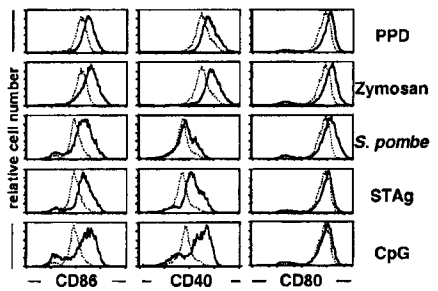

FIGURE 1. DC activation by different microbial stimuli. CD11c-enriched B6 or BALB/c spleen cells were cultured overnight with the indicated agents and then stained for CD11c, CD40, CD80, or CD86 and analyzed by flow cytometry. Histograms show gated CD11c^{bright} cells. Increased CD40, CD80, and CD86 expression was seen on DC cultured with test stimuli (solid lines) vs medium alone (dotted line). Doses: CpG DNA, 1.5 μg/ml; STAg, 5 μg/ml; *S. pombe*, 2 × 10^5 particles/well; zymosan, 50 μg/ml; PPD, 10 μg/ml. Data shown are from multiple experiments. Similar results were seen in more than four experiments performed with each stimulus in various mouse strains.

Microbial stimuli dictate the cytokine response of DC to CD40 triggering

STAg and CpG DNA by themselves elicited modest levels of IL-12 p70 (<1 ng/ml) but no IL-10 from DC-enriched splenocyte populations (Fig. 2*A*). However, little accumulation of IL-12 p70 or IL-10 in culture supernatants was seen in response to any of the other stimuli (Fig. 2*A*, *top*). Because IL-12 p70 production by DC is markedly dependent on a second T cell-derived signal (13), we assessed the effect of CD40 coligation on the cytokine response. Culturing DC-enriched splenocytes on a monolayer of CD40L-expressing fibroblasts was sufficient to induce low levels of IL-12 p70 and IL-10 (Fig. 2*A*). Addition of STAg and CpG DNA caused a significant increase in IL-12 p70 but not in IL-10 levels (Fig. 2*A*, *bottom*). Similar results were obtained with PPD, although IL-12 p70 production in response to PPD was consistently lower than to STAg or CpG DNA (Fig. 2*A*, *bottom*). In contrast, the combination of zymosan or *S. pombe* together with CD40L led to an increase primarily in IL-10 (Fig. 2*A*, *bottom*). Similar induction of IL-10 was seen with a pathogenic yeast, *Candida albicans*, in combination with CD40L (data not shown). Neutralizing Ab to IL-10 did not increase the levels of IL-12 p70 in response to CD40L plus yeasts or zymosan (see below). When IL-12-promoting stimuli (e.g., CpG DNA) and IL-10-promoting zymosan were combined in the presence of CD40L, there was a significant decrease in IL-12 production (Fig. 2*B*), consistent with the known ability of IL-10 to suppress IL-12 synthesis, and a slight decrease in IL-10 production (Fig. 2*B*). These results demonstrate that CD40 triggering in DC does not inevitably lead to IL-12 synthesis but can reveal production of IL-10.

To examine whether physiological levels of T cell feedback signals could substitute for CD40L-expressing fibroblasts, naive TCR transgenic T cells were cultured with DC-enriched populations ± Ag in the presence of IL-12- or IL-10-promoting stimuli. In the absence of microbial stimuli, IL-12 p70 or IL-10 levels were low or undetectable even after T cell activation by Ag (Fig. 2*C*). Microbial stimulation in the absence of Ag elicited only low levels of IL-12 p70 or IL-10. However, in the presence of OVA peptide, the yeasts triggered accumulation of IL-10 but not of IL-12 p70, whereas the opposite was seen with PPD and STAg (Fig. 2*C*). As expected, cytokine accumulation in supernatants was Ag dose dependent (Fig. 2*C*). These results using naive T cells agree with the data obtained with CD40L-expressing fibroblasts. However, anti-CD40L did not entirely block the effect of T cells in this system (R. Spörri and C. Reis e Sousa, unpublished observations), implying that other molecules expressed by naive T cells after activation can also provide feedback signals to amplify DC cytokine production. Inclusion of the microbial stimuli did not affect subsequent T cell proliferation although it had marked effects on Th differentiation (S. P. Manickasingham, A. D. Edwards, and C. Reis e Sousa, manuscript in preparation).

Direct recognition of microbes by DC via TLR-dependent and -independent pathways

The use of partially purified DC preparations in the experiments described above raised the possibility that the measured cytokines were produced by contaminating leukocytes or indirectly by DC in response to signals made by the contaminating cells. To address this issue, CD11c^{bright} pure DC were sorted by FACS and stimulated with microbial products in the presence of CD40L-expressing fibroblasts. Purified DC responded to CpG DNA and PPD by producing IL-12 p70 but only small amounts of IL-10, whereas the converse was seen with zymosan (Fig. 3, *A* and *B*). These results

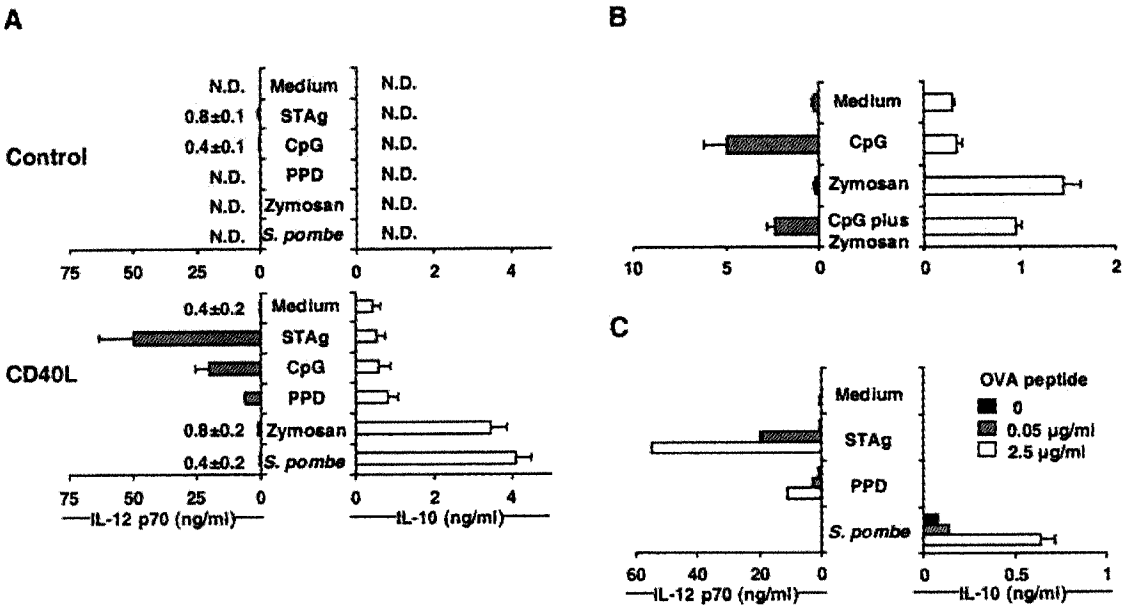

FIGURE 2. CD40L or T cell feedback leads to production of either IL-12 p70 or IL-10 by DC following microbial activation. *A*, CD11c-enriched BALB/c spleen cells (70% DC; 4 × 10^4/well) were cultured overnight on a monolayer of CD40L-expressing or control fibroblasts together with DC-activating agents. Doses: STAg, 5 μg/ml; CpG DNA, 1 μg/ml; PPD, 10 μg/ml; zymosan, 10 μg/ml; *S. pombe*, 10^5 particles/well. *B*, DC as in *A* were cultured on a monolayer of CD40L-expressing fibroblasts together with CpG DNA (1 μg/ml) and/or zymosan (10 μg/ml). *C*, DC as in *A* were cultured with DO11.10 naive T cells (2 × 10^5 total cells/well; DC:T cell ratio, 1:1) in the presence or absence of STAg (1 μg/ml), PPD (5 μg/ml), or *S. pombe* (8 × 10^4 particles/well). OVA peptide was added as indicated, and the cells were cultured overnight. IL-12 p70 and IL-10 in culture supernatants were measured by ELISA. Histograms represent the mean of triplicate wells; all error bars are shown and represent 1 SD from the mean. N.D. (not detectable) indicates that the value was below the detection limit of the ELISA (<100 pg/ml IL-12 p70, <100 pg/ml IL-10). Data are representative of more than four experiments for each stimulus with CD40L-expressing fibroblasts and of three experiments with T cell feedback and with mixtures of stimuli.

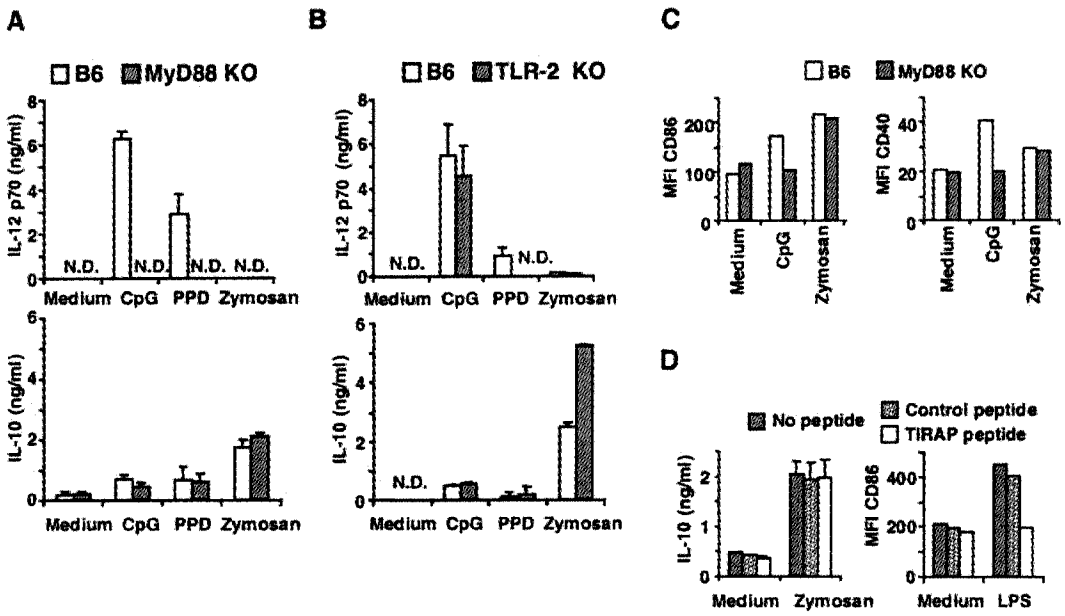

FIGURE 3. TLR2 and MyD88 are required for the IL-12 p70 response to PPD, but the response to zymosan is TLR independent. $CD11c^{bright}$ $CD45.1^-$ donor-derived spleen DC were purified from radiation chimeras of B6.SJL ($CD45.1^+$) mice reconstituted with bone marrow from $CD45.2^+$ $MyD88^{-/-}$, $TLR2^{-/-}$, or control B6 mice. *A*, Purified $MyD88^{-/-}$ or control DC were cultured overnight at 3×10^4/well with the indicated stimuli on a monolayer of CD40L-expressing fibroblasts. Cytokine levels in supernatants were measured by ELISA after 24 h. *B*, Similar to *A* but comparing $TLR2^{-/-}$ vs B6 DC. Doses: CpG, 1 μg/ml; PPD, 20 μg/ml; zymosan, 10 μg/ml. *C*, CD40 and CD86 expression on $MyD88^{-/-}$ or control DC was analyzed by flow cytometry after overnight culture with the indicated stimuli. *D*, CD11c-enriched BALB/c splenocytes (90% DC; 10^5/well) were pretreated for 1 h with 10 μM TIRAP or control peptide. Cells ± peptides were stimulated overnight with zymosan (10 μg/ml) on CD40L-expressing fibroblasts and analyzed for IL-10 production (*left*). As a positive control, the same cells ± peptides were stimulated overnight with LPS (0.5 ng/ml), and CD86 expression on DC was analyzed by flow cytometry (*right*). MFI, Median fluorescence intensity of gated $CD11c^{bright}$ cells. Histograms represent the mean of triplicate wells; all error bars are shown and represent 1 SD from the mean. N.D., not detectable. Data are representative of two experiments with $MyD88^{-/-}$ DC, three experiments with $TLR2^{-/-}$ DC, and two experiments with TIRAP-peptide. KO, Knockout.

demonstrate that DC themselves can directly recognize and discriminate among microbial stimuli and can produce either IL-10 or IL-12 in response to the appropriate combination of signals.

MyD88 is a critical adapter for the transduction of signals from many TLRs, including TLR9 and TLR2, which have been implicated in innate recognition of CpG DNA and zymosan, respectively (20–22). We examined whether MyD88 was required for the response to CpG DNA, PPD, or zymosan. MyD88-deficient DC were purified from the spleens of mice reconstituted with bone marrow from $MyD88^{-/-}$ mice and were compared with DC purified from control chimeras (see *Materials and Methods*). As shown in Fig. 3*A*, $MyD88^{-/-}$ DC did not make IL-12 p70 in response to CpG DNA and PPD plus CD40L. In contrast, MyD88 deficiency did not affect the IL-10 response to zymosan plus CD40L (Fig. 3*A*). Likewise, the up-regulation of CD40 or CD86 in response to zymosan alone was MyD88 independent although, as expected, this adapter was critical for the response to CpG DNA (Fig. 3*C*). A similar comparison revealed that TLR2 was also not necessary for IL-10 production in response to zymosan plus CD40L (Fig. 3*B*). However, $TLR2^{-/-}$ DC made significantly lower levels of IL-12 p70 in response to PPD plus CD40L (Fig. 3*B*). This was not due to a general defect in the ability of such DC to make IL-12 p70 because the same cells mounted a normal response to CpG DNA (Fig. 3*B*).

An additional adapter in TLR signaling, TIRAP/MAL, has been described (19, 23). As expected, a TIRAP-inhibitory peptide but not a control peptide containing the reversed TIRAP sequence (19) abrogated the LPS-induced up-regulation of CD86 by DC (Fig. 3*D*). However, the TIRAP-inhibitory peptide did not affect yeast conditioning for IL-10 production (Fig. 3*D*). These results demonstrate that TLR2 and MyD88 signaling mediate PPD conditioning of DC for CD40-triggered IL-12 p70 production but suggest that TLR signaling is not involved in conditioning by yeasts for IL-10 production.

Plasticity of DC subsets

Spleen DC contain several subsets, which may possess distinct abilities to produce cytokines (24, 25). We addressed the ability of three of these subsets to make IL-10 vs IL-12. Homogeneous populations of $CD11c^{bright}CD8\alpha^+$, $CD4^+$, and $CD8\alpha^-CD4^-$ (double-negative; DN) DC were isolated by cell sorting (Fig. 4*A*). In the presence of control fibroblasts, all DC subsets produced only negligible amounts of IL-12 p70 or IL-10 (not shown). Coculture with CD40L-expressing fibroblasts alone was sufficient to increase the basal production of IL-12 p70 by $CD8\alpha^+$ DC and of IL-10 by all subsets (Fig. 4*B*). Nonetheless, basal cytokine levels were markedly altered by addition of a microbial costimulus. $CD8\alpha^+$ and DN DC produced primarily IL-12 p70 in response to CpG DNA, STAg, or PPD in combination with CD40L although DN DC produced less IL-12 p70 than $CD8\alpha^+$ DC (Fig. 4*B*). Both $CD4^-$ subsets also increased production of IL-10 in response to the combination of zymosan or *S. pombe* plus CD40L (Fig. 4*B*). This was less obvious for $CD8\alpha^+$ DC, which displayed the highest level of basal IL-10 (and IL-12 p70) production in response to CD40L alone but remained statistically significant ($p < 0.01$) (Fig. 4*B*). Zymosan also triggered a small amount of IL-12 p70 production by $CD8\alpha^+$ DC in some experiments (Fig. 4*B*). Interestingly, $CD4^+$ DC failed to make IL-12 p70 in response to any stimulus although they responded to yeast or zymosan plus CD40L by producing high levels of IL-10 (Fig. 4*B*).

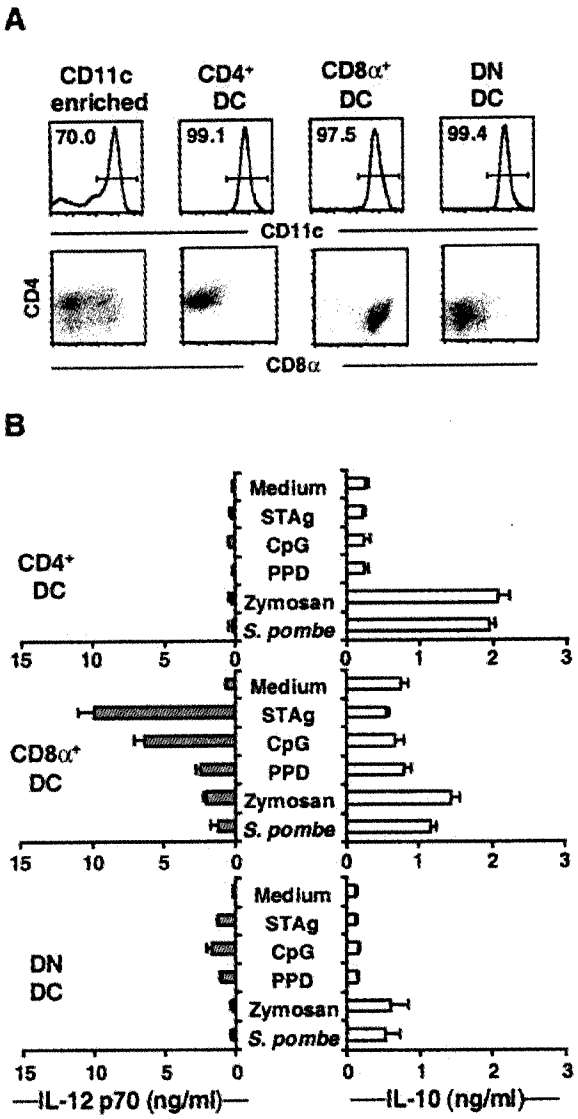

FIGURE 4. Differential cytokine production by individual DC subsets. *A*, FACS analysis of sorted B6 DC subsets. Histograms show the CD11c profile of each population; numbers show the percentage of events corresponding to $CD11c^{bright}$ cells. Dot plots show CD4 vs CD8α profiles of $CD11c^{bright}$ cells, gated as indicated on the histograms. *B*, DC subsets sorted as in *A* were plated at 4×10^4 cells/well on a monolayer of CD40L-expressing fibroblasts with the indicated microbial stimuli. After overnight incubation, IL-10 and IL-12 p70 levels in supernatants were measured by ELISA. Doses: CpG DNA, 1 μg/ml; STAg, 5 μg/ml; PPD, 10 μg/ml; zymosan, 10 μg/ml; *S. pombe*, 5×10^4 particles/well. Histograms represent the mean of triplicate wells; all error bars are shown and represent 1 SD from the mean. Data are representative of seven independent experiments.

IL-10 secretion by $CD8\alpha^+$ DC has not previously been reported. To assess the frequency of IL-10-producing $CD8\alpha^+$ DC, we used a staining method involving IL-10 capture by cell surface-bound Abs followed by detection with a second anti-IL-10 Ab conjugated to a fluorophore (see *Materials and Methods*). To confirm that the staining method identified only those cells producing IL-10 and not $CD8\alpha^+$ DC that passively captured cytokine secreted by neighboring cells, the experiments were conducted with a mixture of live and fixed DC; 20–30% of live $CD8\alpha^+$ DC stained for IL-10 after zymosan plus CD40L stimulation, whereas fixed $CD8\alpha^+$ DC in the same cultures did not stain for the cytokine (Fig. 5*A*). However, both live and fixed cells could be stained to the same extent if incubated with exogenous IL-10 (Fig. 5*A*). In all cases, there was no staining above background when the capture reagent was omitted (not shown). These controls demonstrate that IL-10 staining in live cells accurately reflects cytokine production by individual $CD8\alpha^+$ DC and, under the conditions used here, is not marred by paracrine effects. To determine the frequency of $CD8\alpha^+$ DC producing IL-12, intracellular staining was conducted for the p40 subunit after stimulation with CpG plus CD40L. Compared with baseline staining with an isotype-matched control Ab, essentially all $CD8\alpha^+$ DC stained for IL-12 p40 (Fig. 5*B*). In other experiments, ~15% of $CD8\alpha^+$ DC could also be stained for the bioactive heterodimer, IL-12 p70 (Fig. 5*B*).

Unlike $CD8\alpha^+$ DC, $CD4^+$ DC were unable to produce IL-12 p70 (Fig. 4*B*). To determine whether this was due to autocrine effects of IL-10, DC subsets were cultured on CD40L-expressing fibroblasts in the presence of neutralizing anti-IL-10 Ab. Anti-IL-10 led to an increase in IL-12 p70 production by both $CD8\alpha^+$ and DN DC in response to PPD, which served as a positive control for neutralizing activity. However, IL-10 neutralization did not reveal the ability of $CD4^+$ DC to make IL-12 p70 (Fig. 6). Anti-IL-10 also did not change the nature of the response to zymosan or *S. pombe* in that the yeasts still failed to condition mixed DC populations or the $CD8\alpha^+$ and DN DC to make IL-12 p70 (Fig. 6). These results confirm that both $CD8\alpha^+$ and DN DC are able to produce either IL-12 or IL-10 and show that IL-10 is not responsible for the lack of IL-12 secretion by $CD4^+$ DC.

Differential responses to microbial stimulation are not attributable to quantitative differences in DC subset activation

Differences in the cytokine response of DC subsets to yeasts vs IL-12-promoting stimuli could conceivably arise from quantitative differences in DC activation. In that scenario, the degree rather than the quality of DC activation might determine IL-12 p70 vs IL-10 production in response to CD40 cross-linking. This could be especially relevant because cytokine secretion requires CD40 signaling and CD40 expression is altered by the microbial stimulus itself (Fig. 1). To examine whether the quantity of DC activation affected cytokine production, we chose two prototype IL-12 p70- and IL-10-promoting stimuli (PPD and zymosan, respectively) and examined their ability to 1) induce up-regulation of CD40 and CD86 and 2) promote IL-12 and IL-10 production across a whole dose-response range. There were no obvious differences among DC subsets in sensitivity to either zymosan or PPD in terms of CD86 up-regulation, although $CD8\alpha^+$ DC were more sensitive to PPD than either $CD4^+$ or DN DC when assessed for CD40 expression (Fig. 7*A*). Importantly, PPD conditioned $CD8\alpha^+$ and DN DC to make IL-12 p70 across the entire dose range (Fig. 7*B*). Similarly, zymosan conditioned all three subsets of DC to produce IL-10 at all doses (Fig. 7*B*). The fact that at no point in the dose-response did PPD become an IL-10 inducer or zymosan become an IL-12-promoting stimulus (Fig. 7*B*), demonstrates that qualitative rather than quantitative differences in microbial recognition lie at the heart of differential cytokine responses by DC subsets.

Discussion

Cytokines made by APC play a critical role in responses to infection. Here, we demonstrate four distinct features of cytokine production in murine DC. 1) The activation of individual DC subsets does not result in a preprogrammed pattern of cytokine secretion; it can lead to IL-10 or IL-12 production by $CD8\alpha^+$ and DN DC and to IL-10 production or lack thereof by $CD4^+$ DC. 2) Cytokine

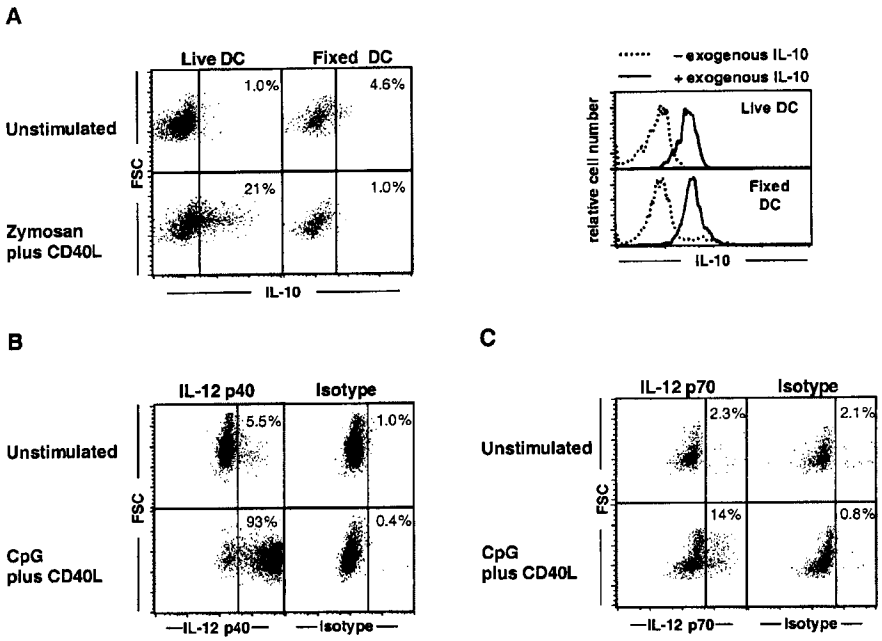

FIGURE 5. Single cell staining of CD8α^+ DC for IL-10 and IL-12. *A*, A 1:1 mixture of labeled live and fixed CD11c-enriched C3H/HeJ spleen cells was cultured with either control fibroblasts or zymosan (50 μg/ml) plus CD40L-expressing fibroblasts as indicated. Cells were assessed for IL-10 production as detailed in *Materials and Methods* and analyzed by flow cytometry. *Left*, Dot plots show IL-10 vs forward scatter profiles of gated CD8α^+CD11c$^+$ DC (FITC$^+$TC$^-$ for live or FITC$^-$TC$^+$ for fixed). *Right*, The same mixture of live and fixed DC was coated with IL-10 capture reagent and incubated $\pm$ exogenous IL-10 (10ng/ml) and then stained with anti-IL-10 and CD8α; histograms show IL-10 staining of CD11c$^+$CD8α^+ DC gated as above. *B*, CD11c-enriched C3H/HeJ spleen cells were cultured either alone or with CpG DNA (1 μg/ml) plus CD40L-expressing fibroblasts. Brefeldin A was added after 4 h, and cells were harvested and fixed 2.5 h later. Cells were permeabilized and stained with Abs to IL-12 p40 or with isotype control Abs, counterstained for CD11c, DEC-205, and CD8α and analyzed by flow cytometry. Dot plots show IL-12 vs forward scatter profiles of CD8α^+DEC-205$^+$CD11c$^+$ cells. *C*, Similar to *B*, using cells from BALB/c mice and staining for IL-12 p70. Dot plots show IL-12 vs forward scatter profiles of CD8α^+ CD11c$^+$ cells. Data for *A–C* are representative of three to four independent experiments.

production can be dictated by direct microbial recognition. Microbial structures from *Toxoplasma* and *Mycobacterium* or CpG-containing DNA condition DC to make IL-12 p70. In contrast, heat-killed yeasts (brewers' yeast, fission yeast, *C. albicans*) or yeast derivatives (zymosan) condition DC to make primarily IL-10. 3) Differential conditioning is dependent on distinct PRR; PPD and CpG DNA act through TLRs and an MyD88-dependent pathway, whereas yeasts act via a TLR-independent pathway. 4) PRR signaling results in limited cytokine production unless is it followed by signals from T cells which amplify DC activation but do not alter the type of cytokine that is made.

TLRs have emerged as key players in DC activation (2, 3). Consistent with this notion, the IL-12-promoting effects of PPD and STAg are absolutely dependent on signaling via MyD88 (Fig. 3 and Ref. 26). PPD contains traces of bacterial DNA, and some of its IL-12-promoting activity can be removed by DNase treatment (A. D. Edwards and C. Reis e Sousa, unpublished observations). However, most of the DC response to PPD appears to be due to TLR2 triggering (Fig. 3*C*), consistent with the fact that this TLR is involved in recognition of mycobacterial lipoarabinomannan and mannosylated phosphatidylinositol (27–29). TLR2 has also been implicated in the activation of macrophages by zymosan (21, 22). Given that DC express functional TLR2 (as determined by its involvement in PPD recognition), it is therefore surprising that zymosan failed to condition DC for IL-12 production even when IL-10 was neutralized (Fig. 6). It is possible that zymosan recognition in macrophages involves heterodimerization with another TLR, which is not expressed on mouse DC. Alternatively, recognition of zymosan by an IL-10-promoting PRR on DC is dominant over TLR2 recognition of the same particle and overwhelmingly conditions the cells for IL-10 production. Indirect support for this hypothesis comes from two observations: 1) in some experiments, the combination of zymosan plus CD40L slightly increased the level of IL-12 production compared with CD40L alone (e.g. Fig. 4*B*); 2) TLR2$^{-/-}$ DC reproducibly made more IL-10 in response to zymosan plus CD40L than controls, as if the IL-10-promoting PRR was now acting unopposed (Fig. 3*B*). The identity of the IL-10-promoting PRR for yeasts on DC is unknown at present, but it is unlikely to belong to the TLR family as it does not signal via MyD88 or TIRAP/MAL (Fig. 3). This would be consistent with the notion that TLR signaling is involved primarily in induction of IL-12 and type 1 adaptive immune responses (4).

We have previously suggested that CD40 signaling in DC acts to amplify innate signals for IL-12 production (13). Here, we show that CD40L is just as critical for amplifying IL-10 secretion (Fig. 2). This may seem contrary to the prevalent view that CD40 signaling leads to IL-12 production by DC (30, 31). However, CD40 signaling also induces IL-10 in monocyte-CSF-primed monocytes (32) and in human monocyte-derived DC exposed to glucocorticoids (33). Furthermore, our data fit with recent experiments showing that CD40 expression by bone marrow-derived DC is critical for priming of a Th2 response to *Schistosoma mansoni* eggs (34). Thus, CD40L and other T cells signals appear to act as neutral amplifiers that are critical for execution of cytokine production programs initiated by pattern recognition. Indeed, analysis of a large panel of IL-12-promoting stimuli shows that, like PPD, most trigger production of the IL-12 p40 subunit but induce little IL-12 p70 until combined with CD40L (A. D. Edwards and C. Reis e Sousa, unpublished observations). Apparent exceptions are CpG DNA and STAg, which can induce production of bioactive IL-12

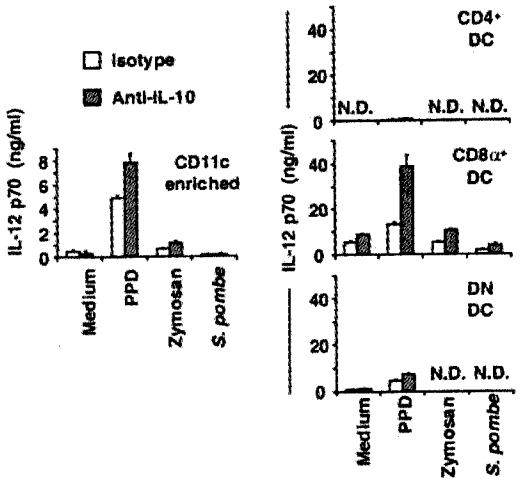

FIGURE 6. Lack of IL-12 p70 production in response to zymosan plus CD40L is not due to suppression by IL-10. CD11c-enriched cells (90% DC; 4×10^4/well) or sorted DC subsets (5×10^4/well) from B6 mice were cultured overnight on CD40L-expressing fibroblasts with the indicated microbial stimuli in the presence of 10 μg/ml of a neutralizing anti-IL-10 mAb or a control rat IgG1 of irrelevant specificity. IL-12 p70 levels in supernatant were measured by ELISA. Doses: PPD, 10 μg/ml; zymosan, 20 μg/ml; and *S. pombe*, 1×10^5particles/well. Histograms represent the mean of triplicate wells; all error bars are shown and represent 1 SD from the mean. N.D., Not detectable. Data are representative of five experiments with CD11c-enriched cells and two experiments with sorted subsets.

p70 by murine CD8α$^+$ and DN DC in the absence of T cell signals (Fig. 2 and Refs. 12, 13). However, CD40 ligation still increases greatly IL-12 p70 production in response to these two stimuli (Fig. 2 and Ref. 13).

The ability of microbes to influence production of IL-12 or IL-10 is not without precedent. Gram-negative bacteria preferentially induce IL-10 production in monocytes, whereas Gram-positive bacteria induce IL-12 (35). A recent report shows that a protein from *Bordetella pertussis* induces IL-10 production in DC (36). However, our use of inactivated microbes and microbial extracts as tools to dissect DC biology raises the question of whether our findings are of significance to natural infections with intact organisms. Production of IL-12 by DC in response to STAg, PPD, or CpG DNA has obvious implications for the development of protective type 1 immune responses to *Toxoplasma*, *Mycobacterium*, and other bacteria. The significance of IL-10 production in response to heat-killed yeasts is less clear. Protection from murine and human candidiasis involves primarily Th1-biased responses, even though a role for IL-10 has been suggested (37). Live *Candida* yeasts trigger IL-12 production by splenic DC (38), and live recombinant yeasts elicit IL-12 production by bone marrow-derived DC (39). Thus, conditioning of DC for IL-10 production in our experiments could reflect preferential destruction by heat treatment of IL-12-inducing yeast components.

It has been argued that different DC subtypes are specialized to make different cytokines and drive distinct forms of T cell differentiation (7). In support of this notion, human blood contains monocytes and plasmacytoid cells that can generate distinct DC1 or DC2 that prime Th1 or Th2 responses, respectively (40). These cells also express distinct TLR repertoires and respond to different microbial stimuli (8–10). In mouse, CD8α$^+$ and CD8α$^-$ subsets of spleen DC differ in their ability to make IL-12 in vitro and in vivo and to prime Th1 and Th2 responses in vivo (12, 13, 24, 25, 41, 42). However, there is also evidence that individual DC types are not necessarily precommitted DC1 or DC2. In both mice and humans, the ability of DC to produce IL-12 p70 and prime Th1 responses can be modulated by exposure to cytokines (24, 43, 44). In addition, mouse DC can produce either IL-12 or IL-4 in response to different forms of the fungus *C. albicans* and direct Th1 or Th2 development (38). Similarly, murine bone marrow-derived DC treated with LPS or Gram-negative bacteria preferentially prime Th1 responses while cells exposed to certain worm products direct Th2 development (34, 45). In the human system, pathogen products have also been shown to dictate the cytokine producing and Th-skewing capacity of monocyte-derived DC (46). Even so-called DC2 plasmacytoid cells can make IL-12 in response to CpG DNA plus CD40L (9) and can prime Th1 responses after exposure to viruses (47, 48), arguing that their Th2-directing ability is not hardwired. Consistent with the notion of flexibility, here we show that DN and CD8α$^+$ DC subsets have a choice of effector cytokines. It remains possible that these DC subsets are heterogeneous and contain DC precommitted to either IL-12 p70 or IL-10 production. However, using single-cell staining methods, we were

FIGURE 7. Differences in cytokine production induced by zymosan and PPD are dose independent. Sorted B6 DC subsets were cultured overnight with varying doses of PPD or zymosan and analyzed for surface marker up-regulation or cytokine production. *A*, Sorted DC subsets (6×10^4/well) were cultured with the indicated concentrations of PPD or zymosan. Duplicate wells were pooled, stained for CD11c, CD40, and CD86 and analyzed by FACS. Mean fluorescence indices (MFI) are expressed as fold increase over medium alone (·····). *B*, DC subsets (6×10^4/well) were cultured overnight on a monolayer of CD40L-expressing fibroblasts with serial dilutions of PPD or zymosan, and supernatants were analyzed for IL-12 p70 and IL-10 by ELISA. Top concentrations were 40 μg/ml for PPD and 10 μg/ml for zymosan; cytokine production with CD40L alone is indicated as 0. Data are the mean of duplicate wells (triplicate for 0). All error bars are shown and represent 1 SD from the mean. Data are representative of three independent experiments.

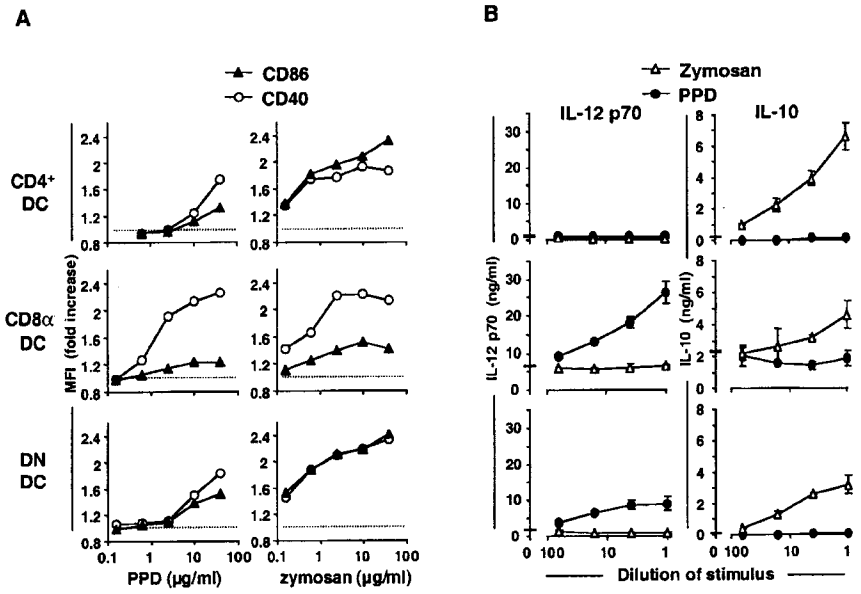

able to show that up to 30% of CD8α^+ DC could produce IL-10 when given zymosan plus CD40L (Fig. 5*A*), and >90% of CD8α^+ DC could make IL-12 p40 in response to an appropriate combination of stimuli (Fig. 5*B* and data not shown). Therefore, we suppose that at least 15–20% of CD8α^+ DC are bipotential for IL-10 and IL-12 p40 production. This is probably an underestimate, as the staining method for IL-10 involves cell resuspension, which disrupts continued CD40 engagement and stops cytokine synthesis (A. D. Edwards and C. Reis e Sousa, unpublished observations). Whether bipotentiality extends to IL-12 p70 production could not be unambiguously determined as only up to 15% of CD8α^+ DC can be stained for the cytokine (Fig. 5). However, IL-12 p70 is produced at 10- to 50-fold lower levels than IL-12 p40 (49) even after CD40-dependent up-regulation of IL-12 p35 (13) and is extremely difficult to detect by staining. Therefore, again, our staining is likely to provide only a gross underestimate of the true frequency of IL-12 p70-producing cells. Thus, we favor the notion that most CD8α^+ and DN DC have the potential to produce alternative cytokines in response to distinct stimuli. This does not exclude the possibility that some DC subsets may have functional specializations, exemplified by the apparent inability of CD4$^+$ DC to produce IL-12 p70 in response to a large panel of stimuli (Figs. 4, 6, and 7 and data not shown), also seen by Hochrein et al. (25). CD4$^+$ DC represent ~50% of splenic DC and constitute the majority of DC in the CD8α^- fraction, which may underlie the observed tendency of CD8α^- DC to induce Th2 responses (24, 41, 42). However, even CD4$^+$ DC do not have a prewired response to activation: they are activated to a similar degree by zymosan and PPD as measured by CD40 and CD86 up-regulation, yet zymosan conditions the cells to make IL-10 whereas PPD does not (Fig. 7). Altogether, these results suggest a model in which all DC irrespective of subset can behave as flexible APC. The fact that innate signals and T cell feedback are both necessary and sufficient for cytokine production by all DC subsets can, therefore, explain Th polarization by these APC without invoking the participation of third-party cells or cytokines.

Acknowledgments

We thank A. Lehmann and C. Lehane for *S. cerevisiae* and *S. pombe* cultures and S. Vogel for LPS. We are grateful to C. Simpson, A. Eddaoudi, and G. Warnes for cell sorting and G. Hutchinson and J. Bee for animal care. We thank N. Hogg and D. Cantrell for comments on the manuscript.

References

1. Reis e Sousa, C. 2001. Dendritic cells as sensors of infection. *Immunity 14:495.*
2. Medzhitov, R., and C. Janeway, Jr. 2000. The Toll receptor family and microbial recognition. *Trends Microbiol. 8:452.*
3. Akira, S., K. Takeda, and T. Kaisho. 2001. Toll-like receptors: critical proteins linking innate and acquired immunity. *Nat. Immunol. 2:675.*
4. Schnare, M., G. M. Barton, A. C. Holt, K. Takeda, S. Akira, and R. Medzhitov. 2001. Toll-like receptors control activation of adaptive immune responses. *Nat. Immunol. 2:947.*
5. Moser, M., and K. M. Murphy. 2000. Dendritic cell regulation of THI-TH2 development. *Nat. Immunol. 1:199.*
6. Lanzavecchia, A., and F. Sallusto. 2001. Regulation of T cell immunity by dendritic cells. *Cell 106:263.*
7. Liu, Y. J. 2001. Dendritic cell subsets and lineages, and their functions in innate and adaptive immunity. *Cell 106:259.*
8. Kadowaki, N., S. Ho, S. Antonenko, R. de Waal Malefyt, R. A. Kastelein, F. Bazan, and Y. J. Liu. 2001. Subsets of human dendritic cell precursors express different toll-like receptors and respond to different microbial antigens. *J. Exp. Med. 194:863.*
9. Krug, A., A. Towarowski, S. Britsch, S. Rothenfusser, V. Hornung, R. Bals, T. Giese, H. Engelmann, S. Endres, A. M. Krieg, and G. Hartmann. 2001. Toll-like receptor expression reveals CpG DNA as a unique microbial stimulus for plasmacytoid dendritic cells which synergizes with CD40 ligand to induce high amounts of IL-12. *Eur. J. Immunol. 31:3026.*
10. Jarrossay, D., G. Napolitani, M. Colonna, F. Sallusto, and A. Lanzavecchia. 2001. Specialization and complementarity in microbial molecule recognition by human myeloid and plasmacytoid dendritic cells. *Eur. J. Immunol. 31:3388.*
11. Kalinski, P., C. M. Hilkens, E. A. Wierenga, and M. L. Kapsenberg. 1999. T-cell priming by type-1 and type-2 polarized dendritic cells: the concept of a third signal. *Immunol. Today 20:561.*
12. Reis e Sousa, C., S. Hieny, T. Scharton-Kersten, H. Charest, D. Jankovic, R. N. Germain, and A. Sher. 1997. In vivo microbial stimulation induces rapid CD40L- independent production of IL-12 by dendritic cells and their re-distribution to T cell areas. *J. Exp. Med. 186:1819.*
13. Schulz, O., A. D. Edwards, M. Schito, J. Aliberti, S. Manickasingham, A. Sher, and C. Reis e Sousa. 2000. CD40 triggering of heterodimeric IL-12 p70 production by dendritic cells in vivo requires a microbial priming signal. *Immunity 13:453.*
14. Murphy, K. M., A. B. Heimberger, and D. Y. Loh. 1990. Induction by antigen of intrathymic apoptosis of CD4$^+$CD8$^+$TCR^{lo} thymocytes in vivo. *Science 250: 1720.*
15. Adachi, O., T. Kawai, K. Takeda, M. Matsumoto, H. Tsutsui, M. Sakagami, K. Nakanishi, and S. Akira. 1998. Targeted disruption of the *MyD88* gene results in loss of IL-1- and IL-18-mediated function. *Immunity 9:143.*
16. Takeuchi, O., K. Hoshino, T. Kawai, H. Sanjo, H. Takada, T. Ogawa, K. Takeda, and S. Akira. 1999. Differential roles of TLR2 and TLR4 in recognition of Gram-negative and Gram-positive bacterial cell wall components. *Immunity 11:443.*
17. Schulz, O., D. Pennington, K. Hodivala-Dilke, M. Febbraio, and C. Reis e Sousa. 2002. CD36 or $\alpha_v\beta_3$ and $\alpha_v\beta_5$ integrins are not essential for MHC class I cross-presentation of cell-associated antigen by CD8α^+ murine dendritic cells. *J. Immunol. 168:6057.*
18. Krieg, A. M., A. K. Yi, S. Matson, T. J. Waldschmidt, G. A. Bishop, R. Teasdale, G. A. Koretzky, and D. M. Klinman. 1995. CpG motifs in bacterial DNA trigger direct B-cell activation. *Nature 374:546.*
19. Horng, T., G. M. Barton, and R. Medzhitov. 2001. TIRAP: an adapter molecule in the Toll signaling pathway. *Nat. Immunol. 2:835.*
20. Hemmi, H., O. Takeuchi, T. Kawai, T. Kaisho, S. Sato, H. Sanjo, M. Matsumoto, K. Hoshino, H. Wagner, K. Takeda, and S. Akira. 2000. A Toll-like receptor recognizes bacterial DNA. *Nature 408:740.*
21. Underhill, D. M., A. Ozinsky, A. M. Hajjar, A. Stevens, C. B. Wilson, M. Bassetti, and A. Aderem. 1999. The Toll-like receptor 2 is recruited to macrophage phagosomes and discriminates between pathogens. *Nature 401:811.*
22. Ozinsky, A., D. M. Underhill, J. D. Fontenot, A. M. Hajjar, K. D. Smith, C. B. Wilson, L. Schroeder, and A. Aderem. 2000. The repertoire for pattern recognition of pathogens by the innate immune system is defined by cooperation between toll-like receptors. *Proc. Natl. Acad. Sci. USA 97:13766.*
23. Fitzgerald, K. A., E. M. Palsson-McDermott, A. G. Bowie, C. A. Jefferies, A. S. Mansell, G. Brady, E. Brint, A. Dunne, P. Gray, M. T. Harte, D., et al. 2001. Mal (MyD88-adapter-like) is required for Toll-like receptor-4 signal transduction. *Nature 413:78.*
24. Maldonado-Lopez, R., C. Maliszewski, J. Urbain, and M. Moser. 2001. Cytokines regulate the capacity of CD8α^+ and CD8α^- dendritic cells to prime Th1/Th2 cells in vivo. *J. Immunol. 167:4345.*
25. Hochrein, H., K. Shortman, D. Vremec, B. Scott, P. Hertzog, and M. O'Keeffe. 2001. Differential Production of IL-12, IFN-α, and IFN-γ by mouse dendritic cell subsets. *J. Immunol. 166:5448.*
26. Scanga, C. A., J. Aliberti, D. Jankovic, F. Tilloy, S. Bennouna, E. Y. Denkers, R. Medzhitov, and A. Sher. 2002. Cutting edge: MyD88 is required for resistance to *Toxoplasma gondii* infection and regulates parasite-induced IL-12 production by dendritic cells. *J. Immunol. 168:5997.*
27. Underhill, D. M., A. Ozinsky, K. D. Smith, and A. Aderem. 1999. Toll-like receptor-2 mediates mycobacteria-induced proinflammatory signaling in macrophages. *Proc. Natl. Acad. Sci. USA 96:14459.*
28. Tsuji, S., M. Matsumoto, O. Takeuchi, S. Akira, I. Azuma, A. Hayashi, K. Toyoshima, and T. Seya. 2000. Maturation of human dendritic cells by cell wall skeleton of *Mycobacterium bovis* bacillus Calmette-Guérin: involvement of toll-like receptors. *Infect. Immun. 68:6883.*
29. Jones, B. W., T. K. Means, K. A. Heldwein, M. A. Keen, P. J. Hill, J. T. Belisle, and M. J. Fenton. 2001. Different Toll-like receptor agonists induce distinct macrophage responses. *J. Leukocyte Biol. 69:1036.*
30. Cella, M., D. Scheidegger, K. Palmer-Lehmann, P. Lane, A. Lanzavecchia, and G. Alber. 1996. Ligation of CD40 on dendritic cells triggers production of high levels of interleukin-12 and enhances T cell stimulatory capacity: T-T help via APC activation. *J. Exp. Med. 184:747.*
31. Koch, F., U. Stanzl, P. Jennewein, K. Janke, C. Heufler, E. Kampgen, N. Romani, and G. Schuler. 1996. High level IL-12 production by murine dendritic cells: upregulation via MHC class II and CD40 molecules and downregulation by IL-4 and IL-10. *J. Exp. Med. 184:741.*
32. Foey, A. D., M. Feldmann, and F. M. Brennan. 2000. Route of monocyte differentiation determines their cytokine production profile: CD40 ligation induces interleukin 10 expression. *Cytokine 12:1496.*
33. Rea, D., C. van Kooten, K. E. van Meijgaarden, T. H. Ottenhoff, C. J. Melief, and R. Offringa. 2000. Glucocorticoids transform CD40-triggering of dendritic cells into an alternative activation pathway resulting in antigen-presenting cells that secrete IL-10. *Blood 95:3162.*
34. MacDonald, A. S., A. D. Straw, N. M. Dalton, and E. J. Pearce. 2002. Cutting edge: Th2 response induction by dendritic cells: a role for CD40. *J. Immunol. 168:537.*
35. Hessle, C., B. Andersson, and A. E. Wold. 2000. Gram-positive bacteria are potent inducers of monocytic interleukin-12 (IL-12) while Gram-negative bacteria preferentially stimulate IL-10 production. *Infect. Immun. 68:3581.*
36. McGuirk, P., C. McCann, and K. H. Mills. 2002. Pathogen-specific T regulatory 1 cells induced in the respiratory tract by a bacterial molecule that stimulates

interleukin 10 production by dendritic cells: a novel strategy for evasion of protective t helper type 1 responses by *Bordetella pertussis*. *J. Exp. Med. 195:221.*

37. Romani, L. 1999. Immunity to *Candida albicans*: Th1, Th2 cells and beyond. *Curr. Opin. Microbiol. 2:363.*
38. d'Ostiani, C. F., G. Del Sero, A. Bacci, C. Montagnoli, A. Spreca, A. Mencacci, P. Ricciardi-Castagnoli, and L. Romani. 2000. Dendritic cells discriminate between yeasts and hyphae of the fungus *Candida albicans*: implications for initiation of T helper cell immunity in vitro and in vivo. *J. Exp. Med. 191:1661.*
39. Stubbs, A. C., K. S. Martin, C. Coeshott, S. V. Skaates, D. R. Kuritzkes, D. Bellgrau, A. Franzusoff, R. C. Duke, and C. C. Wilson. 2001. Whole recombinant yeast vaccine activates dendritic cells and elicits protective cell-mediated immunity. *Nat. Med. 7:625.*
40. Rissoan, M. C., V. Soumelis, N. Kadowaki, G. Grouard, F. Briere, R. de Waal Malefyt, and Y. J. Liu. 1999. Reciprocal control of T helper cell and dendritic cell differentiation. *Science 283:1183.*
41. Pulendran, B., J. L. Smith, G. Caspary, K. Brasel, D. Pettit, E. Maraskovsky, and C. R. Maliszewski. 1999. Distinct dendritic cell subsets differentially regulate the class of immune response in vivo. *Proc. Natl. Acad. Sci. USA 96:1036.*
42. Maldonado-López, R., T. De Smedt, P. Michel, J. Godfroid, B. Pajak, C. Heirman, K. Thielemans, O. Leo, J. Urbain, and M. Moser. 1999. $CD8\alpha^+$ and $CD8\alpha^-$ subclasses of dendritic cells direct the development of distinct T helper cells in vivo. *J. Exp. Med.* 189:587.
43. Hochrein, H., M. O'Keeffe, T. Luft, S. Vandenabeele, R. J. Grumont, E. Maraskovsky, and K. Shortman. 2000. Interleukin (IL)-4 is a major regulatory cytokine governing bioactive IL-12 production by mouse and human dendritic cells. *J. Exp. Med. 192:823.*
44. Kalinski, P., H. H. Smits, J. H. Schuitemaker, P. L. Vieira, M. van Eijk, E. C. de Jong, E. A. Wierenga, and M. L. Kapsenberg. 2000. IL-4 is a mediator of IL-12p70 induction by human Th2 cells: reversal of polarized Th2 phenotype by dendritic cells. *J. Immunol. 165:1877.*
45. Whelan, M., M. M. Harnett, K. M. Houston, V. Patel, W. Harnett, and K. P. Rigley. 2000. A filarial nematode-secreted product signals dendritic cells to acquire a phenotype that drives development of Th2 cells. *J. Immunol. 164:6453.*
46. de Jong, E. C., P. L. Vieira, P. Kalinski, J. H. Schuitemaker, Y. Tanaka, E. A. Wierenga, M. Yazdanbakhsh, and M. L. Kapsenberg. 2002. Microbial compounds selectively induce Th1 cell-promoting or Th2 cell- promoting dendritic cells in vitro with diverse Th cell-polarizing signals. *J. Immunol. 168:1704.*
47. Cella, M., F. Facchetti, A. Lanzavecchia, and M. Colonna. 2000. Plasmacytoid dendritic cells activated by influenza virus and CD40L drive a potent T_H1 polarization. *Nat. Immunol. 1:305.*
48. Kadowaki, N., S. Antonenko, J. Y. Lau, and Y. J. Liu. 2000. Natural interferon α/β-producing cells link innate and adaptive immunity. *J. Exp. Med. 192:219.*
49. Trinchieri, G. 1995. Interleukin-12: a proinflammatory cytokine with immunoregulatory functions that bridge innate resistance and antigen-specific adaptive immunity. *Annu. Rev. Immunol. 13:251.*

Phase I Study of Recombinant Human CD40 Ligand in Cancer Patients

By Robert H. Vonderheide, Janice P. Dutcher, Jeanne E. Anderson, S. Gail Eckhardt, Katherine F. Stephans, Betty Razvillas, Susan Garl, Michael D. Butine, Vicki P. Perry, Richard J. Armitage, Richard Ghalie, Dania A. Caron, and John G. Gribben

Purpose: **To determine the toxicity, maximum-tolerated dose (MTD), and pharmacokinetics of recombinant human CD40 ligand (rhuCD40L) (Avrend; Immunex Corp, Seattle, WA), suggested in preclinical studies to mediate cytotoxicity against CD40-expressing tumors and immune stimulation.**

Patients and Methods: **Patients with advanced solid tumors or intermediate- or high-grade non-Hodgkin's lymphoma (NHL) received rhuCD40L subcutaneously daily for 5 days in a phase I dose-escalation study. Subsequent courses were given until disease progression.**

Results: **Thirty-two patients received rhuCD40L at three dose levels. A total of 65 courses were administered. The MTD was 0.1 mg/kg/d based on dose-related but transient elevations of serum liver transaminases. Grade 3 or 4 transaminase elevations occurred in 14%, 28%, and 57% of patients treated at 0.05, 0.10, and 0.15 mg/kg/d, respectively. Other toxicities were mild to moderate. At the MTD, the half-life of rhuCD40L was calculated at 24.8 ± 22.8 hours. Two patients (6%) had a partial response on study (one patient with laryngeal carcinoma and one with NHL). For the patient with laryngeal cancer, a partial response was sustained for 12 months before the patient was taken off therapy and observed on no additional therapy. Three months later, the patient was found to have a complete response and remains biospy-proven free of disease at 24 months. Twelve patients (38%) had stable disease after one course, which was sustained in four patients through four courses.**

Conclusion: **The MTD of rhuCD40L when administered subcutaneously daily for 5 days was defined by transient serum elevations in hepatic transaminases. Encouraging antitumor activity, including a long-term complete remission, was observed. Phase II studies are warranted.**

J Clin Oncol 19:3280-3287.

THE CELL SURFACE molecule CD40, a member of the tumor necrosis factor receptor superfamily, has been studied as a target for antitumor therapy because of its expression on nearly all B-cell malignancies and the majority of solid tumors.[1-3] This expression includes all types of B-cell tumors, including non-Hodgkin's lymphoma (NHL), acute lymphoblastic leukemia, chronic lymphocytic leukemia, and myeloma. In solid tumors, CD40 expression is found on 35% to 100% of established cell lines, depending on histology, and on more than 60% of tumor biopsy specimens obtained from patients with melanoma and many epithelial tumors (eg, pancreas, lung, ovary, bladder, breast, colon, prostate, and squamous cell cancer of the head and neck).[4,5]

In normal tissues, signaling through CD40 has been implicated in enhanced antigen presentation function and cytokine release.[3,6,7] In B cells, CD40 cross-linking results in immunoglobulin class switching and growth stimulation.[8-10] CD40 has been demonstrated on all normal B-lymphocytes, as well as populations of epithelial cells, $CD34^+$ hematopoietic progenitor cells, monocytes, dendritic cells, endothelial cells, and fibroblasts.[11-15] Although CD40 expression on B-cell malignancies may reflect preexisting expression on nonmalignant precursor cells,[1] the biologic role of CD40 in malignant tissues and, in particular, on solid tumors is unknown.

CD40 ligand (CD40L), also known as CD154, functions as the natural ligand for CD40.[9,16] It is expressed primarily on the surface of activated T lymphocytes[16] but has also been found on activated platelets.[17] The CD40L gene maps to human chromosome Xq26, and its mutation results in X-linked immunodeficiency (hyperimmunoglobulin M) syndrome.[18] CD40L is a major component of T-cell help for B cells in antibody isotype switching and in the formation of memory B cells and germinal centers.[1] Interactions between CD40 and CD40L provide critical costimulatory signals that trigger T-lymphocyte expansion.[19] Antibodies that cross-link CD40 mimic the signal of CD40L[20] and can substitute

From the Department of Adult Oncology, Dana-Farber Cancer Institute; Department of Medicine, Brigham and Women's Hospital; and Harvard Medical School, Boston, MA; Cancer Center, Our Lady of Mercy Hospital, New York Medical College, Bronx, NY; Cancer Therapy and Research Center, Institute for Drug Development, San Antonio, TX; and Immunex Corp, Seattle, WA.

Submitted November 21, 2000; accepted March 27, 2001.

Immunex Corp (Seattle, WA) provided financial institutional support to cover partial costs for the conduct of the study.

Presented in part at the Forty-First Annual Meeting of the American Society of Hematology, New Orleans, LA, December 3-7, 1999.

Address reprint requests to R.H. Vonderheide, MD, DPhil, Dana-Farber Cancer Institute, 44 Binney St, Boston, MA 02115; email: robert_vonderheide@dfci.harvard.edu.

0732-183X/01/1913-3280

for $CD4^+$ lymphocytes in murine models of T-cell–mediated immunity.[21-23]

To enhance the signaling activity of CD40L via cell surface CD40, a trimeric recombinant form of human CD40 ligand (rhuCD40L) (Avrend; Immunex Corp, Seattle, WA) was produced that incorporates an isoleucine zipper motif.[24] Two main observations have suggested that rhuCD40L could be used therapeutically to target CD40-expressing solid tumors and B-cell malignancies.[3] First, rhuCD40L is cytotoxic against CD40-expressing tumors.[25-32] In preclinical studies, rhuCD40L induced in vitro growth inhibition and cell killing of $CD40^+$ human carcinoma and B-cell lymphoma cell lines. Furthermore, rhCD40L improved survival in vivo of severe-combined immunodeficient mice implanted with MDA231 breast cancer cells.[30] Similar protective effects of rhuCD40L were observed in a severe-combined immunodeficient mouse–human lymphoma model.[25]

A second potential antitumor effect of rhuCD40L is related to immune stimulation observed after CD40 cross-linking, including the enhancement of antigen presentation by dendritic cells, monocytes, and B cells, and the triggering of antigen-specific T-cell responses.[3] In B-cell malignancies, treatment with CD40L can even upregulate antigen presentation by tumor cells themselves and can stimulate autologous antitumor T-cell responses,[6,33-35] a notion currently being tested in vivo in patients with B-cell lymphoma or leukemias.[36,37]

In preclinical toxicology studies, rhuCD40L was well tolerated by nonhuman primates treated daily for 28 days and by mice given trimeric recombinant murine CD40L in a total of 10 injections every other day. The most prominent clinical findings included injection site reactions (ISRs) and enlargement of lymphoid organs after subcutaneous administration. At substantially higher doses (four- to 10-fold increase) than planned for phase I investigation in humans, rhuCD40L resulted in moderate to severe myelosuppression and mild hepatotoxicity in monkeys.

Here, we report the results of the first clinical trial to treat cancer patients with rhuCD40L. The main objective of this phase I study was to determine the safety and maximum-tolerated dose (MTD) of rhuCD40L when administered subcutaneously daily for 5 days. Other objectives included the evaluation of the pharmacokinetics of rhuCD40L administered in this fashion and the assessment of antitumor effects in cancer patients.

PATIENTS AND METHODS

To be eligible, patients had to have recurrent intermediate or high-grade NHL (Working Formulation), chemotherapy-resistant solid tumors, or solid tumors for which conventional cytotoxic therapy was considered unlikely to achieve a meaningful antitumor response. Patients had to be older than 18 and younger than 75 years of age, with a Karnofsky performance status greater than 70%. They had to have adequate hematologic function (hemoglobin > 9 g/dL, WBC count $>$ 3,000 cells/mm^3, absolute neutrophil count $>$ 1,500 cells/mm^3, and platelet count $>$ 100,000 cells/mm^3), renal function (serum creatinine < 2.0 mg/dL), and hepatic function (total bilirubin < 2.0 mg/dL and AST and ALT< 2.5 times the upper limit of normal values). For female patients of childbearing potential, a negative pregnancy test was required, taken within 24 hours before the first dose of rhuCD40L. Patients were not eligible if they had a known personal or immediate family history of autoimmune disease; significant chronic neurologic, hepatic, renal, respiratory, dermatologic, endocrinologic, or cardiovascular disease; alcohol abuse or illicit drug use within 12 months of enrollment; or second malignancy within the previous 5 years, except for carcinoma in situ of the uterus and superficial epithelial skin cancers. Use of systemic chemotherapy, radiotherapy, antitumor biologic therapy, or investigational drugs was not allowed within 30 days before the first dose, nor was the use of hematopoietic growth factors allowed within 10 days. Signed, written, and informed consent was obtained, as required, from each patient. The study was approved by the investigational review boards of the three participating institutions, as well as the United States Food and Drug Administration.

Treatment

Patients were stratified by diagnosis, with NHL patients in one group and solid tumor patients in a second. Each dose cohort in the NHL group included three patients, whereas each dose cohort in the solid tumor group had four patients. Determination of CD40 tumor expression was not required for enrollment. CD40 expression in NHL is nearly 100% but is roughly 75% in solid tumors; consequently, solid tumor patient groups were larger than NHL groups because of this lower expected CD40 expression rate. There was no expected difference with regard to the primary end point of toxicity between patients with solid tumors versus those with NHL. Patients received rhuCD40L (Avrend) by daily subcutaneous injection for 5 consecutive days, a treatment schedule based on pharmacologic data from preclinical studies in nonhuman primates. Five doses were scheduled for evaluation: 0.05, 0.10, 0.20, 0.40, and 0.80 mg/kg/d. Escalation between doses was based on tolerance of lower doses. In the absence of progressive disease or grade 3 or 4 major organ toxicity, patients could receive a second 5-day course of rhuCD40L beginning 6 weeks after the first dose in course one. Third and subsequent courses were administered at 4-week intervals. Dose-limiting toxicity (DLT) was defined based on events during the first course of therapy as any grade 3 or 4 major organ toxicity or any grade 3 or 4 nonmajor organ toxicity requiring discontinuation from the study. An isolated, 1-day grade 3 elevation of ALT in one patient was not considered a DLT. Before enrollment at the next dose level was permitted, at least three patients in the stratification group had to complete 5 days of dosing and 28 days of follow-up without DLT. If one patient experienced DLT at a given dose level, three additional patients were enrolled at the same dose level. If two or more patients experienced DLT at a given dose level, the dose level preceding the one at which DLT was observed was considered the MTD. If two or more patients at a given dose level within a stratification group experienced grade 2 major organ toxicity, the dose was only increased 50% in the next dose cohort. If the intermediate dose level was well tolerated, patients were enrolled at the next scheduled dose level; otherwise, the dose immediately preceding the intermediate dose was considered the MTD. Eight additional patients were then enrolled at the MTD.

At the time of enrollment, medical histories were obtained and patients underwent a physical examination, including measurement of weight, vital signs, and performance status. Pretreatment evaluation also included complete blood count, reticulocyte count, serum chemistry profile, urinalysis, prothrombin time, partial thromboplastin time, quantitative serum immunoglobulins, an ECG, a chest radiograph, and assessment of known tumor sites using appropriate imaging techniques. Patients were evaluated for toxicity (common toxicity criteria) on days 1 through 7, 9, 14, 21, 28, and 35 during courses 1 and 2 and slightly less frequently during subsequent courses. Quantitative serum immunoglobulins, an ECG, a chest radiograph, and tumor response evaluation were repeated at least at the end of courses 1 and 2 and every two cycles thereafter.

Pharmacokinetics

For courses 1 and 2, serum samples for pharmacokinetic studies were obtained at baseline; at 1, 2, 4, 6, and 8 hours postdose on day 1; and at 4, 6, 8, 24, 48, 96, and 216 hours after the day 5 dose. Parameters included half-life, maximum concentration, and area under the curve. Enzyme-linked immunosorbent assay (ELISA) plates were coated with a solution of isoleucine zipper-specific monoclonal antibody. RhuCD40L standard (Immunex Corp) and human sera were diluted in a sample buffer, and the rhuCD40L standard curve ranged from 1,600 to 25 pg/mL in two-fold increments. Sera were tested at a minimal dilution of 1:5 and were titrated two-fold in duplicate through four wells. Incubation and washing were followed by a 1-hour incubation with rabbit polyclonal anti-rhuCD40L antiserum. Detection used peroxidase-conjugated goat antirabbit immunoglobulin (Ig) G (H+L), and color was developed with 3,3',5,5'-tetramethylbenzidine. The reaction was stopped with acid, and optical densities (OD) were determined at a wavelength of 450 nm. The standard curve was generated with a four-parameter logistic model, and sample concentrations were estimated by interpolation from the fitted curve.

Immunoassessment

During course 1, blood samples for flow cytometry were collected in heparinized tubes at baseline and on day 5 and shipped immediately overnight at room temperature to a central laboratory. Peripheral-blood mononuclear cells were obtained after Ficoll (Amersham Pharmacia Biotech, Uppsala, Sweden) centrifugation and preincubated at 4°C with 1% normal rabbit serum and 2% normal goat serum in phosphate-buffered saline/NaN_3 to block nonspecific binding of test antibodies. Cells were then incubated for 30 minutes at 4°C with the relevant phycoerythrin– or fluorescein isothiocyanate–conjugated monoclonal antibodies, washed three times in phosphate-buffered saline/NaN_3 and analyzed by flow cytometry using a FACScan (Becton Dickinson, Mountain View, CA). Monoclonal antibodies used in this study were CD3, CD4, CD8, CD14, CD16, CD19, and CD56 (BD Pharmingen, Torrey Pines, CA).

Serum samples obtained at baseline and day 5 were kept frozen at −80°C. Levels of polyclonal IgM, IgG, IgA, and IgE were then determined by ELISA, as described previously.[38] Sera from normal donors (n = 6) was used to determine normal ranges. Antigen-specific titers of IgG were determined by ELISA by coating plates with the following partially purified antigens: tetanus toxoid (Connaught Laboratories Inc, Swiftwater, PA), measles, influenza, or varicella (Viral Antigens Inc, Memphis, TN), followed by biotinylated-antihuman IgG (Cappel, Malvern, PA). Sera from normal donors was used to generate a standard curve for each antigen.

Table 1. Patient Characteristics

Characteristic	Solid Tumor (n = 23) No.	Solid Tumor (n = 23) %	NHL (n = 9) No.	NHL (n = 9) %
Sex				
Women	14	61	4	44
Men	9	39	5	56
Race				
White	17	74	6	67
Hispanic	2	9	3	33
Asian	2	9	0	0
African-American	2	9	0	0
Age, years				
Median	59		53	
Range	23-75		21-71	
Stage IV disease		100		78
Prior cancer therapy				
Chemotherapy		65		100
Radiation		65		67
Biologic		39		67

Serum levels of interleukin 12 (IL-12), macrophage inflammatory protein (MIP1) α, and MIP1β, and regulated upon activation, normal T cell expressed and secreted (RANTES) were determined by ELISA using paired monoclonal and polyclonal antibodies specific for each cytokine (R&D Systems, Minneapolis, MN). The sensitivities of the ELISAs were as follows: IL-12, 6 pg/mL; MIP1α, 23 pg/mL; MIP1β, 6 pg/mL; and RANTES, 15 pg/mL.

rhuCD40L Antibodies

Serum samples obtained on the first, 14th, and last day of each course were tested for the presence of antibodies to rhuCD40L. ELISA plates were coated overnight with rhuCD40L, and after washing, controls and serum samples were added to the wells and incubated. Bound antibody was detected, after washing, with a peroxidase-labeled antihuman Ig conjugate. A sample was scored positive if the posttreatment sample exhibited a statistically significant OD increase when compared with the corresponding pretreatment sample OD.

Confirmation of positive antibody results was tested by assessing the ability of sample to influence the binding of CD40L to CD40. Immobilized CD40 was exposed to sample (preincubated with a fixed quantity of rhuCD40L), washed, and exposed to biotinylated rhuCD40L. Bound biotinylated rhuCD40L was detected with streptavidin-horseradish peroxidase conjugate. A sample was scored positive (confirmed) if it exhibited a statistically significant difference from the control.

RESULTS

Patient Characteristics

Thirty-two patients including 23 with solid tumors and nine with NHL were evaluated in this phase I study from July 1998 to August 1999 at three institutions. Patient characteristics are given in Table 1. Histology of the solid tumors included renal cell carcinoma (n = 10), head and neck cancer (n = 4), cervical cancer (n = 2), sarcoma (n = 2), and one patient each

Table 2. Incidence and Grade of Serum Transaminase Elevations (all courses)

	Solid Tumor (n = 23)						NHL (n = 9)							
	0.05 mg/kg/d (n = 4)		0.10 mg/kg/d (n = 15)		0.15 mg/kg/d (n = 4)		0.05 mg/kg/d (n = 3)		0.10 mg/kg/d (n = 3)		0.15 mg/kg/d (n = 3)		Total (N = 32)	
	No.	%	No.	%	No.	%	No.	%	No.	%	No.	%	No.	%
AST high														
Grade 1	1	25	3	20	0	0	0	0	0	0	2	67	6	19
Grade 2	0	0	2	13	1	25	0	0	2	67	0	0	5	16
Grade 3	1	25	5	33	2	50	0	0	0	0	1	33	9	28
Grade 4	0	0	0	0	1	25	0	0	0	0	0	0	1	3
ALT high														
Grade 1	0	0	4	27	0	0	0	0	0	0	1	33	5	16
Grade 2	0	0	1	7	1	25	0	0	2	67	0	0	4	13
Grade 3	1	25	3	20	2	50	0	0	0	0	1	33	7	22
Grade 4	0	0	0	0	1	25	0	0	0	0	0	0	1	3

with rectal carcinoma, esophageal carcinoma, breast carcinoma, peritoneal carcinomatosis, and adenocarcinoma of unknown primary tumor. Histology in the NHL patients included B-cell NHL (n = 8) and T-cell NHL (n = 1). B-cell NHL diagnoses were diffuse large cell (n = 4); diffuse, mixed small and large cell (n = 1); diffuse, small cleaved cell (n = 1); and transformed follicular (n = 2).

Patients were treated at three different dose levels. The total number of courses administered was 65, and the mean number of courses per patient was two (range, one to 12). Six solid tumor patients and none of the nine NHL patients received three or more courses. Every patient except one completed at least one full 5-day course of therapy. One patient with breast carcinoma developed grade 4 elevations in AST and ALT after four injections of rhuCD40L, so the final day of therapy was not given. This patient was included in the analyses of toxicity and tumor response but not pharmacokinetics.

Hepatic Toxicity and MTD

Dose-related, transient serum elevations in liver transaminases were observed as detailed in Table 2. In the solid tumor cohort of patients, this toxicity defined the MTD of rhuCD40L administered on this schedule to be 0.10 mg/kg/d. No MTD was defined based on NHL patients. Among all patients, grade 3 or 4 elevations of either AST or ALT were observed in 14%, 28%, and 57% of patients treated at 0.05, 0.1, and 0.15 mg/kg/d, respectively. Grade 4 elevation in AST or ALT occurred only at the highest dose. Elevations were transient, usually peaking on day 6, and generally returned to within normal limits by day 14. Two patients with liver metastases had sustained elevations of AST and ALT. In the six patients treated with three or more courses of rhuCD40L, there was no increase in the incidence or severity of liver enzyme elevations with repeated courses. When observed in these six patients, grade 3 or 4 elevations in liver transaminases always initially occurred during the first course, except for one patient who developed grade 3 abnormalities only during the second course.

Hematopoietic Toxicity

Six patients developed grade 3 (n = 5) or grade 4 (n = 1) reductions in hemoglobin, although this toxicity was not clearly dose-dependent. Two patients had grade 3 or 4 leukopenia, and three had grade 3 or 4 neutropenia. Seven (78%) of the nine NHL patients and 15 (68%) of the 23 solid tumor patients had grade 3 lymphopenia, although three of these NHL patients and four of these solid tumor patients had grade 3 lymphopenia at baseline. In the six patients treated with three or more courses of rhuCD40L, there was no increase in the incidence or severity of these hematopoietic toxicities, which when observed always initially occurred during the first course. One patient with renal cell carcinoma, bone metastases, and no evidence of bleeding developed asymptomatic grade 4 reduction in hemoglobin after two courses and was transfused two units of packed RBCs.

Other Toxicities

Other toxicities were generally mild to moderate (Table 3). Grade 3 toxicities included five patients with pain and one patient each with dyspnea, asthenia, dyspepsia, and pneumonia. A grade 3 seizure occurred in one patient who had completed radiation therapy for brain metastases eight months before treatment with rhuCD40L. One patient had two episodes of gastrointestinal bleeding (one grade 3 and one grade 4) relating to an invasive small bowel tumor. One patient developed a renal stone. Two deaths occurred on study, 26 and 30 days after the last dose of rhuCD40L, and each was due to disease progression.

Table 3. Adverse Events Other Than Hepatic and Hematologic Toxicities Occurring in ≥ 10% of All Patients (all grades, all courses)

	Solid Tumor (n = 23)						NHL (n = 9)							
	0.05 mg/kg/d (n = 4)		0.10 mg/kg/d (n = 15)*		0.15 mg/kg/d (n = 4)		0.05 mg/kg/d (n = 3)		0.10 mg/kg/d (n = 3)		0.15 mg/kg/d (n = 3)		Total (N = 32)	
	No.	%	No.	%	No.	%	No.	%	No.	%	No.	%	No.	%
Injection site reaction	2	50	9	60	3	75	0	0	2	67	3	100	23	72
Asthenia	3	75	6	38	0	0	2	67	0	0	1	33	12	38
Fever	2	50	3	19	1	25	2	67	1	33	1	33	10	31
Abdominal pain	3	75	4	25	0	0	1	33	1	33	0	0	9	28
Anorexia	2	50	3	19	0	0	2	67	1	33	0	0	8	25
Constipation	1	25	3	19	0	0	2	67	2	67	0	0	8	25
Dyspnea	2	50	3	19	1	25	2	67	0	0	0	0	8	25
Pain	2	50	3	19	1	25	1	33	1	33	0	0	8	25
Chills	1	25	1	6	1	25	0	0	1	33	1	33	5	16
Diarrhea	1	25	2	13	1	25	1	33	0	0	0	0	5	16
Nausea	2	50	2	13	1	25	0	0	0	0	0	0	5	16
Vasodilation	1	25	2	13	0	0	0	0	1	33	1	33	5	16
Vomiting	2	50	3	19	0	0	0	0	0	0	0	0	5	16
Back pain	2	50	1	6	0	0	0	0	1	33	0	0	4	13
Cough increase	1	25	2	13	0	0	0	0	1	33	0	0	4	13
Pruritus	0	0	1	6	1	25	2	67	0	0	0	0	4	13
Sinusitis	1	25	1	6	0	0	1	33	0	0	1	33	4	13
Tachycardia	1	25	1	6	0	0	0	0	2	67	0	0	4	13
Weight decrease	0	0	2	13	0	0	2	67	0	0	0	0	4	13

*One patient in the solid tumor group who received 0.15 mg/kg/d of rhuCD40L in courses 1 and 2 and 0.10 mg/kg/d in courses 3 and 4 is double-counted such that the denominator is 16 for calculating percentages.

ISRs were the only clinical adverse event that seemed to be dose-related, but were all grade 1 or 2. Among solid tumor patients, ISRs were observed in 50%, 60%, and 75% of patients treated with 0.05, 0.10, and 0.15 mg/kg/d, respectively. Among NHL patients, ISRs were observed in 100% of patients in the 0.15 mg/kg/d group compared with 0% at 0.05 mg/kg/d and 67% at 0.10 mg/kg/d.

One patient with renal cell carcinoma developed subclinical hypothyroidism after one course of rhuCD40L. This patient had received a 5-month course of interleukin-2 therapy 4 months before entering onto the study and was retrospectively found to have had elevated antithyroid peroxidase antibody levels (but normal thyroid function) before treatment with rhuCD40L. No other autoimmune sequelae were observed in patients on this study.

Antitumor Activity

Two patients (6%) had a partial tumor response while on study. One of these patients, a 60-year-old man with stage IV squamous cell carcinoma of the larynx that was progressive despite prior conventional and experimental therapy, had a more than 50% reduction in his laryngeal tumor mass after one course of 0.1 mg/kg/d of rhuCD40L. Prior therapy for recurrent disease included external-beam radiation, four single-agent chemotherapeutic agents, and a phase I agent targeted at the epidermal growth factor receptor. The partial response to rhuCD40L was sustained for 11 additional courses, and he was then taken off treatment after receiving 1 year of rhuCD40L without progression. He was subsequently observed while not receiving any anticancer therapy. Three months after discontinuing rhuCD40L, follow-up endoscopic examination revealed a complete tumor response, which was confirmed pathologically by biopsy 5 months later. The patient remains free of disease 1 year after completing rhuCD40L and 2 years after enrollment.

The second patient with a partial response had a more than 50% reduction in his NHL after one course of 0.05 mg/kg/d of rhuCD40L but was found to have progressive disease after two courses. Prior therapy included two regimens of chemotherapy and six treatments with external-beam radiation. Twelve patients (38%) had stable disease after one course of rhuCD40L, which was sustained in five patients after two courses. Four patients continued with stable disease through the fourth course.

Pharmacokinetics

Serum concentrations of rhuCD40L were barely detectable in the 0.05 mg/kg/d group. For 18 patients treated at 0.10 mg/kg/d and six patients treated at 0.15 mg/kg/d, absorption was rapid after subcutaneous administration, with peak serum concentrations generally observed within 4 hours after dosing. At the MTD of 0.10 mg/kg/d, the terminal half-life was 24.8

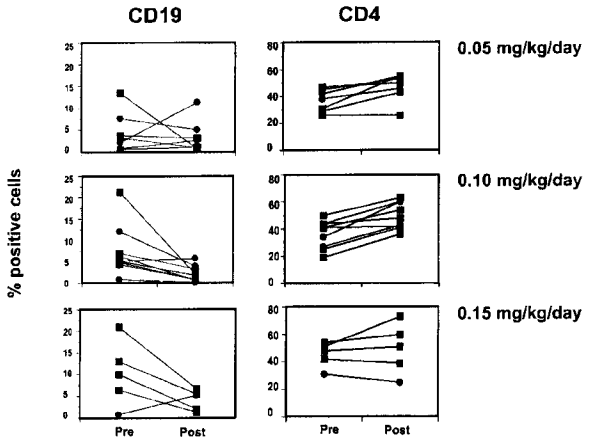

Fig 1. Analysis of CD19$^+$ and CD4$^+$ peripheral lymphocyte subsets from patients before and after the 5-day administration of rhuCD40L at 0.05, 0.10, or 0.15 mg/kg/d. ■, solid tumor patients; ●, NHL patients.

hours (SD, 22.8 hours; range, 12 to 73 hours). The maximum concentration at this dose was 2.9 ± 1.7 ng/mL, and the area under the curve from 0 to 24 hours was 41.6 ± 24.6 ng-hr/mL. There were no significant changes in pharmacokinetic parameters between dosing days.

Immunoassessment

Blood was obtained at baseline and on day 5 from 23 patients (15 with solid tumors and eight with NHL) to measure lymphocyte subsets by flow cytometry. Peripheral-blood mononuclear cells were obtained in sufficient numbers for analysis from 21 patients. For 16 of 21 patients, there was a decrease of at least 5% in the percentage of CD19$^+$ cells on day 5 compared with baseline ($P = .027$ by Fisher's exact test (StatXact 4, Cytel Software, Cambridge, MA), particularly evident at doses of 0.1 mg/kg/d and 0.15 mg/kg/d (Fig 1). In contrast, 17 of 21 patients had increases in the percentage of CD4$^+$ cells of at least 5% on day 5 relative to baseline ($P = .007$). There was no overall trend in the change of CD3$^+$, CD8$^+$, CD14$^+$, or CD16/CD56$^+$ cells before and after treatment (data not shown).

Serum obtained at baseline and on day 5 was used to measure polyclonal and antigen-specific antibody levels and levels of pro-inflammatory cytokines, including IL-12, MIP1α, MIP1β, and RANTES. No significant changes were observed before or after treatment in serum antibody or cytokine levels.

rhuCD40L Antibody

Samples were obtained from 31 of 32 patients for the measurement of antibodies to rhuCD40L, and two patients were confirmed to be positive. In one patient, antibodies developed after one of three courses and were still detectable in the serum 4 months later. This patient did not develop immune complex-related phenomenon nor any other adverse event related to the development of antibodies. In a second patient, anti-rhuCD40L antibodies were detected at day 14 of course 1, but the patient died of progressive disease on day 35 before further follow-up was possible.

DISCUSSION

rhuCD40L is a novel recombinant biologic agent whose receptor, CD40, is expressed on the surface of nearly all B-cell malignancies and the majority of solid tumors. Treatment of tumor cell lines in vitro or tumor-bearing animals in vivo with rhuCD40L leads to tumor death or tumor growth inhibition. Furthermore, CD40L (naturally expressed by activated T lymphocytes) is an important component of T-cell help for B-cell differentiation and provides costimulatory signals for T-cell clonal expansion.[11,19] CD40 ligation has been effectively exploited for the induction of antitumor immunity in several animal models.[39-41]

Here, we report the results of the first phase I clinical trial of rhuCD40L in the treatment of patients with advanced solid tumors and NHL. Thirty-two patients were given rhuCD40L subcutaneously daily for 5 days, which could be repeated every 4 to 6 weeks in the absence of progressive disease or toxicity. Overall, rhuCD40L was well tolerated. Based on transient elevations of liver transaminases, the MTD of this approach was 0.1 mg/kg/d every 4 weeks. The exact cause of the liver function test abnormalities is not known, but a cytotoxic effect of rhuCD40L on CD40$^+$ hepatic cells has been reported in one in vitro experimental model.[42] Anemia, leukopenia, and neutropenia were observed in less than 15% of patients, but only one patient required a blood transfusion, and none simultaneously developed fever. Injection site reactions were dose dependent in frequency but were never worse than grade 2. No autoimmune sequelae were observed except possibly for one patient with preexisting antithyroid peroxidase antibodies who developed subclinical hypothyroidism on study.

Two patients (6%) had a partial tumor response while on study. One of these patients, having achieved a sustained partial response of a laryngeal mass, discontinued rhuCD40L after 12 courses (approximately 1 year) and was observed while not receiving any anticancer therapy. After 3 months without therapy, he was found to have a complete response with the disappearance of the laryngeal mass, a finding that was confirmed pathologically on biopsy of the site. It is tempting to speculate that his transition from partial to complete response was immune-mediated, given

the delay in his tumor response, which is typical of T-cell–mediated antitumor effects.[43]

Determination of CD40 tumor expression was not required for study entry, although five of six pretreatment biopsies that were evaluated showed CD40 expression. Nevertheless, evaluation of a correlation between CD40 tumor expression, tumor response, and toxicity was not possible in this study. However, the potential stimulation of host professional antigen-presenting cells, such as dendritic cells, by treatment with rhuCD40L would be independent of tumor CD40 expression. In tumor-bearing mice, for example, treatment with trimeric CD40L has been shown to be effective against CD40-negative tumors.[40,41,44]

In this study, effects of rhuCD40L on the immune system were monitored in part by flow cytometry of peripheral blood. In 76% of the patients tested, there was a decrease in the percentage of circulating $CD19^+$ B lymphocytes on day 5 compared with baseline, possibly related to the peripheral clearance of these $CD40^+$ cells by binding to rhuCD40L. Such clearance was also observed in mice and nonhuman primates treated with CD40L (Armitage, unpublished observations). In contrast, the percentage of $CD4^+$ T lymphocytes increased during this time in 81% of patients. Levels of serum immunoglobulins and cytokines, such as IL-12, were unchanged, although in vitro CD40L treatment stimulates immunoglobulin class switching in B cells and cytokine production from monocytes, dendritic cells, and B cells. In contrast to preclinical animal testing, rhuCD40L did not lead to lymph node enlargement or splenomegaly in any of the patients.

Monomeric forms of CD40L signal inefficiently via CD40, whereas cross-linking of CD40 by trimeric CD40L or by certain antibodies against CD40 markedly enhances signaling.[24,45] RhuCD40L leads to a cascade of intracellular signals in B-cell lymphomas and $CD40^+$ solid tumor cells (Vonderheide and Battle, unpublished observations)[11]; however, the isoleucine-zipper motif used for trimerization of rhuCD40L presents a potential for the development of anti-rhuCD40L antibodies in patients. Although 94% of patients evaluated did not develop anti-rhuCD40L antibodies, two patients were confirmed to have developed such antibodies. There were no clinical adverse events related to the anti-rhuCD40L antibodies.

Pharmacokinetic monitoring of rhuCD40L serum levels indicated that absorption was rapid after subcutaneous administration. The terminal half-life was approximately 24 hours, but there was considerable variability at the MTD. Intravenous dosing of rhuCD40L is being compared with subcutaneous dosing in subsequent trials.

In summary, encouraging antitumor activity, including the induction of a long-term complete remission in one heavily pretreated patient, was observed in this phase I trial of rhuCD40L. The MTD of this dosing schedule was defined by transient elevations in liver transaminases, but other side effects were quite tolerable. Phase II studies are underway to further refine the dosing, toxicity, and efficacy of this novel agent. Given the observed hepatic toxicity in this study, phase II studies include interim evaluations and stopping rules for toxicity. Important additional end points for these subsequent studies will be correlation of efficacy with tumor CD40 expression and the assessment of the effect of rhuCD40L on patients' immune system. Ultimately, the combination of rhuCD40L with chemotherapy, radiotherapy, serotherapy, and other biologic therapy, as suggested by preclinical studies (unpublished observations),[44] will become an important goal.

REFERENCES

1. Banchereau J, Bazan F, Blanchard D, et al: The CD40 antigen and its ligand. Ann Rev Immunol 12:881-922, 1994

2. Young LS, Eliopoulos AG, Gallagher NJ, et al: CD40 and epithelial cells: Across the great divide. Immunol Today 19:502-506, 1998

3. Schultze J, Johnson P: A stimulating new target for cancer immunotherapy. Lancet 354:1225-1227, 1999

4. Stamenkovic I, Clark EA, Seed B: A B-lymphocyte activation molecule related to the nerve growth factor receptor and induced by cytokines in carcinomas. EMBO J 8:1403-1410, 1989

5. Vestal RE, Wingett DG, Knight LK, et al: Expression of CD40 in breast, colon, lung, and ovarian tumors. Proc Am Assoc Cancer Res 38:230, 1997 (abstr 1550)

6. Schultze JL, Cardoso AA, Freeman GJ, et al: Follicular lymphomas can be induced to present alloantigen efficiently: A conceptual model to improve their tumor immunogenicity. Proc Natl Acad Sci U S A 92:8200-8204, 1995

7. Schultze JL, Michalak S, Lowne J, et al: Human non-germinal center B cell interleukin (IL)-12 production is primarily regulated by T cell signals CD40 ligand, interferon gamma, and IL-10: Role of B cells in the maintenance of T cell responses. J Exp Med 189:1-12, 1999

8. Banchereau J, Rousset F: Growing human B lymphocytes in the CD40 system. Nature 353:678-679, 1991

9. Spriggs MK, Armitage RJ, Strockbine L, et al: Recombinant human CD40 ligand stimulates B cell proliferation and immunoglobulin E secretion. J Exp Med 176:1543-1550, 1992

10. Schultze JL, Michalak S, Seamon MJ, et al: CD40 activated human B cells: An alternative source of highly efficient antigen presenting cells to generate autologous antigen-specific T cells for adoptive immunotherapy. J Clin Invest 100:2757-2765, 1997

11. van Kooten C, Banchereau J: Functions of CD40 on B cells, dendritic cells and other cells. Curr Opin Immunol 9:330-337, 1997

12. Alderson MR, Armitage RJ, Tough TW, et al: CD40 expression by human monocytes: Regulation by cytokines and activation of monocytes by the ligand for CD40. J Exp Med 178:669-674, 1993

13. Caux C, Massacrier C, Vanbervliet B, et al: Activation of human dendritic cells through CD40 cross-linking. J Exp Med 180:1263-1272, 1994

14. Karmann K, Hughes CC, Schechner J, et al: CD40 on human endothelial cells: Inducibility by cytokines and functional regulation of adhesion molecule expression. Proc Natl Acad Sci U S A 92:4342-4346, 1995

15. Yellin MJ, Winikoff S, Fortune SM, et al: Ligation of CD40 on fibroblasts induces CD54 (ICAM-1) and CD106 (VCAM-1) up-regulation and IL-6 production and proliferation. J Leukoc Biol 58:209-216, 1995

16. Armitage RJ, Fanslow WC, Strockbine L, et al: Molecular and biological characterization of a murine ligand for CD40. Nature 357:80-82, 1992

17. Henn V, Slupsky JR, Grafe M, et al: CD40 ligand on activated platelets triggers an inflammatory reaction of endothelial cells. Nature 391:591-594, 1998

18. Allen RC, Armitage RJ, Conley ME, et al: CD40 ligand gene defects responsible for X-linked hyper-IgM syndrome. Science 259: 990-993, 1993

19. Grewal IS, Flavell RA: CD40 and CD154 in cell-mediated immunity. Ann Rev Immunol 16:111-135, 1998

20. Banchereau J, de Paoli P, Valle A, et al: Long-term human B cell lines dependent on interleukin-4 and antibody to CD40. Science 251:70-72, 1991

21. Ridge JP, Di Rosa F, Matzinger P: A conditioned dendritic cell can be a temporal bridge between a CD4+ T-helper and a T-killer cell. Nature 393:474-478, 1998

22. Bennett SR, Carbone FR, Karamalis F, et al: Help for cytotoxic-T-cell responses is mediated by CD40 signaling. Nature 393:478-480, 1998

23. Schoenberger SP, Toes RE, van der Voort EI, et al: T-cell help for cytotoxic T lymphocytes is mediated by CD40-CD40L interactions. Nature 393:480-483, 1998

24. Morris AE, Remmele RL Jr, Klinke R, et al: Incorporation of an isoleucine zipper motif enhances the biological activity of soluble CD40L (CD154). J Biol Chem 274:418-423, 1999

25. Funakoshi S, Longo DL, Beckwith M, et al: Inhibition of human B-cell lymphoma growth by CD40 stimulation. Blood 83:2787-2794, 1994

26. Hess S, Engelmann H: A novel function of CD40: Induction of cell death in transformed cells. J Exp Med 183:159-167, 1996

27. Eliopoulos AG, Dawson CW, Mosialos G, et al: CD40-induced growth inhibition in epithelial cells is mimicked by Epstein-Barr Virus-encoded LMP1: Involvement of TRAF3 as a common mediator. Oncogene 13:2243-2254, 1996

28. Murphy WJ, Asai O, Hirano A, et al: Inhibition of aggressive histology human B cell lymphoma growth by CD40 stimulation in vivo: A comparison of a CD40 antibody and a recombinant soluble CD40 ligand (srCD40L). Blood 88S:89a, 1996 (abstr 343)

29. Eliopoulos AG, Davies C, Knox PG, et al: CD40 induces apoptosis in carcinoma cells through activation of cytotoxic ligands of the tumor necrosis factor superfamily. Mol Cell Biol 20:5503-5515, 2000

30. Hirano A, Longo DL, Taub DD, et al: Inhibition of human breast carcinoma growth by a soluble recombinant human CD40 ligand. Blood 93:2999-3007, 1999

31. Wingett DG, Vestal RE, Forcier K, et al: CD40 is functionally expressed on human breast carcinomas: Variable inducibility by cytokines and enhancement of Fas-mediated apoptosis. Breast Cancer Res Treat 50:27-36, 1998

32. Degli-Eposti MA, Klinke R, Armitage RJ, et al: CD40 ligand, a potent growth factor, causes apoptosis of bladder carcinoma cell lines. Blood 86S:318a, 1995 (abstr 1261)

33. Schultze JL, Seamon MJ, Michalak S, et al: Autologous tumor infiltrating T cells cytotoxic for follicular lymphoma cells can be expanded in vitro. Blood 89:3806-3816, 1997

34. Cardoso AA, Seamon MJ, Afonso HM, et al: Ex vivo generation of human anti-pre-B leukemia-specific autologous cytolytic T cells. Blood 90:549-561, 1997

35. Kato K, Cantwell MJ, Sharma S, et al: Gene transfer of CD40-ligand induces autologous immune recognition of chronic lymphocytic leukemia B cells. J Clin Invest 101:1133-1141, 1998

36. Fisher DC, Van den Abbeele A, Singer S, et al: Phase I trial with CD40-activated follicular lymphoma cells: A novel cellular vaccine strategy for B cell malignancies. Blood 92S:247a, 1998 (abstr 1010)

37. Wierda WG, Cantwell MJ, Woods SJ, et al: CD40-ligand (CD154) gene therapy for chronic lymphocytic leukemia. Blood 96:2917-2924, 2000

38. Armitage RJ, Macduff BM, Spriggs MK, et al: Human B cell proliferation and Ig secretion induced by recombinant CD40 ligand are modulated by soluble cytokines. J Immunol 150:3671-3680, 1993

39. French RR, Chan HT, Tutt AL, et al: CD40 antibody evokes a cytotoxic T-cell response that eradicates lymphoma and bypasses T-cell help. Nat Med 5:548-553, 1999

40. Diehl L, den Boer AT, Schoenberger SP, et al: CD40 activation in vivo overcomes peptide-induced peripheral cytotoxic T-lymphocyte tolerance and augments anti-tumor vaccine efficacy. Nat Med 5:774-779, 1999

41. Sotomayor EM, Borrello I, Tubb E, et al: Conversion of tumor-specific CD4+ T-cell tolerance to T-cell priming through in vivo ligation of CD40. Nat Med 5:780-787, 1999

42. Afford SC, Randhawa S, Eliopoulos AG, et al: CD40 activation induces apoptosis in cultured human hepatocytes via induction of cell surface Fas ligand expression and amplifies Fas-mediated hepatocyte death during allograft rejection. J Exp Med 189:441-446, 1999

43. Alyea E: Adoptive immunotherapy: Insights from donor lymphocyte infusions. Transfusion 40:393-395, 2000

44. Borges L, Miller RE, Jones J, et al: Synergistic action of fms-like tyrosine kinase 3 ligand and CD40 ligand in the induction of dendritic cells and generation of antitumor immunity in vivo. J Immunol 163:1289-1297, 1999

45. Fanslow WC, Srinivasan S, Paxton R, et al: Structural characteristics of CD40 ligand that determine biological function. Semin Immunol 6:267-278, 1994

Prospect of Targeting the CD40 Pathway for Cancer Therapy

Robert H. Vonderheide

Abstract The cell surface molecule CD40 is a member of the tumor necrosis factor receptor superfamily and is broadly expressed by immune, hematopoietic, vascular, epithelial, and other cells, including a wide range of tumor cells. CD40 itself lacks intrinsic kinase or other signal transduction activity but rather mediates its diverse effects via an intricate series of downstream adapter molecules that differentially alter gene expression depending on cell type and microenvironment. As a potential target for novel cancer therapy, CD40 may mediate tumor regression through both an indirect effect of immune activation and a direct cytotoxic effect on the tumor, resulting in a "two-for-one" mechanism of action of CD40 agonists. Several drug formulations that target the CD40 pathway have undergone phase 1 clinical evaluation in advanced-stage cancer patients, and initial findings show objective clinical responses and immune modulation in the absence of major toxicity.

Background

CD40 is best appreciated as a critical regulator of cellular and humoral immunity via its expression on B lymphocytes, dendritic cells, and monocytes (1, 2). CD40 is also expressed on the cell surface of many other normal cells, including endothelial cells, fibroblasts, hematopoietic progenitors, platelets, and basal epithelial cells; the global physiologic effect of the CD40 signaling pathway is profound (1–4). CD40 ligand (CD40L), also known as CD154, is the chief ligand described for CD40 and is expressed primarily by activated T lymphocytes and platelets (2, 5). Atherosclerosis, graft rejection, coagulation, infection control, and autoimmunity are all regulated by CD40-CD40L interactions (1, 2). Curiously, many tumor cells also express CD40, including nearly 100% of B-cell malignancies and up to 70% of solid tumors. Successfully developing novel cancer therapies that target CD40 with an acceptable therapeutic index depends on an understanding of the complex biology of CD40.

CD40 signaling. The physiologic consequences of CD40 signaling are multifaceted, and even biologically opposed, depending on the type of cell expressing CD40 and the microenvironment in which the CD40 signal is provided. For example, CD40-CD40L engagement induces activation and proliferation of B lymphocytes but triggers apoptosis of carcinoma cells. Like some other members of the tumor necrosis factor (TNF) receptor family, CD40 signaling is mediated in large part by an intricate series of downstream adapter molecules rather than by inherent kinase or other signal transduction activity of the CD40 cytoplasmic tail (Fig. 1). As a consequence of CD40 signaling, a number of well-characterized signal transduction pathways are activated, including the nuclear factor-κB, p38 mitogen-activated protein kinase, c-Jun-NH_2-kinase, Janus kinases/signal transducers and activators of transcription, and phosphoinositide 3-kinase pathways (6). These pathways, in turn, regulate alterations in gene expression that are themselves extensive, dynamic, and variable. CD40 is well known to cooperate with, and even require in some cases, other extracellular signals that either induce overlapping downstream pathways or integrate others (Fig. 1). Some attempts have been made to characterize the global integration and regulation of CD40 signaling and gene expression (6); however, overall, a full appreciation of the CD40 circuitry at the level of systems biology remains incomplete. A great need exists for studies in primary cells other than B lymphocytes, primary malignant cells rather than transformed cell lines, and animal models.

CD40-induced immune activation. Signaling via CD40 activates antigen-presenting cells both *in vitro* and *in vivo*. Physiologically, this signal represents a major component of the process known as T-cell "help." Ligation of CD40 on dendritic cells, for example, induces cellular maturation and activation as manifested by increased surface expression of costimulatory and MHC molecules, production of proinflammatory cytokines such as interleukin 12, and enhanced T-cell activation (2, 4). CD40 ligation of resting B cells also increases antigen-presenting function and, in addition, induces proliferation and immunoglobulin class switching (2, 4). Patients with germ line mutations in either CD40 or CD40L are markedly immunosuppressed, susceptible to opportunistic infections, and have deficient T-cell–dependent immune reactions, including IgG production, germinal center formation, and memory B-cell induction (7–9). Similar immunophenotypes are observed in mice deficient in CD40 or CD40L (10–13).

In three articles published simultaneously in *Nature* in 1998, agonist CD40 antibodies were shown to mimic the signal of CD40L and substitute for the function of $CD4^+$ lymphocytes in murine models of T-cell–mediated immunity (14–16). A key

Author's Affiliation: Abramson Family Cancer Research Institute, University of Pennsylvania School of Medicine, Philadelphia, Pennsylvania
Received 7/28/06; accepted 8/3/06.
Grant support: National Cancer Institute grants R01 CA111377 and P50 CA093372.
Requests for reprints: Robert H. Vonderheide, Abramson Family Cancer Research Institute, University of Pennsylvania School of Medicine, 551 BRB II/III, 421 Curie Boulevard, Philadelphia, PA 19104. Phone: 215-573-4265; Fax: 215-573-2652; E-mail: rhv@mail.med.upenn.edu.

doi:10.1158/1078-0432.CCR-06-1893

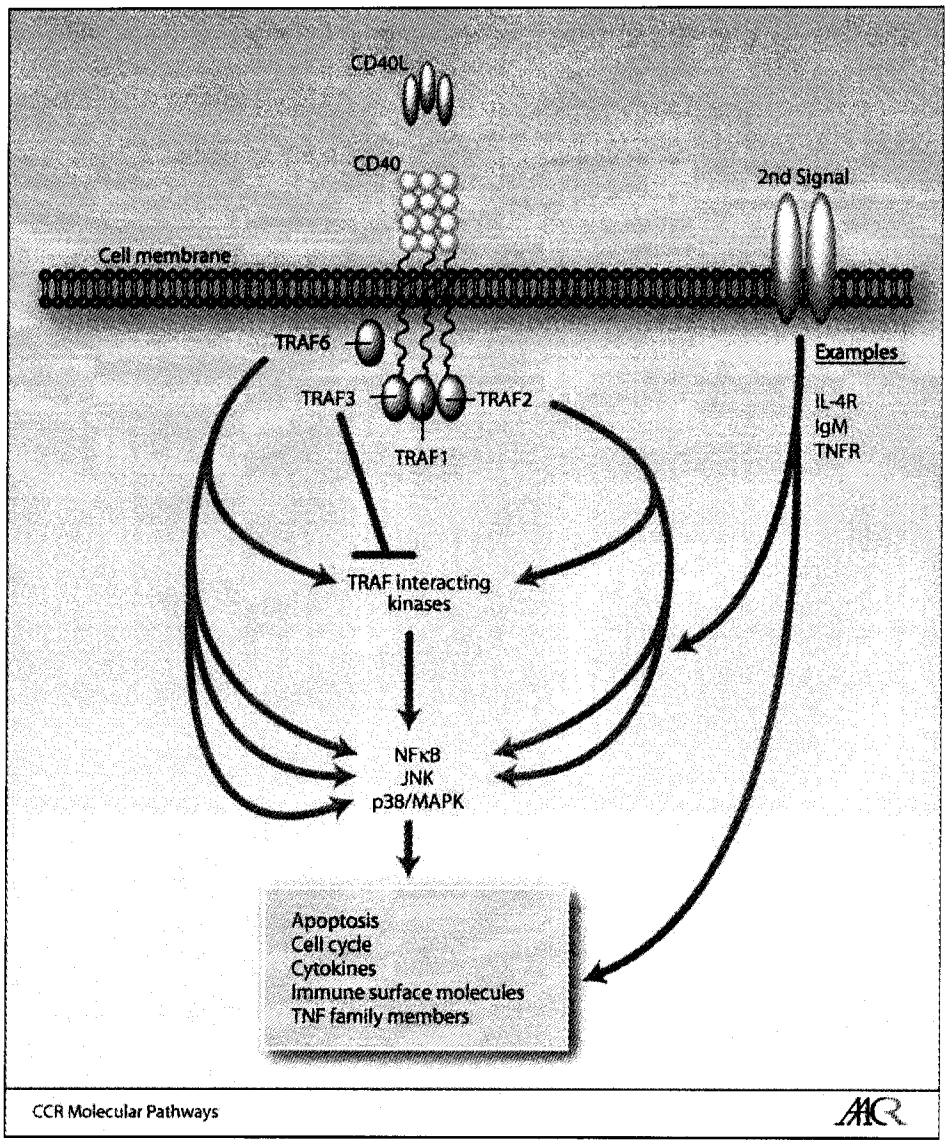

Fig. 1. The CD40 signaling pathway. Engagement of CD40 by multimeric CD40L causes redistribution of CD40 to membrane lipid rafts and a conformational change that recruits adapter molecules known as TNF receptor (*TNFR*) – associated factors (*TRAF*) to at least two distinct binding sites on the CD40 cytoplasmic tail (67, 68). TRAFs then recruit TRAF-interacting kinases and together influence a number of well-characterized signal transduction pathways, including the nuclear factor-κB, p38/mitogen-activated protein kinase (*MAPK*), and c-Jun-NH_2-kinase (*JNK*) pathways (6). TRAF2, for example, interacts with germinal center kinase in B cells and contributes to CD40-induced c-Jun-NH_2-kinase activation and cell proliferation (not shown; ref. 69). In another example, TRAF6 acts in concert with ubiquitin-activating/conjugating enzymes to activate TAK1 kinase complex and ultimately to induce nuclear factor-κB and p38/mitogen-activated protein kinase pathways (refs. 70, 71; not shown). In other circumstances, CD40-TRAF interactions have been shown to be inhibitory (72). Target genes of CD40 signaling regulate apoptosis, cell cycle progression, cytokine production, expression of cell surface immune modulators, and TNF family members and other pathways. Second extracellular signals cooperate with the CD40 signaling pathway, inducing overlapping responses or triggering others. Independent of TRAF-dependent signaling shown here, CD40 signaling can activate the Janus kinases/signal transducers and activators of transcription pathway, for example, via the binding of JAK3 to the CD40 cytoplasmic tail (73), as well as the phosphoinositide 3-kinase pathway (74–76).

mechanism of this effect was felt to be CD40/CD40L-mediated activation of host dendritic cells. These findings raised the hypothesis that CD40 agonists, together with signals involving toll-like receptors, might rescue the function of antigen-presenting cells in tumor-bearing hosts and trigger or restore effective immune responses against tumor-associated antigens. In 1999, three landmark articles in *Nature Medicine* provided the evidence for this hypothesis: agonist CD40 antibodies overcome T-cell tolerance in tumor-bearing mice, evoke effective cytotoxic T-cell responses, and enhance the efficacy of antitumor vaccines (17–19).

Consequences on survival and proliferation. Both proapoptotic and antiapoptotic genes affecting either the intrinsic or extrinsic pathways can be influenced by CD40 (20). In normal and certain malignant B cells, CD40 ligation rapidly rescues cells from apoptosis, an effect involving increased expression of bcl-xL, A20, and Bfl-1, each downstream from CD40-mediated nuclear factor-κB activation (21–24). The antiapoptotic protein survivin is also up-regulated by CD40 in some cells (25). On the other hand, CD40 may induce apoptosis in breast carcinoma cells by increased expression of Bax and in other cells by cooperation with members of the TNF family (26–30).

CD40 target genes also regulate cell cycle progression in certain cells, and, at least in B cells, seem to do so distinctly from the regulation of survival (31). For example, CD40 signaling in B cells increases expression and activation of the cyclin D-dependent kinases 4 and 6 and decreases expression of the cyclin-dependent kinase inhibitor p27kip-1 (32, 33). Pim-1, c-myc, Fas, and telomerase are other important gene products regulated by CD40 signaling (34-37), often in cooperation with second signals such as antigen-receptor ligation in B cells.

CD40-mediated tumor cell death. CD40 ligation on the surface of many tumors mediates a direct cytotoxic effect in the absence of immune accessory cells. CD40 expression is found in nearly all B-cell malignancies and many solid tumors, including melanoma and carcinomas of the lung, breast, colon, prostate, pancreas, kidney, ovary, and head and neck. Engagement of CD40 *in vitro* inhibits the growth of solid tumor cells and high-grade B cell lines, which in most experimental systems has been attributed to the induction of tumor cell apoptosis (29, 30, 38-41). CD40-mediated tumor inhibition has also been observed *in vivo*, including inhibition of breast carcinoma or B-cell lymphoma xenografts in immunocompromised mice in which there is no potential for confounding activation of lymphocytes (26, 38, 42, 43). It has always been puzzling why tumors, particularly epithelial tumors, express CD40, unless it is a remnant from ontogeny, organogenesis, or some other normal process of growth, differentiation, or response to inflammation (3). In primary cutaneous melanoma, CD40 expression has been reported to be a negative prognostic factor (44), yet the expression of CD40 in metastatic melanoma *in situ* is far weaker than in primary melanoma (41).

CD40-mediated tumor cell death seems at least additive and possibly synergic with chemotherapy both *in vitro* and *in vivo* (40, 43, 45). The combination of anti-CD40 agonist antibody and gemcitabine cures most mice with established implanted tumors, and cured mice are resistant to tumor rechallenge (45). This effect is absolutely dependent on CD8 T cells and independent of CD4 T cells and is only seen *in vivo* in the setting of tumor cell death. These findings highlight the hypothesis that immune activation and direct tumor cytotoxicity after systemic CD40 activation can be synergistic for antitumor effects.

Clinical Translational Advances

Several drug formulations that target the CD40 pathway have undergone phase 1 clinical evaluation in advanced-stage cancer patients, and initial results have been promising (Table 1). Most of these investigational drugs are designed as CD40 agonists, with a 2-fold rationale: First, CD40 agonists can trigger immune stimulation by activating host antigen-presenting cells, which then drive T-cell responses directed against tumors to cause tumor cell death. Second, CD40 ligation can impart direct tumor cytotoxicity on tumors that express CD40. Synergy develops if tumor antigens that are shed after a direct cytotoxic hit can be taken up by antigen-presenting cells during the activation process and confer tumor specificity to the resulting T-cell response.

Recombinant human CD40L, engineered with an isoleucine zipper motif to facilitate trimerization, was the first such investigational agent to be tested (46). In collaboration with two other clinic sites, we treated 32 patients with advanced solid tumors or non-Hodgkin's lymphoma with recombinant human CD40L s.c. daily for 5 days of each cycle (46). Transient elevations in serum transaminases were dose limiting, and serum half-life was ~24 h. Two patients had an objective partial response, one of whom was subsequently found to have a complete response several months after discontinuing recombinant human CD40L therapy although the patient had not initiated additional anticancer therapy.

Clinical efforts to target CD40 have accelerated in the past year with the development of anti-CD40 monoclonal

Table 1. Phase 1 studies of CD40-targeted therapy in cancer patients

Drug	Formulation	CD40 signaling	Patient population	Clinical trial findings	Reference
Recombinant CD40L	Recombinant human trimer	Agonist	Solid tumors or NHL (n = 32)	• Increased AST/ALT • Injection site reactions • 2 PR	Vonderheide et al. (46)
CP-870,893	Fully human IgG2 mAb	Agonist	Solid tumors (n = 29)	• CRS • 4 PR	Vonderheide et al. (49)
SGN-40	Humanized IgG1 mAb	Weak agonist	NHL (n = 29; ongoing)	• CRS • 4 PR, 1 CR	Forero-Torres et al. (53)
			Multiple myeloma (n = 23; ongoing)	• CRS • 4 patients with decreases in M-protein	Hussein et al. (54)
HCD 122	Fully human IgG1 mAb	Antagonist	CLL and multiple myeloma		Byrd et al. (77)* Bensinger et al. (78)*
CD40L-expressing CLL cells	Adenovirus gene therapy	Agonist	CLL (n = 11)	• Flu-like symptoms • Reductions in tumor burden	Wierda et al. (57)
Leukemia cells with CD40L and IL-2-expressing fibroblasts	Adenovirus gene therapy	Agonist	Acute or lymphoblastic leukemia in remission (n = 10)	• Well tolerated • 9 patients disease-free at median follow-up of 41 mo	Rousseau et al. (58)

Abbreviations: AST, aspartate aminotransferase; ALT, alanine aminotransferase; NHL, non-Hodgkin's lymphoma; PR, partial response; CR, complete response; CRS, cytokine release syndrome; CLL, chronic lymphocytic leukemia.
*See note added in proof.

antibodies (mAb). CP-870,893 (Pfizer, New London, CT) is a fully human CD40 agonist mAb that has both immune-mediated and nonimmune-mediated effects on tumor cell death (47, 48). CP-870,893 is an IgG2 immunoglobulin (in contrast to most approved mAbs, which are IgG1 immunoglobulins) and as such is unlikely to activate complement or bind Fc receptors efficiently. Any potential biological effect is felt to be primarily related to CD40 signaling. In collaboration with Scott Antonia and colleagues at Moffitt Cancer Center, we completed a first-in-human, dose-escalation trial of 29 patients with advanced solid tumors given single doses of CP-870,893 i.v. (49). The most common adverse event was cytokine release syndrome, which manifest as transient chills, rigors, and fevers on the day of infusion and associated with elevations of serum TNF-α and interleukin 6. CP-870,893–associated cytokine release syndrome most likely reflects CD40 activation of immune and vascular cells, rather than acute target lysis or hypersensitivity, given its fully human IgG2 formulation. Four partial responses were observed upon restaging at 7 weeks; all partial responses were in patients with melanoma. With repeated dosing every 6 to 8 weeks, one patient has a continued response ongoing at 14 months, associated with complete resolution of abnormal tracer activity on positron emission tomography scan.

Pharmacodynamic studies showed that CP-870,893 infusion results in a marked, rapid, and dose-dependent decrease in the percentage of B cells. Among B cells remaining in the blood, there was a rapid and dose-related up-regulation of CD86, a costimulatory molecule fundamental to T-cell activation (49). At the highest dose levels, the percentage of $CD86^+$ B cells increased >8-fold. From these and other findings, we hypothesize that CP-870,893 infusion activates (rather than destroys) peripheral blood B cells, leading to the extravasation of most B cells from the blood. A similar effect may occur for peripheral blood monocytes and dendritic cells after CP-870,893 infusion. Whether CP-870,893 infusion is associated with the induction of cellular tumor-specific immunity remains to be explored. A study of repeated doses of CP-870,893 is under way.

A second CD40 mAb, SGN-40 (Seattle Genetics, Bothell, WA), has been evaluated in two phase 1, dose-escalation studies in patients with relapsed or refractory non–Hodgkin's lymphoma and multiple myeloma, two diseases in which CD40 is nearly uniformly expressed. SGN-40 is a humanized IgG1 immunoglobulin and a weak agonist of CD40 signaling in blood mononuclear cells, including B cells (50). Against a panel of high-grade B-cell lymphoma cell lines, however, SGN-40 mediates potent growth inhibition and apoptosis and facilitates antibody-dependent cellular cytotoxicity (50–52). In one ongoing study, 29 patients with non–Hodgkin's lymphoma received weekly doses of SGN-40 over 4 to 5 weeks, with some patients treated with an intrapatient dose-loading schedule (53). Like CP-870,893, SGN-40 is associated with cytokine release syndrome, most pronounced with the first infusion and extinguished with subsequent dosing in the patients described thus far. Five non–Hodgkin's lymphoma patients have achieved objective tumor responses (four patients with partial response and one with a complete response after one cycle of SGN-40 ongoing at 20 weeks). The experience of 16 multiple myeloma patients treated thus far with SGN-40 has also been reported, with similar adverse events and encouraging antitumor activity (Table 1; ref. 54).

The clearance of both SGN-40 and CP-870,893 seems unusually rapid for IgG1 or IgG2 immunoglobulin molecules administered i.v. CP-870,893, for example, is detectable in serum for <24 h in the single-infusion study, possibly reflecting antibody binding to a broadly expressed target on normal cells (49). SGN-40 investigators suggest that there may be a rapid elimination pathway of SGN-40 or a redistribution volume that is not saturated at certain doses (54). Interestingly, the maximum tolerated dose of a single infusion of CP-870,893 is estimated at 0.2 mg/kg, but doses of SGN-40 at least up to 4 mg/kg have been tolerated in patients (49, 53). These findings may reflect differences in dosing schedules or differences in the agonistic or structural properties of the two mAbs that affect pharmacology or pharmacodynamics.

A third CD40 mAb, HCD 122 (formerly known as CHIR-12.12; Novartis/XOMA, Berkeley, CA), is a fully human IgG1 mAb that mediates antibody-dependent cellular cytotoxicity and blocks CD40L-induced cell survival and proliferation of normal and malignant B cells (55). Distinct from CP-870,893 or SGN-40, HCD 122 does not show any agonist activity in cell proliferation assays. HCD 122 is being tested in phase 1 clinical trial for patients with advanced B-cell malignancies.[1]

Other clinical approaches targeting CD40 in cancer include gene therapy to achieve expression of CD40L in autologous tumor cells before reinfusion. Engagement of CD40L enhances the antigen-presenting function of malignant B cells and enables these cells to generate antitumor immune responses (56). In one study, patients with chronic lymphocytic leukemia were administered autologous leukemia cells transduced with adenovirus encoding recombinant CD40L without major toxicity (57). Reductions in leukemic burden in some patients were associated with the induction of leukemia-specific T cells and increased serum interleukin 12. In another study, leukemic blasts administered with skin fibroblasts transduced with adenoviral vectors encoding human interleukin 2, and CD40L induced leukemic-specific T cells and antibodies after repeated injections (58). Gene therapy and other means can also be used *ex vivo* to activate antigen-presenting cells with CD40L (59, 60). Loaded with a tumor antigen payload, CD40-activated dendritic cells or B cells hold promise as novel cancer vaccines (61).

Most encouraging from these initial clinical trials has been the absence of major toxicity, in light of understandable concerns regarding the potential for CD40-mediated systemic inflammation and autoimmunity (62). In our studies with an agonist CD40 mAb, we have not observed enterocolitis, dermatitis, or hypophysitis that has been observed with other immunomodulatory agents, in particular, blocking anti-CTLA4 mAb (63). Although cytokine release syndrome has been observed with agonist CD40 mAb, the effects have been moderate and transient, and clinically and mechanistically distinct from multiorgan failure observed recently in subjects receiving a single dose of anti-CD28 agonist mAb (64).

Future Directions

Although initial phase 1 studies of CD40 agonists have already achieved objective tumor responses, possibly the

[1] Two additional studies have recently been published. Please see Note Added in Proof for further details.

greatest potential for these drugs will be in combination with other agents. These include chemotherapy, tumor vaccines, toll-like receptor agonists, cytokines, and other TNF receptor family agonists such as DR5 and CD137 mAb. Data from multiple preclinical models suggest the prospect of synergistically enhancing immune activation with such combinations (18, 19, 43, 45, 65, 66). CD40 agonists could also be combined with agents that block negative immune checkpoints (e.g., anti-CTLA4 mAb). Clinical trial designs testing these hypotheses will require careful consideration of both the basic immunology involved and the pharmacology and pharmacodynamics of the agents being investigated.

Note Added in Proof

Additional clinical trial data for SGN-40 and HCD 122 were reported at the annual meeting of the American Society of Hematology in December 2006. Of particular note, HCD 122 investigators reported two partial responses among 24 evaluable patients with chronic lymphocytic leukemia or multiple myeloma (77, 78). Treatment with HCD 122 was associated with transient infusion reactions.

Acknowledgments

I thank James Riley, Carolyn Clark, and Richard Huhn for helpful discussions.

References

1. Grewal IS, Flavell RA. CD40 and CD154 in cell-mediated immunity. Annu Rev Immunol 1998;16:111–35.
2. van Kooten C, Banchereau J. CD40-40 ligand. J Leukoc Biol 2000;67:2–17.
3. Young LS, Eliopoulos AG, Gallagher NJ, Dawson CW. CD40 and epithelial cells: across the great divide. Immunol Today 1998;19:502–6.
4. Quezada SA, Jarvinen LZ, Lind EF, Noelle RJ. CD40/CD154 interactions at the interface of tolerance and immunity. Annu Rev Immunol 2004;22:307–28.
5. Armitage RJ, Fanslow WC, Strockbine L, et al. Molecular and biological characterization of a murine ligand for CD40. Nature 1992;357:80–2.
6. Dadgostar H, Zarnegar B, Hoffmann A, et al. Cooperation of multiple signaling pathways in CD40-regulated gene expression in B lymphocytes. Proc Natl Acad Sci U S A 2002;99:1497–502.
7. Allen RC, Armitage RJ, Conley ME, et al. CD40 ligand gene defects responsible for X-linked hyper-IgM syndrome. Science 1993;259:990–3.
8. Ferrari S, Giliani S, Insalaco A, et al. Mutations of CD40 gene cause an autosomal recessive form of immunodeficiency with hyper IgM. Proc Natl Acad Sci U S A 2001;98:12614–9.
9. Etzioni A, Ochs HD. The hyper IgM syndrome—an evolving story. Pediatr Res 2004;56:519–25.
10. Castigli E, Alt FW, Davidson L, et al. CD40-deficient mice generated by recombination-activating gene-2-deficient blastocyst complementation. Proc Natl Acad Sci U S A 1994;91:12135–9.
11. Kawabe T, Naka T, Yoshida K, et al. The immune responses in CD40-deficient mice: impaired immunoglobulin class switching and germinal center formation. Immunity 1994;1:167–78.
12. Renshaw BR, Fanslow WC III, Armitage RJ, et al. Humoral immune responses in CD40 ligand-deficient mice. J Exp Med 1994;180:1889–900.
13. Xu J, Foy TM, Laman JD, et al. Mice deficient for the CD40 ligand. Immunity 1994;1:423–31.
14. Bennett SR, Carbone FR, Karamalis F, Flavell RA, Miller JF, Heath WR. Help for cytotoxic-T-cell responses is mediated by CD40 signalling. Nature 1998;393:478–80.
15. Ridge JP, Di Rosa F, Matzinger P. A conditioned dendritic cell can be a temporal bridge between a $CD4^+$ T-helper and a T-killer cell. Nature 1998;393:474–8.
16. Schoenberger SP, Toes RE, van der Voort EI, Offringa R, Melief CJ. T-cell help for cytotoxic T lymphocytes is mediated by CD40-40L interactions. Nature 1998;393:480–3.
17. French RR, Chan HT, Tutt AL, Glennie MJ. CD40 antibody evokes a cytotoxic T-cell response that eradicates lymphoma and bypasses T-cell help. Nat Med 1999;5:548–53.
18. Diehl L, den Boer AT, Schoenberger SP, et al. CD40 activation *in vivo* overcomes peptide-induced peripheral cytotoxic T-lymphocyte tolerance and augments anti-tumor vaccine efficacy. Nat Med 1999;5:774–9.
19. Sotomayor EM, Borrello I, Tubb E, et al. Conversion of tumor-specific $CD4^+$ T-cell tolerance to T-cell priming through *in vivo* ligation of CD40. Nat Med 1999;5:780–7.
20. Dallman C, Johnson PW, Packham G. Differential regulation of cell survival by CD40. Apoptosis 2003;8:45–53.
21. Choi MS, Boise LH, Gottschalk AR, Quintans J, Thompson CB, Klaus GG. The role of bcl-XL in CD40-mediated rescue from anti-μ-induced apoptosis in WEHI-231 B lymphoma cells. Eur J Immunol 1995;25:1352–7.
22. Sarma V, Lin Z, Clark L, et al. Activation of the B-cell surface receptor CD40 induces A20, a novel zinc finger protein that inhibits apoptosis. J Biol Chem 1995;270:12343–6.
23. Zhang X, Li L, Choe J, et al. Up-regulation of Bcl-xL expression protects CD40-activated human B cells from Fas-mediated apoptosis. Cell Immunol 1996;173:149–54.
24. Lee HH, Dadgostar H, Cheng Q, Shu J, Cheng G. NF-κB-mediated up-regulation of Bcl-x and Bfl-1/A1 is required for CD40 survival signaling in B lymphocytes. Proc Natl Acad Sci U S A 1999;96:9136–41.
25. Granziero L, Ghia P, Circosta P, et al. Survivin is expressed on CD40 stimulation and interfaces proliferation and apoptosis in B-cell chronic lymphocytic leukemia. Blood 2001;97:2777–83.
26. Wingett DG, Vestal RE, Forcier K, Hadjokas N, Nielson CP. CD40 is functionally expressed on human breast carcinomas: variable inducibility by cytokines and enhancement of Fas-mediated apoptosis. Breast Cancer Res Treat 1998;50:27–36.
27. Afford SC, Randhawa S, Eliopoulos AG, Hubscher SG, Young LS, Adams DH. CD40 activation induces apoptosis in cultured human hepatocytes via induction of cell surface fas ligand expression and amplifies fas-mediated hepatocyte death during allograft rejection. J Exp Med 1999;189:441–6.
28. Grell M, Zimmermann G, Gottfried E, et al. Induction of cell death by tumour necrosis factor (TNF) receptor 2, CD40 and CD30: a role for TNF-R1 activation by endogenous membrane-anchored TNF. EMBO J 1999;18:3034–43.
29. Eliopoulos AG, Davies C, Knox PG, et al. CD40 induces apoptosis in carcinoma cells through activation of cytotoxic ligands of the tumor necrosis factor superfamily. Mol Cell Biol 2000;20:5503–15.
30. Tong AW, Papayoti MH, Netto G, et al. Growth-inhibitory effects of CD40 ligand (CD154) and its endogenous expression in human breast cancer. Clin Cancer Res 2001;7:691–703.
31. Harnett MM. CD40: a growing cytoplasmic tale. Sci STKE 2004:pe25.
32. Ishida T, Kobayashi N, Tojo T, Ishida S, Yamamoto T, Inoue J. CD40 signaling-mediated induction of Bcl-XL, Cdk4, and Cdk6. Implication of their cooperation in selective B cell growth. J Immunol 1995;155:5527–35.
33. Han H, Nomura T, Honjo T, Tsubata T. Differential modulation of cyclin-dependent kinase inhibitor p27Kip1 by negative signaling via the antigen receptor of B cells and positive signaling via CD40. Eur J Immunol 1996;26:2425–32.
34. Zhu N, Ramirez LM, Lee RL, Magnuson NS, Bishop GA, Gold MR. CD40 signaling in B cells regulates the expression of the Pim-1 kinase via the NF-κB pathway. J Immunol 2002;168:744–54.
35. Schauer SL, Wang Z, Sonenshein GE, Rothstein TL. Maintenance of nuclear factor-κB/Rel and c-myc expression during CD40 ligand rescue of WEHI 231 early B cells from receptor-mediated apoptosis through modulation of IκB proteins. J Immunol 1996;157:81–6.
36. Galibert L, Burdin N, de Saint-Vis B, et al. CD40 and B cell antigen receptor dual triggering of resting B lymphocytes turns on a partial germinal center phenotype. J Exp Med 1996;183:77–85.
37. Igarashi H, Sakaguchi N. Telomerase activity is induced in human peripheral B lymphocytes by the stimulation to antigen receptor. Blood 1997;89:1299–307.
38. Funakoshi S, Longo DL, Beckwith M, et al. Inhibition of human B-cell lymphoma growth by CD40 stimulation. Blood 1994;83:2787–94.
39. Hess S, Engelmann H. A novel function of CD40: induction of cell death in transformed cells. J Exp Med 1996;183:159–67.
40. Eliopoulos AG, Dawson CW, Mosialos G, et al. CD40-induced growth inhibition in epithelial cells is mimicked by Epstein-Barr Virus-encoded LMP1: involvement of TRAF3 as a common mediator. Oncogene 1996;13:2243–54.
41. von Leoprechting A, van der Bruggen P, Pahl HL, Aruffo A, Simon JC. Stimulation of CD40 on immunogenic human malignant melanomas augments their cytotoxic T lymphocyte-mediated lysis and induces apoptosis. Cancer Res 1999;59:1287–94.
42. Hirano A, Longo DL, Taub DD, et al. Inhibition of human breast carcinoma growth by a soluble recombinant human CD40 ligand. Blood 1999;93:2999–3007.
43. Ghamande S, Hylander BL, Oflazoglu E, Lele S, Fanslow W, Repasky EA. Recombinant CD40 ligand therapy has significant antitumor effects on CD40-positive ovarian tumor xenografts grown in SCID mice and demonstrates an augmented effect with cisplatin. Cancer Res 2001;61:7556–62.
44. van den Oord JJ, Maes A, Stas M, et al. CD40 is a prognostic marker in primary cutaneous malignant melanoma. Am J Pathol 1996;149:1953–61.
45. Nowak AK, Robinson BW, Lake RA. Synergy between chemotherapy and immunotherapy in the treatment of established murine solid tumors. Cancer Res 2003;63:4490–6.
46. Vonderheide RH, Dutcher JP, Anderson JE, et al.

Phase I study of recombinant human CD40 ligand in cancer patients. J Clin Oncol 2001;19:3280–7.

47. Gladue R, Cole S, Donovan C, et al. *In vivo* efficacy of the CD40 agonist antibody CP-870,893 against a broad range of tumor types: impact of tumor CD40 expression, dendritic cells, and chemotherapy. J Clin Oncol 2006;24:103s.
48. Bedian V, Donovan C, Garder J, et al. *In vitro* characterization and pre-clinical pharmacokinetics of CP-870,893, a human anti-CD40 agonist antibody. J Clin Oncol 2006;24:109s.
49. Vonderheide RH, Flaherty KT, Khalil M, et al. Clinical activity and immune modulation in cancer patients treated with CP-870,893, a novel CD40 agonist monoclonal antibody. J Clin Oncol 2007, in press.
50. Law CL, Gordon KA, Collier J, et al. Preclinical antilymphoma activity of a humanized anti-CD40 monoclonal antibody, SGN-40. Cancer Res 2005;65:8331–8.
51. Tai YT, Catley LP, Mitsiades CS, et al. Mechanisms by which SGN-40, a humanized anti-CD40 antibody, induces cytotoxicity in human multiple myeloma cells: clinical implications. Cancer Res 2004;64:2846–52.
52. Kelley SK, Gelzleichter T, Xie D, et al. Preclinical pharmacokinetics, pharmacodynamics, and activity of a humanized anti-CD40 antibody (SGN-40) in rodents and non-human primates. Br J Pharmacol 2006;148:1116–23.
53. Forero-Torres A, Furman RR, Rosenblatt JD, Younes A, Harrop K, Drachman JG. A humanized antibody against CD40 (SGN-40) is well tolerated and active in non-Hodgkin's lymphoma (NHL): results of a phase 1 study. J Clin Oncol 2006;24:430s.
54. Hussein MA, Berenson JR, Niesvizky R, et al. A phase I humanized anti-CD40 monoclonal antibody (SGN-40) in patients with multiple myeloma [abstract 2572]. Blood 2005;106.
55. Tong X, Georgakis GV, Long L, O'Brien S, Younes A, Luqman M. *In vitro* activity of a novel fully human anti-CD40 antibody CHIR-12.12 in chronic lymphocytic leukemia: blockade of CD40 activation and induction of ADCC [abstract 2504]. Blood 2005;106.
56. Schultze JL, Cardoso AA, Freeman GJ, et al. Follicular lymphomas can be induced to present alloantigen efficiently: a conceptual model to improve their tumor immunogenicity. Proc Natl Acad Sci U S A 1995;92:8200–4.
57. Wierda WG, Cantwell MJ, Woods SJ, Rassenti LZ, Prussak CE, Kipps TJ. CD40-ligand (CD154) gene therapy for chronic lymphocytic leukemia. Blood 2000;96:2917–24.
58. Rousseau RF, Biagi E, Dutour A, et al. Immunotherapy of high-risk acute leukemia with a recipient (autologous) vaccine expressing transgenic human CD40L and IL-2 after chemotherapy and allogeneic stem cell transplantation. Blood 2006;107:1332–41.
59. Schultze JL, Michalak S, Seamon MJ, et al. CD40 activated human B cells: an alternative source of highly efficient antigen presenting cells to generate autologous antigen-specific T cells for adoptive immunotherapy. J Clin Invest 1997;100:2757–65.
60. Coughlin CM, Vance BA, Grupp SA, Vonderheide RH. RNA-transfected CD40-activated B cells induce functional T-cell responses against viral and tumor antigen targets: implications for pediatric immunotherapy. Blood 2004;103:2046–54.
61. Schultze J, Johnson P. A stimulating new target for cancer immunotherapy. Lancet 1999;354:1225–7.
62. Tong AW, Stone MJ. Prospects for CD40-directed experimental therapy of human cancer. Cancer Gene Ther 2003;10:1–13.
63. Kapadia D, Fong L. CTLA-4 blockade: autoimmunity as treatment. J Clin Oncol 2005;23:8926–8.
64. Farzaneh L, Kasahara N, Farzaneh F. The strange case of TGN1412. Cancer Immunol Immunother 2007;56:129–34.
65. Ahonen CL, Doxsee CL, McGurran SM, et al. Combined TLR and CD40 triggering induces potent $CD8^+$ T cell expansion with variable dependence on type I IFN. J Exp Med 2004;199:775–84.
66. Uno T, Takeda K, Kojima Y, et al. Eradication of established tumors in mice by a combination antibody-based therapy. Nat Med 2006;12:693–8.
67. Pham LV, Tamayo AT, Yoshimura LC, et al. A CD40 signalosome anchored in lipid rafts leads to constitutive activation of NF-κB and autonomous cell growth in B cell lymphomas. Immunity 2002;16:37–50.
68. McWhirter SM, Pullen SS, Holton JM, Crute JJ, Kehry MR, Alber T. Crystallographic analysis of CD40 recognition and signaling by human TRAF2. Proc Natl Acad Sci U S A 1999;96:8408–13.
69. Bishop GA, Hostager BS. The CD40-154 interaction in B cell-T cell liaisons. Cytokine Growth Factor Rev 2003;14:297–309.
70. Deng L, Wang C, Spencer E, et al. Activation of the IκB kinase complex by TRAF6 requires a dimeric ubiquitin-conjugating enzyme complex and a unique polyubiquitin chain. Cell 2000;103:351–61.
71. Wang C, Deng L, Hong M, Akkaraju GR, Inoue J, Chen ZJ. TAK1 is a ubiquitin-dependent kinase of MKK and IKK. Nature 2001;412:346–51.
72. Hostager BS, Bishop GA. Cutting edge: contrasting roles of TNF receptor-associated factor 2 (TRAF2) and TRAF3 in CD40-activated B lymphocyte differentiation. J Immunol 1999;162:6307–11.
73. Hanissian SH, Geha RS. Jak3 is associated with CD40 and is critical for CD40 induction of gene expression in B cells. Immunity 1997;6:379–87.
74. Ren CL, Morio T, Fu SM, Geha RS. Signal transduction via CD40 involves activation of lyn kinase and phosphatidylinositol-3-kinase, and phosphorylation of phospholipase Cγ2. J Exp Med 1994;179:673–80.
75. Fruman DA, Snapper SB, Yballe CM, et al. Impaired B cell development and proliferation in absence of phosphoinositide 3-kinase p85α. Science 1999;283:393–7.
76. Suzuki H, Terauchi Y, Fujiwara M, et al. Xid-like immunodeficiency in mice with disruption of the p85α subunit of phosphoinositide 3-kinase. Science 1999;283:390–2.
77. Byrd JC, Flinn IW, Khan KD, et al. Pharmacokinetics and pharmacodynamics from a first-in-human phase 1 dose escalation study with antagonist anti-CD40 antibody, HCD 122 (formerly CHIR-12.12), in patients with relapsed and refractory chronic lymphocytic leukemia [abstract 2837]. Blood 2006;108.
78. Bensinger W, Jagannath S, Becker PS, et al. A phase 1 dose escalation study of a fully human, antagonist anti-CD40 antibody, HCD 122 (formerly CHIR-12.12), in patients with relapsed and refractory multiple myeloma [abstract 3575]. Blood 2006;108.

VOLUME 25 · NUMBER 7 · MARCH 1 2007

JOURNAL OF CLINICAL ONCOLOGY ORIGINAL REPORT

Clinical Activity and Immune Modulation in Cancer Patients Treated With CP-870,893, a Novel CD40 Agonist Monoclonal Antibody

Robert H. Vonderheide, Keith T. Flaherty, Magi Khalil, Molly S. Stumacher, David L. Bajor, Natalie A. Hutnick, Patricia Sullivan, J. Joseph Mahany, Maryann Gallagher, Amy Kramer, Stephanie J. Green, Peter J. O'Dwyer, Kelli L. Running, Richard D. Huhn, and Scott J. Antonia

From the Abramson Family Cancer Research Institute, Abramson Cancer Center, Division of Hematology-Oncology, Department of Medicine, University of Pennsylvania School of Medicine, Philadelphia, PA; Thoracic Oncology Program, Department of Interdisciplinary Oncology, H. Lee Moffitt Cancer Center and Research Institute, University of South Florida College of Medicine, Tampa, FL; and Pfizer Inc, New London, CT.

Submitted July 19, 2006; accepted December 4, 2006.

Supported by Pfizer Inc, New London, CT, and by National Cancer Institute Grant No. P50 CA093372 (R.H.V.).

Authors' disclosures of potential conflicts of interest and author contributions are found at the end of this article.

Address reprint requests to Robert H. Vonderheide, MD, PhD, Abramson Family Cancer Research Institute, University of Pennsylvania School of Medicine, 551 BRB II/III, 421 Curie Blvd, Philadelphia, PA 19104; e-mail: rhv@mail.med.upenn.edu.

0732-183X/07/2507-876/$20.00

DOI: 10.1200/JCO.2006.08.3311

ABSTRACT

Purpose
The cell-surface molecule CD40 activates antigen-presenting cells and enhances immune responses. CD40 is also expressed by solid tumors, but its engagement results in apoptosis. CP-870,893, a fully human and selective CD40 agonist monoclonal antibody (mAb), was tested for safety in a phase I dose-escalation study.

Patients and Methods
Patients with advanced solid tumors received single doses of CP-870,893 intravenously. The primary objective was to determine safety and the maximum-tolerated dose (MTD). Secondary objectives included assessment of immune modulation and tumor response.

Results
Twenty-nine patients received CP-870,893 in doses from 0.01 to 0.3 mg/kg. Dose-limiting toxicity was observed in two of seven patients at the 0.3 mg/kg dose level (venous thromboembolism and grade 3 headache). MTD was estimated as 0.2 mg/kg. The most common adverse event was cytokine release syndrome (grade 1 to 2) which included chills, rigors, and fever. Transient laboratory abnormalities affecting lymphocytes, monocytes, platelets, D-dimer and liver function tests were observed 24 to 48 hours after infusion. Four patients with melanoma (14% of all patients and 27% of melanoma patients) had objective partial responses at restaging (day 43). CP-870,893 infusion resulted in transient depletion of CD19+ B cells in blood (93% depletion at the MTD for < 1 week). Among B cells remaining in blood, we found a dose-related upregulation of costimulatory molecules after treatment.

Conclusion
The CD40 agonist mAb CP-870,893 was well tolerated and biologically active, and was associated with antitumor activity. Further studies of repeated doses of CP-870,893 alone and in combination with other antineoplastic agents are warranted.

J Clin Oncol 25:876-883. © 2007 by American Society of Clinical Oncology

INTRODUCTION

The cell-surface molecule CD40, a member of the tumor necrosis factor (TNF) receptor superfamily, broadly regulates immune activation, mediates tumor apoptosis, and has been studied as a target for novel cancer therapy.[1-3] CD40 is expressed by dendritic cells, B lymphocytes, monocytes, and other benign cells. Considerable data demonstrate that signaling via CD40 activates antigen-presenting cells (APCs)[1-5] including dendritic cells and B cells. The natural ligand for CD40 is CD154, which is expressed primarily on the surface of activated T lymphocytes[6] and provides a major component of T-cell "help" for immune responses.[7-9] Agonistic CD40 antibodies substitute for the function of CD4+ lymphocytes in murine models of T cell–mediated immunity.[7-9] In tumor-bearing hosts, CD40 agonists trigger effective immune responses against tumor-associated antigens.[10-13]

CD40 is also expressed on many tumor cells and mediates a direct cytotoxic effect.[2] CD40 expression has been reported on 30% to 70% of primary samples of human solid tumors, including melanoma and carcinomas. Engagement of CD40 on tumor cells results in apoptosis in vitro and impaired tumor growth in vivo.[14-18]

CP-870,893 is a fully human and selective CD40 agonist monoclonal antibody (mAb) and has both direct (non–immune-mediated) and indirect

(immune-mediated) effects on tumor cell death. CP-870,893 activates human APCs in vitro and inhibits growth of human tumors in both immune-deficient and immune-reconstituted SCID-beige mice.[19,20] Binding of CP-870,893 does not compete with CD154.

Here, we report results of the first human clinical trial of the agonistic CD40 mAb CP-870,893. This study was designed to determine the safety and maximum-tolerated dose (MTD) of a single intravenous infusion of CP-870,893 and to assess immune modulation and clinical activity in patients.

PATIENTS AND METHODS

Patients

Twenty-nine patients with advanced solid malignancies were enrolled between April 2004 and September 2005 at the Abramson Cancer Center, University of Pennsylvania (Philadelphia, PA), and the H. Lee Moffitt Cancer Center, University of South Florida (Tampa, FL). This was the first human, open label, phase I dose-escalation study of a single intravenous infusion of CP-870,893. The protocol and informed consent forms were approved by the local institutional review boards. The primary objective was to determine the safety, tolerability, and MTD of a single dose of CP-870,893. Secondary objectives were to characterize pharmacokinetics, pharmacodynamics, immune modulation, and antitumor activity.

Patients had to be at least 18 years old with an Eastern Cooperative Oncology Group (ECOG) performance status of 0 to 1 and adequate end organ function. Signed informed consent was required. Patients with autoimmune disorders, coagulopathies, or major illness and those who were pregnant or lactating were excluded. Concurrent treatment with anticancer drugs was not allowed.

Study Design

At least three patients per dose level were enrolled, with additional patients enrolled in case of toxicity, which was graded according to National Cancer Institute (NCI) Common Terminology Criteria for Adverse Events version 3.0. Dose-limiting toxicity (DLT) was defined as treatment-related nonhematologic grade 3 to 4 adverse events despite optimal supportive care; grade 3 hematologic adverse events, other than lymphopenia, that do not recover to grade 0 to 1 or baseline; grade 4 lymphopenia if complicated by infection or other grade 4 hematologic adverse event; or grade 2 or worse infusion reaction that affects vital organs. The MTD was estimated as the highest dose at which fewer than two of six patients experienced DLT. CP-870,893 was supplied by Pfizer Inc (New London, CT) as a solution in vials containing 10 mg/mL of IgG2 protein.

Study Procedures

Patients were evaluated for adverse events for 6 weeks. A panel of 12 autoantibodies were measured at baseline and day 43. Serum for pharmacokinetics and to determine human antihuman antibodies was obtained at baseline and various times after infusion. Plasma levels of TNF alpha (TNF-α), interleukin-6 (IL-6), and tryptase were determined by enzyme-linked immunosorbent assay (ELISA) at baseline and within 1 hour of infusion.

Tumor Response

Tumor response was assessed according to Response Evaluation Criteria in Solid Tumors (RECIST).

Pharmacokinetics of CP-870,893

Serum CP-870,893 concentrations determined using CD40-hu-Ig (Pfizer, Groton, CT) and a validated sandwich enzyme immunoassay (Alta Analytic Laboratory, San Diego, CA). The lower limit of quantification for the assay was 0.0038 μg/mL, and the working range of the assay was 0.0038 to 0.090 μg/mL. Test samples were diluted 100-fold for assay, so the effective working range of the assay was 0.38 to 9.0 μg/mL. The mean intra-assay precision (as coefficient of variation) was 3.7% to 18.2%, and the mean inter-assay precision was 8.1% to 21.5%. Pharmacokinetic parameters were estimated using standard noncompartmental analytic techniques.

Pharmacodynamics of CP-870,893

Single-dose pharmacodynamics of CP-870,893 was assessed by flow cytometry of peripheral blood performed according to good laboratory practices. Peripheral-blood leukocytes were stained with the following mAbs: fluorescein isothiocyanate (FITC) -conjugated CD45 (leukocyte common antigen), PerCP-Cy5.5-conjugated CD19 (B cell marker), and phycoerythrin (PE) -conjugated CD86 (costimulatory molecule). Cells were analyzed using an FACSCaliber (Becton Dickinson, Mountain View, CA) and molecules of equivalent soluble fluorochrome (MESF) was calculated.

Statistical Analysis

SAS PROC MIXED (SAS Institute Inc, Cary, NC) was used to analyze the change from baseline of pharmacodynamic end points. A repeat measure analysis of variance was done with time (class variable), dose (continuous variable), and time-dose interaction terms. A heterogeneous autoregressive covariance structure [ARH[1]] was assumed for the repeat measures across time. Log values of the end points and of dose were used in the models.

RESULTS

Patient Characteristics, Toxicity, and Determination of MTD

Twenty-nine patients with advanced solid tumors were evaluated (Table 1). Six dose levels were explored, with the majority of patients treated with 0.2 mg/kg (n = 9) or 0.3 mg/kg (n = 7) of CP-870,893.

Table 1. Patient Characteristics (N = 29)

Characteristic	No.	%
Sex		
Male	15	52
Female	14	48
Age, years		
Median	60	
Range	23-79	
Race/ethnicity		
White	28	97
Asian	1	3
ECOG PS		
0	23	79
1	6	21
Tumor types		
Melanoma	15	52
Non-small-cell lung cancer	5	17
Sarcoma	3	10
Cholangiocarcinoma	2	7
Breast cancer	1	3
Thyroid cancer	1	3
Unknown primary	1	3
Mesothelioma	1	3
Tumor stage		
IV	27	100
III	2	
Prior treatment		
Chemotherapy	15	48
Radiation	12	41
Surgery	29	100
Immunotherapy	5	17
Investigational drug	3	10
Other	7	24

Abbreviation: ECOG PS, Eastern Cooperative Oncology Group performance status.

Infusion was well tolerated, and adverse events and abnormal laboratory values are summarized in Tables A1 and A2 (online only). Three DLT events were observed: venous thromboembolism (one patient at 0.3 mg/kg), grade 3 headache (one patient at 0.3 mg/kg), and grade 3 transient elevations in serum transaminases (one patient at 0.2 mg/kg). Because two patients in the 0.3 mg/kg cohort had DLT, the MTD was estimated as 0.2 mg/kg per the clinical protocol.

Cytokine Release Syndrome

The most common adverse event was dose-related cytokine release syndrome (CRS; grade 1 to 2). This syndrome was clinically evident within minutes to hours after infusion, manifested by varying combinations of chills, rigors, fever, rash, nausea, vomiting, muscle aches, and back pain. The syndrome was most pronounced in patients receiving 0.2 mg/kg or 0.3 mg/kg, and was associated in these patients with elevations in serum TNF-α and IL-6 (Fig 1). Serum tryptase levels were not elevated, indicating that the syndrome was not an anaphylactic or allergic reaction. Rigors were readily treated with meperidine, and the syndrome fully resolved within 24 hours in all but one patient, who experienced an ongoing and severe headache for 8 days after infusion (classified as a DLT). Prophylactic use of acetaminophen and antihistamines was instituted after the first two patients at 0.2 mg/kg dose level were noted to have grade 2 CRS, but this did not prevent grade 2 CRS in subsequent patients.

Hematologic Toxicity and Laboratory Abnormalities

Infusion of CP-870,893 was associated with dose-related and transient decreases peripheral lymphocytes, monocytes, and platelets (Figs 2A to 2C). The nadir was observed 24 to 48 hours after infusion. Recovery of counts was prompt and complete in most patients by day 8. This effect manifests as grade 3 lymphopenia in 11 patients and grade 4 lymphopenia in 2 patients. Three patients, each at the 0.3 mg/kg dose level, developed grade 2 thrombocytopenia. None of these abnormalities was considered a DLT.

Modest, transient elevations in serum D-dimer were observed in most patients treated at the two highest dose levels (Fig 2D). Similarly, there was an elevation in thrombin–antithrombin 3 complex formation on day 3 in most patients at the two highest dose levels (data not shown). Other standard coagulation parameters were not affected by CP-870,893 infusion. There were no signs of disseminated intravascular coagulation.

A patient with mesothelioma treated at 0.3 mg/kg developed dyspnea and hypoxia 1 hour after CP-870,893 was infused via a central venous catheter. The patient was found to have a thrombus in the superior vena cava associated with the catheter and was diagnosed with a pulmonary embolism (grade 4 thrombosis). He was treated with systemic anticoagulation. This patient had a history of a lower extremity deep venous thrombosis and had completed a course of coumadin before enrollment. The event was considered a DLT because attribution to study drug could not be ruled out.

Hepatic Toxicity

Dose-related, transient elevations in serum liver transaminases and total bilirubin were observed after infusion, peaking at 24 to 48 hours, and normalizing in most patients by day 8 (Figs 2E to 2G). One patient at 0.2 mg/kg was found to have asymptomatic grade 3 elevations in AST and ALT at 24 hours (considered a DLT), with resolution delayed until day 22. Another patient had grade 3 elevation of AST (but normal ALT and bilirubin) in the setting of pneumonia at day 15, which was not considered DLT. Five patients developed transient grade 1 or 2 hyperbilirubinemia.

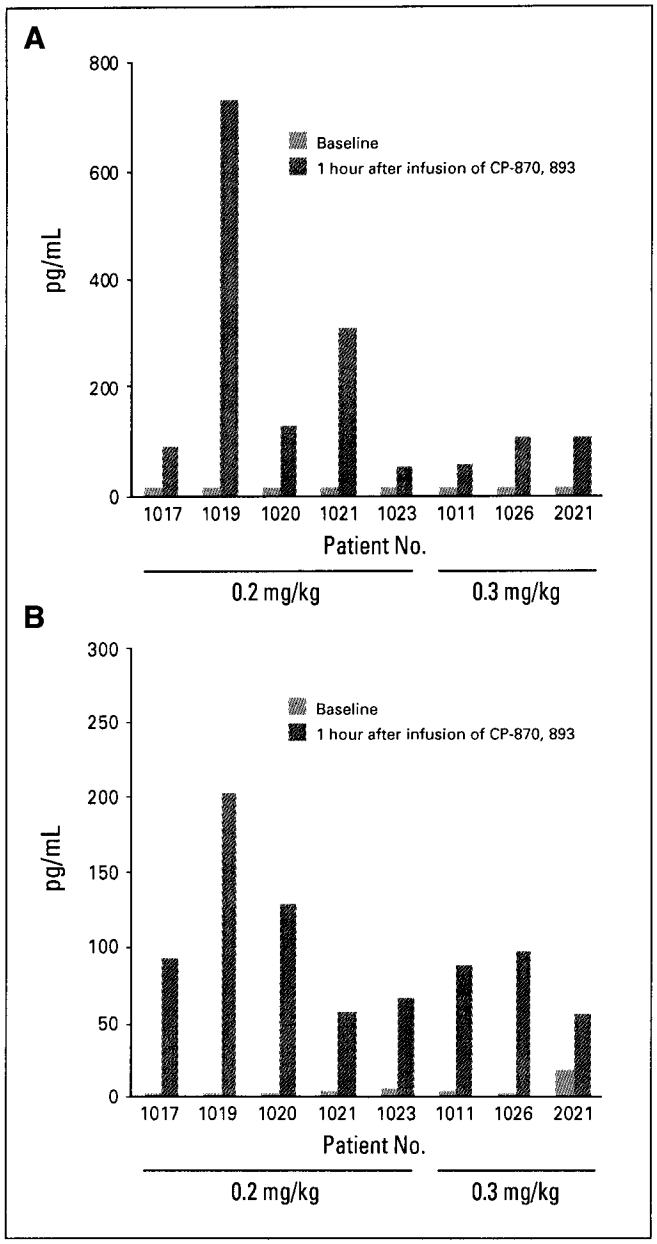

Fig 1. Serum cytokine concentrations before (yellow bars) and 1 hour after (blue bars) CP-870,893 in patients treated with 0.2 mg/kg (n = 5) or 0.3 mg/kg (n = 3). (A) tumor necrosis factor alpha; (B) interleukin-6.

Other Toxicities

Other adverse events included a grade 4 seizure, grade 3 pericardial effusion, and grade 3 bone pain, each related to progressive tumor (Table A1, online only). One patient developed pneumonia (grade 3) 2 weeks after treatment. Eight other grade 3 laboratory abnormalities were observed, but none was considered a DLT (Table A2, online only). Sixteen patients (55%) developed grade 1 (n = 11) or grade 2 (n = 5) proteinuria that was evident on day 2

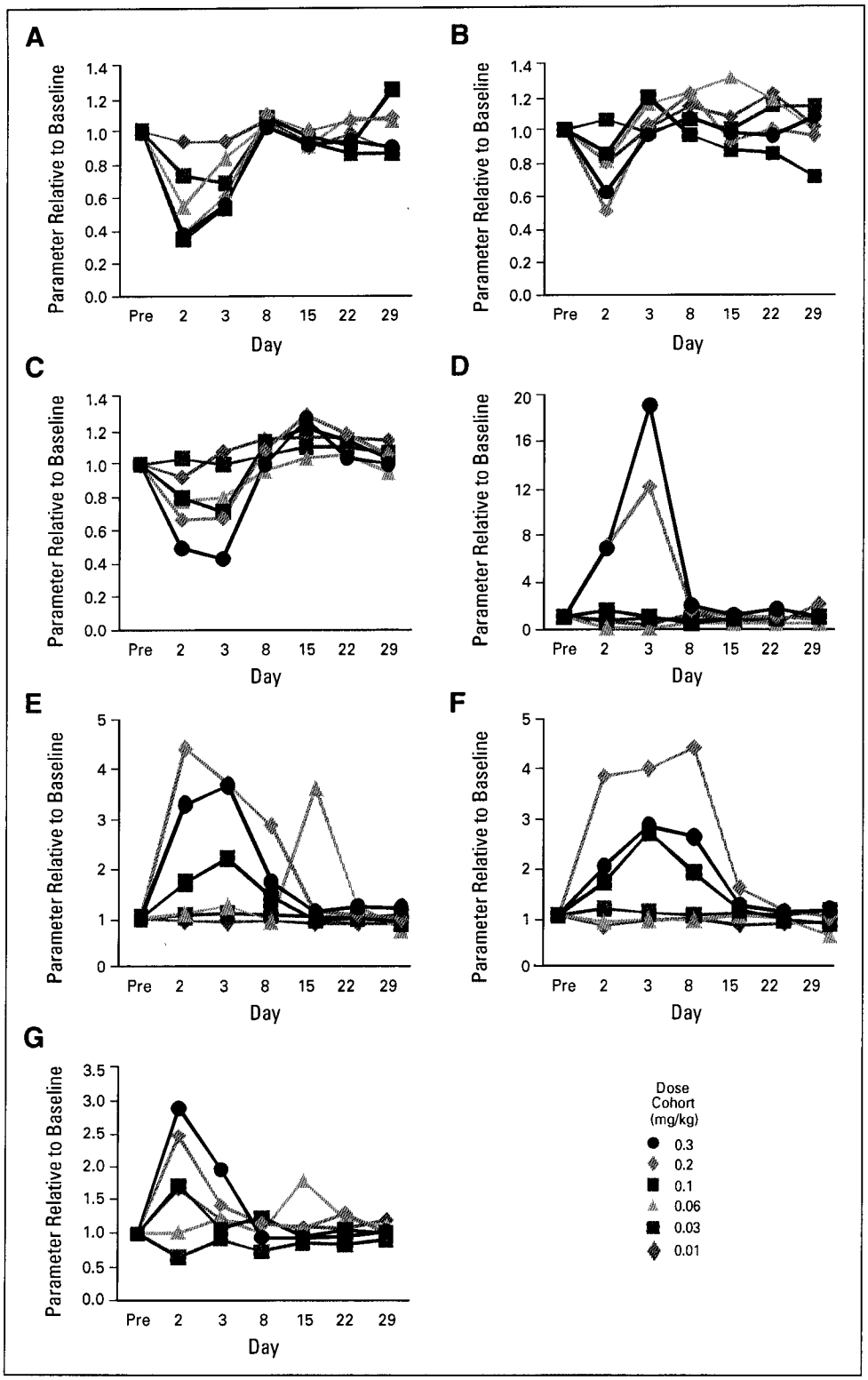

Fig 2. Change relative to baseline in hematologic and serum chemistry parameters after infusion of CP-870,893. (A) Absolute lymphocyte count (ALC); (B) absolute monocyte count (AMC); (C) platelets; (D) D-dimer (University of Pennsylvania patients only); (E) AST; (F) ALT; and (G) total bilirubin. Data are grouped for all patients in a given dose level cohort and reported as mean values. Blue diamonds, 0.01 mg/kg; red squares, 0.03 mg/kg; yellow triangles, 0.06 mg/kg; brown squares, 0.1 mg/kg; gray diamonds, 0.2 mg/kg; dark blue circles, 0.3 mg/kg.

and resolved by day 8. One patient developed a mild, asymptomatic elevated antinuclear antibody (1:160), and one patient developed a positive direct antiglobulin test. No human antihuman antibodies against CP-870,893 were identified.

Antitumor Activity

Four patients, each with stage IV melanoma, were found to have a partial response (PR) on restaging at the end of study (day 43; Table A3, online only). Three of these patients were treated with

0.2 mg/kg of CP-870,893, and one received 0.3 mg/kg. Each patient had progressive disease at the start of the study despite treatments including surgery (n = 4), chemotherapy (n = 2), radiation (n = 1), and high-dose interferon (n = 1). PR was evident by regression of lesions in the liver, skin, lung, and muscle. Overall, 14% of patients had an objective response, including 27% of patients with melanoma. Seven patients (24%) had stable disease (SD; Table A3, online only), including one patient with cholangiocarcinoma at the 0.06 mg/kg level who had regression of a large hepatic metastasis that did not meet RECIST criteria for PR. A patient with melanoma at the 0.2-mg/kg dose level had regression of pulmonary, lymph node, and subcutaneous lesions that met criteria for SD but not PR.

Redosing With CP-870,893

Seven patients with SD or PR were redosed with CP-870,893 without intervening anticancer therapy. The time to second dose of CP-870,893 was 2 to 4 months due to regulatory issues. Six patients had progressive disease after a second dose. One patient (0.2 mg/kg) had a sustained PR after the second dose and has subsequently been treated with seven additional doses (for a total of eight) at dosing intervals of roughly 2 months. At baseline, this patient had metastatic disease with a mass involving the left iliopsoas region (Fig 3). Restaging after six doses showed a nearly complete resolution of this disease and complete resolution of abnormal fluorodeoxyglucose tracer activity in this region and no evidence for disease anywhere else in the patient (Fig 3). The patient remains in partial remission at 14 months. Re-treatment was not associated with additional treatment-related toxicities.

Pharmacokinetics

Serum concentrations of CP-870,893 were measurable (> 0.38 μg/mL) only in patients treated with 0.1 mg/kg or more of CP-870,893 (Fig 4). At the highest dose level, CP-870,893 concentrations were measurable for only 8 hours after dosing. The half-life of CP-870,893 was not estimated at any dose level as it was felt to be extremely unlikely that the terminal disposition phase for a monoclonal antibody, such as CP-870,893, would be present as early as 8 hours after dosing.

Pharmacodynamics

To assess pharmacodynamic actions of CP-870,893, flow cytometry analysis was performed to evaluate CD19+ B cells in blood before and after treatment. We found that CP-870,893 infusion resulted in a marked, rapid, and dose-dependent decrease in the percentage of CD19+ B cells among peripheral-blood lymphocytes, with an effect evident within 1 hour of infusion and sustained for at least 2 days (Fig 5A). The peripheral-blood concentration of CD19+ B cells (ie, percentage of CD19+ B cells multiplied by the absolute lymphocyte count) also rapidly decreased, with a maximum effect observed at 24 hours for each dose level (Fig 5B). On average, for all patients, the concentration of CD19+ B cells decreased from 173 cells/mm^3 (standard deviation, 176 cells/mm^3) before treatment to 16 cells/mm^3 (standard deviation, 19 cells/mm^3) on day 2 (paired t test $P < .0001$).

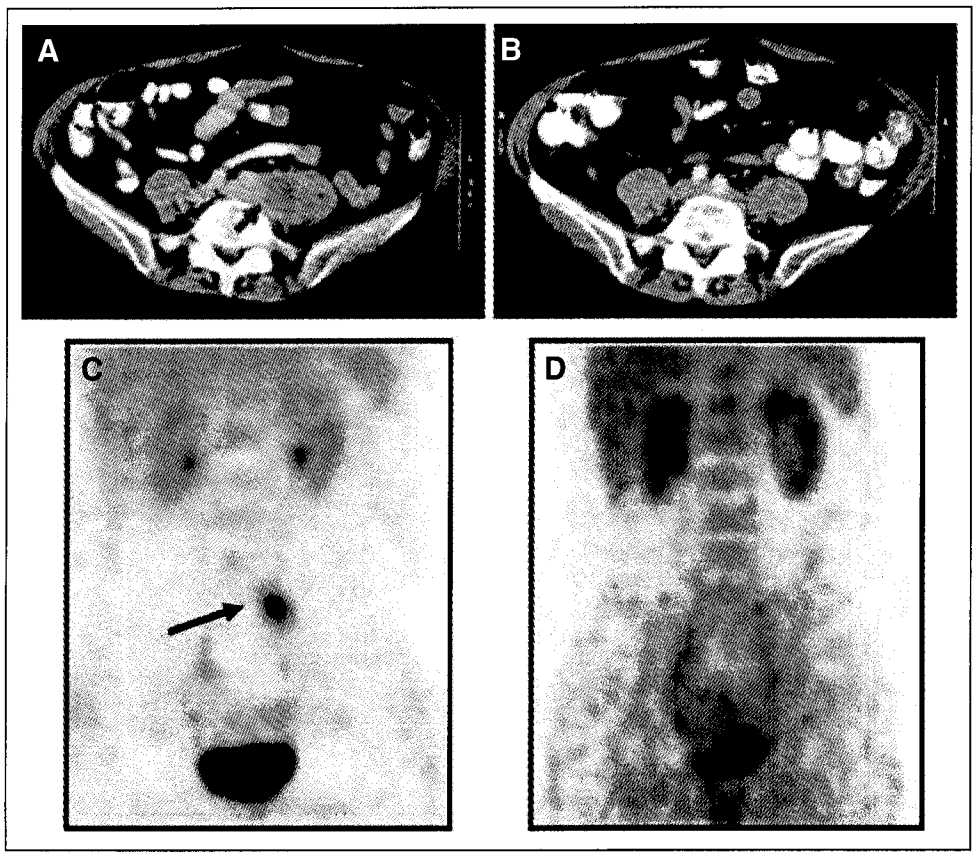

Fig 3. Tumor response to CP-870,893. (A, B) Radiographic evidence for objective partial response in patient 1017 and (C, D) fluorodeoxyglucose positron emission tomography images in same patient. (A, C) baseline; (B, D) after six doses of CP-870,893. Red arrow, metastatic disease at baseline; black arrow, abnormal tracer activity of tumor at baseline.

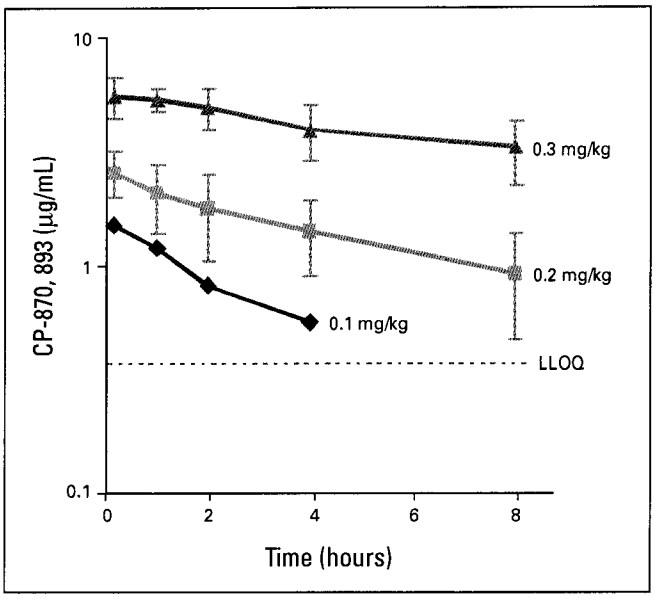

Fig 4. Serum concentration of CP-870,893 after a single, intravenous infusion at 0.1 mg/kg (n = 2 patients), 0.2 mg/kg (n = 9 patients), or 0.3 mg/kg (n = 5) of drug. Bars indicate standard deviation for patients at 0.3-mg/kg and 0.2-mg/kg dose levels. Standard deviations for the 0.1 mg/kg dose level are smaller than the size of the symbol. LLOQ, lower limit of quantification.

We then evaluated the expression of the costimulatory molecule CD86 on patient B cells before and after treatment as a potential pharmacodynamic effect of CP-870,893. Exposure of B cells to CP-870,893 in vitro upregulates CD86 without inducing apoptosis (Table A4, online only). In patients in vivo, we found a marked, rapid, and dose-related upregulation of the costimulatory molecule CD86 after infusion of CP-870,893. Both the percentage of CD86+ cells among CD19+ B cells and the MESF for CD86 among CD86+, CD19+ B cells increased after infusion (Fig 5C to 5D). At the highest dose levels, there was an eight- to 10-fold increase in the percentage of CD86+ cells and a 1.5- to 2.5-fold increase in the MESF of CD86.

Results of repeat-measure analysis of variance demonstrated that changes from baseline differed significantly over time for percentage of CD19+ B cells, percentage of CD86+, CD19+ B cells, and the MESF of CD86 on CD86+, CD19+ B cells ($P < .01$ for each). Changes from baseline at 1 hour, 8 hours, 2 days, and 3 days after infusion were significantly different from zero, whereas days 15 and 43 were not. There was also a linear association of log dose with change in percentage of CD19+ B cells and change in percentage of CD86+, CD19+ B cells, meaning that differences from baseline were larger for higher doses. Dose-time interactions were also significant, indicating that the dose relationships differed across time.

DISCUSSION

The purpose of this investigation was to evaluate the safety and biologic impact of treating cancer patients with a single intravenous infusion of CP-870,893, a fully human agonist mAb against the

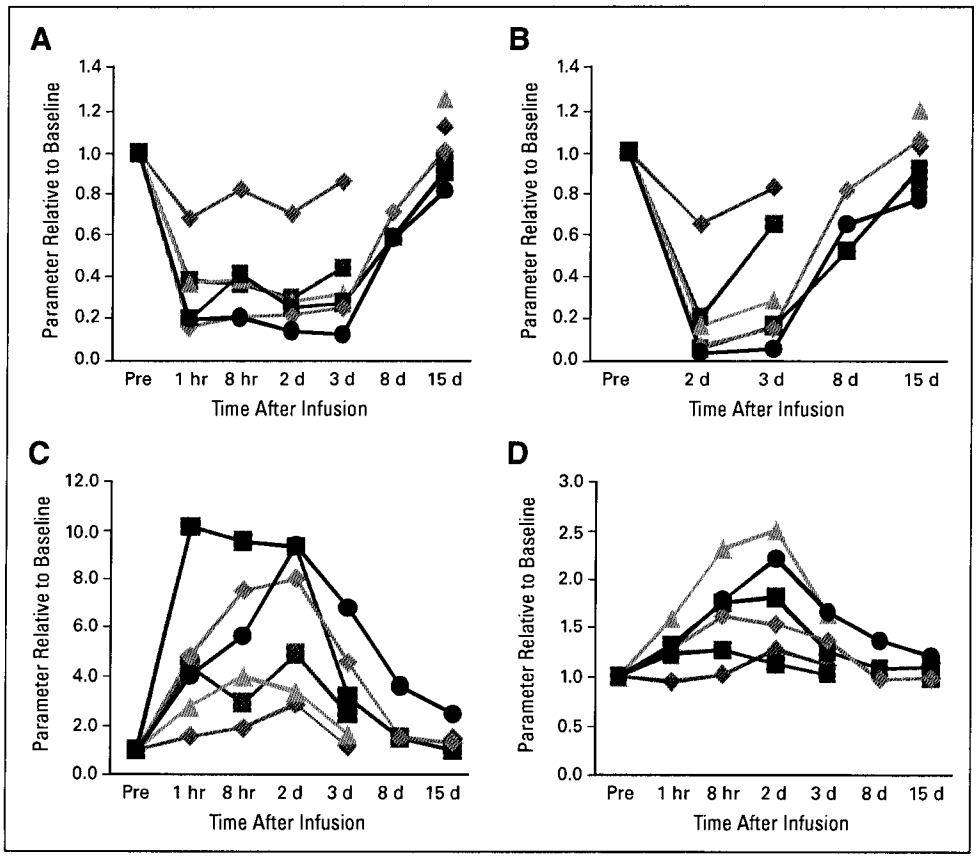

Fig 5. Pharmacodynamics of CP-870,893 after a single intravenous infusion. Parameters are shown relative to baseline. (A) Percentage of CD19+ B cells; (B) absolute $CD19^+$ B cell count; (C) percentage of CD86+ cells among CD19+ B cells; and (D) molecules of equivalent soluble fluorochrome (MESF) of CD86 expression among CD86+, CD19+ B cells. Data are grouped for all patients in a given dose-level cohort and reported as mean values. Blue diamonds, 0.01 mg/kg; orange squares, 0.03 mg/kg; yellow triangles, 0.06 mg/kg; brown squares, 0.1 mg/kg; gray diamonds, 0.2 mg/kg; dark blue circles, 0.3 mg/kg. hr, hour; d, day.

cell-surface molecule CD40. Treatment with a single infusion of CP-870,893 was well tolerated and was associated with objective tumor responses, including four patients with PR, of which one is sustained at 14 months and associated with complete resolution of abnormal tracer activity on fluorodeoxyglucose positron emission tomography. Clinical and pharmacodynamic evaluations demonstrate broad physiologic activation via CD40 after infusion.

The most common adverse event was transient grade 1 to 2 CRS, occurring in 55% of patients and associated with acute elevations in serum TNF-α and IL-6. Although the mechanism of CRS after CP-870,893 infusion is not fully understood, it is likely related to the mAb's binding its target on immune or vascular cells rather than hypersensitivity. CP-870,893 is a fully human molecule containing no murine sequences. It binds to Fc receptors poorly, which is typical of the immunoglobulin (Ig) G2 isotype. Other fully human non-CD40 IgG2 mAbs do not cause CRS.[21]

CP-870,893 binds to a wide variety of benign cells that express CD40, including lymphocytes, monocytes, platelets, endothelial cells, and hepatocytes. As a likely reflection of these interactions in vivo, a pattern of transient hematologic and metabolic laboratory abnormalities was observed after infusion, including decreased lymphocytes, monocytes, and platelets; elevated D-dimer; and elevated AST, ALT, and total bilirubin. For some parameters, the changes may reflect toxicity at the end organ. CD40+ hepatocytes, for example, undergo apoptosis after CD40 activation.[22] For lymphocytes, monocytes, and platelets, CP-870,893 most likely triggers alteration in circulation and extravasation, rather than apoptosis, given the rapidity of recovery. CD40 ligation on endothelium has complex effects, involving adhesion molecules, cytokines, chemokines, and coagulation factors.[23-27] D-dimer elevations in our patients may reflect low-grade activation of coagulation. In contrast to the 3-week half-life for other IgG2 mAbs,[21] the serum half-life of CP-870,893 is short, with the drug measurable in serum for less than 24 hours, a finding most likely related to binding of the antibody to a widely distributed target.

We observed objective PR in four patients with metastatic melanoma. The mechanism of tumor regression may involve an indirect effect of immune activation, a direct cytotoxic against CD40+ tumors cells, or both. Evaluation of tumor CD40 expression was not an eligibility criterion in this study. CD40 activation in tumor-bearing animals induces tumor-specific cytotoxic T lymphocytes, primarily through activation of APCs and cross presentation of tumor antigens[10-13] and even for tumors that are CD40 negative.[10,13] Direct cytotoxicity of tumor cells, including melanoma, after CD40 ligation has also been described.[2,17] Although CD40 is expressed in primary melanoma lesions in vivo, CD40 expression in metastatic lesions of melanoma is weak.[17] A lack of CD40 expression on metastatic melanoma would make a direct cytotoxic effect of CP-870,893 unlikely.

In a trial using human CD40-ligand (rhCD40L) as a CD40 agonist in cancer patients,[28] objective responses were also observed in the first human study but unlike in our experience with CP-870,893, CRS was not reported, and the MTD of rhCD40L was defined on the basis of transient elevations in serum transaminases.

CP-870,893 is a potent activator of CD40-expressing APCs in vitro.[1,5] To determine the pharmacodynamics of CP-870,893, we utilized flow cytometry to evaluate peripheral-blood CD19+ B cells, which uniformly express CD40. The in vitro effects of CD40 activation of human B cells, including upregulation of costimulatory molecules, are well described.[29,30] CP-870,893 infusion resulted in a rapid but transient decline in both the percentage and absolute count of CD19+ B cells in peripheral blood. B cells remaining in blood after treatment demonstrated a dose-related upregulation of CD86, but a difficulty with this assay is that the maximal effect of CD86 upregulation occurs at the time of maximal B-cell depletion. Activation of B cells no longer in circulation is unknown. Nevertheless, we hypothesize that CP-870,893 infusion globally activates (rather than destroys) peripheral-blood B cells, as evidenced by the rapid return of B cells into the circulation coincident with the decline of CP-870,893 plasma levels at 24 to 48 hours. A similar effect may occur for peripheral-blood monocytes and dendritic cells after CP-870,893 infusion. Whether CP-870,893 infusion is associated with enhanced tumor-antigen presentation and induction of cellular tumor-specific immunity remains to be explored in future studies.

AUTHORS' DISCLOSURES OF POTENTIAL CONFLICTS OF INTEREST

Although all authors completed the disclosure declaration, the following authors or their immediate family members indicated a financial interest. No conflict exists for drugs or devices used in a study if they are not being evaluated as part of the investigation. For a detailed description of the disclosure categories, or for more information about ASCO's conflict of interest policy, please refer to the Author Disclosure Declaration and the Disclosures of Potential Conflicts of Interest section in Information for Contributors.

Employment: Stephanie J. Green, Pfizer; Kelli L. Running, Pfizer; Richard D. Huhn, Pfizer **Leadership:** N/A **Consultant:** N/A **Stock:** Stephanie J. Green, Pfizer; Kelli L. Running, Pfizer; Richard D. Huhn, Pfizer **Honoraria:** Scott J. Antonia, Pfizer **Research Funds:** Robert H. Vonderheide, Pfizer; Peter J. O'Dwyer, Pfizer; Scott J. Antonia, Pfizer **Testimony:** N/A **Other:** N/A

AUTHOR CONTRIBUTIONS

Conception and design: Robert H. Vonderheide, Keith T. Flaherty, Peter J. O'Dwyer, Kelli L. Running, Richard D. Huhn, Scott J. Antonia
Financial support: Robert H. Vonderheide, Peter J. O'Dwyer
Administrative support: Robert H. Vonderheide, Amy Kramer, Peter J. O'Dwyer, Kelli L. Running, Scott J. Antonia
Provision of study materials or patients: Robert H. Vonderheide, Keith T. Flaherty, Peter J. O'Dwyer, Scott J. Antonia
Collection and assembly of data: Robert H. Vonderheide, Keith T. Flaherty, Magi Khalil, Molly S. Stumacher, David L. Bajor, Natalie A. Hutnick, Patricia Sullivan, J. Joseph Mahany, Maryann Gallagher, Amy Kramer, Peter J. O'Dwyer, Kelli L. Running, Richard D. Huhn, Scott J. Antonia
Data analysis and interpretation: Robert H. Vonderheide, Keith T. Flaherty, Magi Khalil, Molly S. Stumacher, David L. Bajor, Natalie A. Hutnick, Maryann Gallagher, Amy Kramer, Stephanie J. Green, Peter J. O'Dwyer, Kelli L. Running, Richard D. Huhn, Scott J. Antonia
Manuscript writing: Robert H. Vonderheide, Keith T. Flaherty, Stephanie J. Green, Richard D. Huhn, Scott J. Antonia
Final approval of manuscript: Robert H. Vonderheide, Keith T. Flaherty, Magi Khalil, Molly S. Stumacher, David L. Bajor, Natalie A. Hutnick, Patricia Sullivan, J. Joseph Mahany, Maryann Gallagher, Amy Kramer, Stephanie J. Green, Peter J. O'Dwyer, Kelli L. Running, Richard D. Huhn, Scott J. Antonia

REFERENCES

1. van Kooten C, Banchereau J: CD40-CD40 ligand. J Leukoc Biol 67:2-17, 2000
2. Eliopoulos AG, Young LS: The role of the CD40 pathway in the pathogenesis and treatment of cancer. Curr Opin Pharmacol 4:360-367, 2004
3. Tong AW, Stone MJ: Prospects for CD40-directed experimental therapy of human cancer. Cancer Gene Ther 10:1-13, 2003
4. Banchereau J, Bazan F, Blanchard D, et al: The CD40 antigen and its ligand. Annu Rev Immunol 12:881-922, 1994
5. Grewal IS, Flavell RA: CD40 and CD154 in cell-mediated immunity. Annu Rev Immunol 16:111-135, 1998
6. Armitage RJ, Fanslow WC, Strockbine L, et al: Molecular and biological characterization of a murine ligand for CD40. Nature 357:80-82, 1992
7. Bennett SR, Carbone FR, Karamalis F, et al: Help for cytotoxic-T-cell responses is mediated by CD40 signalling. Nature 393:478-480, 1998
8. Ridge JP, Di Rosa F, Matzinger P: A conditioned dendritic cell can be a temporal bridge between a CD4+ T- helper and a T-killer cell. Nature 393:474-478, 1998
9. Schoenberger SP, Toes RE, van der Voort EI, et al: T-cell help for cytotoxic T lymphocytes is mediated by CD40-CD40L interactions. Nature 393: 480-483, 1998
10. French RR, Chan HT, Tutt AL, et al: CD40 antibody evokes a cytotoxic T-cell response that eradicates lymphoma and bypasses T-cell help. Nat Med 5:548-553, 1999
11. Diehl L, den Boer AT, Schoenberger SP, et al: CD40 activation in vivo overcomes peptide-induced peripheral cytotoxic T-lymphocyte tolerance and augments anti-tumor vaccine efficacy. Nat Med 5:774-779, 1999
12. Sotomayor EM, Borrello I, Tubb E, et al: Conversion of tumor-specific CD4+ T-cell tolerance to T-cell priming through in vivo ligation of CD40. Nat Med 5:780-787, 1999
13. van Mierlo GJ, den Boer AT, Medema JP, et al: CD40 stimulation leads to effective therapy of CD40(-) tumors through induction of strong systemic cytotoxic T lymphocyte immunity. Proc Natl Acad Sci U S A 99:5561-5566, 2002
14. Hess S, Engelmann H: A novel function of CD40: Induction of cell death in transformed cells. J Exp Med 183:159-167, 1996
15. Wingett DG, Vestal RE, Forcier K, et al: CD40 is functionally expressed on human breast carcinomas: Variable inducibility by cytokines and enhancement of Fas-mediated apoptosis. Breast Cancer Res Treat 50:27-36, 1998
16. Hirano A, Longo DL, Taub DD, et al: Inhibition of human breast carcinoma growth by a soluble recombinant human CD40 ligand. Blood 93:2999-3007, 1999
17. von Leoprechting A, van der Bruggen P, Pahl HL, et al: Stimulation of CD40 on immunogenic human malignant melanomas augments their cytotoxic T lymphocyte-mediated lysis and induces apoptosis. Cancer Res 59:1287-1294, 1999
18. Eliopoulos AG, Davies C, Knox PG, et al: CD40 induces apoptosis in carcinoma cells through activation of cytotoxic ligands of the tumor necrosis factor superfamily. Mol Cell Biol 20:5503-5515, 2000
19. Bedian V, Donovan C, Garder J, et al: In vitro characterization and pre-clinical pharmacokinetics of CP-870,893, a human anti-CD40 agonist antibody. J Clin Oncol 24:109s, 2006 (suppl; abstr 2539)
20. Gladue R, Cole S, Donovan C, et al: In vivo efficacy of the CD40 agonist antibody CP-870,893 against a broad range of tumor types: Impact of tumor CD40 expression, dendritic cells, and chemotherapy. J Clin Oncol 24:103s, 2006 (suppl; abstr 2514)
21. Ribas A, Camacho LH, Lopez-Berestein G, et al: Antitumor activity in melanoma and anti-self responses in a phase I trial with the anti-cytotoxic T lymphocyte-associated antigen 4 monoclonal antibody CP-675,206. J Clin Oncol 23:8968-8977, 2005
22. Afford SC, Randhawa S, Eliopoulos AG, et al: CD40 activation induces apoptosis in cultured human hepatocytes via induction of cell surface fas ligand expression and amplifies fas-mediated hepatocyte death during allograft rejection. J Exp Med 189:441-446, 1999
23. Karmann K, Hughes CC, Schechner J, et al: CD40 on human endothelial cells: Inducibility by cytokines and functional regulation of adhesion molecule expression. Proc Natl Acad Sci U S A 92:4342-4346, 1995
24. Dechanet J, Grosset C, Taupin JL, et al: CD40 ligand stimulates proinflammatory cytokine production by human endothelial cells. J Immunol 159: 5640-5647, 1997
25. Zhou L, Stordeur P, de Lavareille A, et al: CD40 engagement on endothelial cells promotes tissue factor-dependent procoagulant activity. Thromb Haemost 79:1025-1028, 1998
26. Miller DL, Yaron R, Yellin MJ: CD40L-CD40 interactions regulate endothelial cell surface tissue factor and thrombomodulin expression. J Leukoc Biol 63:373-379, 1998
27. Thienel U, Loike J, Yellin MJ: CD154 (CD40L) induces human endothelial cell chemokine production and migration of leukocyte subsets. Cell Immunol 198:87-95, 1999
28. Vonderheide RH, Dutcher JP, Anderson JE, et al: Phase I study of recombinant human CD40 ligand in cancer patients. J Clin Oncol 19:3280-3287, 2001
29. Schultze JL, Michalak S, Seamon MJ, et al: CD40 activated human B cells: An alternative source of highly efficient antigen presenting cells to generate autologous antigen-specific T cells for adoptive immunotherapy. J Clin Invest 100:2757-2765, 1997
30. Coughlin CM, Vance BA, Grupp SA, et al: RNA-transfected CD40-activated B cells induce functional T-cell responses against viral and tumor antigen targets: Implications for pediatric immunotherapy. Blood 103:2046-2054, 2004

Acknowledgment

We thank DuPont Guerry, Lynn Schuchter, Charles Abrams, Colleen Redlinger, and Ambika Sohal (University of Pennsylvania), Patrick Stauffer, Sem Bastien, and Michael Langevin (Moffitt), and Vahe Bedian, Ronald Gladue, Antonio Gualberto, and Dennis Noe (Pfizer).

Appendix

The Appendix is included in the full-text version of this article, available online at www.jco.org. It is not included in the PDF version (via Adobe® Reader®).

APPENDIX D

OTHER REFERENCES

CITED IN REPLY

Combined TLR/CD40 Stimulation Mediates Potent Cellular Immunity by Regulating Dendritic Cell Expression of CD70 In Vivo[1]

Phillip J. Sanchez,* Jennifer A. McWilliams,* Catherine Haluszczak,* Hideo Yagita,† and Ross M. Kedl[2]*

We previously showed that immunization with a combination of TLR and CD40 agonists (combined TLR/CD40 agonist immunization) resulted in an expansion of Ag-specific CD8 T cells exponentially greater than the expansion observed to immunization with either agonist alone. We now show that the mechanism behind this expansion of T cells is the regulated expression of CD70 on dendritic cells. In contrast to previous results in vitro, the expression of CD70 on dendritic cells in vivo requires combined TLR/CD40 stimulation and is not significantly induced by stimulation of either pathway alone. Moreover, the exponential expansion of $CD8^+$ T cells following combined TLR/CD40 agonist immunization is CD70 dependent. Thus, the transition from innate stimuli (TLRs) to adaptive immunity is controlled by the regulated expression of CD70. *The Journal of Immunology,* **2007, 178: 1564–1572.**

It is generally agreed upon that the successful immunotherapeutic treatment of chronic infectious diseases and cancer requires the generation of a strong cellular immune response. Vaccines based on attenuated infectious agents typically generate some degree of cellular immunity, but their use in the clinic is often complicated by numerous problems ranging from the practical concerns of vaccine production and storage to public health issues, such as adverse reactions or reversion to virulence in some portion of the population. Additionally, not all pathogens can be attenuated for use as a vaccine. Therefore, one of the main goals of vaccine development is to create a noninfectious vaccine that mimics a natural infection's ability to stimulate a strong cellular immune response. As such, much effort has concentrated on the development of novel and potent vaccine adjuvants. Unfortunately, the majority of vaccine adjuvants developed thus far have not facilitated the generation of clinically significant cell-mediated immunity. At this point, the only approved vaccine adjuvant for general clinical use is alum, which is inadequate for generating cellular responses (1). Additionally, alum preferentially promotes the formation of Th2-type responses, which can be counterproductive to the kinds of inflammatory responses necessary to eradicate established chronic diseases (2–4).

Agonists for TLRs represent a class of vaccine adjuvant that has been the topic of intense study in recent years. Various bacterial- or viral-derived molecular structures (di- and triacylated lipoproteins, ssRNA and dsRNA, LPS, flagellin, unmethylated CpG sequences) are agonists for 1 of 10 known human TLRs and are potent activators of innate immunity (5). Cells important in both innate and adaptive immunity, such as dendritic cells (DCs),[3] express high levels of various TLRs, and stimulation of a DC through its TLR(s) generally results in the activation of the DC to produce cytokines, upregulate costimulatory marker expression, and migrate into T cell areas of lymphoid tissue (4, 6). As such, TLR agonists appear to be optimal for use as vaccine adjuvants for the generation of cellular immunity. However, the use of purified TLR agonists as vaccine adjuvants has been disappointing at best, demonstrating an inability to generate T cell responses on par with the responses observed during an actual infection (7–16). These results have been both surprising and frustrating to those in the field attempting to construct molecular vaccine formulations as alternatives to attenuated infectious vaccines. Collectively, the data are most consistent with a necessary but not sufficient role of TLR stimulation in the progression of events that leads to protective cellular immunity.

Although the development of a cellular immunity-generating vaccine has been fraught with complications, a number of signaling pathways and receptor/ligand pairs have been identified which have the potential, if they could be targeted, to significantly influence the development of CD4 and $CD8^+$ T cell responses. One such signaling receptor/ligand pair is CD27/CD70. Although the downstream signaling events are not completely defined, CD27-CD70 interactions are critical for the development of potent cell-mediated immunity in a number of model systems. Mice deficient in CD27 exhibit both impaired primary and memory antiviral T cell responses (17). Conversely, enhanced stimulation of CD27, through either forced cellular expression or soluble administration of CD70, results in enhanced T cell expansion, antiviral immunity,

*Integrated Department of Immunology, University of Colorado Health Sciences Center, Denver, CO 80206; and †Department of Immunology, Juntendo University School of Medicine, Tokyo, Japan

Received for publication October 10, 2006. Accepted for publication November 11, 2006.

The costs of publication of this article were defrayed in part by the payment of page charges. This article must therefore be hereby marked *advertisement* in accordance with 18 U.S.C. Section 1734 solely to indicate this fact.

[1] This work was supported by funds from the University of Colorado and National Institutes of Health Grants R21AI070038-01 and R01AI06877-01.

[2] Address correspondence and reprint requests to Dr. Ross M. Kedl, Integrated Department of Immunology, University of Colorado, National Jewish and Medical Research Center, 1400 Jackson Street, Denver, CO 80206. E-mail address: ross.kedl@uchsc.edu

[3] Abbreviations used in this paper: DC, dendritic cell; VVova, OVA-expressing vaccina virus; poly(I:C), polyinosinic:polycytidylic acid; TNFL, TNF ligand; WT, wild type; MFI, mean fluorescence intensity; Pam_3Cys, *N*-palmitoyl-*S*-[2,3-bis(palmitoyloxy)-(2*R*,*S*)-propyl]-(*R*)-cysteine-(S)serine-(S)lysine 4; MPL, monophosphoryl lipid A.

and antitumor CD8$^+$ T cell responses (18–29). Thus, the development of a vaccine strategy capable of facilitating the CD27-CD70 interaction would be invaluable.

Although it is clear that the forced expression of CD70 can significantly augment T cell expansion, the natural regulation and cellular expression of CD70 in vivo is largely unknown. Most studies describing the induction of CD70 expression on various cell types have used in vitro model systems examining in vitro-stimulated cells (20, 27, 29, 30). For example, studies have shown that bone marrow-derived DCs, T cells, and B cells could be induced, by various stimuli to express CD70 in vitro (20, 27, 30, 31). However, the little in vivo data available have examined CD70 expression/induction on various cell types in nonlymphoid tissues (30, 32), or in Rag-deficient hosts (33), and essentially no data are available regarding CD70 expression on normal DC subsets in vivo. As a result, the exploitation of the CD27-CD70 interaction for vaccine purposes has remained elusive.

We previously demonstrated that immunization with Ag in combination with both a TLR agonist and an anti-CD40 Ab (combined TLR/CD40 agonist immunization) induces potent CD8$^+$ T cell expansion (8). After a single immunization, this response is 10- to 20-fold higher than immunization with either agonist alone and is on par with the magnitude of T cell expansion often observed in response to infectious agents such as lymphocytic choriomeningitis virus or *Listeria monocytogenes*.

The only mechanistic data available at the time determined that the T cell response to this form of immunization demonstrated an intriguing variable dependence upon type I IFN (8). In our present findings, we demonstrate that the mechanism underlying the CD8$^+$ T cell expansion in response to combined TLR/CD40 agonist immunization is determined by the expression of CD70. In contrast to previous in vitro (20, 27, 29, 30) and in vivo (33) data, the up-regulation of CD70 expression on normal DC subsets in vivo is not induced by either TLR or CD40 stimulation alone, but requires the combined stimulation of TLR/CD40. This expression of CD70 plays an essential role in mediating the expansion of CD8$^+$ T cells following combined TLR/CD40 agonist immunization. In addition to providing a mechanism behind the CD8$^+$ T cell responses elicited from combined TLR/CD40 agonist immunization, the data show that the induction of CD70 on DCs is a central mechanism by which innate signaling pathways integrate with CD40 for the induction of cellular immunity.

Materials and Methods

Mice and injections

Six- to 12-wk-old C57BL/6 mice purchased from The Jackson Laboratory were immunized with 0.1–0.5 mg of whole OVA as previously described (8). In brief, whole protein was injected (i.p. or s.c.) in combination with a TLR agonist (50 μg of *N*-palmitoyl-*S*-[2,3-bis(palmitoyloxy)-(2*R*,*S*)-propyl]-(*R*)-cysteine-(S)serine-(S)lysine 4 (Pam_3Cys), 10 of μg flagellin, 100 μg of polyinosinic:polycytidylic acid (poly(I:C)), 150 μg of 27609, 100 μg of 3M012, and 50 μg of CpG1826), the anti-CD40 Ab FGK45 (50 μg), or both. OVA was purchased from Sigma-Aldrich and contaminating LPS was removed using a Triton X-114 LPS detoxification methodology as previously described (34). Following this detoxification method, the OVA was tested for LPS contamination by *Limulus* assay and found to have <1 endotoxin unit of LPS activity (~0.1 ng) for the amount injected in vivo. Injection of this amount of LPS has no observable effects on spleen DCs in vivo (data not shown). The TLR agonists used were either purchased (Pam_3Cys, InvivoGen; poly(I:C), Amersham Biosciences/GE Healthcare), provided through a material transfer agreement (27609, 3M012; 3M Pharmaceuticals), or isolated in house (flagellin). Flagellin was decontaminated of LPS using the same protocol as described above for OVA detoxification. TNF ligand (TNFL)-blocking Abs (see below) were injected i.p. between days −1 and +2 of Ag challenge. For vaccinia virus challenge, mice were injected i.p. with 0.5–1 × 10^7 PFU of an OVA-expressing vaccinia virus (VVova (35)).

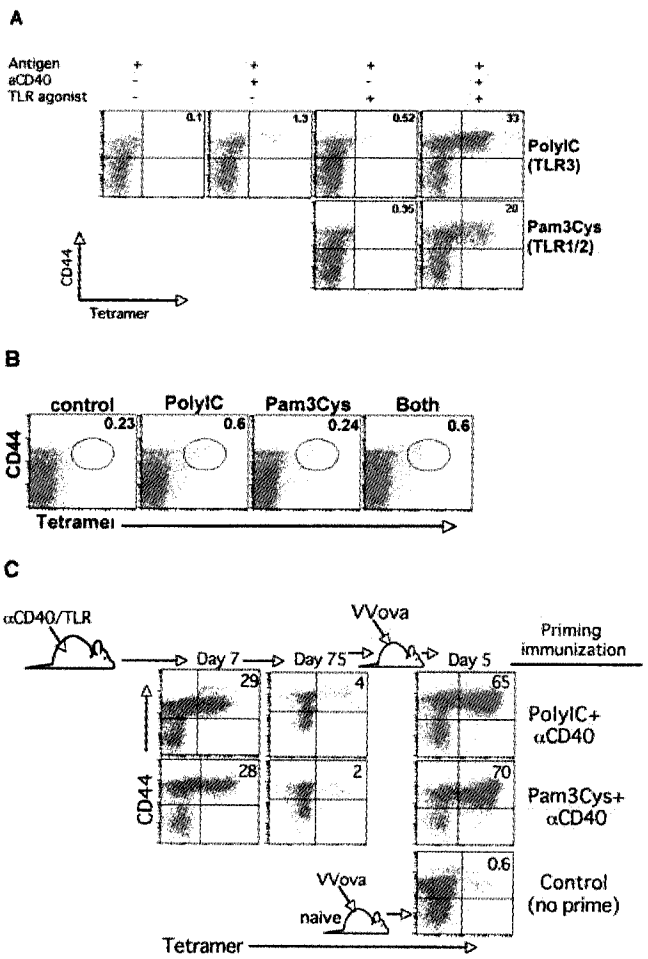

FIGURE 1. Combined TLR/CD40 agonist immunization generates potent primary and memory CD8$^+$ T cell responses. *A*, C57BL/6 mice were immunized i.p. with the indicated combinations of 500 μg of whole OVA (<0.5 endotoxin units), 50 μg of anti-CD40 Ab FGK45, 100 μg of poly(I:C) (TLR3 agonist), or 50 μg of Pam_3Cys (TLR1/2 agonist). Seven days after immunization (primary), PBLs were isolated and stained with K^b/SIINFEKL tetramer and CD8, B220, and CD44 Abs as previously described (8, 35). The magnitude of the Ag-specific T cell response was determined by gating on all CD8$^+$B220$^-$ events following FACS analysis (FACSCaliber; BD Biosciences). The numbers in the *upper right-hand quadrant* of each dot plot indicate the percentage of Ag-specific (tetramer staining) CD8$^+$ T cells of total CD8$^+$ T cells in the blood. *B*, C57BL/6 mice were immunized i.p. with 1 mg of whole OVA in combination with Pam_3Cys (50 μg), poly(I:C) (100 μg), or both. T cell responses were analyzed by K^b/B8R tetramer staining 7 days after challenge as in *A*. *C*, Mice were primed with the combined TLR/CD40 agonist immunization as in *A*. Seventy-five days later, the mice were challenged with 5 × 10^6 PFU of VVova. Naive mice were challenged with VVova as a control. Five days after challenge, the mice were sacrificed and K^b/SIINFEKL tetramer staining was performed on PBLs as described in *A*. The dot plots shown are representative of two mice per treatment group. The results shown are representative of at least four experiments performed.

Antibodies

CD11c allophycocyanin (clone HL3), CD11b PerCP-Cy5.5 (clone M1/70), CD8 allophycocyanin-Cy7 (clone 53-6.7), CD70 PE (clone FR70), CD86 FITC (clone GL1), CD80 FITC (clone 16-10A1), CD40 FITC (clone 3/23), and H-2K^b FITC (clone F6-88.5) were purchased from BD Pharmingen. CD30L PE (clone RM153), OX40L PE (clone RM134L), and 4-1BBL PE (clone TKS-1) were purchased from eBioscience. PDCA-1 biotin (clone JF05- 1C2.4.1) was purchased from Miltenyi Biotec. Streptavidin-Pacific Blue was purchased from Molecular Probes.

Purified CD70 (clone FR70), CD30L (clone RM153), OX40L (clone RM134L), and 4-1BBL (clone TKS-1) were produced as previously described (24).

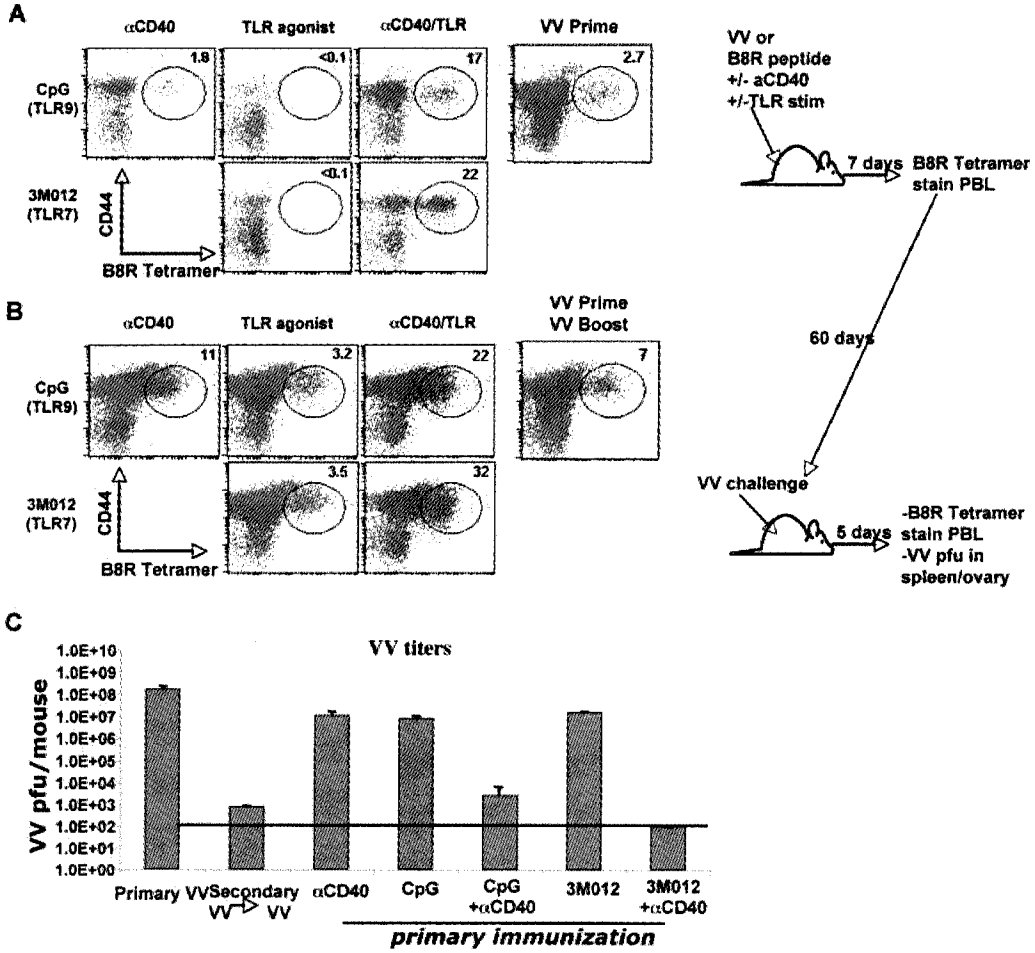

FIGURE 2. Combined TLR/CD40 agonist immunization elicits potent protective $CD8^+$ T cell memory. C57BL/6 mice were immunized with 50 μg B8R peptide and the indicated combinations of anti-CD40 (50 μg) and/or TLR agonists (50 μg of CpG1826 or 100 μg of 3M012). *A*, Peripheral blood was taken by tail vein 7 days later and stained with tetramer to identify B8R-specific $CD8^+$ T cells as described in *Materials and Methods*. Control mice were challenged with VVova and analyzed for their B8R-specific $CD8^+$ T cell response. Numbers in the dot plots indicate the percent tetramer positive of total $CD8^+$ T cells. *B*, Sixty days after initial priming, the mice were then challenged with 5×10^6 PFU of VVova. Five days after challenge, the T cell responses were again measured by tetramer staining of peripheral blood. Control mice were both primed and boosted with VVova. *C*, Ovaries from the mice in *B* were removed, and viral titers were determined by plaque assay. Horizontal line, Lower limit of detection of the plaque assay. Each treatment group had three mice per treatment. Error bars, SD.

TLR agonists

The TLR7 agonist S27609 (27609) (6) and the related molecule 3M012 (9) were synthesized at 3M Pharmaceuticals as previously described (36). They were reconstituted in either water (27609) or DMSO (3M012) at 10 mg/ml and diluted in PBS for injection into mice. Other TLR agonists used were poly(I:C) (Amersham Biosciences/GE Healthcare), Pam_3Cys (InvivoGen), monophosphoryl lipid A (MPL) or LPS (Sigma-Aldrich), and flagellin isolated from *Salmonella choleraesuis* subsp. *choleraesuis* serovar *Minnesota* (American Type Culture Collection) as previously described (37, 38).

Cell preparation

Seven days after primary challenge (i.p. or s.c.) or 5 days after secondary challenge, PBLs were isolated via tail vein or dorsal aorta bleed. In some experiments, spleens were removed and homogenized into single-cell suspensions. RBC were lysed using an ammonium chloride buffer followed by washing. Cells were resuspended in Complete Medium: SMEM (BioSource International), 10% heat-inactivated FBS (BioSource International), 1 mM sodium pyruvate, 0.1 mM nonessential amino acids, 1% penicillin-streptomycin, and 1% L-glutamine (Sigma-Aldrich). Spleen cells were resuspended at $\sim 2-4 \times 10^7$ cells/ml. PBLs were resuspended in 500 μl of complete buffer. Fifty to 100 μl of cells was used in subsequent tetramer or intracellular IFN-γ stains.

Enrichment and phenotype of DCs

B6, B6 $MyD88^{-/-}$, or B6 $Rag1^{-/-}$ mice were challenged i.p. or s.c. with a given TLR agonist, anti-CD40, or both. At 12–48 h after challenge, spleens were removed, placed into wells of a 6-well plate containing 2 ml of click's (EHAA) medium containing collagenase D (0.5 mg/ml) and DNase (50 μg/ml), and teased apart with forceps. Plates were incubated at 37°C for 40 min, after which 2 ml of 0.1 M EDTA (in HBSS) was added to each well and incubated an additional 5 min at 37°C. The cell suspension was passed through a strainer into a 50-ml tube and washed with 5 mM EDTA (in HBSS). Cells were pelleted by centrifugation and subsequently resuspended in ammonium chloride buffer to lyse RBC. Cells were then washed and resuspended in HBSS containing 5 mM EDTA and 0.1% FBS. For the DC phenotype, 5×10^6 cells were first stained with PDCA-1 biotin and then washed twice in FACS buffer (PBS containing 0.1% FBS and 0.1% sodium azide). The cells were then stained with CD11c allophycocyanin, CD11b PerCP-Cy5.5, CD8 allophycocyanin-Cy7, streptavidin-Pacific Blue, and a FITC- and PE-conjugated Ab specific for the indicated activation marker. Five- or six-color flow cytometry was performed on a CyAn LX flow cytometer (DakoCytomation) and analyzed with Weasel version 2.2 software (The Walter and Eliza Hall Institute of Medical Research, Melbourne, Australia).

Tetramer staining and flow cytometry

Cells were stained with K^b/OVA tetramer as previously described (35). Briefly, cells were plated in 96-well plates and stained with tetramer for 1.5 h at 37°C. Abs against CD8, CD44, CD27, and B220 were added, and the cells were incubated an additional 20 min at 37°C. The cells were then washed, fixed, and resuspended in FACS buffer for flow cytometric analysis. Four- to five-color FACS data were collected on a BD FACScan flow cytometer, retrofitted with a second laser (Cytek), using CellQuest and Rainbow software, and analyzed using CellQuest software. For analysis,

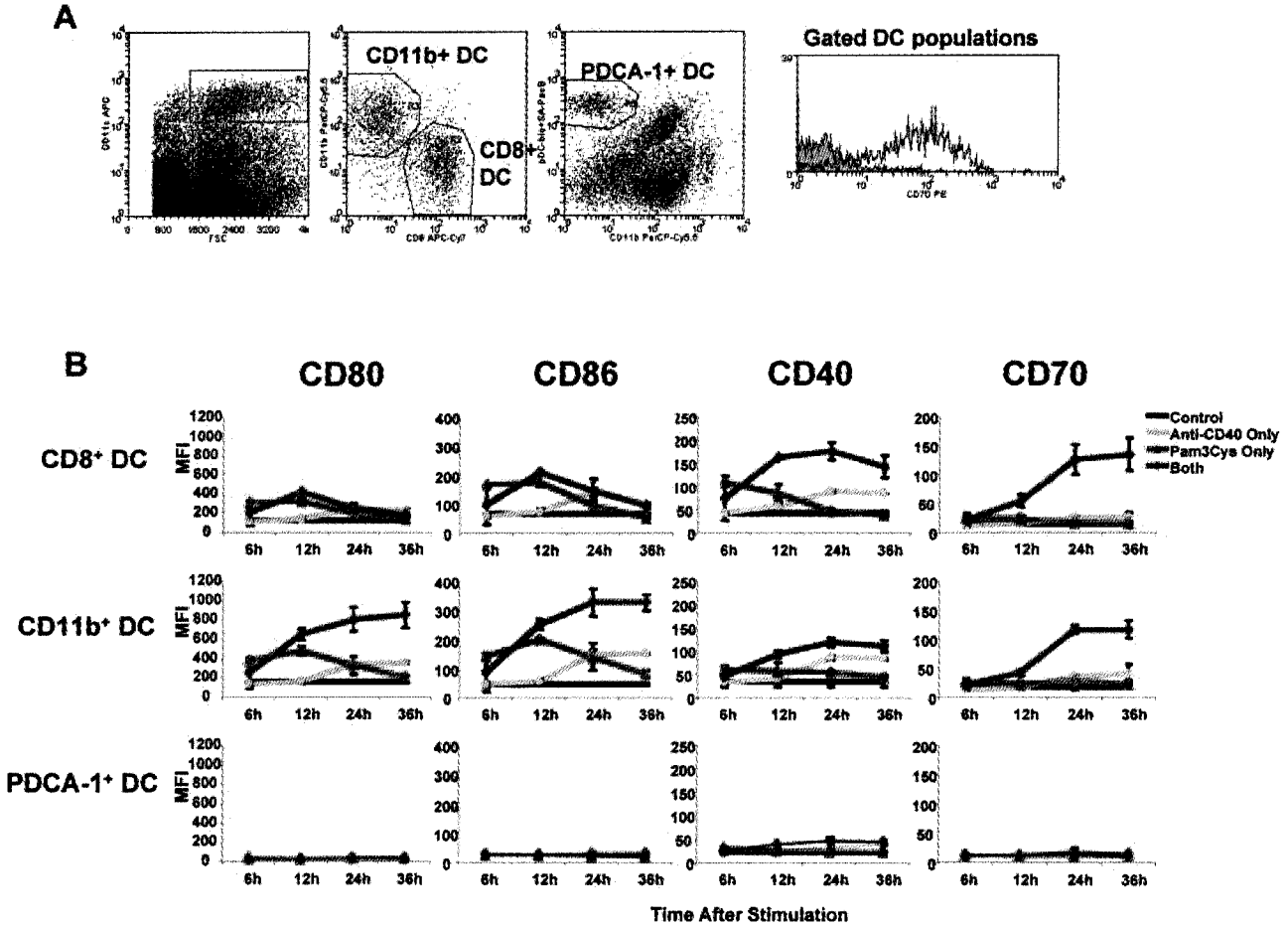

FIGURE 3. Increased surface expression of CD70 on DC subsets requires both TLR and CD40 agonists. *A*, Gating scheme for analyzing phenotypes of DC subsets. Mouse splenocytes were stained for six-color flow cytometry. $CD8^+$ and $CD11b^+$ DCs were identified by gating on $CD11c^{high}$ cells. PDCA-1^+ DCs were identified by gating on $CD11c^+$ cells. Surface marker expression was determined by plotting histograms gated on the particular DC subset. *B*, Surface marker expression of DC subsets. Mice were injected i.p. with agonistic anti-CD40 Ab (50 μg), Pam_3Cys (TLR1/2 agonist, 50 μg), or both. At 6, 12, 24, and 36 h, mouse splenocytes were stained for six-color flow cytometry. Data shown are the mean fluorescence intensities (MFI) of the indicated surface maker at each time point. The same scale was used for each DC subset within the indicated surface marker to show the relative expression level between DC subsets. Error bars, SD. Data are representative of two independent experiments. Graphs are representative of similar data obtained using poly(I:C) (TLR3), MPL (TLR4), and 27609 (TLR7) as the TLR agonist.

the data were gated on $CD8^+B220^-$ events and then analyzed for tetramer staining by the activation marker CD44, the Ag-specific cells being $CD44^{high}$. CD27/tetramer staining was also analyzed and gave results essentially identical to those of CD44/tetramer.

Results

Combined TLR/CD40 agonist immunization generates primary and secondary $CD8^+$ immunity comparable to viral challenge

We previously reported that immunization of a host with Ag in the presence of agonists for both CD40 and a TLR (combined TLR/CD40 agonist immunization) generates $CD8^+$ T cell responses exponentially larger than those observed in response to immunization with either agonist alone (8). Given the magnitude of the response to this form of immunization, we sought to determine whether combined TLR/CD40 agonist immunization promoted both primary and secondary protective immunity on par with viral challenge. Mice were immunized with the indicated combinations of Ag (OVA), an agonistic anti-CD40 Ab (FGK45), and a TLR agonist. Seven days later, peripheral blood was isolated from the mice and stained with K^b/SIINFEKL MHC class I tetramers to identify Ag-specific $CD8^+$ T cells. Similar to previously published data of splenic CD8 responses (8), the combined TLR/CD40 agonist immunization elicited a potent expansion of OVA-specific $CD8^+$ T cells, detectable in the peripheral circulation, compared with any other immunization (Fig. 1*A*). These Ag-specific cells in the peripheral blood were also functional with respect to IFN-γ production and lytic function (data not shown and Ref. 8).

The stimulation of DCs in vitro with combinations of TLR agonists has been reported to have a synergistic effect both on the activation of the DC as well as on the subsequent T cell response stimulated by the DCs (39). However, we found that in vivo, immunization of mice with similar combinations of TLR agonists had little effect on the subsequent T cell response (Fig. 1*B*). This was also true of other combinations of TLR agonists such as MPL (TLR4) and 27609 (TLR7), and 27609 and CpG1826 (TLR9) (data not shown). At best, the combinations of TLR agonists had an additive effect on the resulting T cell response (data not shown), but synergy to the same degree as combined TLR/CD40 agonist immunization was never observed (Fig. 1*B*).

In addition to inducing potent primary $CD8^+$ T cell expansion, combined TLR/CD40 agonist immunization resulted in the generation of a competent pool of memory cells capable of even greater

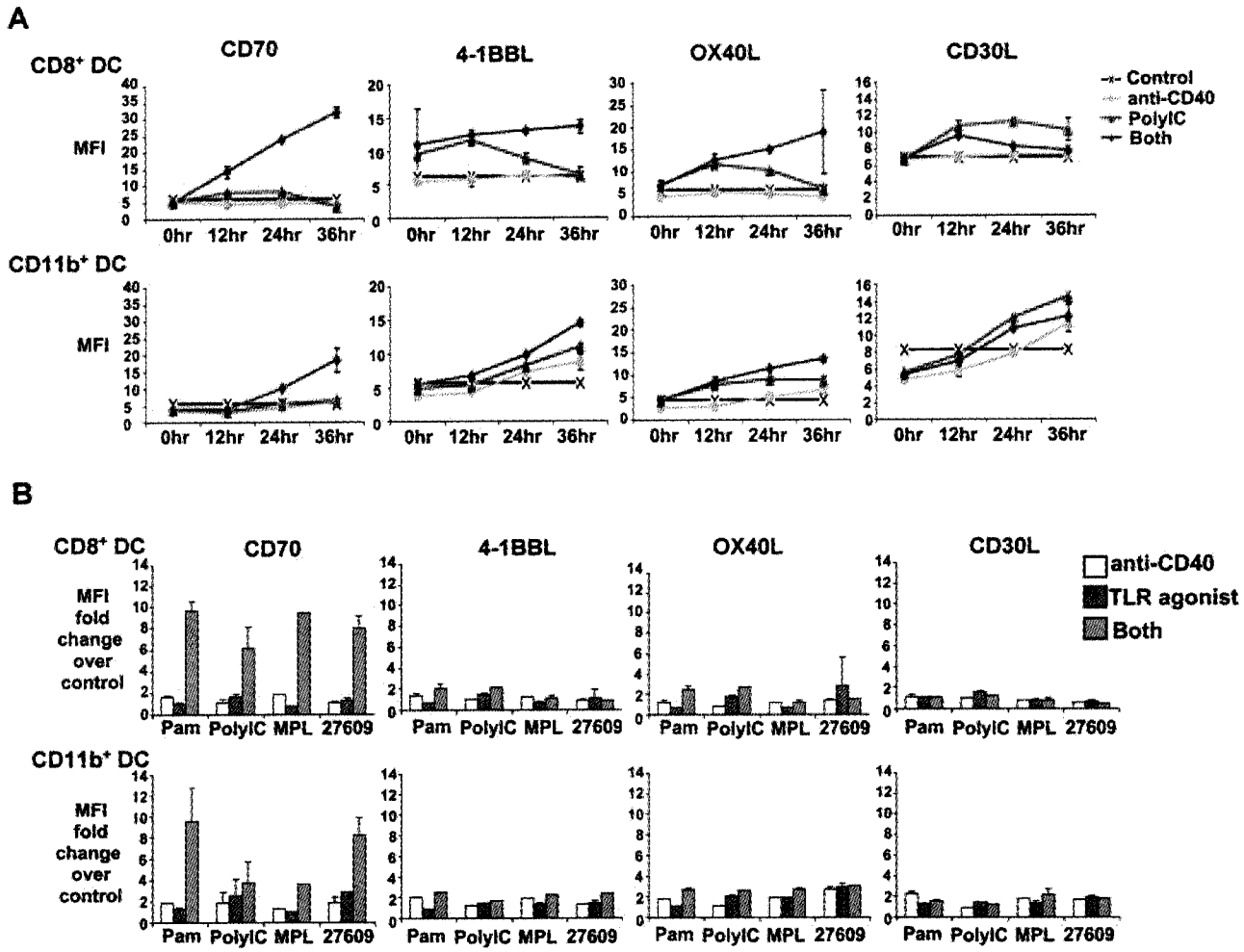

FIGURE 4. TLR/CD40 agonist stimulates a greater increase in surface CD70 than other members of the TNFL superfamily. *A*, DC subset surface expression of TNFL superfamily members. Mice were injected i.p. with agonistic anti-CD40 Ab (50 μg), poly(I:C) (TLR3 agonist, 100 μg), or both. At 6, 12, 24, and 36 h, mouse splenocytes were stained for six-color flow cytometry. Data shown are the MFI of the indicated surface marker at each time point. The same scale was used for each DC subset within the indicated surface marker to show the relative expression level between DC subsets. Error bars, SD. Graphs are representative of similar data obtained using Pam_3Cys (TLR1/2), MPL (TLR4), and 27609 (TLR7) as the TLR agonist. *B*, Relative increase in surface expression of TNFL superfamily members on DC subsets. Values represent the fold increase, over naive controls, of the surface marker expression at 24 h postinjection (the peak of expression stimulated by TLR/CD40 agonist combination). The fold increase was calculated as the MFI of the surface marker on the DC from stimulated mice divided by the MFI of the same surface marker on DC from unstimulated mice. The CD70 graphs were generated from the means of two independent experiments. Error bars, SE. Values in the 4-1BBL, OX40L, and CD30L graphs represent the mean ± SD from single experiments.

expansion upon secondary challenge. Seventy-five days after initial combined TLR/CD40 agonist immunization, the mice were challenged with VVova. VVova challenge induced a robust secondary response of the OVA-specific T cells in the peripheral blood (Fig. 1*C*). Interestingly, a secondary expansion of $CD8^+$ T cells was minimally detectable in the spleen or lymph nodes following VVova challenge (data not shown). In previously published work, we also observed minimal memory responses in the lymph nodes and spleen following secondary challenge with either peptide or protein (8). This indicates that the detectable response in these sites is a vast underestimate of the total secondary response, consistent with previous reports from the literature (40, 41).

To establish the degree to which combined TLR/CD40 agonist immunization was able to provide protective immunity, mice were primed against the dominant vaccinia class I peptide epitope B8R (16), in the context of the indicated combinations of TLR agonist, anti-CD40, or vaccina virus (Fig. 2*A*). Sixty days later, the mice were challenged with vaccinia virus, and the secondary expansion of memory B8R-specific $CD8^+$ T cells (in peripheral blood) and viral titers (in the ovary) were measured 5 days after challenge. Prior immunization with combined TLR/CD40 agonists again resulted in an elevated secondary expansion of memory B8R-specific T cells (Fig. 2*B*), as well as the elimination of viral replication (Fig. 2*C*). In contrast, prior immunization with either TLR or CD40 agonists alone resulted in only minimal reduction in viral titers compared with virus-challenged naive mice. Thus, combined TLR/CD40 agonist immunization elicits potent primary $CD8^+$ T cell responses that culminate in the generation of protective memory.

CD70 expression is regulated in vivo by combined TLR and CD40 signaling

We next sought to determine the mechanism responsible for the synergy between the TLR and CD40 pathways for inducing such potent $CD8^+$ T cell responses. Given their constitutive expression of CD40 and large repertoire of TLRs (4), we reasoned that DCs were the likely cellular target of the coadministered anti-CD40 Ab and the TLR agonist. Upon stimulation through either molecular pathway, DCs are activated to migrate into T cell zones of lymphoid organs, produce cytokines, and increase expression of

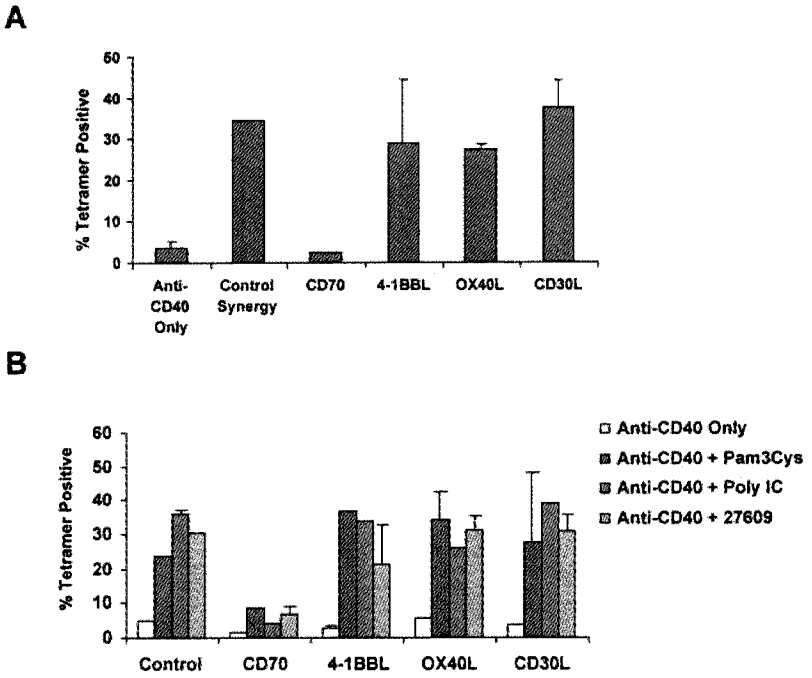

FIGURE 5. Blocking CD70, but not other TNFL members, inhibits TLR/CD40 agonist-mediated expansion of Ag-specific $CD8^+$ T cells. C57BL/6 mice were immunized i.p. with whole OVA and 50 μg of agonistic anti-CD40 Ab alone or in combination with 50 μg of Pam_3Cys (*A*) or the indicated TLR agonist (50 μg of Pam_3Cys, 100 μg of poly(I:C), or 150 μg of 27609) (*B*). Blocking Abs (250 μg per injection for each Ab) specific for the indicated TNFL were administered i.p. 1 day before immunization and 1, 3, and 5 days after immunization. Seven days after immunization, PBL were stained for Ag-specific $CD8^+$ T cells. Values represent the percentage of $CD8^+$ T cells that stained with K^b/SIINFEKL tetramer. Error bars, SD. Graphs are representative of four independent experiments.

costimulatory markers (4, 6). These changes in DC phenotype during activation are crucial for priming of naive T cells and the development of Ag-specific immunity. We therefore determined whether there was a change in DC phenotype that was unique to the combination of anti-CD40 and TLR agonist compared with either stimulus alone. To examine the phenotype of activated splenic DCs, mice were injected with a TLR agonist, anti-CD40, or both. Splenic $CD8^+$, $CD11b^+$, and PDCA-1^+ DCs ($CD11c^+$) (Fig. 3*A*) were analyzed directly ex vivo at 6, 12, 24, and 36 h after the injection for the expression of the surface markers CD80, CD86, CD40, and CD70.

The expression of any of these surface markers was relatively unaffected on PDCA-1^+ DCs (Fig. 3*B*) and, as a result, phenotypic data for this DC subset is not shown in subsequent experiments. In $CD8^+$ and $CD11b^+$ DCs, administration of agonistic anti-CD40 Ab or TLR agonist alone induced varying levels of increased CD80, CD86, and CD40 expression, which peaked at 6–12 and 24–36 h, respectively (Fig. 3*B*). The increase in these activation markers was prolonged in mice challenged with combined TLR/CD40 agonists. However, only combined TLR/CD40 stimulation induced significant up-regulation of CD70 expression on the major DC subsets (Fig. 3*B*), with little or no increase in CD70 observed in response to challenge with either agonist alone. Surface levels of CD70 were increased within 6–12 h of administration and were sustained at their peak levels between 24 and 36 h (Fig. 3*B*). Therefore, of the markers analyzed, only the expression of CD70 correlated directly with the magnitude of the $CD8^+$ T cell response observed following individual or concomitant stimulation of TLR and CD40.

CD70 expression is uniquely regulated by TLR/CD40 agonist stimulation compared with other TNFLs

CD70 is a member of the TNFR ligand superfamily. Other members of the TNFL superfamily, including CD30L, OX40L, and 4-1BBL, can have costimulatory effects on T cells and can function to sustain T cell responses after initial T cell activation (42). We examined the expression of these molecules on activated splenic DCs from mice that were injected with TLR agonist with or without anti-CD40 as described above.

The expression of CD70, 4-1BBL, OX40L, and CD30L remained unchanged on $CD8^+$ DCs in mice treated with agonistic anti-CD40 Ab alone (Fig. 4*A*). The same treatment resulted in a slight increase in the expression of 4-1BBL, OX40L, and CD30L on the $CD11b^+$ DCs (Fig. 4*A*). TLR agonist alone stimulated a small transient increase in the expression of 4-1BBL and OX40L and a more sustained increase in CD30L on the $CD8^+$ DC subset (Fig. 4*A*). For the $CD11b^+$ DC subset, TLR agonist alone stimulated a small sustained increase in the expression of 4-1BBL, OX40L, and CD30L, but CD70 expression was unaffected (Fig. 4*A*). The combined TLR/CD40 agonist challenge stimulated small increases in the expression of 4-1BBL, OX40L, and CD30L on both DC subsets examined (Fig. 4*A*) but, again, significantly larger increases in CD70 expression compared with any other TNFL (Fig. 4, *A* and *B*). Thus, although increased expression of other TNFL family members could be observed, their regulation was more similar to the expression of CD80/86/40, being increased to one degree or another with either CD40 or TLR stimulation alone and prolonged in expression after stimulation of both (Fig. 4*A*). Additionally, whereas the increase in 4-1BBL, OX40L, and CD30L was no greater than 3-fold on either DC subset in the presence of agonists for both TLR and CD40 (Fig. 4*B*), the increase in CD70 expression was 6- to 10-fold on $CD8^+$ DCs and 4-to10-fold on $CD11b^+$ DCs, depending on the TLR agonist that was administered. This was true at all time points between 12 and 48 h (data not shown). Thus, even in relation to other TNFL family members, DC expression of CD70 is uniquely regulated, showing a significant increase only after stimulation of both TLR and CD40 pathways.

$CD8^+$ T cell expansion, following combined TLR/CD40 agonist immunization, is CD70 dependent

Because the expression of CD70 best correlated with the magnitude of the $CD8^+$ T cell response elicited, we examined the dependency of the $CD8^+$ T cell response on CD70-mediated signaling following combined TLR/CD40 agonist immunization. Blocking Abs to CD70, 4-1BBL, OX40L, and CD30L (24) were administered to mice 1 day before immunization to OVA with

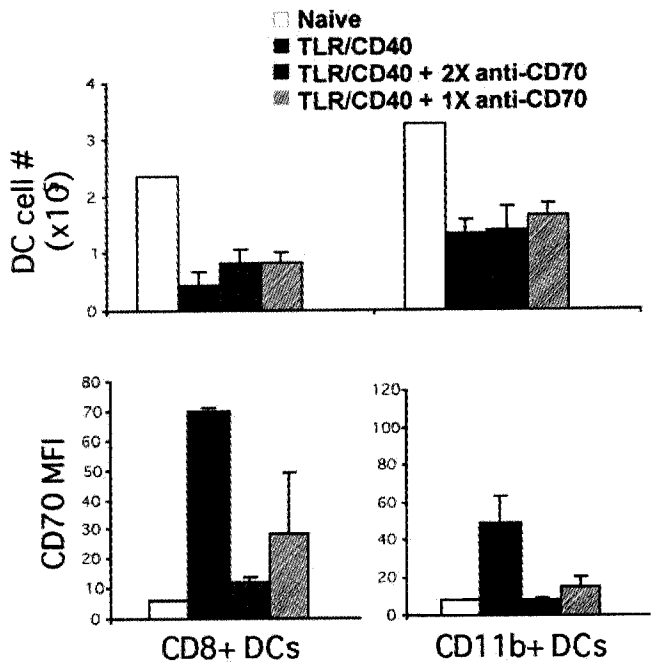

FIGURE 6. In vivo administration of anti-CD70 Ab does not deplete splenic DCs. C57BL/6 mice were immunized s.c. with 50 μg of anti-CD40 Ab and 150 μg of 27609. Some mice received 250 μg of anti-CD70 i.p. 36 h before immunization and 7–8 h postimmunization (anti-CD70, two times) or 7–8 h postimmunization only (anti-CD70, one time). Mice were sacrificed 24 h after combined TLR/CD40 agonist challenge, and spleen DCs were collected and analyzed as described in Fig. 2 and *Materials and Methods*. The percentages of $CD8^+$ and $CD11b^+$ DC were determined by flow cytometry (*upper panels*). Upon isolation, the DCs were stained for CD70 expression to verify the degree of CD70 blockade by the anti-CD70 Ab (*lower panels*). Values represent the total number of splenic $CD8^+$ and $CD11b^+$ DC as calculated by multiplying the percentage of $CD11c^{high}CD8^+$ and $CD11c^{high}CD11b^+$ cells by the total number of splenic leukocytes. Error bars, SD.

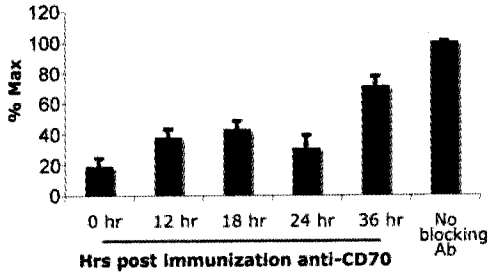

FIGURE 7. CD70 must be blocked within 24 h after immunization for effective reduction of the $CD8^+$ T cell response. Mice were challenged with whole OVA, poly(I:C), and antiCD40. At the same time as Ag challenge, and at the indicated times thereafter, representative mice were injected i.p. with 500 μg of anti-CD70. Seven days after immunization, PBL were stained for Ag-specific $CD8^+$ T cells as described in *Materials and Methods*. The response from the anti-CD70 treatment groups is divided by the response from the non-anti-CD70-injected control mice (no blocking Ab) to be expressed as the percentage of maximum response.

agonistic anti-CD40 Ab and TLR agonist. Injection of the blocking Abs was repeated on days 1, 3, and 5 after immunization. On day 7, mice were bled and the percentage of tetramer-staining $CD8^+$ T cells was determined.

In contrast to the administration of blocking Abs to 4-1BBL, OX40L, and CD30L, administration of the anti-CD70-blocking Ab to the TLR/CD40 agonist-treated mice inhibited the generation of Ag-specific $CD8^+$ T cells back to the level observed in response to immunization with anti-CD40 alone (Fig. 5*A*). This was consistent for all the TLR agonists that were tested, including Pam_3Cys (TLR1/2), poly(I:C) (TLR3), 27609 (TLR7) (Fig. 5*B*), MPL (TLR4), and flagellin (TLR5) (data not shown). The reduced T cell response in the presence of anti-CD70-blocking Ab was not due to the elimination of DCs by the anti-CD70 Ab, because DC numbers were not significantly different in immunized mice with or without the injection of the anti-CD70 Ab (Fig. 6) or Abs against the other TNFL family members (data not shown). In addition, the DCs in the CD70-blocked mice expressed high levels of CD80, CD86, and CD40, further indicating that the resident DCs were not eliminated by the CD70 Ab and replaced by recent naive immigrants from the circulation.

Although CD70 expression has been demonstrated on numerous cell types (30, 43), we did not observe any significant expression of CD70 on T cells, B cells, or monocyte/macrophages within the first 48 h after challenge (data not shown). Furthermore, we observed that unless the anti-CD70 Ab was administered within the first 12–24 h of TLR/CD40 agonist immunization, effective blocking of $CD8^+$ T cell expansion was not observed (Fig. 7). Collectively, these data indicate that the expansion of Ag-specific $CD8^+$ T cells requires interaction with a CD70-bearing DC within 24 h of antigenic challenge.

Interestingly, the minimal $CD8^+$ response to CD40 alone (Fig. 5*B*), or even to TLR stimulation alone (data not shown), was also reduced in the presence of CD70-blocking Ab. This indicates that even the fractional induction of CD70 on DCs by these stimuli is apparently important for the generation of a $CD8^+$ T cell response. However, the effects of CD70 blockade are most readily observed following combined TLR/CD40 agonist immunization where CD70 appears to mediate the synergy that exists between the CD40 and TLR pathways for the induction of $CD8^+$ T cell expansion.

Discussion

CD70-CD27 interactions are known to influence the generation of primary and memory T cell responses (18–20, 22–26, 29, 32, 44, 45). However, the regulated expression of CD70 and other TNFL family members on DCs in vivo has not been extensively examined. Furthermore, the overall importance of these ligands in the generation of immunity has generally been viewed as another example of redundancy in immune signaling. In the present work, we have uncovered mechanisms by which CD70 expression on DCs is uniquely regulated in vivo, even with respect to other TNFL family members, by concomitant signaling of the TLR/CD40 pathways. This expression of CD70 is critical for eliciting potent $CD8^+$ T cell responses, because blocking CD70 during this immunization all but eliminates Ag-specific $CD8^+$ T cell expansion.

The results we show here begin to shed some light on the discrepancy between the ability of TLR agonists to activate DCs and their comparable inability to generate cellular immunity in a vaccine setting. Stimulation of DCs with TLR agonists alone instigates increases in the expression of classical markers of DC activation such as CD80, CD86, and CD40, as well as many inflammatory cytokines in many DC subsets (46). At least some of these increases are necessary, because we previously demonstrated that $CD8^+$ T cell responses to combined TLR/CD40 agonist immunization are B7 dependent (8). This is not surprising, because almost all T cell responses are dependent on initial CD28 stimulation (47). However, the induction of CD80/86 by the TLR agonist alone does not result in a substantial $CD8^+$ T cell response (Ref. 8 and Fig. 1). Although the prolonged expression of CD80/

86, in response to combined TLR/CD40 stimulation, may play a supporting role in the ensuing $CD8^+$ T cell response, it is clear that the expression of CD80/86 is necessary, but not sufficient, for mediating the potent expansion of Ag-specific $CD8^+$ T cells. Similarly, CD40 agonists alone also activate many DC functions, and yet have also been unsuccessful, both preclinically (48–50) and clinically (51), at generating long-term cellular immunity. Collectively, these results can now be explained by our data showing 1) maximal CD70 expression requires the combined stimulus of both the CD40 and TLR pathways and 2) the potent $CD8^+$ T cell response following combined TLR/CD40 agonist vaccination is CD70 dependent. Given these data, the rational design of novel and potent vaccine adjuvants should use the induction of CD70 expression on DCs in vivo as a clinically relevant readout.

It should be noted that our results showing the requirement for both TLR and CD40 stimulation for optimal DC CD70 expression in vivo are in apparent contradiction to recently published data by Taraban et al. (33). This recent publication documented increased CD70 expression on splenic DCs in vivo after injection with a high dose (500 μg) of anti-CD40 (33). There are two possible explanations for the discrepancies between our data and the data of Taraban et al (33). First, Taraban et al. (33) used 10-fold more anti-CD40 than we did. We have repeated our experiments using this amount of anti-CD40 and have found a small increase in CD70 expression on the DCs in vivo as well (data not shown). However, this increase in CD70 was abrogated in $MyD88^{-/-}$ mice (data not shown), suggesting that this amount of Ab may contain enough contaminating LPS to synergize with the CD40 in wild-type (WT) mice. Second, Taraban et al. (33) actually used $Rag^{-/-}$ mice, not WT, when examining DC activation and CD70 expression in vivo. We have also repeated these experiments using a high dose of anti-CD40 in $Rag^{-/-}$ mice and have found a surprising difference in the regulation of CD70 expression between $Rag^{-/-}$ and WT mice. Following high-dose anti-CD40 challenge of $Rag^{-/-}$ mice, we find exactly the same results as Taraban et al. (33), namely, that a significant population of $CD11c^+$ cells express high levels of CD70 (data not shown). In contrast, the DCs in WT mice show only a minor, though detectable, increase in CD70 to high doses of anti-CD40, which again is eliminated in $MyD88^{-/-}$ hosts. As a positive control, the addition of poly(I:C) (which does not signal through MyD88 (52)) to the antiCD40 resulted in the greatest upregulation of CD70 in all strains. Given these data, there appears to be no real contradiction between our data shown here and the previous work by Taraban et al. (33). We would explain the apparent discrepancies as the result of either contaminating LPS, due to the high dose of anti-CD40 used, a fundamental difference between DCs in WT and $Rag^{-/-}$ mice, or a combination of both. Given the phenotype of CD70 expression in the $Rag^{-/-}$ hosts, we find the second explanation the most likely, although it is unclear at present what the significance of these findings are. Given the lack of regulatory T cells in the $Rag^{-/-}$ hosts, an intriguing possibility is that these results have uncovered a role for regulatory T cells in the regulation of DC CD70 expression.

That being said, we do see minimal increases in DC expression of CD70 in vivo following challenge with TLR or CD40 agonists alone, and even these limited amounts of CD70 expression appear to be physiologically relevant, because CD70 blockade reduced even the minimal $CD8^+$ expansion observed in response to immunization with either agonist alone (see Fig. 4*B*). However, optimal CD70 expression on DCs in WT B6 mice in vivo cannot be achieved with either agonist alone, suggesting that the differences between previous in vitro results and the data presented here are due to differences between bone marrow-derived DCs and normal DC subsets, between in vitro and in vivo stimulation of DCs, or both.

We previously also showed an important role for type 1 IFN in determining the $CD8^+$ T cell response from some TLR/CD40 agonist combinations (8). This IFN dependence was observed only when the TLR stimulation elicited significant IFN production in the host. Interestingly, we have recently determined that this IFN dependency is based on the same immunologic principle that mediates the $CD8^+$ T cell expansion to TLR/CD40 immunization, namely, the induction of CD70 expression on DCs, and is the subject of a manuscript currently in preparation. Thus, we now have evidence that multiple innate signaling pathways integrate with CD40 for the induction of potent cellular immunity through CD70.

Our data further support the role of CD70 as the primary factor mediating the licensing of DCs for productive interaction with $CD8^+$ T cells (27). Previous experimental models showed that CD4-dependent $CD8^+$ T cell responses could be recovered in CD4-depleted or deficient mice by the administration of an agonistic CD40 Ab (53–55). These previous data demonstrated that, following CD40 stimulation, DCs were enabled, or licensed, to productively stimulate $CD8^+$ T cells. Our results are consistent with those of others (27), which demonstrate that CD70 can provide this licensing role and that CD70 may arguably be the definitive licensing signal for CD4-independent, $CD8^+$ T cell responses.

Finally, our data show that the engagement of TLR and one TNFR/L pair (CD40/L) leads to the eventual expression and engagement of another TNFR/L pair (CD27/CD70). It may be that TNFR/L superfamily members generally play a role in the positive feedback regulation of primary, and possibly secondary, T cell expansion. Although we observed a critical role for CD27-CD70 interactions in primary $CD8^+$ T cell responses, secondary T cell expansion appears to be relatively independent of CD70 (P. J. Sanchez and R. M. Kedl, unpublished observations). As shown above, the TNFL OX40L and 4-1BBL are induced to some degree by TLR stimulation alone. Memory cells are known to be more sensitive to secondary Ag challenge (56, 57), and this may be due in part because they are more responsive to TNFL family members whose expression is achieved under conditions of minimal inflammation. Understanding the relationship between the regulated expression of the different TNFL members and primary/secondary T cell expansion will result in the development of clinical prime-boost regimens that optimally promote long-term cellular immunity.

Acknowledgment

We thank Jill Slansky for helpful discussions concerning this manuscript.

Disclosures

The authors have no financial conflict of interest.

References

1. Baylor, N. W., W. Egan, and P. Richman. 2002. Aluminum salts in vaccines: US perspective. *Vaccine* 20: S18–S23.
2. Audibert, F. 2003. Adjuvants for vaccines, a quest. *Int. Immunopharmacol.* 3: 1187–1193.
3. Hadden, J. W. 1994. T-cell adjuvants. *Int. J. Immunopharmacol.* 16: 703–710.
4. Pulendran, B. 2004. Modulating vaccine responses with dendritic cells and Toll-like receptors. *Immunol. Rev.* 199: 227–250.
5. Akira, S. 2003. Mammalian Toll-like receptors. *Curr. Opin. Immunol.* 15: 238.
6. Doxsee, C. L., T. R. Riter, M. J. Reiter, S. J. Gibson, J. P. Vasilakos, and R. M. Kedl. 2003. The immune response modifier and TLR7 agonist S-27609 selectively induces IL-12 and TNFα production in $CD11c^+CD11b^+CD8^-$ dendritic cells. *J. Immunol.* 171: 1156–1163.
7. Rhee, E. G., S. Mendez, J. A. Shah, C. Y. Wu, J. R. Kirman, T. N. Turon, D. F. Davey, H. Davis, D. M. Klinman, R. N. Coler, et al. 2002. Vaccination with

heat-killed leishmania antigen or recombinant leishmanial protein and CpG oligodeoxynucleotides induces long-term memory $CD4^+$ and $CD8^+$ T cell responses and protection against leishmania major infection. *J. Exp. Med.* 195: 1565–1573.
8. Ahonen, C. L., C. L. Doxsee, S. M. McGurran, T. R. Riter, W. F. Wade, R. J. Barth, J. P. Vasilakos, R. J. Noelle, and R. M. Kedl. 2004. Combined TLR and CD40 triggering induces potent $CD8^+$ T cell expansion with variable dependence on type I IFN. *J. Exp. Med.* 199: 775–784.
9. Wille-Reece, U., C. Y. Wu, B. J. Flynn, R. M. Kedl, and R. A. Seder. 2005. Immunization with HIV-1 Gag protein conjugated to a TLR7/8 agonist results in the generation of HIV-1 Gag-specific Th1 and $CD8^+$ T cell responses. *J. Immunol.* 174: 7676–7683.
10. Lore, K., M. R. Betts, J. M. Brenchley, J. Kuruppu, S. Khojasteh, S. Perfetto, M. Roederer, R. A. Seder, and R. A. Koup. 2003. Toll-like receptor ligands modulate dendritic cells to augment cytomegalovirus- and HIV-1-specific T cell responses. *J. Immunol.* 171: 4320–4328.
11. Tritel, M., A. M. Stoddard, B. J. Flynn, P. A. Darrah, C. Y. Wu, U. Wille, J. A. Shah, Y. Huang, L. Xu, M. R. Betts, et al. 2003. Prime-boost vaccination with HIV-1 Gag protein and cytosine phosphate guanosine oligodeoxynucleotide, followed by adenovirus, induces sustained and robust humoral and cellular immune responses. *J. Immunol.* 171: 2538–2547.
12. Busch, D. H., and E. G. Pamer. 1999. T lymphocyte dynamics during *Listeria monocytogenes* infection. *Immunol. Lett.* 65: 93–98.
13. Busch, D. H., and E. G. Pamer. 1999. T cell affinity maturation by selective expansion during infection. *J. Exp. Med.* 189: 701–710.
14. Butz, E., and M. J. Bevan. 1998. Dynamics of the $CD8^+$ T cell response during acute LCMV infection. *Adv. Exp. Med. Biol.* 452: 111–122.
15. Butz, E. A., and M. J. Bevan. 1998. Massive expansion of antigen-specific $CD8^+$ T cells during an acute virus. *Infect. Immun.* 8: 167–175.
16. Tscharke, D. C., G. Karupiah, J. Zhou, T. Palmore, K. R. Irvine, S. M. Haeryfar, S. Williams, J. Sidney, A. Sette, J. R. Bennink, and J. W. Yewdell. 2005. Identification of poxvirus $CD8^+$ T cell determinants to enable rational design and characterization of smallpox vaccines. *J. Exp. Med.* 201: 95–104.
17. Hendriks, J., L. A. Gravestein, K. Tesselaar, R. A. van Lier, T. N. Schumacher, and J. Borst. 2000. CD27 is required for generation and long-term maintenance of T cell immunity. *Nat. Immunol.* 1: 433–440.
18. Arens, R., K. Schepers, M. A. Nolte, M. F. van Oosterwijk, R. A. van Lier, T. N. Schumacher, and M. H. van Oers. 2004. Tumor rejection induced by CD70-mediated quantitative and qualitative effects on effector $CD8^+$ T cell formation. *J. Exp. Med.* 199: 1595–1605.
19. Arens, R., K. Tesselaar, P. A. Baars, G. M. van Schijndel, J. Hendriks, S. T. Pals, P. Krimpenfort, J. Borst, M. H. van Oers, and R. A. van Lier. 2001. Constitutive CD27/CD70 interaction induces expansion of effector-type T cells and results in IFN-γ-mediated B cell depletion. *Immunity* 15: 801–812.
20. Bullock, T. N., and H. Yagita. 2005. Induction of CD70 on dendritic cells through CD40 or TLR stimulation contributes to the development of $CD8^+$ T cell responses in the absence of $CD4^+$ T cells. *J. Immunol.* 174: 710–717.
21. Cormary, C., R. Gonzalez, J. C. Faye, G. Favre, and A. F. Tilkin-Mariame. 2004. Induction of T-cell antitumor immunity and protection against tumor growth by secretion of soluble human CD70 molecules. *Cancer Gene Ther.* 11: 497–507.
22. Couderc, B., L. Zitvogel, V. Douin-Echinard, L. Djennane, H. Tahara, G. Favre, M. T. Lotze, and P. D. Robbins. 1998. Enhancement of antitumor immunity by expression of CD70 (CD27 ligand) or CD154 (CD40 ligand) costimulatory molecules in tumor cells. *Cancer Gene Ther.* 5: 163–175.
23. Douin-Echinard, V., P. D. Robbins, M. T. Lotze, G. Favre, and B. Couderc. 1998. Enhancement of anti-tumor immunity by injection of fibroblasts genetically engineered to produce IL-12 and to express CD70. *Adv. Exp. Med. Biol.* 451: 353–357.
24. Florido, M., M. Borges, H. Yagita, and R. Appelberg. 2004. Contribution of CD30/CD153 but not of CD27/CD70, CD134/OX40L, or CD137/4-1BBL to the optimal induction of protective immunity to *Mycobacterium avium*. *J. Leukocyte Biol.* 76: 1039–1046.
25. Lorenz, M. G., J. A. Kantor, J. Schlom, and J. W. Hodge. 1999. Anti-tumor immunity elicited by a recombinant vaccinia virus expressing CD70 (CD27L). *Hum. Gene Ther.* 10: 1095–1103.
26. Rowley, T. F., and A. Al-Shamkhani. 2004. Stimulation by soluble CD70 promotes strong primary and secondary $CD8^+$ cytotoxic T cell responses in vivo. *J. Immunol.* 172: 6039–6046.
27. Taraban, V. Y., T. F. Rowley, and A. Al-Shamkhani. 2004. Cutting edge: a critical role for CD70 in CD8 T cell priming by CD40-licensed APCs. *J. Immunol.* 173: 6542–6546.
28. Tesselaar, K., L. A. Gravestein, G. M. van Schijndel, J. Borst, and R. A. van Lier. 1997. Characterization of murine CD70, the ligand of the TNF receptor family member CD27. *J. Immunol.* 159: 4959–4965.
29. Yamada, A., A. D. Salama, M. Sho, N. Najafian, T. Ito, J. P. Forman, R. Kewalramani, S. Sandner, H. Harada, M. R. Clarkson, et al. 2005. CD70 signaling is critical for CD28-independent $CD8^+$ T cell-mediated alloimmune responses in vivo. *J. Immunol.* 174: 1357–1364.
30. Tesselaar, K., Y. Xiao, R. Arens, G. M. van Schijndel, D. H. Schuurhuis, R. E. Mebius, J. Borst, and R. A. van Lier. 2003. Expression of the murine CD27 ligand CD70 in vitro and in vivo. *J. Immunol.* 170: 33–40.
31. Iwamoto, S., M. Ishida, K. Takahashi, K. Takeda, and A. Miyazaki. 2005. Lipopolysaccharide stimulation converts vigorously washed dendritic cells (DCs) to nonexhausted DCs expressing CD70 and evoking long-lasting type 1 T cell responses. *J. Leukocyte Biol.* 78: 383–392.
32. Laouar, A., V. Haridas, D. Vargas, X. Zhinan, D. Chaplin, R. A. van Lier, and N. Manjunath. 2005. $CD70^+$ antigen-presenting cells control the proliferation and differentiation of T cells in the intestinal mucosa. *Nat. Immunol.* 6: 698–706.
33. Taraban, V. Y., T. F. Rowley, D. F. Tough, and A. Al-Shamkhani. 2006. Requirement for CD70 in $CD4^+$ Th cell-dependent and innate receptor-mediated $CD8^+$ T cell priming. *J. Immunol.* 177: 2969–2975.
34. Adam, O., A. Vercellone, F. Paul, P. F. Monsan, and G. Puzo. 1995. A nondegradative route for the removal of endotoxin from exopolysaccharides. *Anal. Biochem.* 225: 321–327.
35. Kedl, R. M., W. A. Rees, D. A. Hildeman, B. Schaefer, T. Mitchell, J. Kappler, and P. Marrack. 2000. T cells compete for access to antigen-bearing antigen-presenting cells. *J. Exp. Med.* 192: 1105–1114.
36. Gibson, S. J., L. M. Imbertson, T. L. Wagner, T. L. Testerman, M. J. Reiter, R. L. Miller, and M. A. Tomai. 1995. Cellular requirements for cytokine production in response to the immunomodulators imiquimod and S-27609. *J. Interferon Cytokine Res.* 15: 537–545.
37. Gomez-Gomez, L., G. Felix, and T. Boller. 1999. A single locus determines sensitivity to bacterial flagellin in *Arabidopsis thaliana*. *Plant J.* 18: 277–284.
38. Felix, G., J. D. Duran, S. Volko, and T. Boller. 1999. Plants have a sensitive perception system for the most conserved domain of bacterial flagellin. *Plant J.* 18: 265–276.
39. Napolitani, G., A. Rinaldi, F. Bertoni, F. Sallusto, and A. Lanzavecchia. 2005. Selected Toll-like receptor agonist combinations synergistically trigger a T helper type 1-polarizing program in dendritic cells. *Nat. Immunol.* 6: 769–776.
40. Masopust, D., V. Vezys, A. L. Marzo, and L. Lefrancois. 2001. Preferential localization of effector memory cells in nonlymphoid tissue. *Science* 291: 2413–2417.
41. Reinhardt, R. L., A. Khoruts, R. Merica, T. Zell, and M. K. Jenkins. 2001. Visualizing the generation of memory CD4 T cells in the whole body. *Nature* 410: 101–105.
42. Watts, T. H. 2005. Tnf/Tnfr family members in costimulation of T cell responses. *Annu. Rev. Immunol.* 23: 23–68.
43. Lens, S. M., K. Tesselaar, M. H. van Oers, and R. A. van Lier. 1998. Control of lymphocyte function through CD27-CD70 interactions. *Semin. Immunol.* 10: 491–499.
44. Arens, R., M. A. Nolte, K. Tesselaar, B. Heemskerk, K. A. Reedquist, R. A. van Lier, and M. H. van Oers. 2004. Signaling through CD70 regulates B cell activation and IgG production. *J. Immunol.* 173: 3901–3908.
45. Ochsenbein, A. F., S. R. Riddell, M. Brown, L. Corey, G. M. Baerlocher, P. M. Lansdorp, and P. D. Greenberg. 2004. CD27 expression promotes long-term survival of functional effector-memory $CD8^+$ cytotoxic T lymphocytes in HIV-infected patients. *J. Exp. Med.* 200: 1407–1417.
46. Doxsee, C. L., T. R. Riter, M. J. Reiter, S. J. Gibson, J. P. Vasilakos, and R. M. Kedl. 2003. The immune response modifier and Toll-like receptor 7 agonist S-27609 selectively induces IL-12 and TNF-α production in $CD11c^+CD11b^+$ $CD8^-$ dendritic cells. *J. Immunol.* 171: 1156–1163.
47. Sharpe, A. H., and G. J. Freeman. 2002. The B7-CD28 superfamily. *Nat. Rev. Immunol.* 2: 116–126.
48. Erickson, L. D., B. G. Durell, L. A. Vogel, B. P. O'Connor, M. Cascalho, T. Yasui, H. Kikutani, and R. J. Noelle. 2002. Short-circuiting long-lived humoral immunity by the heightened engagement of CD40. *J. Clin. Invest.* 109: 613–620.
49. Kedl, R. M., M. Jordan, T. Potter, J. Kappler, P. Marrack, and S. Dow. 2001. CD40 stimulation accelerates deletion of tumor-specific $CD8^+$ T cells in the absence of tumor-antigen vaccination. *Proc. Natl. Acad. Sci. USA* 98: 10811–10816.
50. Mauri, C., L. T. Mars, and M. Londei. 2000. Therapeutic activity of agonistic monoclonal antibodies against CD40 in a chronic autoimmune inflammatory process. *Nat. Med.* 6: 673–679.
51. Vonderheide, R. H., J. P. Dutcher, J. E. Anderson, S. G. Eckhardt, K. F. Stephans, B. Razvillas, S. Garl, M. D. Butine, V. P. Perry, R. J. Armitage, et al. 2001. Phase I study of recombinant human CD40 ligand in cancer patients. *J. Clin. Oncol.* 19: 3280–3287.
52. Akira, S., and S. Sato. 2003. Toll-like receptors and their signaling mechanisms. *Scand. J. Infect. Dis.* 35: 555–562.
53. Bennett, S. R., F. R. Carbone, F. Karamalis, R. A. Flavell, J. F. Miller, and W. R. Heath. 1998. Help for cytotoxic-T-cell responses is mediated by CD40 signalling. *Nature* 393: 478–480.
54. Ridge, J. P., F. Di Rosa, and P. Matzinger. 1998. A conditioned dendritic cell can be a temporal bridge between a $CD4^+$ T-helper and a T-killer cell. *Nature* 393: 474–478.
55. Schoenberger, S. P., R. E. Toes, E. I. van der Voort, R. Offringa, and C. J. Melief. 1998. T-cell help for cytotoxic T lymphocytes is mediated by CD40-CD40L interactions. *Nature* 393: 480–483.
56. Kedl, R. M., and M. F. Mescher. 1998. Qualitative differences between naive and memory T cells make a major contribution to the more rapid and efficient memory $CD8^+$ T cell response. *J. Immunol.* 161: 674–683.
57. Byrne, J. A., J. L. Butler, and M. D. Cooper. 1988. Differential activation requirements for virgin and memory T cells. *J. Immunol.* 141: 3249–3257.

Stimulation of Cell Surface CCR5 and CD40 Molecules by Their Ligands or by HSP70 Up-Regulates APOBEC3G Expression in CD4$^+$ T Cells and Dendritic Cells[1]

Jeffrey Pido-Lopez,* Trevor Whittall,* Yufei Wang,* Lesley A. Bergmeier,† Kaboutar Babaahmady,* Mahavir Singh,‡ and Thomas Lehner[2]*

Apolipoprotein B mRNA-editing, enzyme-catalytic, polypeptide-like-3G (A3G) is an intracellular innate antiviral factor that deaminates retroviral cytidine to uridine. In an attempt to harness the anti-HIV effect of A3G, we searched for an agent that would up-regulate A3G and identify the receptors involved. Stimulation of cell surface CCR5 with CCL3 and CD40 with CD40L or both molecules with microbial 70-kDa heat shock protein (HSP)70 up-regulated A3G mRNA and protein expression in human CD4$^+$ T cells and monocyte-derived dendritic cells (DC), demonstrated by real-time PCR and Western blots, respectively. The specificity of CCR5 and CD40 stimulation was established by inhibition with TAK 779 and mAb to CD40, as well as using human embryonic kidney 293 cells transfected with CCR5 and CD40, respectively. A dose-dependent increase of A3G in CCL3- or HSP70-stimulated CD4$^+$ T cells was associated with inhibition in HIV-1 infectivity. To differentiate between the inhibitory effect of HSP70-induced CCR5 binding and that of A3G, GFP-labeled pseudovirions were used to infect human embryonic kidney 293 cells, which showed inhibition of pseudovirion uptake, consistent with A3G being responsible for the inhibitory effect. Ligation of cell surface CCR5 receptors by CCL3 or CD40 by CD40L activated the ERK1/2 and p38 MAPK signaling pathways that induced A3G mRNA expression and production of the A3G protein. These in vitro results were corroborated by in vivo studies in rhesus macaques in which A3G was significantly up-regulated following immunization with SIVgp120 and p27 linked to HSP70. This novel preventive approach may in addition to adaptive immunity use the intracellular innate antiviral effect of A3G. ***The Journal of Immunology,*** **2007, 178: 1671–1679.**

The difficulties encountered with the development of a preventive or therapeutic vaccine against HIV-1 infection have focused attention to the innate arm of immunity (1–3). The innate immune response is rapid, does not rely on immunological memory, and may be involved in driving adaptive immunity. There are three components to innate immunity: cellular (dendritic cells (DC),[3] macrophages, NK, and γδ cells), which involve the TLR (4); extracellular factors (type I and II IFN, cellular antiviral factor, CC chemokines, and complement); and intracellular factors (apolipoprotein B mRNA-editing, enzyme-catalytic, polypeptide-like-3G (A3G) (5), tripartite motif (6), and Murr1 (7)). Intracellular innate immunity against HIV-1 has acquired considerable importance since the discovery of A3G. This is an enzyme with a molecular mass of 46 kDa, which is packaged into retroviral virions and deaminates viral cytidine to uridine, rendering them nonfunctional and inhibiting viral replication. Recently, A3G has also been found to inhibit HIV by an additional mechanism, possibly at or before reverse-transcription (RT) stage of the viral RNA (8). This innate mechanism of resistance to retroviral infection is counteracted by the HIV-1 viral infectivity factor (Vif), which protects the virus by preventing incorporation of A3G into virions and by rapidly inducing its ubiquitination and proteasomal degradation (9–12).

A3G is found in human T lymphocytes, monocytes, and macrophages, and lethally hypermutates viral DNA shortly after it is synthesized by RT (11–15). A3G was also demonstrated in testes, ovaries, and a number of tumor cell lines (14). There is limited information concerning the factors that control expression of A3G, but its level of mRNA does not change with HIV-1 infection (11, 16). A3G inhibits both the R5 and X4 strains of HIV-1 (5). Phorbol esters up-regulate A3G mRNA in a T cell line (H9), and this is mediated by the protein kinase C/mitogen-activated protein/ERK signaling cascade (13). PHA also up-regulates A3G (11), whereas IFN-α and IFN-γ stimulate an increase in A3G in macrophages (13, 14), leading to inhibition of HIV-1 replication in these cells.

To prevent HIV-1 infection, we attempted to identify cell surface molecules that might be involved in stimulating A3G expression. We explored recent findings that 70-kDa heat shock protein (HSP)70 significantly inhibits HIV-1 infectivity of human CD4$^+$ T cells (K. Babaahmady, M. Singh, and T. Lehner, manuscript in preparation), and that it elicits chemokine and cytokine functions by engaging CCR5 and CD40 molecules (17–19). Indeed, we have found that in vitro stimulation of the cell surface CCR5 and CD40 molecules up-regulates A3G in CD4$^+$ T cells and DC. Immunization of rhesus macaques with HSP70 linked to SIV Ags also up-regulates A3G in PBMC, suggesting the application of HSP70

*Mucosal Immunology Unit, Kings College, London, United Kingdom; †Department of Oral Medicine and Pathology, Kings College, London, United Kingdom; and ‡Lionex Diagnostics and Therapeutics, Braunschweig, Germany

Received for publication August 3, 2006. Accepted for publication November 6, 2006.

The costs of publication of this article were defrayed in part by the payment of page charges. This article must therefore be hereby marked *advertisement* in accordance with 18 U.S.C. Section 1734 solely to indicate this fact.

[1] This work was supported by European Community Grants LSHP-CT-2003-503558 and LSHP-CT-2003-503240.

[2] Address correspondence and reprint requests to Dr. Thomas Lehner, Mucosal Immunology Unit, Guy's Tower Floor 28, Guy's Hospital, London SE1 9RT, U.K. E-mail address: thomas.lehner@kcl.ac.uk

[3] Abbreviations used in this paper: DC, dendritic cell; A3G, apolipoprotein B mRNA-editing enzyme-catalytic polypeptide-like-3G; HEK, human embryonic kidney; HSP, heat shock protein; LMM, low molecular mass; MFI, mean fluorescence intensity; RT, reverse transcription; Vif, viral infectivity factor; VSV, vesicular stomatitis virus; ct, cycle threshold.

or other CCR5 and CD40 ligands to preventive and therapeutic vaccination against HIV-1 infection.

Materials and Methods

Preparation of microbial HSP70

Recombinant *Mycobacterium tuberculosis* HSP70 was prepared from the *Escherichia coli* pop strain (20). HSP70 was purified by ion-exchange chromatography using Q-Sepharose, followed by ATP affinity chromatography. The HSP70 preparation was further treated with polymixin B-coated beads (Sigma-Aldrich) to remove LPS. The LPS content of the HSP preparations was determined by the *Limulus* amebocyte lysate assay (Sigma-Aldrich), and showed <0.006 U/μg HSP70 or 5 pg/1 μg HSP70 preparation. Any contamination with LPS was further excluded by calcium mobilization elicited by HSP70, but not LPS and proteinase K treatment, which inhibited TNF-α production stimulated by HSP70, but not by LPS (data not presented; see Refs. 17 and 18). Furthermore, dose-dependent inhibition by pertussis toxin producing TNF-α and IL-12 was found with HSP70, but not with LPS. In many assays, LPS was used as a control, so as to exclude further the possibility that any LPS contaminant might have been responsible for the results (21, 22).

LPS, CD40L, CCL-3 (MIP-1α), CXCL-12, and TAK 779

LPS derived from *E. coli* strain 0111B4 was purchased from Sigma-Aldrich. Soluble CD40L trimer was donated by F. Villinger (Department of Immunology, Emory University, Atlanta, GA). CCL3 (MIP-1α) and CXCL12 were purchased from R&D Systems. TAK 779 was obtained from the Medical Research Council AIDS Research Reagents Programme.

Preparation of human CD4$^+$ and CD8$^+$ T cells, monocytes, and DC

Volunteers were recruited from the staff and postgraduate students at Guy's Hospital. Permission was obtained for this investigation from the ethics committees of Guy's and St. Thomas' Hospital Medical School. Approximately 50 ml of venous blood was taken, and PBMC was separated by Ficoll-Hypaque gradient centrifugation (Lymphoprep; Nycomed). CD4$^+$ and CD8$^+$ T cells were enriched from PBMC by negative selection on MACS columns (Miltenyi Biotec), through a combination of Abs to CD11b, CD16, CD19, CD36, and CD56, with either CD4 or CD8 (CD8-T cell isolation kit, or CD4-T cell isolation kit; Miltenyi Biotec). Eluted cells that were not bound to the columns were enriched CD4-positive or CD8-positive T cells, and contained <5% of CD8$^-$ or CD4-positive cells, respectively, and <1% monocytes. Human primary monocytes were isolated from PBMC prepared from healthy donors. CD14$^+$ monocytes were enriched by depletion of CD14$^-$ cells using the Monocyte Isolation Kit (MACS; Miltenyi Biotec). The purity of isolated monocytes was consistently >90% when analyzed by flow cytometry with Ab to CD14. Human DC were generated by culturing monocytes in RPMI 1640, 10% FCS, GM-CSF (400 U/ml), and IL-4 (100 U/ml) for 5 days. These monocyte-derived DC were considered to be immature DC, defined by surface expression of DC markers CD83, CD80, CD86, and CD40, and were CD14$^-$. To generate mature DC, immature DC were further stimulated with 20 μg/ml HSP70, and for some experiments with 10 ng/ml LPS or 10 ng/ml CD40L for 48 h.

Cell lines and stimulation

Human embryonic kidney (HEK) cell line (HEK 293) and stably transfected HEK 293 cells with CCR5 were obtained from the National Institutes of Health AIDS Research and Reference Reagent Program. The cells showed 85% (mean fluorescence intensity (MFI) 173) CCR5 and were maintained in DMEM medium supplemented with 10% FCS, 100 μg/ml penicillin and streptomycin, and 2 mM glutamine. For CCR5-transfected HEK 293 cells, 500 μg/ml G418 (Sigma-Aldrich) was included in the medium. HEK 293 T cells were provided by K. Bishop and M. Malim (Kings College, London, U.K.). Aliquots of 2 $\times$ 10^6 purified CD4$^+$ or CD8$^+$ T cells, monocytes, and immature or mature DC in 1 ml of RPMI 1640 with 10% FCS were added to each well of a 24-well plate. Cells were incubated in 5% CO_2 at 37°C with HSP70 (20μg/ml), LPS (10 ng/ml), CD40L (10 ng/ml), CCL3, or CXCL12 each at 10 ng/ml or left untreated. For the dose responses, CD4$^+$ T cells or immature DC were treated with 0, 6.25, 12.5, 25, or 50 μg/ml microbial HSP70; 0, 2.5, 5, 10, or 20 ng/ml CCL3 or CXCL12; and 2.5, 5, 10, or 20 ng/ml CD40L or LPS. Incubation periods were 28 h for CD4$^+$ and CD8$^+$ T cells and 18 h for monocytes, immature or mature DC, and HEK 293 T cells or HEK 293 cells.

Isolation of RNA

RNA was isolated from ~2 $\times$ 10^6 cells using a Total RNA Isolation Kit (Promega), and cDNA was generated from RNA by RT-PCR using the Reverse Transcription System (Promega), according to the manufacturer's instructions.

Transfection

Full-length human CD40 cDNA in the pCDM8 plasmid vector (Invitrogen Life Technologies) was provided by B. Seed (Department of Genetics, Harvard University, Boston, MA). The HEK 293 T cells were cultured in 25-cm^2 flasks until 30–50% confluence and transfected using LipofectAmine Plus (Invitrogen Life Technologies). Transfection was performed, according to the manufacturer's protocol, and CD40 was detected by flow cytometry using FITC-conjugated CD40 mAb.

Receptor inhibition

CCR5-transfected HEK 293 cells were treated with 0, 10, 50, 100, or 500 nM TAK 779 to block CCR5 over 1 h, and then stimulated with 20 μg/ml HSP70 for 18 h. CD40-transfected HEK 293 T cells were treated with 0, or 15 μg/ml anti-CD40 Ab for 1 h, and then stimulated with 20 μg/ml HSP70 for 18 h.

PCR of A3G

Aliquots of 100 ng of the cDNA were added to a PCR mix containing *Taq* polymerase, reaction buffer, 3 mM $MgCl_2$, 0.2 mM dNTP, and 12 μM each A3G primer (5′-TACAGGGTTACCTGCTTCACCTCC-3′ and 5′-AAG TAATGCACTCTAATTTTTAAA-3′). PCR conditions were 95°C for 5 min, then 90°C for 1 min, 57°C for 1 min, and 72°C for 2 min (for 32 cycles), and then 72°C for 10 min. PCR products (500 bp long) were run on a 1% agarose gel containing 0.001% ethidium bromide. Samples were normalized using GAPDH PCR amplification as an endogenous control. Inhibition of HSP70-stimulated A3G was by treating the cells with mAb to CD40 (1.5 μg/ml) and control with the IgG2a isotype (1.5 μg/ml).

Real-time PCR of A3G mRNA

A3G mRNA expression was determined by real-time PCR using the ABI Prism 5700 (Applied Biosystems). Approximately 100 ng of cDNA was added in duplicate to a PCR mix containing TaqMan Universal Mastermix (Applied Biosystems) and commercially available A3G primers and fluorescent labeled probes (Assays on Demand; Applied Biosystems). The cDNA was amplified on the ABI Prism 5700, according to the manufacturer's instructions. Real-time PCR amplification within samples was normalized using GAPDH amplification (23). GAPDH primers and fluorescent labeled probes were obtained from Assays on Demand (Applied Biosystems). The sensitivity of the A3G and GAPDH PCR was initially tested and validated by amplification of the target product from serially diluted cDNAs. A difference in the cycle threshold (ct) value by cycles at every $\log_{10}$ dilution of the cDNA concentration and similar and parallel trends of the curves for GAPDH and A3G reaction graphs (slope $\leq$0.1) were taken as confirmation of the validity of the GAPDH and A3G PCR (data not shown). Data analysis was performed following the $2^{-\lambda\lambda ct}$ comparative method outlined in the ABI Prism user bulletin to obtain the fold difference in mRNA expression between two different samples, which is stimulated relative to unstimulated cells.

Western blots of A3G protein

To detect A3G protein, 2 $\times$ 10^6 cells were treated for 24 h with HSP70 (25 μg/ml), CD40L (1 μg/ml), or PHA (10 μg/ml), and then lysed in HBBS, with 10 mM HEPES (pH 7.4) with 1% Nonidet P-40. Lysates were cleared by centrifugation, and an equal volume of SDS sample buffer was added before SDS-PAGE under reducing conditions. For the experiments with macaque cells and comparison of different cells, A3G was immunoprecipitated using polyclonal rabbit anti-human A3G (Immunodiagnostics) and protein G-Sepharose (Amersham Pharmacia). Bound A3G was released by addition of SDS sample buffer for SDS-PAGE, as above. After transfer of proteins to a polyvinylidene difluoride membrane, Western blotting was conducted with mouse mAb to A3G (Immunodiagnostics) or β-actin (Sigma-Aldrich), using biotinylated anti-mouse Ab, streptavidin-peroxidase, and ECL-plus reagents (Amersham).

Signaling

To study the signaling pathway, DC were incubated with 20 μM p38 MAPK inhibitor SB 203580 or 10 μM ERK1/2 inhibitor PD 098059 (both Sigma-Aldrich) for 30 min and stimulated with HSP70 (20 μg/ml) or PHA

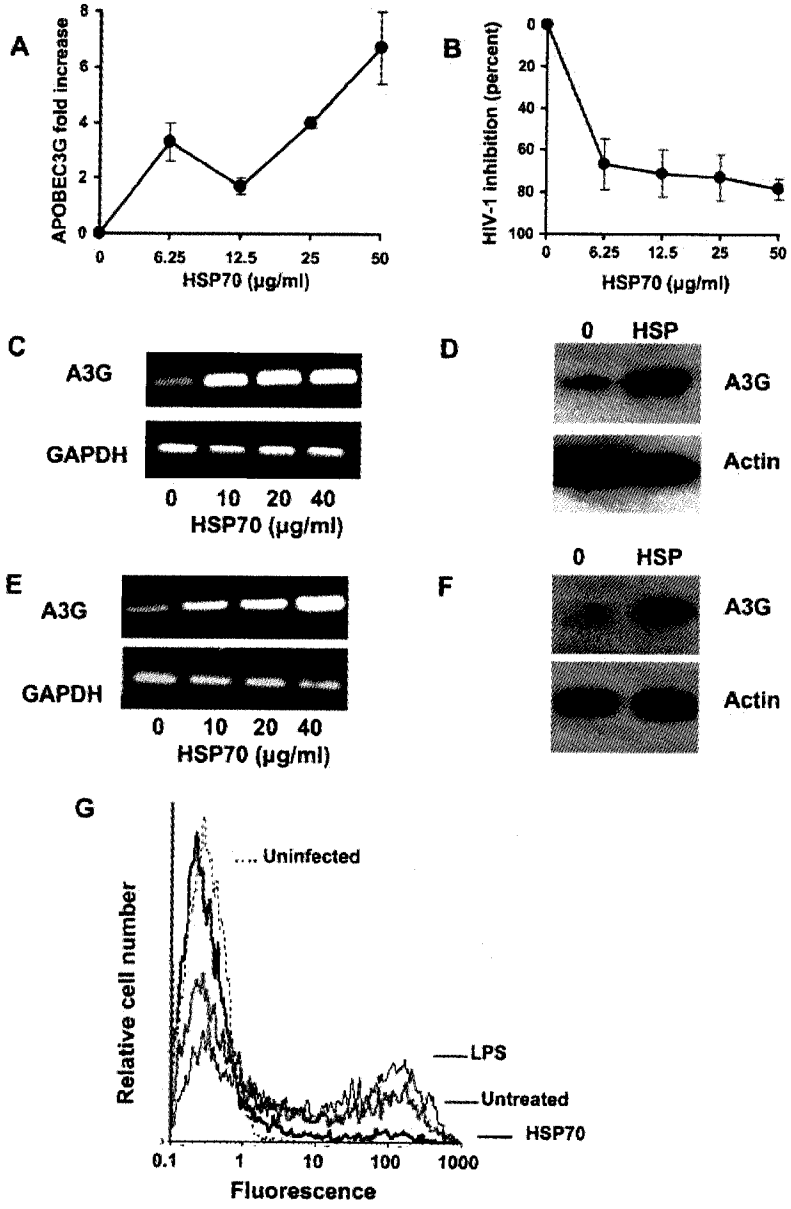

FIGURE 1. Evidence that dose-dependent stimulation of primary $CD4^+$ T cells with HSP70 up-regulates A3G mRNA expression shown by RT-PCR (*A*), inhibits HIV-1 infectivity (*B*), and up-regulates A3G mRNA shown by PCR (*C*) and protein expression demonstrated by Western blots (*D*). Stimulation of A3G mRNA expression by HSP70 in immature DC shown by PCR (*E*) and protein demonstrated by Western blots (*F*); inhibition of HSP70-treated (*G*), compared with untreated or LPS-treated GFP-labeled pseudovirions of HEK 293 cells (representative sample of three experiments).

(10 μg/ml) for 24 h, and then A3G expression was determined. β-Actin was used as a loading control for A3G, and the cells were checked for direct toxic effect of the inhibitors by trypan blue, which showed no impaired viability of the cells.

The effect of HSP70 on HIV-1 infectivity

The CCR5 strain of HIV-1 (BaL) isolate was obtained from the National Institutes of Health AIDS Research and Reference Reagent Program. PBMCs were stimulated with PHA (Sigma-Aldrich) and IL-12 (Schiaparelli Biosystems), using standard protocol to grow the virus. RT activity in the culture supernatants was monitored using Quan-T RT kit (Amersham Biosciences), and the virus was harvested at a peak time point. The-HIV-1_{Bal} stock titers were determined by RT, and the 50% tissue culture infective dose of the virus was then determined.

To test HIV-1 infectivity, we separated CD4-positive T cells from PBMC using the $CD4^+$ T cell separating kit (Miltenyi Biotec). CD4-positive cells were activated with 10 μg/ml PHA in RPMI 1640 medium supplemented with penicillin, streptomycin, 10% FCS, and 20 IU of IL-2 (Schiaparelli Biosystems) for 3 days, and then washed with medium and counted. Cells were infected with primary HIV-1 BaL (CCR5-binding strain), using 100 μl (20,000 cpm) of the virus to infect 10^6 cells. They were incubated for 3 h and washed three times with medium, and 10^5 cells/well were cultured in triplicate in 96-well plates. HSP70 (0–50 μg/ml) were added to the cells, and every 2 days 100 μl of culture supernatant was replaced with 100 μl of medium supplemented with 20 IU of IL-2 and HSP70. RT activity was measured on days 1 and 7 using the Amersham Quan-T RT kit; the results are given for day 7.

In vivo studies of A3G in immunized macaques with HSP70

PBMC were separated from the blood of five groups of rhesus macaques in which blood was taken 2–4 wk after the last of three immunizations. Group 1 unimmunized animals ($n = 3$) were compared with group 2 ($n = 3$), immunized with SIVgp120 (200 μg) and *gag* p27 (200 μg) covalently linked to HSP70 (200 μg). Group 3 macaques ($n = 3$) were immunized with SIVgp120 and *gag* p27 (100 μg each), covalently linked to HSP70 (200 μg); in addition to comparing pre- and postimmunization PBMC, they were also compared with group 4 macaques ($n = 3$) immunized with alum (200 μg Alugel; Uniscience) adsorbed with HIVgp140 (100 μg) and SIV*gag* p27 (200 μg). Increase in A3G was assayed by real-time PCR in PBMC from naive macaques, HSP70-SIV Ags, alum-HIV/SIV Ags, and HSP70-immunized animals without Ags (group 5, $n = 2$). The animals were housed and handled in accordance with the U.K. Home Office and European guidelines.

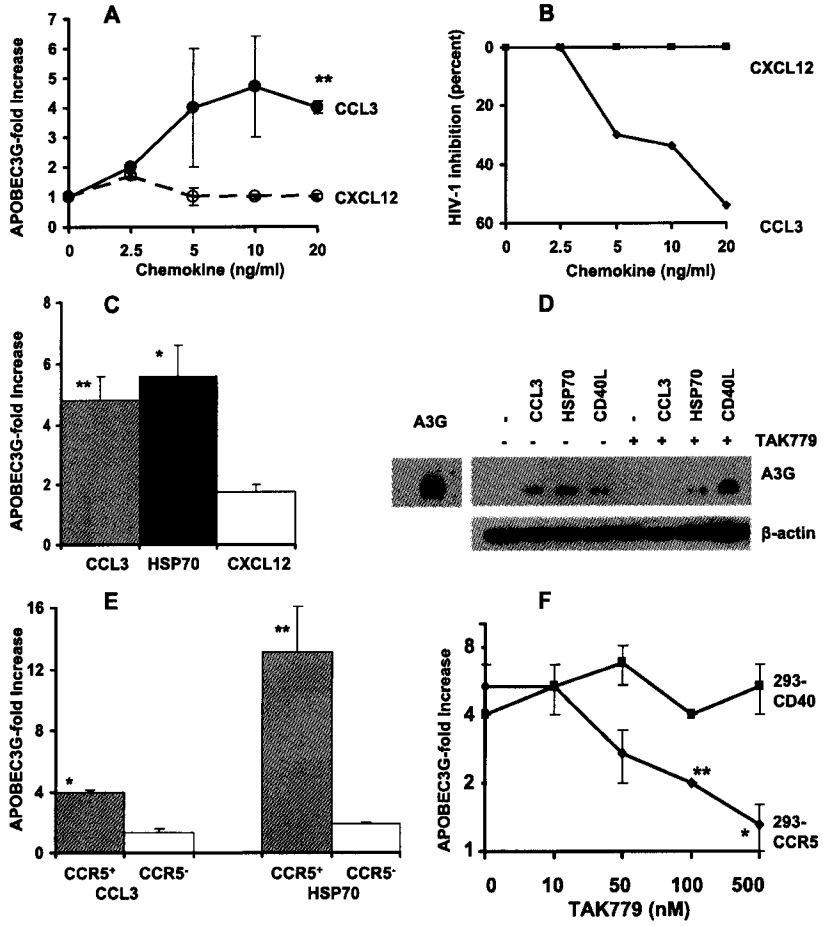

FIGURE 2. Evidence that stimulation of CCR5 with CCL3 (10 ng/ml) or HSP70 (20 μg/ml) upregulates A3G expression. *A*, Dose-dependent effect of CCL3 compared with CXCL12 (10 ng/ml) on expression of A3G (**, $p < 0.0001$); *B*, inhibition of HIV-1 infectivity in primary $CD4^+$ T cells; *C*, mRNA in DC stimulated with CCL3 compared with CXCL12 and HSP70 ($n = 4$; *, $p = 0.04$; **, $p = 0.002$); *D*, inhibition of CCR5-mediated production of A3G protein by TAK 779 in DC stimulated with CCL3 or HSP70 compared with the CD40L control and β-actin; *E*, mRNA in $CCR5^+$ compared with $CCR5^-$ HEK 293 cells stimulated with CCL3 ($n = 4$; $p = 0.015$) or HSP70 ($n = 9$; **, $p = 0.006$); and *F*, inhibition by TAK 779 of A3G mRNA in $CCR5^+$ compared with $CD40^+$ HEK 293 cells stimulated with HSP70 (*, $p = 0.057$; **, $p = 0.0001$).

Preparation of the HIV-GFP virus

To prepare GFP-labeled HIV-1, HEK 293 T cells were transfected with plasmids p8.91 (encoding for HIV-1 *gag*, *pol*, *tat*, and *rev*), pCSGW (encoding for GFP), and pVSV-G (encoding for vesicular stomatitis virus (VSV) viral envelope) provided by M. Malim and K. Bishop (Kings College, London, U.K.) (24). The VSV viral envelope avoided the requirement of CD4 and HIV coreceptors for cell entry by virions. The transfection was conducted by the lipofectin (Invitrogen Life Technologies) method, according to the manufacturer's instructions. Virions were harvested 3–4 days posttransfection and normalized by p24 *gag* ELISA (Gentaur).

To infect HEK 293 cells expressing CCR5, $\sim 5 \times 10^4$ cells/well, in 0.5 ml of DMEM with 10% FCS, were plated into 12-well plates and treated with either HSP70 (20 μg/ml) or LPS (10 ng/ml) and incubated at 37°C and 5% CO_2 for 18 h. The cells were infected with 1 ml of GFP-virus extract, containing 30–50 pg/ml p24, and incubated for 3 days. Cells were then harvested and assessed for viral infection by GFP expression using FACS analysis.

Real-time PCR of rhesus macaque A3G mRNA

PBMC (3×10^6, 500 μl/well) were distributed into 24-well plates and incubated in RPMI 1640 (supplemented with 10% FCS, 2 μM glutamine, and 100 μg of penicillin and streptomycin) for 18 h with 10 μg/ml HSP70 or 10 μg/ml PHA. The cells were then harvested and washed with PBS. The RNA was extracted using a Total RNA kit, and cDNA was prepared using the RT system (Promega), as described above.

Quantification of A3G mRNA was conducted by real-time PCR (ABI Prism 5700) using the PlatinumSYBR green qPCR SuperMix-UDG with ROX (Invitrogen Life Technologies). The primers used for rhesus macaques A3G were as follows: 5′-CTG TCC ACT GAC CCA AGG TT-3′ (right); 5′-ACA TGC CAC GAA GAT CA-3′ (left). The amplification conditions were 2 min at 50°C, 2 min at 95°C, 40 cycles of 15 s at 95°C, and 30 s at 60°C. The results were standardized within samples using rhesus macaques GAPDH mRNA (primers: 5′-GGA GCT CTC CAG AAC ATC ATC CCT-3′ (right); 5′-CCT TGA GGG GGC CCT CCG ACG CCT-3′ (left)). Melting curve analysis was performed in every assay, and the products were also analyzed on agarose gel to confirm the specificity of amplified products. The data analysis was described above.

Statistics

The results are expressed as mean (±SEM) and were analyzed with the appropriate Student *t* test.

Results

Stimulation of mRNA and protein of A3G by HSP70 in primary $CD4^+$ T cells and the effect on HIV-1 infectivity

The rationale for exploring HSP70 as an agent that will stimulate A3G production was based on the inhibitory effect of HSP70 on HIV-1 replication (K. Babaahmady, M. Singh, and T. Lehner, manuscript in preparation). Dose-dependent increase in A3G mRNA expression was demonstrated by real-time PCR in primary $CD4^+$ T cells stimulated with HSP70 (Fig. 1*A*), and these cells showed corresponding inhibition of HIV-1 infectivity (Fig. 1*B*), using an R5 strain of HIV-1 (BaL). Increased A3G mRNA (Fig. 1*C*) and protein (Fig. 1*D*) expression were also found after HSP70 stimulation of $CD4^+$ T cells and monocyte-derived immature DC (Fig. 1, *E* and *F*), respectively. The GAPDH control showed little or no change (Fig. 1, *C* and *E*). Thus, stimulation by HSP70 induced a dose-dependent increase in A3G mRNA and protein expression that was associated with inhibition of HIV-1 infection in $CD4^+$ T cells and monocyte-derived DC.

Inhibition of GFP-labeled HIV-1 virions

To differentiate between HSP70 binding CCR5 directly or via CC chemokines and A3G, we used single-round infection assay by GFP-labeled HIV-1 pseudovirions to infect $CCR5^+$ HEK 293

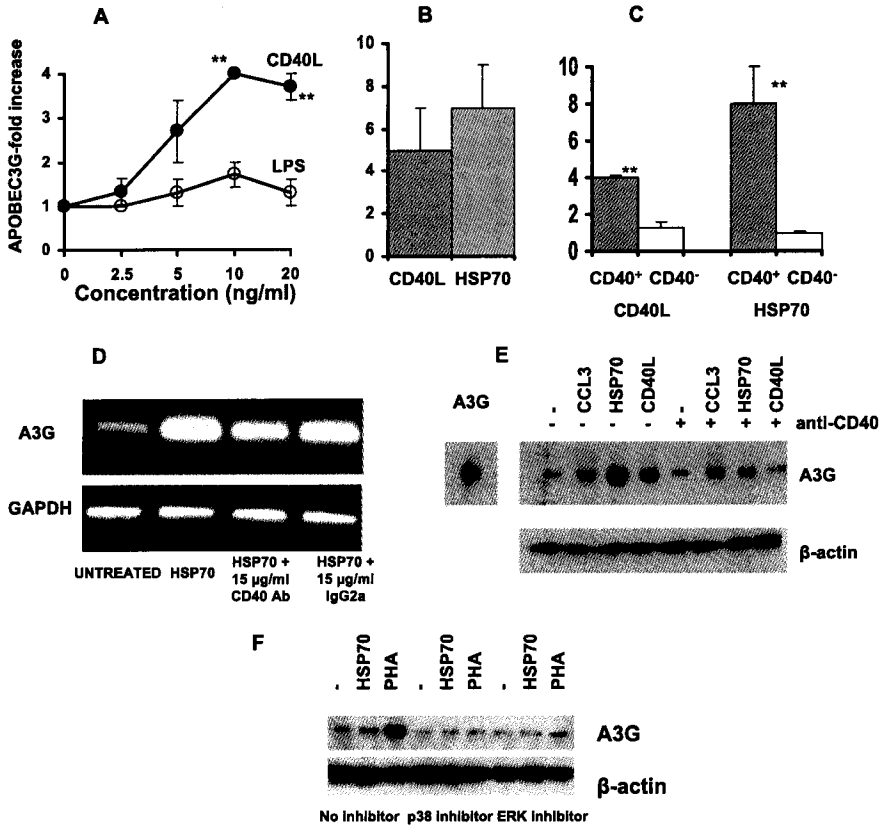

FIGURE 3. Evidence that stimulation of CD40 with CD40L or HSP70 up-regulates A3G expression. *A*, Dose-dependent increase of mRNA in human DC stimulated with CD40L (10 ng/ml) compared with LPS (10 ng/ml) ($n = 3$; **, $p = 0.02$), and *B*, CD40L (10 ng/ml) compared with HSP70 (20 μg/ml) ($n = 7$); *C*, mRNA in CD40-transfected and untransfected HEK 293 cells stimulated with HSP70 ($n = 7$; **, $p = 0.02$) or CD40L; *D*, inhibition with mAb to CD40 of HSP70-stimulated induction of A3G mRNA in DC assessed by PCR, and *E*, inhibition of induction of A3G protein by CCL3 (10 ng/ml), HSP70 (20 μg/ml), or CD40L (10 ng/ml) analyzed by Western blot; *F*, inhibition of HSP70-stimulated DC by p38 MAPK (20 μM) and ERK (10 μM) inhibitors; **, $p \leq 0.01$.

cells. Before pseudovirion exposure, the $CCR5^+$ HEK 293 cells were treated overnight with either 20 μg/ml mHSP70 or 10 ng/ml LPS. FACS analysis of cells 3 days postexposure to the GFP^+ virions revealed that the percentage of GFP^+ cells was 5- to 6-fold greater for the untreated (44.2%; MFI 176.2) or LPS-treated cells compared with the HSP70-treated cells (8.6%; MFI 125.5) (Fig. 1*G*).

Time course of HSP70 stimulation of $CD4^+$ T cells and DC

A time course of HSP70 stimulation (20 μg/ml) of $CD4^+$ T cells at 0, 8, 18, 28, and 38 h showed an optimum 4-fold increase in A3G mRNA at 28 h, which was applied in all subsequent studies (data not shown). A corresponding time course with immature DC showed a 6.7 (+1.3)-fold increase in A3G, which was optimal at 18 h (data not shown), and this was used for all subsequent investigations.

Up-regulation of A3G expression mediated by stimulation of the CCR5 molecules

Having prior knowledge that the CCR5 and CD40 molecules mediate HSP70 stimulation in $CD4^+$ T cells and DC (17–19), we first examined the possibility that ligation of CCR5 will up-regulate A3G. Stimulation of primary human $CD4^+$ T cells (Fig. 2*A*) or immature DC (data not presented) with CCL3 showed a dose-dependent increase in A3G mRNA expression, compared with CXCL12, which does not bind CCR5 and showed no change. A corresponding dose-dependent inhibition of HIV-1 infectivity was found when the primary $CD4^+$ T cells were treated with CCL3, but not CXCL12 (Fig. 2*B*). The effect of CCL3 (10 ng/ml) was then compared with HSP70 (20 μg/ml) in immature DC, which showed an increase in A3G expression (4.8 ± 0.8- and 5.6 ± 0.9-fold, respectively), whereas CXCL12 (10 ng/ml) showed negligible increases in A3G (1.7 ± 0.25; $p = 0.002$ and 0.04, respectively; Fig. 2*C*). A3G protein was also up-regulated following treatment with the above concentration of HSP70 and to a lesser extent with CCL3 and CD40L, but only CCL3- and HSP70-stimulated increases in A3G generation were inhibited by TAK 779, a specific CCR5 inhibitor, as CD40L-stimulated increase in A3G is mediated by CD40 and not CCR5 molecules (Fig. 2*D*). The β-actin control remained largely unchanged. CCR5-mediated stimulation of A3G expression was further supported by stimulating CCR5-transfected HEK 293 cells with CCL3, which induced greater A3G expression (4.0 ± 0-fold) than stimulating untransfected cells (1.3 ± 0.3-fold; $p = 0.015$), whereas stimulation with HSP70 showed greater A3G expression in CCR5-transfected cells (13.3 ± 3.0-fold) than untransfected cells (1.9 ± 1.1-fold; $p = 0.006$) (Fig. 2*E*). The specificity of HSP70-binding CCR5 was confirmed by treatment of the CCR5-transfected HEK 293 cells with TAK 779, which showed a significant dose-dependent inhibition of HSP70-induced A3G expression, unlike the CD40-transfected cells (Fig. 2*F*).

Up-regulation of A3G expression mediated by stimulation of CD40 molecules

We then studied CD40, which is engaged by the CD40L (CD154), and is an important molecule in the costimulatory pathway of cognate immunity (25). Indeed, stimulation of DC with CD40L resulted in a significant dose-dependent increase in A3G, which was not found when DC were stimulated with LPS (**, $p = 0.02$; Fig. 3*A*). A comparative study of stimulating DC with CD40L or HSP70 showed 5.4 ± 1.9-fold increase in A3G expression with CD40L, which was similar to that stimulated by HSP70 (6.8 ± 1.8-fold; Fig. 3*B*). This was supported by significant CD40L-stimulated increase in A3G mRNA expression in CD40-transfected (4.0 ± 0-fold), compared with untransfected HEK 293 T cells

(1.3 ± 0.33; $p = 0.015$; Fig. 3*C*). A significant increase in A3G expression was also found following HSP70 stimulation of CD40-transfected (8.0 ± 2.3-fold), compared with untransfected (1.0 ± 0.03; $p = 0.022$) HEK 293 T cells (Fig. 3*C*). Furthermore, inhibition of HSP70-stimulated A3G mRNA expression and protein in monocyte-derived DC was demonstrated using mAb to CD40 by PCR (Fig. 3*D*). Examination of A3G protein by Western blots also showed increases in A3G production stimulated by CCL3, HSP70, or CD40L (Fig. 3*E*), and treatment with CD40 Abs inhibited CD40L- and HSP70-, but not CCL3-stimulated up-regulation of A3G. The control β-actin showed little change, except for an increased concentration with CD40L and anti-CD40 treatment, which, however, was converse to the A3G expression (Fig. 3*E*). These results in monocyte-derived DC and CD40-transfected 293 cells suggest that activation of the CD40 cell surface molecules induces A3G expression.

Signaling by the ERK1/2 and p38 phosphorylation pathways

The signaling pathway of A3G stimulation mediated by CCR5 and CD40 was then explored. Treatment of HSP70- or PHA-stimulated DC with ERK1/2 (PD09859) or p38 (SB203580) inhibitor showed a decrease in A3G protein, compared with untreated DC (Fig. 3*F*). These results are consistent with ERK1/2 and p38 phosphorylation pathways being involved in the CCR5- and/or CD40-mediated activation of A3G expression.

Comparative study of mRNA and protein expression of A3G in five subsets of human PBMC

A comparative study of mRNA and protein expression of A3G was then pursued in $CD4^+$ and $CD8^+$ T cells, monocytes, and immature and mature DC. Resting $CD8^+$ T cells expressed more A3G protein than $CD4^+$ T cells (Fig. 4*A*). Stimulation with HSP70 for 28 h resulted in an increase in A3G, which was relatively greater in $CD4^+$ than $CD8^+$ T cells. A similar comparison of the monocyte and immature and mature DC series demonstrated greater protein levels of A3G in the unstimulated monocytes and DC than in the T cell subsets (Fig. 4*A*). HSP70 stimulation again resulted in increased expression of A3G in all three subsets of monocytes and DC. Real-time PCR was then used to assess quantitatively the effect of HSP70 stimulation on the expression of A3G mRNA. A3G was up-regulated with a mean (±SEM) fold increase of 1.7 (±0.21) in $CD8^+$ T cells and 3.0 (±0.4) in $CD4^+$ T cells ($p = 0.04$; Fig. 4*B*). Very significant increase in HSP70-stimulated A3G mRNA expression was found in immature (6.8 ± 1.3) and mature DC (11.2 ± 2.5), compared with monocytes (1.7 ± 0.4) ($p = 0.001$; Fig. 4*B*). Clearly, a direct association between A3G mRNA and protein levels was not observed for all of the cell subsets examined. Stimulation of the $CD4^+$ or $CD8^+$ T cells and immature DC with HSP70 was then compared with that of LPS (Fig. 4*C*). The results suggest that A3G in $CD4^+$ T cells is significantly up-regulated with HSP70 (3.0 ± 0.45), compared with LPS (1.25 ± 0.25; $p = 0.014$), and this was also found to a lesser extent with $CD8^+$ T cells ($p = 0.013$; Fig. 4*C*). Immature DC also showed significantly greater increase in A3G when stimulated with HSP70 (6.9 ± 1.84) than with LPS (2.4 ± 0.43; $p = 0.04$) (Fig. 4*C*). Thus, HSP70 is significantly more potent than LPS in up-regulating A3G in all three cell subsets. Furthermore, when LPS or CD40L was used for maturation of DC and these were then stimulated with HSP70, comparable A3G expression was found to that resulting from inducing DC maturation with HSP70 (data not presented).

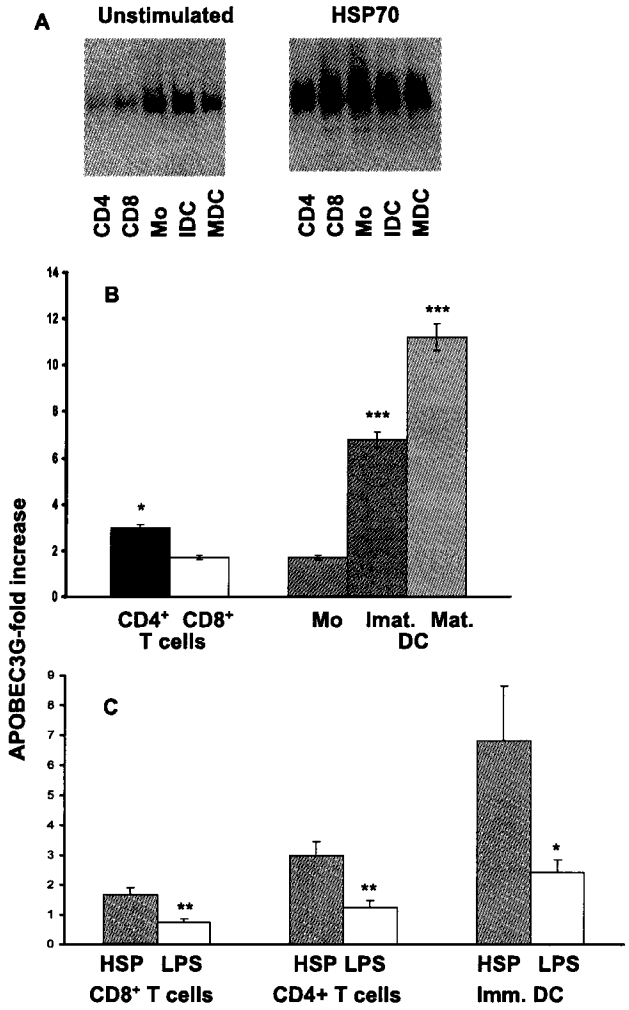

FIGURE 4. *A*, Comparison of A3G expression in five subsets of human PBMC or DC and HSP70-stimulated (20 μg/ml) $CD4^+$ and $CD8^+$ T cells, monocytes, and immature and mature DC demonstrated by Western blots; *B*, the same subsets of cells assayed for mRNA by real-time PCR (n = 6–10); *C*, HSP70 (20 μg/ml) compared with LPS (10 ng/ml) stimulation of cells (*, $p = 0.04$; **, $p = 0.013$; ***, $p = 0.005$).

In vivo up-regulation of A3G following immunization with HSP70 in rhesus macaques

The in vitro studies were followed by a retrospective in vivo investigation of five groups of rhesus macaques. PBMC from naive animals (group 1) was compared with those from HSP70 linked to SIVgp120- and p27-immunized (×3) macaques (group 2), 2–4 wk after the last immunization to determine whether A3G can be up-regulated in vivo. A3G mRNA and the protein showed increases in HSP70-immunized compared with the unimmunized macaques (Fig. 5, *A* and *B*), suggesting that HSP70 immunization induces an increase in A3G expression. This was confirmed by real-time PCR analysis, which showed a mean increase of 3.2 ± 0.12-fold in A3G expression in the cells from immunized, as compared with those from naive (1.0 ± 0.0) ($p = 0.07$) animals (Fig. 5*C*). Further studies of A3G were then pursued before and 2–4 wk after immunization in a third group of macaques immunized with HSP70 linked to SIVgp120 and p27, and compared with a fourth group of macaques given alum-adsorbed SIVgp120 and p27. Whereas PBMC of the HSP70 vaccine-immunized macaques showed significant fold increase in A3G expression of 5.1 ± 0.48 after immunization relative to the preimmunization level ($p = 0.013$), the

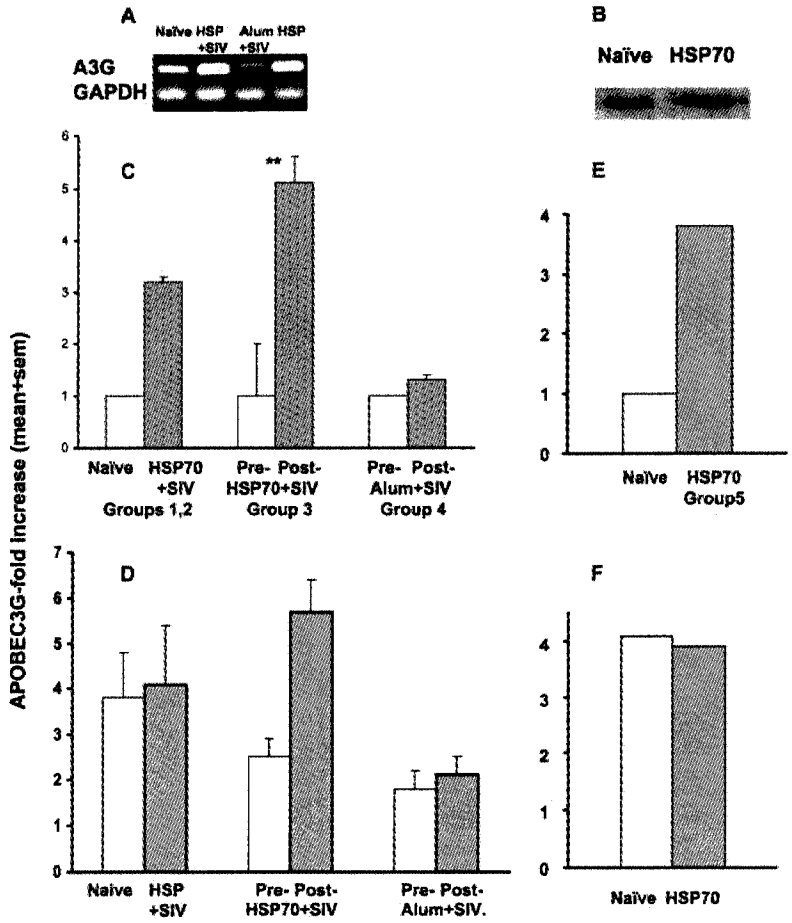

FIGURE 5. The effect of immunization on the expression of A3G in five groups, each consisting of three macaques. Naive animals were compared with those 2–4 wk after they were immunized with HSP70 linked to SIVgp120 and p27, or animals immunized with alum adsorbed to the same SIV proteins by conventional PCR (*A*), by Western blot (*B*), and using real-time PCR (*C*); *D*, the same groups of macaques were restimulated in vitro with HSP70 (20 μg/ml); *E*, a further group of two macaques was immunized with HSP70 alone, and *F*, treated in vitro with HSP70 (**, $p = 0.013$).

alum-immunized macaques showed little or no change (1.2 ± 0.1; Fig. 5*C*). This was corroborated by the conventional PCR (Fig. 5*A*). A comparison between SIV Ags linked to HSP70 and those adsorbed to alum showed a significant increase in A3G expression with HSP70 ($p = 0.032$). Additional in vitro stimulation with HSP70 of PBMC from naive macaques showed an increase in A3G (3.8 ± 1.0) (Fig. 5*D*), but PBMC from the HSP70-immunized macaques showed only a slight further increase in A3G (4.1 ± 1.3) over the level without in vitro treatment with HSP70 (3.2 ± 0.12). Similarly, in vitro stimulation with HSP70 of PBMC from the third group of macaques showed an increase in A3G that was greater in the pre- than in postimmunized macaques (Fig. 5, *D* compared with *C*), unlike the alum-immunized animals that showed only a slight increase in A3G with HSP70. Thus, the increase in A3G can be attributed to immunization with HSP70, as immunization with HIVgp120 and SIV p27 adsorbed to alum failed to up-regulate A3G (1.2 ± 0.09) (Fig. 5*C*). This is consistent with immunization of two macaques with HSP70 alone, which also up-regulated A3G (mean 3.8; Fig. 5*E*), and showed no further increase in A3G following restimulation with HSP70 in vitro, unlike in the naive animals (Fig. 5*F*).

Discussion

It has been established that the HIV-1-inhibitory activity of A3G is neutralized by Vif (9–12). This interaction has raised therapeutic potentials, by either inhibiting Vif activity or boosting A3G levels above the neutralizing capacity of Vif to inhibit virus replication (5, 26). The present studies have been confined to exploring the potential of up-regulating A3G expression first in vitro and then in vivo. The overall results suggest that up-regulation of A3G expression can be mediated by the CCR5 and CD40 molecules, which were stimulated by the chemokine CCL3 and CD40L (CD154), respectively, as well as by HSP70. This was supported by the finding that A3G mRNA expression is up-regulated following stimulation of either CCR5- or CD40-transfected, but not untransfected cell lines, and by the corresponding ligands or HSP70. The primary human cells that showed significant increase in A3G expression when stimulated with CCL3 or HSP70 were $CD4^+$ T cells (3.0 ± 0.4) and immature (6.8 ± 1.3) and mature DC (11.2 ± 2.5), which serve as the major cellular targets of HIV-1. Macrophages were not studied in this work, but show an increase in A3G expression upon stimulation with IFN-α (14).

The specificity of CCR5 stimulation was confirmed by the lack of response of $CCR5^-$ HEK 293 cells or by stimulation with CXCL12, as well as the dose-dependent inhibition of A3G by TAK 779. These findings suggest that CCL3 may not only block and down-regulate CCR5, thereby inhibiting pre-entry of HIV-1 (27, 28), but also stimulate A3G expression, which inhibits postentry replication of HIV-1. Thus, HIV-1 inhibition with CCL3 or HSP70 cannot be ascribed solely to up-regulation of A3G expression. The GFP-labeled virions infecting $CCR5^+$ HEK 293 cells are independent of CD4 and CCR5 expression due to the presence of a VSV envelope, so inhibition of the viral infection is most likely to be due to the intracellular A3G generated by stimulation with HSP70. Furthermore, the pseudo virus features only a single round of infection, which suggests that the A3G-inhibitory effect occurs during the early stages of infection, as observed recently with the low molecular mass (LMM) form of A3G (8). Interestingly, there is evidence that LMM A3G may be resistant to the actions of Vif,

thus making it more desirable as an anti-HIV agent than its non-Vif-resistant high molecular mass A3G counterpart (8). Whether HSP70 up-regulates only the LMM or both forms of A3G requires further investigation. The A3G-inhibiting mechanism involves deaminating deoxycytidine to deoxyuridine of the minus viral ssDNA during RT, and this enzymatic editing of HIV-1 reverse transcripts induces degradation of deaminated minus strand DNA, leading to inhibition of HIV-1 replication (9, 10, 29, 30).

Unlike CCR5, CD40 molecules are expressed on immature and mature DC, Langerhans cells, and macrophages, but not on $CD4^+$ T cells. The specificity of the CD40-mediated response has been demonstrated by A3G mRNA up-regulation in $CD40^+$, but not $CD40^-$ HEK 293 T cells and inhibition of A3G mRNA and protein expression by mAb to CD40. The signaling pathway following stimulation of cell surface CD40 by CD40L or CCR5 by CCL3 was then studied, and this suggested that activation of the ERK1/2 and p38 MAPK signaling pathway induces A3G mRNA expression, which is translated to A3G production. Because the CD40L-CD40 costimulatory pathway between $CD4^+$ T cells and APCs is essential in adaptive immunity between TCRs and peptide-HLA Ags (25), the finding that CD40 stimulation may increase expression of A3G is important. It has been well recognized that activation of $CD4^+$ T cells enhances HIV-1 infectivity, raising concern that immunization might facilitate HIV-1 infection. The finding that CD40 activation by CD40L up-regulates A3G is arguably the first evidence that the enhanced infectivity of activated cells may be counteracted by concomitant increase in A3G expression. Indeed, CD40L is expressed by Ag-specific $CD4^+$ T cells (31), which bind CD40 on DC and probably macrophages that may up-regulate A3G in these cells. Whether a reciprocal stimulation of A3G can be elicited in $CD4^+$ T cells remains to be determined.

The mechanism for up-regulation of A3G can thus be activated by CCL3 stimulating CCR5, CD40L stimulating CD40, or HSP70 stimulating both molecules. An increased expression in CCR5 molecules does not take place; indeed, CC chemokines bind and down-regulate CCR5 on $CD4^+$ T cells or CCR5-transfected Chinese hamster ovary cells (27, 28) and HSP70 down-regulates CCR5 on mature DC (18). However, CD40 is up-regulated in stimulating immature DC with HSP70, so it is possible that the greater cell surface expression of CD40 on mature DC might enhance activation of these cells. Nonetheless, a common MAPK signaling pathway for CCR5 and CD40 molecules involves activation of ERK1/2 and p38, which induce A3G mRNA expression and is translated to protein production. Persistence of A3G expression 2–4 wk after the last immunization with the HSP70-SIV vaccine raises at least two possibilities, as follows: 1) that HSP70 is retained by macrophages and when they undergo necrosis HSP70 is released and bystander macrophages or DC are stimulated to produce A3G (32); 2) that A3G production by $CD4^+$ T cells or DC may retain an immune-like memory, despite it being considered to be an innate immune factor. Both these possibilities will be actively investigated.

The comparative investigation of A3G in the $CD4^+$ and $CD8^+$ T cells showed that whereas resting $CD8^+$ T cells expressed more A3G protein than $CD4^+$ T cells, stimulation of these cells with HSP70 resulted in significantly greater up-regulation of A3G mRNA and protein in $CD4^+$ than $CD8^+$ T cells. A somewhat similar relationship in A3G mRNA was revealed between monocytes and DC, in that HSP70 stimulation induced significantly greater increase in A3G mRNA expression in both immature and mature DC than monocytes. Further quantitative studies will need to be pursued to ascertain whether the final A3G protein levels have reached maximum expression in each of the five subsets of cells studied. The differential effect on HIV-1 infectivity between the $CD4^+$ $CCR5^+$ immature and $CD4^+CCR5^-$ mature DC is also of interest, as the maximal expression of A3G mRNA in mature DC is consistent with lack of HIV-1 infectivity (in contrast to transient carriage) of mature compared with immature DC. Furthermore, there are differences both in timing and magnitude of A3G up-regulation in $CD4^+$ T cells and monocyte-derived DC, suggesting that A3G is more readily up-regulated in DC than $CD4^+$ T cells. This finding might be significant in primary cervicovaginal and rectal mucosal transmission of HIV-1 by Langerhans cells and DC that migrate to the regional lymphoid tissue and infect $CD4^+$ T cells (33–35).

The potential application of HSP70 as an A3G up-regulating agent in both preventive and therapeutic immunization was studied in vivo in rhesus macaques. Indeed, HSP70 alone or covalently linked to HIV or SIV Ags administered by the mucosal or systemic route significantly up-regulated A3G mRNA and protein in PBMC of macaques, whereas alum mixed with HIV and SIV Ags failed to affect A3G expression. Whether other adjuvants will affect the expression of A3G needs to be examined. The overall results suggest that HSP70 might be used as an HIV-designer adjuvant in preventive and therapeutic vaccination, as HSP70 may inhibit both pre-entry transmission of HIV-1 into $CD4^+$ T cells or DC by generating CC chemokines (17, 18), and postentry replication of HIV-1 by up-regulating A3G. Whereas the conventional concept of innate immunity has been that it lacks memory, this may not apply to all innate immune responses, as demonstrated recently with NK cells in delayed hypersensitivity (36). It seems that the CC chemokines, CCL3, CCL4, and CCL5, are increased by repeated immunization with SIVgp120 and p27 in macaques (37), but the effect of repeated in vivo immunization on A3G expression will need to be studied. An important question, whether up-regulation of A3G following HSP70 stimulation can be maintained beyond the 4 wk shown in the present studies, will have to be determined, although preliminary indications are that this might be achieved. Thus, stimulation of the CCR5 molecule, which is the major coreceptor of R5 strains of HIV-1 (38, 39), or the CD40 (25) molecule, which is part of a major costimulatory pathway, up-regulates A3G and results in postentry inhibition of HIV-1 replication. This novel finding may be important in enhancing the innate intracellular anti-HIV-1 response and provides a complementary strategy in protective and therapeutic immunization against HIV-1.

Acknowledgments

We thank Drs. Mike Malim and Kate Bishop for their advice and supplying the reagents for the GFP-labeled virions.

Disclosures

The authors have no financial conflict of interest.

References

1. Levy, J. A. 2001. The importance of the innate immune system in controlling HIV infection and disease. *Trends Immunol.* 22: 312–316.
2. Lehner, T., Y. Wang, M. Cranage, L. A. Bergmeier, E. Mitchell, L. Tao, G. Hall, M. Dennis, N. Cook, R. Brookes, et al. 1996. Protective mucosal immunity elicited by targeted iliac lymph node immunization with a subunit SIV envelope and core vaccine in macaques. *Nat. Med.* 2: 767–775.
3. Lehner, T. 2002. Innate immunity in HIV infection. In *AIDS Vaccine Research.* F. Wong-Staal and R. C. Gallo, eds. Marcel Dekker, New York, pp. 283–307.
4. Iwasaki, A., and A. Medzhitov. 2004. Toll-like receptor control of the adaptive immune responses. *Nat. Immunol.* 10: 987–995.
5. Sheehy, A. M., N. C. Gaddis, J. D. Choi, and M. H. Malim. 2002. Isolation of a human gene that inhibits HIV-1 infection and is suppressed by the viral Vif protein. *Nature* 418: 646–650.
6. Stremlau, M., C. M. Owens, M. J. Perron, M. Kiessling, P. Autissier, and J. Sodroski. 2004. The cytoplasmic body component TRIM5α restricts HIV-1 infection in Old World monkeys. *Nature* 427: 848–853.

7. Ganesh, L., E. Burstein, A. Guha-Niyogi, M. K. Louder, J. R. Mascola, L. W. J. Klomp, C. Wijmenga, C. S. Duckett, and G. J. Nabel. 2003. The gene product Murr1 restricts HIV-1 replication in resting $CD4^+$ lymphocytes. *Nature* 426: 853–857.
8. Chiu, Y.-L., V. B. Soros, J. F. Kreisberg, K. Stopak, W. Tonemoto, and W. C. Greene. 2005. Cellular APOBEC3G restricts HIV-1 infection in resting $CD4^+$ T cells. *Nature* 435: 108–114.
9. Marin, M., K. M. Rose, S. L. Kozak, and D. Kabat. 2003. HIV-1 Vif protein binds the editing enzyme APOBEC3G and induces its degradation. *Nat. Med.* 9: 1398–1403.
10. Sheehy, A. M., N. C. Gaddis, and M. H. Malim. 2003. The antiretroviral enzyme APOBEC3G is degraded by the proteasome in response to HIV-1 Vif. *Nat. Med.* 9: 1404–1407.
11. Stopak, K., C. de Noronha, W. Yonemoto, and W. C. Greene. 2003. HIV-1 vif blocks the antiviral activity of APOBEC3G by impairing both its translation and intracellular stability. *Mol. Cell* 12: 591–601.
12. Mariani, R., D. Chen, B. Schrofelbauer, F. Navarro, R. Konig, B. Bollman, C. Munk, H. Nymark-McMahon, and N. R. Landau. 2003. Species-specific exclusion of APOBEC3G from HIV-1 virions by Vif. *Cell* 114: 21–31.
13. Rose, K. M., M. Marin, S. L. Kozak, and D. Kabat. 2004. Transcriptional regulation of APOBEC3G, a cytidine deaminase that hypermutates human immunodeficiency virus. *J. Biol. Chem.* 279: 41744–41749.
14. Peng, G., K. J. Lei, W. Jin, T. Greenwell-Wild, and S. M. Wahl. 2006. Induction of APOBEC3 family proteins, a defensive maneuver underlying interferon-induced anti-HIV-1 activity. *J. Exp. Med.* 203: 41–46.
15. Jarmuz, A., A. Chester, J. Bayliss, J. Gisbourne, I. Dunham, J. Scott, and N. Navatatnam. 2002. An anthropoid-specific locus of orphan C to U RNA-editing enzymes on chromosome 22. *Genomics* 79: 285–296.
16. Mehle, A., B. Strack, P. Ancuta, C. Zhang, M. McPike, and D. Gabuzda. 2004. Vif overcomes the innate antiviral activity of APOBEC3G by promoting its degradation in the ubiquitin-proteasome pathway. *J. Biol. Chem.* 279: 7792–7798.
17. Wang, Y., C. G. Kelly, J. T. Kartunen, T. Whittall, P. J. Lehner, L. Duncan, P. MacAry, J. S. Younson, M. Singh, W. Oehlmann, et al. 2001. CD40 is a cellular receptor mediating mycobacterial heat shock protein 70 stimulation of CC chemokines. *Immunity* 15: 971–983.
18. Wang, Y., C. G. Kelly, M. Singh, E. G. McGowan, A.-S. Carrara, L. A. Bergmeier, and T. Lehner. 2002. Stimulation of Th1-polarizing cytokines, C-C chemokines, maturation of dendritic cells and adjuvant function by the peptide binding fragment of heat shock protein 70. *J. Immunol.* 169: 2422–2429.
19. Whittall, T., Y. Wang, J. Younson, C. Kelly, L. Bergmeier, B. Peters, M. Singh, and T. Lehner. 2006. Interaction between the CCR5 chemokine receptors and microbial HSP70. *Eur. J. Immunol.* 36: 2304–2314.
20. Singh, M., A. B. Andersen, J. E. G. McCarthy, M. Rhode, H. Schutte, E. Sanders, and K. N. Timmis. 1992. The *Mycobacterium tuberculosis* 38-kDa antigen: overproduction in *Escherichia coli*, purification and expression. *Gene* 117: 53–60.
21. Gao, B., and M. F. Tsann. 2003. Endotoxin contamination in recombinant human heat shock protein 70 (Hsp70) preparation is responsible for the induction of tumor necrosis factor α release by murine macrophages. *J. Biol. Chem.* 278: 174–179.
22. Bausinger, H., D. Lipsker, U. Ziylan, S. Manie, J. P. Briand, J. P. Cazanave, S. Muller, J. F. Haeuw, C. Ravanat, H. de la Salle, and D. Hanau. 2003. Endotoxin-free heat-shock protein 70 fails to induce APC activation. *Eur. J. Immunol.* 32: 3708–3713.
23. Weinberger, B., A. Plentz, K. M. Weinberger, J. Hahn, E. Holler, and W. Jilg. 2004. Quantitation of Epstein-Barr virus mRNA using reverse transcription and real-time PCR. *J. Med. Virol.* 74: 612–618.
24. Soneoka, Y., P. M. Cannon, E. E. Ramsdale, J. C. Griffiths, G. Romano, S. M. Kingsman, and A. J. Kingsman. 1995. A transient three-plasmid expression system for the production of high titer retroviral vectors. *Nucleic Acids Res.* 23: 628–633.
25. Grewal, J. S., and J. Flavell. 1998. CD40 and CD154 in cell mediated immunity. *Annu. Rev. Immunol.* 16: 111–135.
26. Chiu, Y.-L., and W. C. Greene. 2006. APOBEC3G cytidine deaminases: distinct antiviral actions along the retroviral life cycle. *J. Biol. Chem.* 281: 8309–8312.
27. Mueller, A., E. Kelly, and P. G. Strange. 2002. Pathways for internalization and recycling of the chemokine receptor CCR5. *Blood* 99: 785–791.
28. Signoret, N., A. Pelchen-Matthews, M. Mack, A. E. Proudfoot, and M. Marsh. 2000. Endocytosis and recycling of the HIV coreceptor CCR5. *J. Cell Biol.* 151: 1281–1294.
29. Zhang, H., B. Yang, R. J. Pomerantz, C. Zhang, S. C. Arunachalam, and L. Gao. 2003. The cytidine deaminase CEM15 induces hypermutation in newly synthesized HIV-1 DNA. *Nature* 424: 94–98.
30. Mangeat, B., P. Turelli, G. Caron, M. Friedi, L. Perrin, and D. Trono. 2003. Broad antiretroviral defense by human APOBEC3G through lethal editing of nascent reverse transcripts. *Nature* 424: 99–103.
31. Chattopadhyay, P. K., J. Yu, and M. Roederer. 2005. A live-cell assay to detect antigen-specific $CD4^+$ T cells with diverse cytokine profiles. *Nat. Med.* 11: 1113–1117.
32. Basu, S., R. J. Binder, R. Suto, K. M. Anderson, and P. K. Srivastava. 2000. Necrotic but not apoptotic cell death releases heat shock proteins, which deliver a partial maturation signal to dendritic cells and activate the NF-κB pathway. *Int. Immunol.* 12: 1539–1546.
33. Hu, J., M. B. Gardner, and C. J. Miller. 2000. Simian immunodeficiency virus rapidly penetrates the cervicovaginal mucosa after intravaginal inoculation and infects intraepithelial dendritic cells. *J. Virol.* 74: 6087–6095.
34. Spira, A. I., P. A. Marx, B. K. Patterson, J. Mahoney, R. A. Koup, S. M. Wolinsky, and D. D. Ho. 1996. Cellular targets of infection and route of viral dissemination after an intravaginal inoculation of simian immunodeficiency virus into rhesus macaques. *J. Exp. Med.* 183: 215–225.
35. Steinman, R. M., A. Ganelli-Piperno, M. Pope, R. Trumpfheller, G. Ignatius, G. Arrode, P. Racz, and K. Tenner-Racz. 2003. The interaction of immunodeficiency viruses with dendritic cells. *Curr. Top. Microbiol. Immunol.* 276: 1–30.
36. O'Leary, J. G., M. Goofdarzi, D. L. Drayton, and U. H. von Andrian. 2006. T cell- and B cell-independent adaptive immunity mediated by natural killer cells. *Nat. Immunol.* 5: 507–516.
37. Wang, Y., L. Tao, E. Mitchell, L. A. Bergmeier, C. Doyle, and T. Lehner. 1999. The effect of immunization on chemokines and CCR5 and CXCR4 coreceptor functions in SIV binding and chemotaxis. *Vaccine* 17: 1826–1836.
38. Lu, Z., J. F. Berson, V. Chen, J. D. Turner, T. Zhang, M. Sharron, M. H. Jenks, Z. Wang, J. Kim, J. Rucker, et al. 1997. Evolution of HIV-1 coreceptor usage through interactions with distinct CCR5 and CXCR4 domains. *Proc. Natl. Acad. Sci. USA* 94: 6426–6431.
39. Berger, E. A., P. M. Murphy, and J. M. Farner. 1999. Chemokine receptors as HIV-1 coreceptors: roles in viral entry, tropism and disease. *Annu. Rev. Immunol.* 17: 657–700.

Immunity, Vol. 15, 971–983, December, 2001, Copyright ©2001 by Cell Press

CD40 Is a Cellular Receptor Mediating Mycobacterial Heat Shock Protein 70 Stimulation of CC-Chemokines

Yufei Wang,[1] Charles G. Kelly,[2] Jaana T. Karttunen,[3] Trevor Whittall,[1] Paul J. Lehner,[3] Lidia Duncan,[3] Paul MacAry,[3] Justine S. Younson,[2] Mahavir Singh,[4] Wulf Oehlmann,[4] Genhong Cheng,[5] Lesley Bergmeier,[1] and Thomas Lehner[1,6]

[1]Peter Gorer Department of Immunobiology
[2]Immunology Unit
Department of Oral Medicine
Guy's, King's, and St. Thomas' Medical School
KCL, London
[3]Division of Immunology
Department of Pathology
Cambridge Institute for Medical Research
University of Cambridge
Addenbrooke's Hospital
Cambridge
United Kingdom
[4]Lionex Diagnostics and Therapeutics
GmbH, Braunschweig
Germany
[5]Department of Microbiology and Molecular Genetics
Jonsson Comprehensive Cancer Center
University of California, Los Angeles
Los Angeles, California 90095

Summary

The 70 kDa mycobacterial heat shock protein (Mtb HSP70) stimulates mononuclear cells to release CC-chemokines. We now show that this function of Mtb HSP70, but not human HSP70, is dependent on the cell surface expression of CD40. Deletion of the CD40 cytoplasmic tail abolished, and CD40 antibody inhibited, Mtb HSP70 stimulation of CC-chemokine release. Mtb HSP70 stimulated THP1, KG1 cells, and monocyte-derived dendritic cells to produce RANTES. Specific binding of CD40-transfected HEK 293 cells to Mtb HSP70 was demonstrated by surface plasmon resonance. Coimmunoprecipitation of Mtb HSP70 with CD40 indicates a physical association between these molecules. The results suggest that CD40 is critical in microbial HSP70 binding and stimulation of RANTES production.

Introduction

Heat shock protein 70 (HSP70) is a member of a family of molecular chaperones that play an important part in protein synthesis, folding, and translocation (Lindquist and Craig, 1988; Pilon and Schekman, 1999). The HSP family is among the most highly conserved proteins, which carry out many of their regulatory activities via protein-protein interactions (Rothman, 1989; Gething and Sambrook, 1992). *Mycobacterium tuberculosis*-derived HSP70 (Mtb HSP70) is well characterized and functions as an adjuvant in stimulating the host immune response. Antigenic peptides linked to HSP70 can elicit both MHC class I-restricted $CD8^+$ and MHC class II-restricted $CD4^+$ T cell responses (Udono and Srivastava, 1993; Suto and Srivastava, 1995; Suzue and Young, 1996; Ciupitu et al., 1998; Huang et al., 2000). HSP70 can be translocated across cell membranes to gain cytoplasmic and nuclear entry (Fujihara and Nadler, 1999). This property may enable HSP70 to deliver peptides into the endoplasmic reticulum and MHC class I pathway, although the mechanism involved in membrane translocation has not been identified. However, a receptor-mediated endocytic pathway for HSP70 was demonstrated in antigen-presenting cells (Castellino et al., 2000; Binder et al., 2000a; Arnold-Schild et al., 1999; Basu et al., 2001). Endocytosis allows HSP70-bound peptides or proteins to enter the MHC class I and class II processing pathway (Castellino et al. 2000).

Recently we have found that Mtb HSP70 stimulates both in vivo and in vitro antigen-primed and to a lesser extent naive PBMC to produce the CC-chemokines RANTES, MIP-1α, and MIP-1β (Lehner et al., 2000). This finding may explain the adjuvant function of Mtb HSP70 (Suzue and Young, 1996; Lussow et al., 1991; Perraut et al., 1993), as CC-chemokines attract antigen processing and presenting macrophages, dendritic cells (DC), and effector T and B cells (Baggiolini, 1998). The innate function of Mtb HSP70 in stimulating CC-chemokines is mediated by host receptors for Mtb HSP70, although the identity of these receptors has not been determined.

In view of the adjuvanticity of Mtb HSP70, we have considered the hypothesis that Mtb HSP70 might upregulate CC-chemokines via the costimulatory receptors. This was based on the report that CC-chemokines are upregulated by ligation of the CD28 molecule with B7 (Herold et al., 1997) or interaction of CD40 with CD40 ligand (Kombluth et al., 1998; McDyer et al., 1999). CD40 is a 50 kDa member of the TNF receptor family and is expressed on B cells, monocytes, mature DC, and nonhematopoietic cells (Banchereau et al., 1994; Young et al., 1998). CD40/CD40L interaction plays a major role in regulating both humoral and cellular immune responses. Ligation of CD40 activates antigen-presenting cells by increasing expression of the accessory molecules CD80, CD86, and CD54 (Caux et al., 1994; Sallusto and Lanzavecchia, 1994). The CD40/CD40L interaction also leads to production of inflammatory cytokines, such as TNFα, IL-1, IL-6, and IL-12 in macrophages and DC (Kiener et al., 1995; Cella et al., 1996). Stimulation of cytokines and chemokines may promote the innate mechanism to instruct the adaptive immune response to generate a diverse repertoire of antigen-specific receptors distributed on clonally expanded T and B cells (Medzhitov and Janeway, 1997; Hoffmann et al., 1999). Indeed, recent studies demonstrated a central role for ligation of CD40 on macrophages and DC in the induction of MHC class I-restricted antigen-specific $CD8^+$ T cell responses and protective immunity (Ridge et al., 1998; Bennett et al., 1998; Schoenberger et al., 1998).

Here we report that CD40 can mediate Mtb HSP70 stimulation of the human monocyte-derived cell line

[6]Correspondence: thomas.lehner@kcl.ac.uk

(THP1), activated myelo-monocytic cell line (KG1), CD40-transfected HEK 293 cell line, blood monocytes, and PBMC to produce the CC-chemokines RANTES, MIP-1α, and MIP-1β. The CD40-mediated stimulation of production of RANTES was also found with *E. coli* HSP70 but not human HSP70. Furthermore, we demonstrated an association between Mtb HSP70 and CD40 by coimmunoprecipitation and by a binding assay using surface plasmon resonance. These results suggest that CD40 acts as a receptor for microbial HSP70 stimulation of CC-chemokines.

Results

Mtb HSP70 Stimulation of CC-Chemokines in the Monocyte Cell Line (THP1) Is Mediated by CD40

We first studied the induction of CC-chemokines in the monocytic-derived cell line (THP1). Incubation of THP1 cells with Mtb HSP70-stimulated secretion of RANTES, MIP-1α, and MIP-1β in a dose-dependent manner. The increased secretion of CC-chemokines was detected as early as 4 hr after Mtb HSP70 stimulation and this increased steadily by days 2 and 3 (data not shown). Maximal concentration of the three CC-chemokines was observed after 3 days of culture with 10–20 μg/ml of Mtb HSP70 (Figure 1A). There was no further increase of the three CC-chemokines at higher doses of Mtb HSP70 (50 μg/ml), suggesting that saturation of Mtb HSP70 stimulation of monocytes may have taken place as shown in the binding assay (Figure 4F). Mtb HSP70 elicited greater than 100-fold increase of RANTES (4728 ± 252.5 pg/ml) as compared with the unstimulated level (45 ± 5.2 pg/ml), and this applied also to MIP-1α (2940 ± 123 compared with 22.2 ± 10 pg/ml), and MIP-1β (12,743 ± 130.4 compared with 131.7 ± 15.5 pg/ml). In order to rule out nonspecific stimulation, THP1 cells were treated with human serum albumin, and the concentration of the three CC-chemokines remained unchanged (Figure 1A).

HSP70 stimulation of monocytes is dependent on the intracellular calcium flux, which is different from calcium-flux-independent LPS stimulation (McLeish et al., 1989; Asea et al., 2000). In order to differentiate between Mtb HSP70 and LPS and to elaborate the mechanism of Mtb HSP70 stimulation of CC-chemokines, we used an intracellular calcium chelator BAPTA-AM. This demonstrated that Mtb HSP70 stimulation of THP1 cells producing RANTES was inhibited in a dose-dependent manner (in a range of 1–100 μM) by the intracellular calcium chelator BAPTA-AM (Figure 1B). In contrast, stimulation of THP1 cells by LPS was not affected by the treatment with 1–100 μM of BAPTA-AM. Thus, Mtb HSP70, unlike LPS is calcium dependent and the stimulation of RANTES production by the Mtb HSP70 material is not due to any LPS contaminant.

We then treated Mtb HSP70 materials with "Kuttsu Clean" which removes greater than 99% of LPS (data not shown) or added polymyxin B (50 μg/ml) to the cultures and found that this had no effect on Mtb HSP70-induced RANTES production at concentrations of 5–50 μg/ml (Figure 1C). In contrast, polymyxin B suppressed more than 90% RANTES production induced by a range of concentrations of LPS (10–1000 ng/ml). These results rule out the possibility that any contamination with LPS played a role in the induction of CC-chemokines by Mtb HSP70 and indicate that Mtb HSP70 and LPS activate monocytes by different mechanisms.

Phenotypic analysis revealed that resting cultures of monocytic THP1 cells expressed CD40 (99.3% ± 3.1%), CD14 (93.9% ± 4.8%), and CD11b (76.4% ± 3.7%), but little CD91 (1.3% ± 3.2%) or CD40L (1.7% ± 2.7%). Stimulation of CD40 with CD40L on monocytes leads to the production of CC-chemokines (Kornbluth et al., 1998; McDyer et al., 1999). We have also found that culturing THP1 cells with soluble CD40L trimer (CD40LT), a biologically functional oligomer of CD40L, elicited a dose-dependent increase in production of RANTES (data not shown). In order to determine the specificity of CD40 interaction with Mtb HSP70, we carried out inhibition assays with antibodies to CD40. Two anti-CD40 mAbs (MAB89 and LOB/89) were identified which did not stimulate THP1 cells to produce CC-chemokines (data not shown). The clone MAB89 (but not LOB) mAb inhibited RANTES production in THP1 cells in a dose-dependent manner (Figure 1D). Similar results were also observed with MIP-1α (data not shown). The mAb to CD14 (MY4) failed to affect the concentration of RANTES elicited by Mtb HSP70 (Figure 1E). However, LPS-stimulated production of CC-chemokines was inhibited in a dose-dependent manner with anti-CD14 mAb but not with anti-CD40 (Figure 1E), suggesting that CD40, but not CD14, mediated Mtb HSP70 stimulation of CC-chemokines. The isotype control antibody had no effect on Mtb HSP70 or LPS-induced CC-chemokine production (Figures 1D and 1E).

Induction of CC-Chemokines in the CD34$^+$ Myelo-Monocytic Cell Line Is Dependent on Induction of CD40

The CD34$^+$ myelo-monocytic cell line (KG1) differentiates into cells with DC features upon stimulation with PMA and cytokines. During this process, a number of DC markers are upregulated, including CD40 (Louis et al., 1999). Analysis of the surface molecules expressed by KG1 cells showed that unstimulated KG1 cells expressed little CD83, a marker of mature or fully differentiated DC (Zhou and Tedder, 1995) or CD40, and virtually no CD80, CD86, CD14, or CD40L. Stimulation of KG1 cells with 10 μg/ml of Mtb HSP70 for 3 days upregulated CD83 (from 2.7% ± 0.5% to 6.1% ± 1.5%) and CD40 (from 3.2% ± 1.8% to 7.6% ± 2.6%), but not CD80, CD86, CD14, or CD40L. Stimulation with PMA, GM-CSF, and IL-4 also induced a proportion of KG1 cells to express CD83 (11.2% ± 1.7%) and CD40 (7.3% ± 1.9%). Furthermore, adding Mtb HSP70 to PMA and the cytokines, enhanced the expression of both CD83 (14.6% ± 0.9%) and CD40 (11.3% ± 2.3%) without any marked effect being observed on the other costimulatory molecules (CD80, 1.7% ± 0.8%; CD86, 3.3% ± 2.5%), CD14 (0.5% ± 0.2%), or CD40L (0.1% ± 0.1%). The results suggest that the KG1 cells are activated to express CD40 (Figure 2A) and that the increased CD40 stimulated by Mtb HSP70 plus PMA and cytokines reached the 5% significant level ($t = 7.363$, $p < 0.01$), as compared with the untreated KG1 cells.

Production of CC-chemokines was then examined in resting and activated KG1 cells. Resting KG1 cells pro-

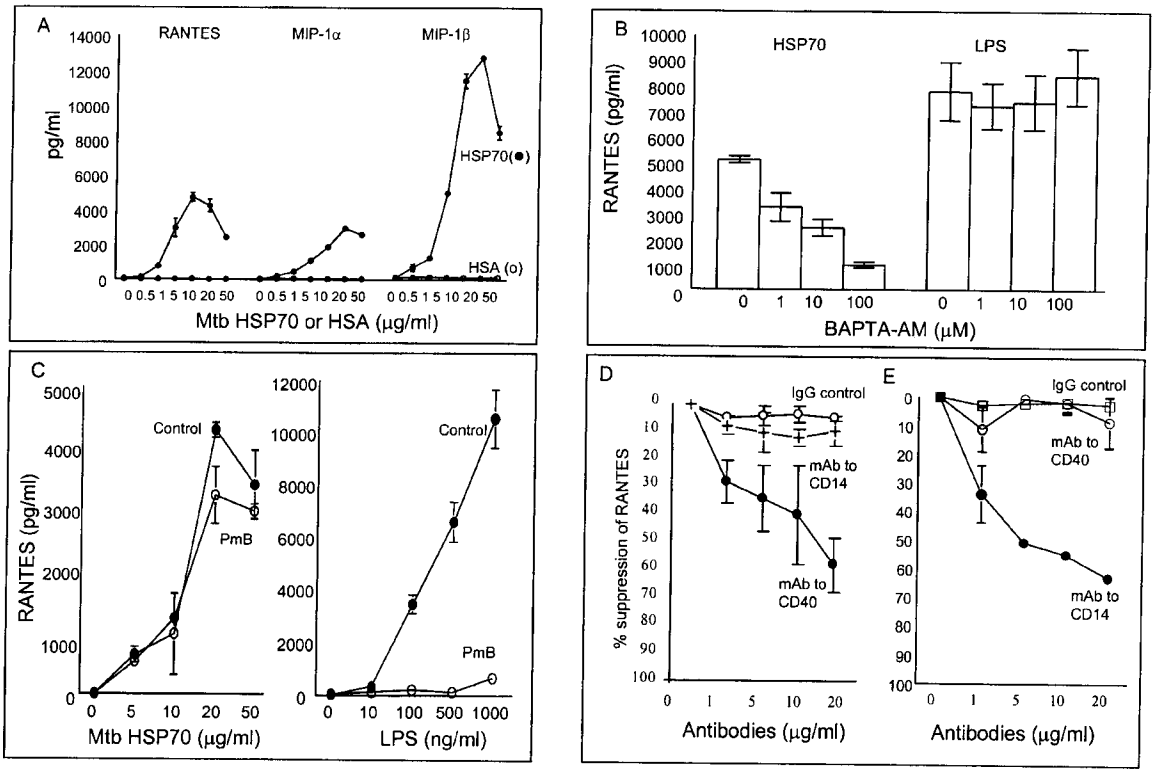

Figure 1. Stimulation of CC-Chemokine Production by Mtb HSP70, as Compared with LPS

(A) Stimulation of CC-chemokine production by Mtb HSP70. THP1 cells (2×10^5 per ml) were stimulated with 0–50 μg/ml Mtb HSP70 (●) or HSA (O) for 3 days, and the supernatants were collected for assays of RANTES, MIP-1α, and MIP-1β. The results of three experiments were presented as means ± SD.

Effects of intracellular calcium chelator BAPTA-AM (B) and polymyxin B (PmB) (C) on Mtb HSP70 stimulation of RANTES production. THP1 cells were stimulated with 20 μg/ml of Mtb HSP70 or 200 ng/ml of LPS in the presence of three concentrations of BAPTA-AM. For inhibition, 50 μg/ml of polymyxin B was added to Mtb HSP70 or LPS-stimulated THP1 cells. After 3 day culture, RANTES was assayed in the culture supernatants.

Suppression of CC-chemokine production in THP1 cells stimulated by Mtb HSP70 (D) or LPS (E). (D) THP1 cells were stimulated with 10 μg/ml of Mtb HSP70 in the presence of 1–20 μg/ml of antibodies to CD40 (MAB89, ●), CD14 (+), and control IgG (O). (E) THP1 cells stimulated with LPS (200 ng/ml) were treated with increasing concentrations of mAb to CD14 (●), CD40 (O), or control IgG (□). After 3 days, the supernatants were used to assay RANTES and MIP-1α. The results from three independent experiments are presented and expressed as mean % suppression ± SD.

duced very low concentrations of RANTES (11.2 ± 6 pg/ml) or MIP-1α (10.8 ± 5.5 pg/ml) and addition of Mtb HSP70 up to 50 μg/ml failed to elicit any increase in RANTES or MIP-1α (Figure 2B). Similarly, PMA, GM-CSF, and IL-4 were also unable to induce CC-chemokine production (Figure 2B). However, Mtb HSP70 elicited a dose-dependent increase in RANTES and MIP-1α production by KG1 cells, in the presence of PMA, GM-CSF, and IL-4 that reached concentrations >100 times those of the activated cells without stimulation with Mtb HSP70 (Figure 2B). LPS failed to elicit an increase in RANTES or MIP-1α in doses up to 1000 ng/ml in both resting and PMA-, GM-CSF-, and IL-4-activated KG1 cells (Figure 2B).

To confirm that the $CD40^+$ cell population was responsible for producing the Mtb HSP70-stimulated CC-chemokines, activated KG1 cells were separated by cell sorting into greater than 95% $CD40^+$ cells and greater than 99% $CD40^-$ cells. RANTES was produced in a dose-dependent manner only by the $CD40^+$ cells when stimulated with Mtb HSP70, independently of PMA, GM-CSF, and IL-4 stimulation. In contrast, no production of RANTES was observed in the $CD40^-$ KG1 cell population stimulated with Mtb HSP70 (0.5–50 μg/ml) alone or in the presence of PMA plus GM-CSF and IL-4 (Figure 2C). The specificity of CD40 in mediating Mtb HSP70-stimulated CC-chemokine production by KG1-derived DC was further examined by inhibition assays. Anti-CD40-specific antibodies inhibited in a dose-dependent manner Mtb HSP70-induced production of RANTES (Figure 2D). Thus, Mtb HSP70 stimulates the production of CC-chemokines only from the $CD40^+$ cell subset of activated KG1 cells, and the specificity of CD40 was demonstrated by inhibition with antibodies to CD40.

Induction of CC-Chemokines by Mtb HSP70-Stimulating PBMC-Derived Monocytes or $CD14^+$ Monocyte-Derived DC

To establish that CD40 is involved in CC-chemokine induction by stimulation with Mtb HSP70 not only in human cell lines but also in cells isolated from the circu-

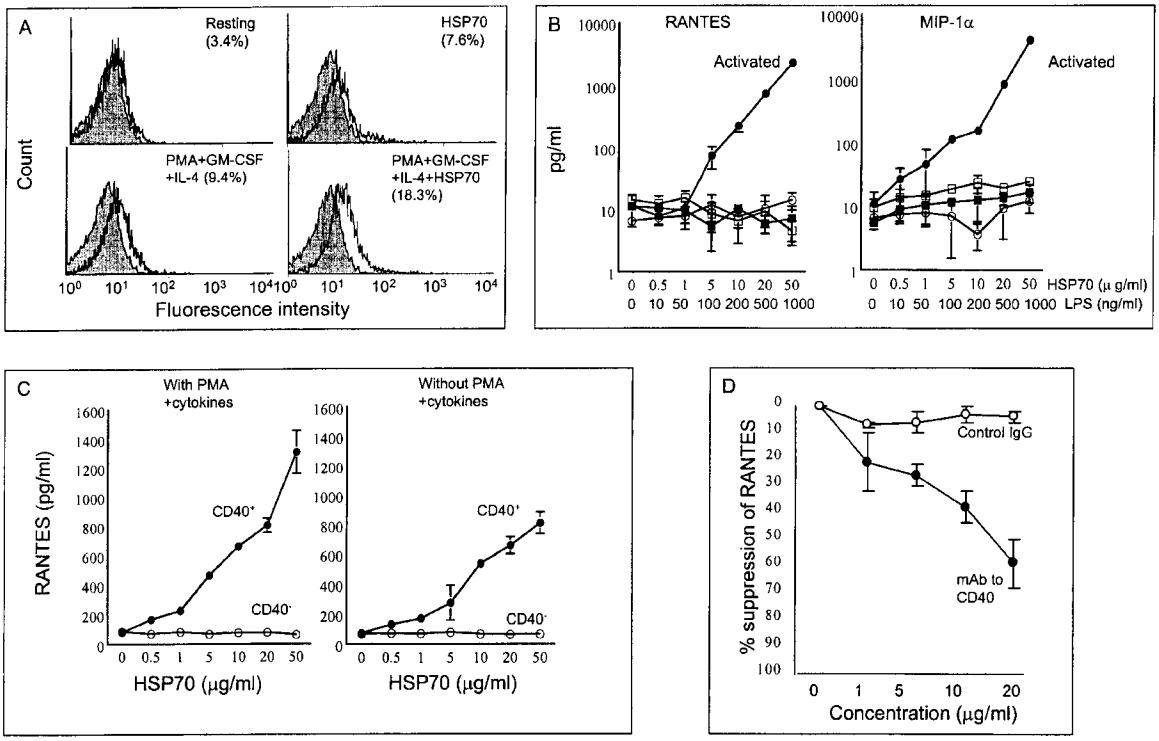

Figure 2. Production of CC-Chemokines by CD40$^+$ and CD40$^-$ KG1 Cells, Stimulated with HSP70

(A) Expression of CD40 on KG1 cells following activation. KG1 cells were treated with Mtb HSP70 (10 μg/ml), PMA (10 ng/ml), GM-CSF (400 U/ml), and IL-4 (20 U/ml) or a combination of Mtb HSP70, PMA, and the cytokines. Three days after stimulation, 5×10^5 cell pellets were incubated with 1 μg PE-conjugated antibody to CD40. PE-conjugated IgG isotype served as a control. The result presented is representative of four experiments.

(B) Induction of CC-chemokines in KG1 cells. KG1 cells (5×10^5 cells per ml) were stimulated with Mtb HSP70 in the absence (O) or presence (●) of PMA (10 ng/ml) with GM-CSF (400 U/ml) and IL-4 (20 U/ml), or stimulated with LPS with (□) or without (■) PMA and cytokines. After 72 hr the culture supernatants were removed for the assay of RANTES and MIP-1α.

(C) Production of RANTES by CD40$^+$ and CD40$^-$ KG 1 cells. CD40$^+$ (●) and CD40$^-$ (O) KG1 cells were purified from activated KG1 by cell sorting and stimulated with Mtb HSP70 (0–50 μg/ml) in the presence or absence of PMA (10 ng/ml) with GM-CSF (400 U/ml) and IL-4 (20 U/ml). After 3 days, the supernatants were used to assay RANTES.

(D) Inhibition of RANTES production by anti-CD40 antibodies. The inhibition was carried out by adding increasing concentrations of anti-CD40 antibodies to Mtb HSP70- (20 μg/ml) stimulated KG1 cells in the presence of PMA with GM-CSF and IL-4.

lation, we studied human PBMC-derived monocytes or CD14$^+$ monocyte-derived DC. Human blood monocytes (>98% purity) were isolated from PBMC by a cell sorter using mAb to CD14. DC were prepared by culturing CD14$^+$ blood monocytes for 7–9 days in the presence of GM-CSF and IL-4 (Sallusto and Lanzavecchia, 1994). A dose-dependent increase in RANTES was found when PBMC-derived monocytes or immature DC were stimulated with Mtb HSP70 (Figures 3A and 3B). The production of RANTES by primary monocytes or CD14$^+$ monocyte-derived DC was significantly inhibited ($p < 0.05$) with antibodies to CD40 (Figures 3C and 3D). The results with human monocytes or DC are consistent with those derived from the monocytic cell lines, suggesting that Mtb HSP70-induced CC-chemokines is mediated by CD40 receptors.

Induction of RANTES Is Dependent on a Signaling-Competent CD40 Receptor

To demonstrate the requirement for CD40 in Mtb HSP70-stimulated CC-chemokine production, we transfected HEK 293 cells with the cDNA encoding human CD40. Three days following transfection over 90% cells expressed cell surface CD40 molecules (Figure 4A). Mtb HSP70 stimulated a dose-dependent increase in the concentration of RANTES in wild-type CD40-transfected, but not the control Lac-Z-transfected HEK 293 cells (Figure 4B), which expressed no CD40 (Figure 4A). There was greater than 20-fold increase in the concentration of RANTES when stimulated with Mtb HSP70, though the level was higher when stimulated with the CD40L trimer (Figure 4B). Surprisingly, only RANTES was induced with Mtb HSP70 or CD40LT-stimulated CD40 transfected-HEK 293 cells, and we failed to detect any MIP-1α or MIP-1β. This suggests a different intracellular mechanism for the production of the three CC-chemokines in the HEK 293 cells as compared with the monocytic THP1 cells or the KG1 cells.

To establish a requirement for CD40 signaling in Mtb HSP70-induced release of RANTES, we made use of a CD40 molecule lacking a cytoplasmic tail (CD40Δ*cyt.*) This truncated form of CD40 has been previously shown

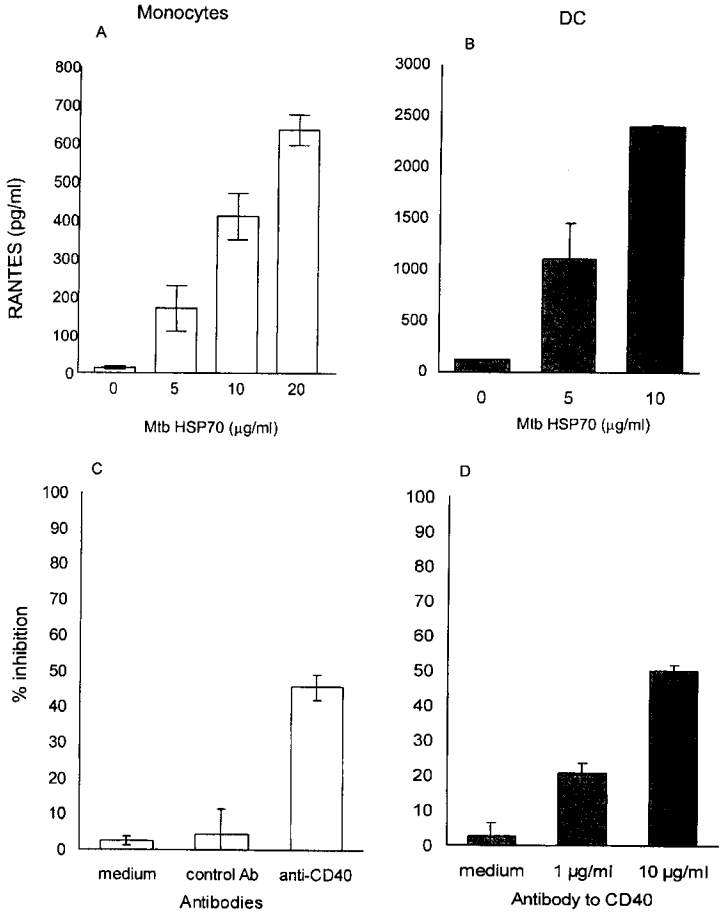

Figure 3. Induction of CC-Chemokines by Human Monocytes and CD14$^+$ Monocyte-Derived DC Stimulated with Mtb HSP70

Induction of CC-chemokines by human monocytes and CD14$^+$ monocytes derived DC stimulated with Mtb HSP70. Aliquots of (A) 5 $\times$ 10^5/ml human monocytes and (B) monocyte-derived DC were stimulated for 3 days with 5, 10, and 20 μg/ml of Mtb HSP70. In the inhibition assay (C and D), mAb to CD40 (10 μg/ml) and the control antibody isotype were added to Mtb HSP70- (10 μg/ml) stimulated monocytes and DC. Three days after culture, the supernatants were removed to assay RANTES.

to lack signaling activity required for costimulation (Lee et al., 1999). HEK 293 cells were transfected with cDNA encoding CD40Δ*cyt*. Flow cytometric analysis shows that the majority of cells transfected with CD40Δ*cyt* express cell surface CD40, as seen with the wild-type CD40 construct (Figure 4A). However, in contrast with HEK 293 cells expressing the wild-type CD40 construct, neither Mtb HSP70 nor the CD40LT stimulated release of RANTES in HEK 293 cells expressing CD40Δ*cyt* (Figure 4B). These results confirm both the specificity of CD40 and the need for CD40 signaling in Mtb HSP70-induced CC-chemokine release.

Binding of Mtb HSP70 to CD40-Transfected HEK 293 Cells

Our results demonstrate a requirement for CD40 in Mtb HSP70-induced CC-chemokine release. Saturation binding of HSP70 to CD40 was then determined using FITC-labeled Mtb HSP70. There was a dose-dependent increase in Mtb HSP70 binding to CD40-transfected cells, as compared with the control Lac-Z-transfected HEK 293 cells (Figure 4C). Saturation of the CD40$^+$, but not CD40$^-$ cells, was reached with 25 μg/ml of Mtb HSP70. Although there was no significant binding to Lac-Z-transfected cells at low concentration of Mtb HSP70 (1.5–12.5 μg/ml), nonspecific binding was observed at concentrations greater than 12.5 μg/ml of Mtb HSP70. However, no binding was observed with FITC-BSA (Figure 4C). Binding of FITC-Mtb HSP70 was inhibited by adding 40-fold excess of unlabeled Mtb HSP70, as shown by the reduction of fluorescence intensity (Figure 4C). Mtb HSP70 binding was also inhibited by a 40-fold excess of *E.coli* HSP70, but not that of human HSP70, suggesting that human HSP70 binding used distinct receptors from Mtb HSP70 binding and was independent of CD40 (Figure 4C). In contrast, the FITC-Mtb HSP70 binding was not affected by addition of unlabeled human serum albumin.

To determine whether Mtb HSP70 binds to the cell surface CD40, we used surface plasmon resonance. Mtb HSP70 was immobilized on the surface of the sensorchip and binding of fluid phase CD40-transfected or Lac-Z- (control) transfected cells in DMEM supplemented with 10% FCS was measured (Figure 5A). CD40 transfected HEK 293 cells bound to immobilized HSP70 and saturation of binding (approximately 275 resonance units) was found at a concentration of 1.5 $\times$ 10^7 cells/ml. In contrast, binding of control Lac-Z-transfected cells was much lower (75 resonance units) at the same concentration. To confirm the specificity of binding, antibody inhibition experiments were performed. Results of a representative experiment are shown in Figure 5B.

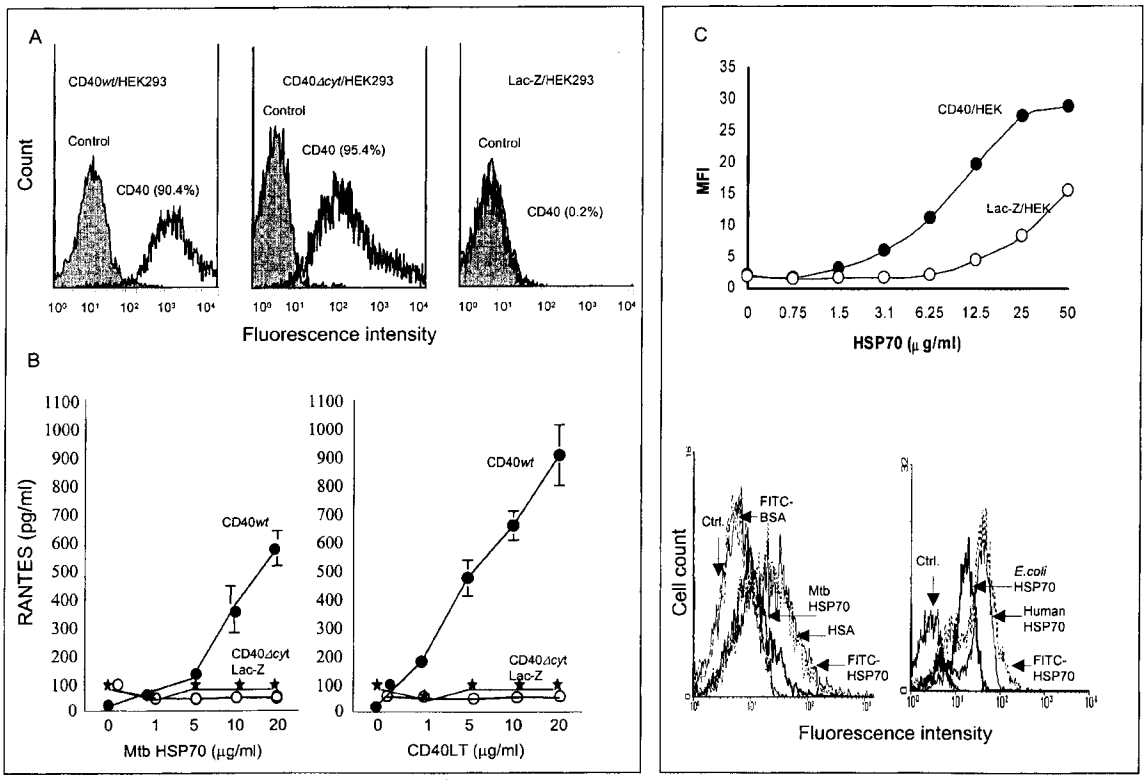

Figure 4. The Cell Surface Expression and Specificity of CD40 Interaction with HSP70 in CD40-Transfected HEK 293 Cells and Saturation Binding of Labeled Mtb HSP70

(A) Cell surface expression of CD40 in HEK 293 cells transfected with wild-type CD40, CD40Δ*cyt*, or Lac-Z. An aliquot of 5×10^5 single-cell suspension of CD40-transfected or Lac-Z-transfected HEK 293 was incubated with 1 μg PE-conjugated antibody to CD40. PE-conjugated IgG isotype served as a control.

(B) Stimulation of RANTES production in CD40-transfected HEK 293 cells by Mtb HSP70 or CD40LT. 24 hr after transfection with the cDNA encoding wild-type CD40, CD40Δ*cyt*, or the control Lac-Z, increasing concentrations of Mtb HSP70 or CD40LT were added to the cell cultures. The supernatants were collected from day 1 to day 6 and RANTES was assayed. The optimum production of RANTES was seen on day 3 and this data is presented. The experiments were repeated four times.

(C) Saturation binding of FITC-labeled Mtb HSP70 and the inhibition of FITC-Mtb HSP70 binding by unlabeled Mtb HSP70, HSA, or *E. coli* HSP70. A cell suspension of CD40 or Lac-Z-transfected HEK 293 cells was incubated with FITC-Mtb HSP70 at 4°C at doses of 0–50 μg/ml. For inhibition, CD40-transfected HEK 293 cells were preincubated for 30 min with 40-fold excess of unlabeled Mtb HSP70, *E. coli* HSP70, human HSP70, or HSA (indicated by arrows), followed by incubation with 25 μg/ml of FITC-Mtb HSP70 for a further 30 min on ice. The cells were also incubated with 25 μg/ml of FITC-BSA as a control. After washing, the cells were analyzed by flow cytometry. The data are representative of four independent experiments.

Binding of CD40-transfected cells was inhibited in a dose-dependent manner by addition of anti-CD40 mAb, whereas the control anti-CD14 mAb had no effect.

Association of Mtb HSP70 with CD40

To ascertain whether Mtb HSP70 associates with the CD40 molecule, detergent extracts from CD40-expressing THP1 cells were incubated with recombinant Mtb HSP70. CD40-associated proteins were then immunoprecipitated with the mAb to CD40, separated by SDS-PAGE, transferred to Immobilon-P membrane, and probed with antisera specific for Mtb HSP70 (Figure 6A). Immunoblot analysis with the Mtb HSP70-specific antibodies showed a 70 kDa band, which corresponds to Mtb HSP70, coimmunoprecipitated with the CD40 molecule. This interaction between CD40 with Mtb HSP70 was specific, as no association was seen in immunoprecipitations performed in the absence of recombinant Mtb HSP70 (Figure 6A). No specific bands were seen when blotted with control antiserum (data not shown). No specific Mtb HSP70 bands were coprecipitated with antibodies to either CD14 or control IgG isotype antibody (Figure 6A). To show that the CD40 association was specific for Mtb HSP70, similar immunoprecipitations were performed following incubation with human HSP70 (Figure 6B). No bands were coimmunoprecipitated with CD40.

To confirm that Mtb HSP70 interacts specifically with cell surface-expressed CD40, further immunoprecipitations were performed with THP1 cells that were surface-labeled by biotinylation. Intact, labeled cells were incubated with Mtb HSP70 at 0 and 50 μg/ml on ice. Unbound HSP70 was removed by washing, and cells were incubated with antibody to Mtb HSP70, CD40, or isotype-matched control antibody (on ice) prior to washing and lysis. Immune complexes, recovered by incubation with protein

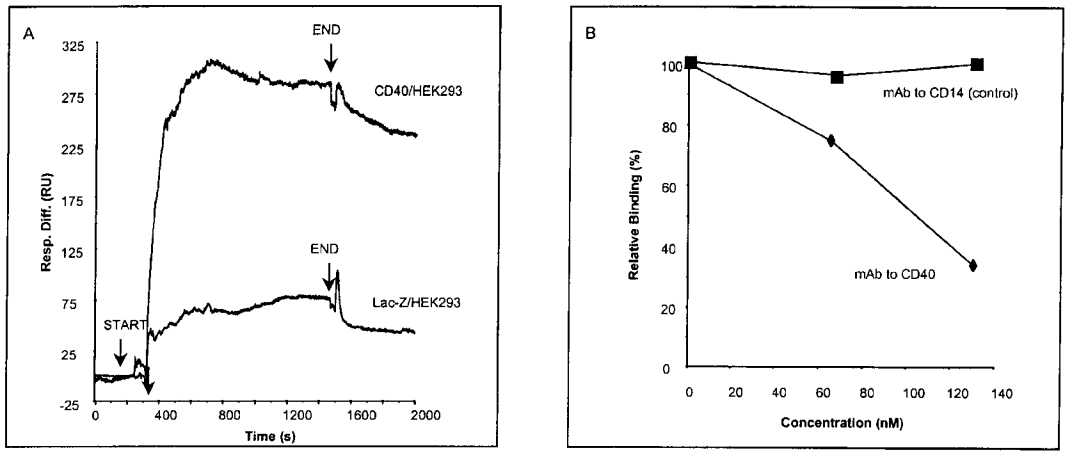

Figure 5. Binding of Mtb HSP70 to CD40-Transfected HEK 293 Cells by Surface Plasmon Resonance

Binding of Mtb HSP70 to CD40-transfected HEK 293 cells. Binding of fluid-phase HEK 293 cells transfected with CD40 or Lac-Z (control) to immobilized Mtb HSP70 was determined by surface plasmon resonance.

(A) Comparison of CD40 and Lac-Z-transfected cells. The superimposed sensorgrams show binding at a concentration of 1.5×10^7 cells/ml. Flow rate was 1 μl/min and injection volume was 20 μl. The period of injection (association phase) is indicated by arrow (↓). In this experiment, binding of CD40-transfected cells reaches saturation.

(B) Inhibition of binding in the presence of anti-CD40 mAb (MAB89). CD40-transfected cells were injected in the presence of anti-CD40 or control anti-CD14 mAb at 130 nM and 65 nM concentrations. Results of a representative experiment are shown as binding (%) relative to binding in the absence of mAb. Magnitude of binding was measured as the difference (resonance units) over the period of injection as in (A).

G-Sepharose, were analyzed by SDS-PAGE. Following electrophoretic transfer onto a nitrocellulose membrane, biotinylated polypeptides were visualized by chemiluminescence using streptavidin-conjugated HRP. Antibody to CD40 precipitated a polypeptide of approximately 42 kDa, and a band with the same electrophoretic mobility was also coimmunoprecipitated by antibody to Mtb HSP70 (Figure 6C, left panel). The identity of this polypeptide band was confirmed to be CD40 by immunoblot analysis with the antibody to CD40 of immunoprecipitates prepared in an identical manner using unlabeled cells (Figure 6C, right panel). An isotype matched control antibody failed to precipitate CD40.

Stimulation of CC-Chemokines by Mtb HSP70 N- and C-Terminal Fragments or *E. coli* HSP70 and Human HSP70

HSP70 consists of two major functionally distinct domains: N-terminal ATPase portion (aa 1–358) and a C-terminal peptide binding domain (aa 359–540), with an adjacent portion (aa 541–625) of unknown function. Stimulation of monocytic THP1 cells with the HSP70 C-terminal fragment (aa 359–610), but not the N-terminal fragment (aa 1–358), elicited a dose-dependent increase in production of RANTES (Figure 7A).

E. coli HSP70 or human HSP70 also stimulated THP1 cells to produce RANTES in a dose-dependent manner (Figure 7A), which was similar to that observed with Mtb HSP70. However, human HSP70, unlike Mtb HSP70, was inhibited by antibodies to CD14 but not antibodies to CD40 (Figure 7B), which is consistent with the report that CD14 is a receptor for human HSP70 (Asea et al., 2000). In contrast, antibodies to CD40, but not to CD14, significantly inhibited *E. coli* HSP70 stimulation of RANTES (Figure 7C). The CD40-dependent stimulation by Mtb $HSP70_{359-610}$ or *E. coli* HSP70 was further studied by using CD40-transfected HEK 293 cells. Mtb $HSP70_{359-610}$ or *E. coli* HSP70 stimulated a dose-dependent increase in production of RANTES in CD40-transfected, but not in Lac-Z-transfected HEK 293 cells (Figures 7D and 7E). In contrast, incubation with increasing doses of human HSP70 (up to 50 μg/ml) failed to elicit significant production of RANTES in CD40-transfected and the control Lac-Z-transfected HEK 293 cells (Figure 7F). The results suggest that CD40 mediates *E. coli* HSP70, but not human HSP70, stimulation of CC-chemokines.

Discussion

The primary function of CC chemokines is to attract antigen-processing and -presenting macrophages and DC, as well as effector T and B cells. We report here that Mtb HSP70 stimulates a human monocyte-derived cell line (THP1), $CD34^+$ myelo-monocytic cell line (KG1), which on activation differentiates into dendritic-like cells, blood monocytes, and $CD14^+$-derived DC to produce CC-chemokines. A significant finding of this study is that induction of CC-chemokines by Mtb HSP70 is dependent on the cell-surface expression of CD40. The CD40 specificity was established (a) by inhibiting RANTES production with anti-CD40 antibodies or (b) by transfecting mutagenized CD40 molecule on HEK 293 cells, (c) by a physical association between Mtb HSP70 and CD40 demonstrated by binding assay using surface plasmon resonance, and (d) by immunoprecipitation with CD40 specific antiserum. CD40-mediated activation of DC and monocytes by Mtb HSP70 may be an important mechanism in the innate function of Mtb HSP70 stimulation of CC-chemokines.

The monocytic THP1 cell line used in this study expresses

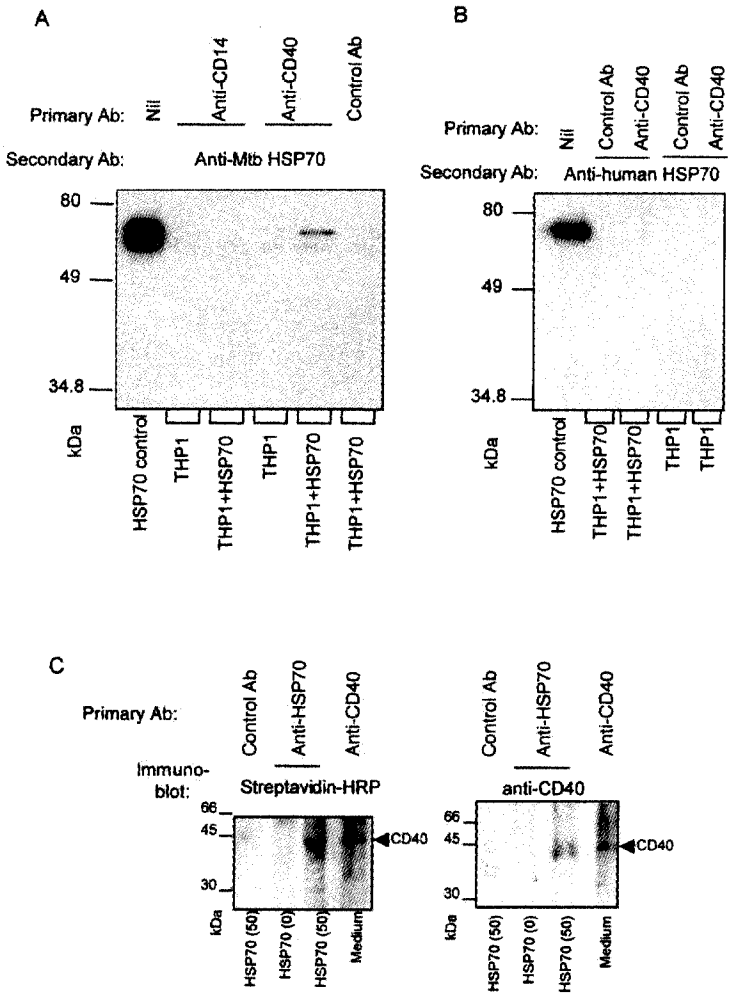

Figure 6. Immunoblot Analysis of Mtb or Human HSP70 Association with CD40 Using Antibodies to CD40 or CD14

Immunoprecipitation of Mtb HSP70 with antibodies to CD40. THP1 cell lysates that had been incubated with recombinant Mtb HSP70 (A) or human HSP70 (B) were precipitated with rabbit antibodies to CD40, rabbit control IgG, mAb to CD14 (A), or isotype control mAb (primary antibodies). The immunoprecipitated products were then analyzed by immunoblot with antibodies (secondary antibody) to Mtb HSP70 (A) or to human HSP70 (B). (C) Immunoprecipitation of cell surface CD40 by Mtb HSP70 was carried out on THP1 cells. Biotinylated THP1 cells were treated with 0 and 50 μg/ml of Mtb HSP70, followed by antibody to Mtb HSP70 or CD40. THP1 cells incubated with 50 μg/ml of Mtb HSP70 were also treated with isotype-matched control antibody. After detergent lysis, immune complexes were recovered by incubation with protein G-Sepharose, separated on SDS-PAGE, and visualized directly with streptavidin-HRP (left panel). Immune complexes prepared in an identical manner to the unlabeled cells were probed with antibody to CD40 (right panel).

CD40 (99%), but stimulation with Mtb HSP70 upregulates the cell surface expression of CD40 and generates high levels of RANTES, MIP-1α, and MIP-1β. We failed to detect CD40L expression on resting or Mtb HSP70-activated THP1 cells, and this eliminated the possibility that CD40 and CD40L interaction between monocytes was responsible for the generation of CC-chemokines, as has been previously shown (Kombluth et al., 1998). Stimulation of KG1 cells with Mtb HSP70 upregulates the CD83 maturation marker of DC, as well as CD40 molecules. These results were similar to those induced by PMA with GM-CSF and IL-4 which drive KG1 cells to differentiate to dendritic-like cells (Louis et al., 1999), suggesting that Mtb HSP70 may play a role in DC maturation, as has been demonstrated with mammalian HSP70 (Basu et al., 2000). It is noteworthy that Mtb HSP70 elicited CC-chemokine production only in KG1 cells activated with PMA, GM-CSF, and IL-4 in which CD40 expression was significantly upregulated. Upregulation of CD40 to a threshold may be essential for stimulation of RANTES production. Indeed, unlike the $CD40^-$ population, cell sorter separated $CD40^+$ KG1 cells (greater than 90%) were capable of producing CC-chemokines following Mtb HSP70 stimulation in the absence of PMA and the cytokines. This is consistent with the findings that the CD40 receptors are involved in Mtb HSP70-induced CC-chemokine production. The specificity of CD40-mediated activation of KG1 cells by Mtb HSP70 was demonstrated by inhibition of CC-chemokine production by antibodies to CD40, which is consistent with the report that ligation of CD40 on DC induces CC-chemokines (McDyer et al., 1999).

Receptor-mediated HSP binding has been shown on antigen-presenting cells (Castellino et al., 2000; Binder et al., 2000a; Basu et al., 2001; Arnold-Schild et al., 1999). CD14 and Toll-like receptor 4 have been described as receptors for human HSP65 and HSP70 in stimulation of antigen-presenting cells (Asea et al., 2000; Kol et al., 2000; Ohashi et al., 2000). A recent study indicates that the α2 macroglobulin receptor (CD91) is a surface receptor shared by the human HSP70, HSP90, and gp96 in priming CD8 cytotoxic T lymphocytes (Binder et al., 2000b; Basu et al., 2001). However, so far no receptor has been described for HSP derived from prokaryotic cells. Although HSPs are conserved across species, usage of receptors differs; human but not bacterial HSP60 utilize CD14 (Ohashi et al., 2000). We have found that CD40 mediates Mtb, but not human HSP70, to generate CC-chemokines.

In the receptor-mediated binding assay, FITC-labeled Mtb HSP70 binds to CD40-transfected HEK 293 cells in

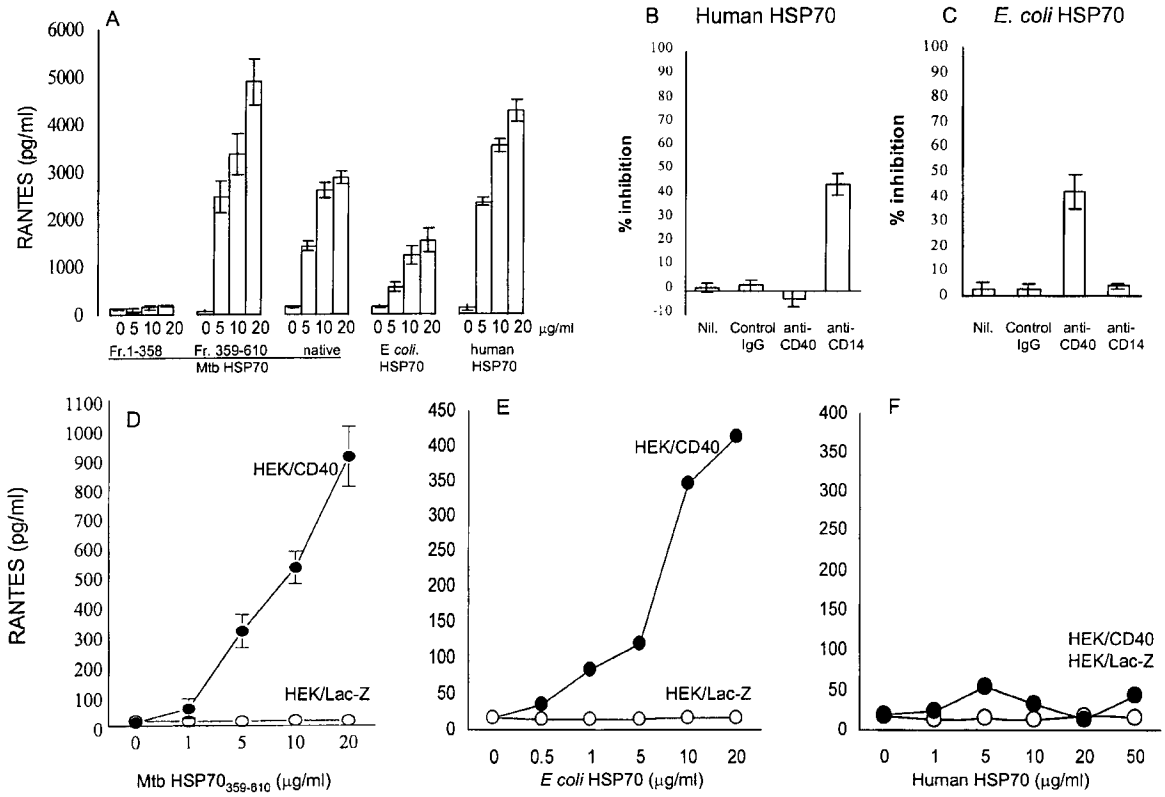

Figure 7. A Comparison of Stimulation of THP1 Cells with Native Mtb HSP70 or Its Two Fragments, *E. Coli* HSP70 and Human HSP70

Stimulation of THP1 cells with native Mtb HSP70 or its two fragments, *E. coli* HSP70 and human HSP70 (A) and effects of antibodies to CD40 or CD14 on the HSP70 stimulation (B and C). Aliquots of 2×10^5 THP1 cells were treated with different doses of native Mtb HSP70 or its two fragments, *E. coli* HSP70 and human HSP70. In the inhibition assays 20 μg/ml of antibodies to CD40, CD14, or control IgG isotype were included. The supernatant was taken 3 days after stimulation to assay RANTES. For induction of RANTES in CD40-transfected HEK 293 cells, confluent CD40, or Lac-Z-transfected HEK 293 cells were incubated with 1–20 μg/ml of the C-terminal Mtb HSP70 (359–610) fragment (D), *E.coli* HSP70 (E), or human HSP70 (F) for 4–5 days. The supernatant was then assayed for the production of RANTES. These experiments were repeated three times and the data presented as mean ± SEM.

a dose-dependent manner, as compared with the same cell lines transfected with the control Lac-Z. The binding was saturated at 25–50 μg/ml of Mtb HSP70 and could be competed by excess unlabeled Mtb or *E. coli* HSP70. Immunoprecipitation also demonstrated a physical association between CD40 and Mtb HSP70. Using surface plasmon resonance, we consistently found that CD40 transfected-, but not Lac-Z transfected-HEK 293 cells, bind specifically to Mtb HSP70, which can be inhibited by antibodies to CD40. This technique is most commonly applied to analysis of fluid phase molecules but has also been used to determine binding of intact cells (Quinn et al., 1997; Seo et al., 1997). It is not clear at present if CD40 alone is adequate to function as a receptor or whether CD40 is a constituent part of a receptor complex, which serves as a pattern recognition receptor that can discriminate between human and pathogenic bacterial HSP70. We are mindful of the increasing complexity of the LPS-CD14 receptor interaction, which requires LPS binding protein and a Toll-like receptor (Wright et al., 1990; Yang et al., 1999; Qureshi et al., 1999).

LPS induces a high concentration of CC-chemokines (Verani et al., 1997), so it was essential to exclude any contaminating LPS. LPS stimulation is independent of calcium flux, unlike the calcium flux-dependent HSP stimulation (McLeish et al., 1989; Asea et al., 2000). Treatment of THP1 cells with an intracellular calcium chelator (BAPTA-AM) prior to stimulation with Mtb HSP70 or LPS inhibited RANTES production with the former but not with the latter. A number of further control experiments indicated that neither contaminating LPS nor other bacterial products were involved in Mtb HSP70-induced CC-chemokine production. Antibodies to CD14, but not those to CD40, suppressed CC-chemokines induced by LPS. The LPS inhibitor polymyxin B inhibited LPS-induced, but not Mtb HSP70-induced CC-chemokines. Treatment of Mtb HSP70 with "Kuttsu Clean" which removes >99% of LPS from the Mtb HSP70 preparation did not alter the Mtb HSP70 activity in the induction of CC-chemokines (data not shown). Furthermore, a preparation of the recombinant Mtb HSP70 N-terminal ATPase fragment purified by the same procedures as Mtb HSP70 failed to stimulate CC-chemokine production, indicating that contamination with a bacterial product was unlikely to be involved.

HSP70 is one of the most conserved protein families among various species. There is about 60% homology between human and Mtb HSP70 and 70% between

E. coli and Mtb HSP70 (Bardwell and Craig, 1984). We have reported here that Mtb HSP70 and *E. coli* HSP70 stimulated THP1 cells to produce RANTES and that both were mediated by CD40, unlike, human HSP70 which is CD14 dependent. We do not have an explanation for this differential receptor usage, but a homology plot of conserved amino acids between human and *E. coli* HSP70 varies between 20% and 80% (Hunt and Morimoto, 1985). However, the epitope resides within the C-terminal peptide binding domain ($HSP70_{359-610}$), which stimulated production of RANTES and not the N-terminal fragment (aa 1–358).

In summary, this study demonstrated that Mtb HSP70 stimulates monocytes and DC to produce CC-chemokines and that this stimulation is mediated by the CD40 molecule and is inhibited by anti-CD40 but not anti-CD14 antibodies. CD40 transfected with the wild-type, unlike a mutagenized CD40, was essential for stimulation of monocytes by HSP70. Coimmunoprecipitation of CD40 with HSP70 and binding of HSP70 to CD40 expressed on the cell surface suggest that CD40 is a receptor or part of a receptor complex for Mtb HSP70.

Experimental Procedures

Reagents

The recombinant Mtb HSP70 was prepared from the *E.coli*. pop strain, which is deficient in bacterial HSP70. The protein was purified by Q-Sepharose followed by ATP affinity chromatography. The Q-Sepharose chromatography was repeated in order to remove endotoxin, which was tested by the Limulus amebocyte lysate assay and showed 1.2 pg of endotoxin per 1 μg Mtb HSP70 protein. In some experiments Mtb HSP70 was further treated with Kuttsu Clean (Maruha Corporation, Ibaraki, Japan), which removes greater than 99% of LPS. DNA encoding the N-terminal ATPase (aa 1–358) domain of HSP70 was cloned and expressed in *E. coli* using the pET 22b vector. Similarly, DNA encoding the C-terminal peptide binding domain (aa 359–610) was expressed using pJLA603 vector (Singh et al., 1992). Cloned inserts were verified by DNA sequence analysis. In both cases, recombinant polypeptides were prepared by affinity chromatography using Ni^{2+}-chelating resin and identity of the polypeptides was confirmed by N-terminal sequence analysis (ten cycles for each). Human recombinant HSP70 was a kind gift from Dr. S. Jindal (Cambridge, MA). *E. coli*. HSP70 was obtained from Stressgen (Bioquote, York, UK). Soluble CD40 ligand trimer (CD40LT, Immunex) was kindly donated by Dr. F. Villinger (Atlanta, Georgia). Monoclonal antibodies to CD14 (clone MY4), CD40 (clone MAB89), CD80, and CD86 were purchased from Immunotech (Oxford, UK). The antibodies to CD14, CD40 (clone LOB), CD40L, CD83, and control murine monoclonal antibody isotypes were obtained from Serotec (Oxford, UK). MAb to CD91 was obtained from Dako (clone A2MRα-2, Cambridgeshire, UK) and mAb to TLR4 (MTS510), which reacts with mouse and human TLR4, was kindly donated by Dr. Miyake (Saga Medical School, Japan). The human recombinant GM-CSF was obtained from Leucomax (Sandoz Pharmaceuticals, Surrey, UK) and human recombinant IL-4 from R&D System (Abingdon, UK). BAPTA-AM, polymyxin B, LPS, and PMA were obtained from Sigma (Dorset, UK).

Antibodies for Immunoprecipitation and Western Blot

Two antibodies to CD40 were used in the immunoprecipitation and Western blot experiments. An affinity-purified rabbit polyclonal antibody to CD40 showed specificity to a peptide mapping at the carboxyl terminus, as demonstrated by Western blot and was obtained from Santa Cruz Biotechnology (Wiltshire, UK). The immunoprecipitation antibody specific to the surface CD40 was murine monoclonal antibody and was obtained from Serotec. The CD14 murine monoclonal antibody used for immunoprecipitation and Western blot was purchased from Santa Cruz. The antibody to Mtb HSP70 was raised in our laboratory, by immunizing rhesus macaques with recombinant Mtb HSP70. An IgG fraction was prepared by ion exchange chromatography on DEAE cellulose. The specificity was demonstrated by Western blotting and dose-dependent adsorption with Mtb HSP70-coated Sepharose-4B beads by ELISA.

Cell Lines

The monocytic THP1 cell line was obtained from the MRC (NIBSC, Potters Bar, UK). The nonadherent THP1 cell line was cultured in RPMI 1640 medium supplemented with 10% FCS, 100 μg/ml of penicillin and streptomycin, and 2 mM glutamine, and the medium was replaced every 3–4 days. KG1 cells were a generous gift from Dr. K. Lee of the Naval Medical Research Institute, Bethesda, MD.. The cells were maintained in RPMI 1640 medium supplemented with 10% FCS, 10% minimum essential medium (MEM), 100 μg/ml of penicillin and streptomycin, and 2 mM glutamine. The human embryonic kidney cell line (HEK 293 cells) was acquired from the NIH (Bethesda, MD) and was maintained in DMEM supplemented with 10% FCS, 2 mM glutamine, 100 μg/ml of penicillin and streptomycin, and passaged every 3–4 days. All three types of cell lines were found to be CD40L negative (data not shown).

Transfection of HEK 293 Cells with Wild-Type or Mutagenized CD40

Full-length human CD40 cDNA in the pCDM8 plasmid vector (Invitrogen, San Diego, CA) was a kind gift from Dr B. Seed (Stamenkovic et al., 1989). A deletion mutant lacking the cytoplasmic tail of CD40 (CD40Δ*cyt*) (Lee et al., 1999) was subcloned from the pBABEpuro CD40Δ*cyt* vector into pCDM8. This was performed by replacing the pCDM8 wild-type CD40 Sph1/Not1 fragment with the Sph1/Sal1 fragment from the pBABEpuro CD40Δ*cyt* vector. pCDM8 encoding the *E. coli* β-galactosidase (Lac-Z) was used as a control. The cells were cultured in 25 cm^2 flasks or 24-well plates until 30%–50% confluence and transfected using LipofectAmine Plus (GIBCO Life Technologies, Paisley, UK). Transfection was performed according to the manufacturer's protocol and CD40 was detected by flow cytometry using PE-conjugated CD40 mAb. The assays were carried out sequentially at days 2, 3, 4, and 5 after transfection, and the percentage of $CD40^+$ cells was consistently greater than 65%.

Induction of CC-Chemokines

THP1 cells (2×10^5 ml), KG1 cells (5×10^5/ml), or transfected HEK 293 cells (80%–90% confluent) were cultured in 24-well plates and incubated with various concentrations of HSP70 (0.5–50 μg/ml), or CD40LT (0.1–5 μg/ml). Human serum albumin was used as a negative control. To rule out the effect of any remaining contamination with LPS in the HSP70 preparation, 50 μg/ml of polymyxin B was added to the cultures of monocytes stimulated with either HSP70 or LPS. To activate KG1 cells, PMA (20 ng/ml), GM-CSF (400 U/ml), and IL-4 (20 U/ml) were added to the KG1 cell cultures (Louis et al., 1999). After 3–5 days, the supernatant was used to assay CC-chemokines.

Cell Sorting

$CD40^+$ and $CD40^-$ KG1 cells were sorted on a MoFlo flow cytometer (Cytomation, Colorado) by using PE-conjugated antibodies to CD40 (10 μl per 10^6 cells). Positive and negative CD40 subsets were collected, and the purity was monitored after every sorting and showed consistently >98%. Collected $CD40^+$ and $CD40^-$ population were washed and resuspended in RPMI medium containing 10% FCS and MEM, 2 mM glutamine, and 100 μg/ml of penicillin and streptomycin at a concentration of 2×10^5 per ml. The cells were placed onto 96-well plates and incubated overnight. After 24 hr culture, Mtb HSP70 was added at various concentrations in the presence or absence of PMA plus GM-CSF and IL-4. Following culture for 3 days, the supernatants were collected for the CC-chemokine assay.

Inhibition of Production of CC-Chemokines

THP1 cells or KG1 cells were stimulated with either 10 μg/ml of HSP70 or 100 ng/ml of LPS in the presence of antibodies to CD14 (1–20 μg/ml), CD40 (1–20 μg/ml), or the isotype-matched control antibody. After 3 days of culture, the supernatants were collected for CC-chemokine assays.

Induction of CC-Chemokines in Primary Cultures of Monocytes, DC, and PMBC

Human blood was taken from healthy laboratory workers and PBMC were prepared by Ficoll-Hypaque gradient centrifugation at 1000 × g for 15 min. The cells were washed and resuspended in 10% FCS-RPMI medium at a concentration of 1×10^6 per ml. Human PBMC-derived monocytes were isolated by cell sorting (MoFlo) using PE-conjugated antibodies to CD14 as described above. DC were generated by culturing $CD14^+$ monocytes for 7–9 days in the presence of GMCSF and IL-4. Purified monocytes (>98%) were resuspended at 5×10^5/ml, and these as well as the DC were stimulated with increasing concentrations of Mtb HSP70. For the inhibition studies, 10 μg/ml of anti-CD40 antibodies or controls were added, and after 3 days the supernatant were used to assay CC-chemokines.

ELISA for RANTES, MIP-1α, and MIP-1β

The CC-chemokines were assayed in the culture supernatants generated by stimulation of THP1, KG1, and HEK 293 cells with HSP70. The supernatants collected from THP1 cells were diluted ten times and KG1 or HEK 293 cell culture supernatant five times. Specific ELISA kits were used for CC-chemokines (R&D System), and the results were expressed in pg/ml.

Flow Cytometry Analysis

Aliquots of 2×10^5 either THP1 or KG1 cells were incubated with 10 μl of PE-conjugated antibodies to CD40, CD40L, or CD14 and PE-conjugated mouse IgG1 isotype for 30 min on ice. After washing twice, the cells were fixed in 1% formaldehyde before analysis by flow cytometry. For indirect staining, the cells were incubated with the primary antibodies to CD80, CD83, CD86, or CD40L for 30 min on ice, followed by FITC-labeled rabbit anti-mouse IgG (Dako, Bucks, UK) for further 30 min. The cells were analyzed on a Coulter XL-MCL cytometer, and the data was analyzed on a Software WinMID.

Binding Assay Using FITC-Mtb HSP70

FITC-labeled Mtb HSP70 was prepared by incubation of recombinant Mtb HSP70 with FITC celite (Sigma). A single-cell suspension of HEK 293 cells was prepared by dissociation of CD40-transfected or Lac-Z-transfected HEK 293 cell cultures with 0.1% EDTA solution. The cells were resuspended at 10^6 cells per ml in PBS, containing 0.1% sodium azide and 2% bovine serum albumin. Aliquots of 20 μl of cells were incubated with various concentrations of FITC-Mtb HSP70 or control FITC-BSA in 20 μl of the PBS medium on ice for 30 min prior to washing. In order to compete with FITC-Mtb HSP70 binding, unlabeled Mtb HSP70 was added at a 40-fold greater concentration than that of the FITC-labeled Mtb HSP70. Binding of labeled Mtb HSP70 or BSA was analyzed by flow cytometry as described above.

HSP70 Binding Assay by Surface Plasmon Resonance

Mtb HSP70 was immobilized on the surface of a CM5 sensorchip (Biacore AB, Stevenage, UK) at 40 μg/ml in 10 mM Na acetate (pH 4.0). Between 3000–8000 resonance units were coupled on each occasion in flow cell 2 while bovine serum albumin was coupled (at the same level) to flow cell 1 which served as reference. Single-cell suspensions of transfected HEK 293 cells expressing CD40 or Lac-Z were prepared by dissociation with 0.1% EDTA solution. Cells were resuspended in DMEM supplemented with 10% FCS and binding of fluid-phase cells over a range of concentrations was determined at 25°C by surface plasmon resonance using the BIAcore X (Biacore AB, Stevenage, UK). DMEM supplemented with 10% FCS was used as buffer throughout, flow rate was 1μl/min, and injection volume was 20μl. The sensorchip surface was regenerated with a pulse (1 μl) of 100 mM HCl. For inhibition analyses, anti-CD40 mAb, a control mAb of irrelevant specificity (Guy's 13), or anti-CD14 mAb (MY4) was added to the cell suspensions immediately before injection.

Immunoprecipitation and Immunoblot Analysis

Monocytic THP1 cells (1×10^7) were washed twice with PBS and lysed with 500 μl of lysis buffer (0.5% Nonidet P-40, 0.14% M NaCl, 50 mM NaF, 20 mM Tris [pH 7.4], 2 mM EDTA, 2 mM orthovanadate, 2 mM PMSF, 2% aprotinin, and 2–4 μg/ml pepstatin, antipain, and leupeptin). After 15 min centrifugation, the supernatant from the cell lysate was incubated with 50 μg/ml of Mtb HSP70 or human HSP70 at 4°C. The mixture was then incubated with rabbit antibodies to CD40, rabbit control antibodies, or mouse anti-CD14 mAb or isotype control mAb for 60 min, followed by 1 hr incubation with protein G-Sepharose. The precipitate was washed three times in lysis buffer, suspended in Laemmli sample buffer, and separated by SDS-PAGE, followed by electrophoretic transfer to a nitrocellulose membrane (Immobilon, Millipore UK). The membranes were probed with either rabbit antibodies to CD40, mAb to CD14, simian antibodies to Mtb HSP70, or control antibody, and detected by chemiluminescence (Amersham, Buckinghamshire, UK).

For immunoprecipitation of cell surface CD40, THP1 cells were surface biotinylated and then incubated with Mtb HSP70 at 0 and 50 μg/ml for 30 min on ice. After washing, the cells were incubated with antibody to Mtb HSP70, CD40, or isotype-matched control antibody on ice for further 30 min. After further washing, the cells were lysed using 150 mM isotonic tris-HCL buffer (pH 7.3) with 1% CHAPS (lysis buffer) for 30 min at 4°C. Insoluble material was removed by centrifugation and the supernatant was incubated with protein G-Sepharose at 4°C for 30 min. Sepharose beads were then washed three times with lysis buffer and incubated with sample buffer containing 1% SDS for 3 min at 100°C. The complexes were separated by SDS-PAGE, transferred to nitrocellulose membrane, and visualized by chemiluminescence. Immunoprecipitates prepared in an identical manner from unlabeled cells were analyzed by Western blot with antibody to CD40.

Statistical Analysis

The differences of the groups were analyzed by the Anova *F*-test, and the significance was analyzed by the paired "t" test.

Acknowledgments

We thank Dr. Q. Liu for his expert technical help in some of the immunoprecipitation experiments and Mr. R. McCord for cell sorting on the MoFlo flow cytometer. This work is supported by grants from the European Community Concerted Action against AIDS and the Special Trustees of Guy's and St. Thomas' Hospital. PJL, JK, PM, and LD are supported by the Wellcome Trust.

Received April 9, 2001; revised October 12, 2001.

References

Arnold-Schild, D., Hanau, D., Spehner, D., Schmid, C., Rammensee, H-G., de la Salle, H., and Schild, H. (1999). Cutting edge: receptor-mediated endocytosis of heat shock proteins by professional antigen-presenting cells. J. Immunol. *162*, 3757–3760.

Asea, A., Kraeft, S.K., Kurt-Jones, E.A., Stevenson, M.A., Chen, L.B., Finberg, R.W., Koo, G.C., and Calderwood, S.K. (2000). HSP70 stimulates cytokine production through a CD14-dependent pathway, demonstrating its dual role as a chaperone and cytokine. Nat. Med. *6*, 435–442.

Baggiolini, M. (1998). Chemokines and leukocyte traffic. Nature. *392*, 565–568.

Banchereau, J., Bazan, F., Blanchard, D., Brière, F. Galizzi, J.P., van Kooten, C., Liu, Y.J., Rousset, F., and Saeland, S. (1994). The CD40 antigen and its ligand. Annu. Rev. Immunol. *12*, 881–922.

Bardwell, J.C., and Craig, E.A. (1984). Major heat shock gene of *Drosophila* and the *Escherichia coli* heat-inducible dnaK gene are homologous. Proc. Natl. Acad. Sci. USA *81*, 848–852.

Basu, S., Binder, R.J., Suto, R., Anderson, K.M., and Srivastava, P.K. (2000). Necrotic but not apoptotic cell death releases heat shock proteins, which deliver a partial maturation signal to dendritic cells and activate the NF-kappa B pathway. Int. Immunol. *12*, 1539–1546.

Basu, S., Binder, R.J., Ramalingam, T., and Srivastava, P.K. (2001). CD91 is a common receptor for heat shock proteins gp96, hsp90, hsp70, and calreticulin. Immunity *14*, 303–313.

Bennett, S.R.M., Carbone, F.R., Karamalis, F., Flavell, R.A., Miller, J.F.A.P., and Heath, W.R. (1998). Help for cytotoxic-T-cell responses is mediated by CD40 signalling. Nature *393*, 478–480.

Binder, R.J., Han, D.K., and Srivastava, P.K. (2000a). CD91: a receptor for heat shock protein gp96. Nat. Immunol. *1*, 151–155.

Binder, R.J., Harris, M.L., Menoret, A., and Srivastava, P.K. (2000b). Saturation, competition, and specificity in interaction of heat shock proteins (hsp) gp96, hsp90 and hsp70 with CD11b$^+$ cells. J. Immunol. *165*, 2582–2587.

Castellino, F., Boucher, P.E., Eichelberg, K., Mayhew, M., Rothman, J.E., Houghton, A.N., and Germain, R.N. (2000). Receptor-mediated uptake of antigen/heat shock protein complexes results in major histocompatibility complex class I antigen presentation via two distinct processing pathways. J. Exp. Med. *191*, 1957–1964.

Caux, C., Massacrier, C., Vanbervliet, B., Dubois, B., Van Kooten, C., Durand, I., and Banchereau, J. (1994). Activation of human dendritic cells through CD40 cross-linking. J. Exp. Med. *180*, 1263–1272.

Cella, M., Scheidegger, D., Palmer-Lehmann, K., Lane, P., Lanzavecchia, A., and Alber, G. (1996). Ligation of CD40 on dendritic cells triggers production of high levels of IL-12 and enhances T cell stimulatory capacity: T-T help via APC activiation. J. Exp. Med. *184*, 747–752.

Ciupitu, A.-M.T., Petersson, M., O'Donnell, C.L., Williams, K., Jindal, S., Kiessling, R., and Welsh, R.M. (1998). Immunization with a lymphocytic choromeningitis virus peptide mixed with heat shock protein 70 results in protective antiviral immunity and specific cytotoxic T lymphocytes. J. Exp. Med. *187*, 685–691.

Fujihara, S.M., and Nadler, S.G. (1999). Intranuclear targeted delivery of functional NF-κB by 70 kDa heat shock protein. EMBO J. *18*, 411–419.

Gething, M.J., and Sambrook, J. (1992). Protein folding in the cell. Nature. *335*, 33–45.

Herold, K.C., Lu, J., Rulifson, I., Vezys, V., Taub, D., Grusby, M.J., and Bluestone, J.A. (1997). Cutting edge: regulation of C-C chemokine production by murine T cells by CD28/B7 costimulation. J. Immunol. *159*, 4150–4153.

Hoffmann, J.A., Kafatos, F.C., Janeway, C.A., Jr., and Ezekowitz, R.A.B. (1999). Phylogenetic perspectives in innate immunity. Science *284*, 1313–1318.

Huang, Q., Richmond, J.F.L., Suzue, K., Eisen, H.M., and Young, R.A. (2000). In vivo cytotoxic T lymphocyte elicitation by mycobacterial heat shock protein 70 fusion proteins maps to a discrete domain and is CD4$^+$ T cell independent. J. Exp. Med. *191*, 403–408.

Hunt, C., and Morimoto, R.I. (1985). Conserved features of eukaryotic HSP70 genes revealed by comparison with the nucleotide sequence of human HSP70. Proc. Natl. Acad. Sci. USA *82*, 6455–6459.

Kiener, P.A., Moran-Davis, P., Rankin, B.M., Wahl, A.F., Aruffo, A., and Hollengaugh, D. (1995). Stimulation of CD40 with purified soluble gp39 induces proinflammatory responses in human monocytes. J. Immunol. *155*, 4917–4295.

Kol, A., Lichtman, A.H., Finberg, R.W., Libby, P., and Kurt-Jones, E.A. (2000). Cutting edge: heat shock protein (HSP) 60 activates the innate immune response: CD14 is an essential receptor for HSP60 activation of mononuclear cells. J. Immunol. *164*, 13–17.

Kornbluth, R.S., Kee, K., and Richman, D.D. (1998). CD40 ligand (CD154) stimulation of macrophages to produce HIV-1-suppressive β-chemokines. Proc. Natl. Acad. Sci. USA *95*, 5205–5210.

Lee, H.H., Dempsey, P.W., Parks, T.P., Zhu, X., Baltimore, D., and Cheng, G. (1999). Specificity of CD40 signaling: involvement of TRAF2 in CD40-induced NF-κB activation and intercellular adhesion molecule-1 up-regulation. Proc. Natl. Acad. Sci. USA *96*, 1421–1426.

Lehner, T., Bergmeier, L.A., Wang, Y., Tao, L., Sing, M., Spallek, R., and van der Zee, R. (2000). Heat shock protein generates β-chemokines which function as innate adjuvants enhancing adaptive immunity. Eur. J. Immunol. *30*, 594–603.

Lindquist, S., and Craig, E.A. (1988). The heat-shock proteins. Annu. Rev. Genet. *22*, 631–677.

Louis, D.C., Woodcock, J.B., Fransozo, G., Blair, P.J., Carlson, L.M., Murillo, M., Wells, M.R., Williams, A.J., Smoot, D.S., Kaushal, S., et al. (1999). Evidence for distinct intracellular signalling pathways in CD34$^+$ progenitor to dendritic cell differentiation from a human cell line model. J. Immunol. *162*, 3237–3248.

Lussow, A.R., Barrios, C., van Embden, J., Van der Zee, R., Verdini, A.S., Pessi, A., Louis, J.A., Lambert, P.H. and Del Giudice, G. (1991). Mycobacterial heat-shock proteins as carrier molecules. Eur. J. Immunol. *21*, 2297–2302.

McDyer, J.F., Dybul, M., Goletz, T.J., Kinter, A.L., Thomas, E.K., Berzofsky, J.A., Fauci, A.S., and Seder, R.A. (1999). Differential effects of CD40 ligand/trimer stimulation on the ability of dendritic cells to replicate and transmit HIV infection: evidence for CC-chemokine-dependent and -independent mechanisms. J. Immunol. *162*, 3711–3717.

McLeish, K.R., Dean, W.L., Wellhausen, S.R., and Stelzer, G.T. (1989). Role of intracellular calcium in priming of human peripheral blood monocytes by bacterial lipopolysacchride. Inflammation *13*, 681–692.

Medzhitov, R., and Janeway, C.A., Jr. (1997). Innate immunity: the virtues of a nonclonal system of recognition. Cell *91*, 295–298.

Ohashi, K., Burkart, V., Flohé, S., and Kolb, H. (2000). Cutting edge: heat shock protein 60 is a putative endogenous ligand of the toll-like receptor-4 complex. J. Immunol. *164*, 558–561.

Perraut, R., Gavoille, S., Garraud, O., Matile, H., Tougne, C., van Embden, J., van der Zee R., Lambert, P.H., and Gysin, J. (1993). Successful primate immunization with peptide conjugated to purified protein derivative or mycobacterial heat shock proteins in the absence of adjuvants. Clin. Exp. Immunol. *93*, 382–386.

Pilon, M., and Schekman, R. (1999). Protein translocation: how hsp70 pulls it off. Cell *97*, 679–682.

Ridge, J.P., Di Rosa, F., and Matzinger, P. (1998). A conditioned dendritic cell can be a temporal bridge between a CD4$^+$ T-helper and a T-killer cell. Nature *393*, 474–478.

Rothman, J.E. (1989). Polypeptide chain binding protein: catalysis of protein folding and related processes in cells. Cell *59*, 591–601.

Quinn, J.G., O'Kennedy, R., Smyth, M., Moulds, J., and Frame, T. (1997). Detection of blood group antigens utilising immobilised antibodies and surface plasmon resonance. J. Immunol. Methods *206*, 87–96.

Qureshi, S.T., Larivière, L., Leveque, G., Clermont, S., Moore, K.J., Gros, P., and Malo, D. (1999). Endotoxin-tolerant mice have mutations in Toll-like receptor 4 (Tlr4). J. Exp. Med. *189*, 615–625.

Sallusto, F., and Lanzavecchia, A. (1994). Efficient presentation of soluble antigen by cultured human dendritic cells is maintained by granulocyte/macrophage colony-stimulating factor plus interleukin 4 and downregulated by tumor necrosis factor α. J. Exp. Med. *179*, 1109–1118.

Schoenberger, S.P., Toes, R.E.M., van der Boort, E.I.H., Offringa, R., and Melief, C.J.M. (1998). T-cell help for cytotoxic T lymphocytes is mediated by CD40-CD40L interactions. Nature *393*, 480–483.

Seo, J.K., Choi, S.Y., Kim, Y., Baek, S.H., Kim, K.T., Chae, C.B., Lambeth, J.D., Suh, P.G., and Ryu, S.H. (1997). A peptide with unique receptor specificity: stimulation of phosphoinositide hydrolysis and induction of superoxide generation in human neutrophils. J. Immunol. *158*, 1895–1901.

Singh, M., Andersen, A.B., McCarthy, J.E.G., Rhode, M., Schütte, H., Sanders, E., and Timmis, K.N. (1992). The *Mycobacterium tuberculosis* 38-kDa antigen: overproduction in *Escherichia coli*, purification and expression. Gene *117*, 53–60.

Stamenkovic, I., Clark, E.A., and Seed, B. (1989). A B-lymphocyte activation molecule related to the nerve growth factor receptor and induced by cytokines in carcinomas. The EMBO J. *8*, 1403–1410.

Suto, R., and Srivastava, P.K. (1995). A mechanism for the specific immunogenecity of heat shock protein-chaperoned peptides. Science *269*, 1585–1588.

Suzue, K., and Young, R.A. (1996). Adjuvant-free hsp70 fusion protein system elicits humoral and cellular immune responses to HIV-1 p24. J. Immunol. *158*, 873–879.

Udono, H., and Srivastava, P.K. (1993). Heat shock protein 70-associated peptides elicit specific cancer immunity. J. Exp. Med. *178*, 1391–1396.

Verani, A., Scarlatti, G., Comar, M., Tresoldi, E., Polo, S., Giacca, M., Lusso, P., Siccardi, A.G., and Vercelli, D. (1997). C-C chemokines

released by lipopolysaccharide (LPS)-stimulated human macrophages suppress HIV-1 infection in both macrophages and T cells. J. Exp. Med. *185*, 805–816.

Wright, S.D., Ramos, R.T., Tobias, P.S., Ulevitch, R.J., and Mathison, J.C. (1990). CD14, a receptor for complex of lipopolysaccharide (LPS) and LPS binding protein. Science *249*, 1431–1433.

Yang, R.-B., Mark, M.R., Gurney, A., and Godowski, P.J. (1999). Signaling events induced by lipopolysaccharide-activated Toll-like receptor 2. J. Immunol. *163*, 639–641.

Young, L.S., Eliopoulos, A.G., Gallagher, N.J., and Dawson, C.W. (1998). CD40 and epithelial cells: across the great divide. Immunol. Today *19*, 502–506.

Zhou, L.J., and Tedder, T.F. (1995). Human blood dendritic cells selectively express CD83, a member of the immunoglobulin superfamily. J. Immunol. *154*, 3821–3835.

nature
chemical biology

C_3-symmetric peptide scaffolds are functional mimetics of trimeric CD40L

Sylvie Fournel[1], Sébastien Wieckowski[1], Weimin Sun[1,5], Nathalie Trouche[1], Hélène Dumortier[1], Alberto Bianco[1], Olivier Chaloin[1], Mohammed Habib[2], Jean-Christophe Peter[1], Pascal Schneider[3], Bernard Vray[2], René E Toes[4], Rienk Offringa[4], Cornelis J M Melief[4], Johan Hoebeke[1] & Gilles Guichard[1]

Interaction between CD40, a member of the tumor necrosis factor receptor (TNFR) superfamily, and its ligand CD40L, a 39-kDa glycoprotein, is essential for the development of humoral and cellular immune responses[1,2]. Selective blockade or activation of this pathway provides the ground for the development of new treatments against immunologically based diseases[3,4] and malignancies[5,6]. Like other members of the TNF superfamily, CD40L monomers self-assemble around a threefold symmetry axis to form noncovalent homotrimers that can each bind three receptor molecules[7,8]. Here, we report on the structure-based design of small synthetic molecules with C_3 symmetry that can mimic CD40L homotrimers. These molecules interact with CD40, compete with the binding of CD40L to CD40, and reproduce, to a certain extent, the functional properties of the much larger homotrimeric soluble CD40L. Architectures based on rigid C_3-symmetric cores may thus represent a general approach to mimicking homotrimers of the TNF superfamily.

CD40L is expressed mainly on activated T cells, whereas its cognate receptor, CD40, is constitutively expressed on dendritic cells (DC), macrophages and B cells. The engagement of CD40 by its ligand contributes to regulation of B cell proliferation, immunoglobulin production, immunoglobulin class switching, germinal center formation and development of B cell memory[1]. Moreover, CD40-CD40L interaction has an essential role in cellular immune response in which CD40 ligation activates DCs, 'licensing' them to present antigen to cytotoxic T cells by increasing MHC and costimulatory molecule expression and by producing high levels of IL-12, a T cell–stimulating cytokine[9–11]. Antibodies against CD40 with agonist activity have been used to increase immune response in infectious diseases[12,13] and in cancer immunotherapy[5,6]. All of these results underscore the important therapeutic applications that could emerge from the development of small-molecule CD40 agonists.

Although ligand-induced dimerization is a general mechanism for activating receptors of cytokines and growth factors[14], signaling through receptors of the TNFR superfamily strongly relies on the formation of stoichiometrically defined C_3-symmetric complexes[7]. The structures of several TNF family members in complex with their cognate receptors show that each ligand homotrimer interacts with three monomeric receptor chains[7,15,16]. The geometry of the resulting 3:3 hexameric complex is favorable to the formation of an internal 3:3 signaling complex between the intracellular tail of the receptor and transduction proteins, ultimately activating downstream effector pathways[7].

Despite the difficulty in identifying small molecules that can disrupt protein-protein interactions, synthetic agonists of homodimeric cytokine receptors have been reported[17,18]. The ability of these molecules to dimerize cell-surface receptors is a major determinant of their effector functions[19]. In the present study, we have developed CD40L mimetics by integrating threefold symmetry as a design principle. We reasoned that such trimeric architectures, besides providing the correct geometry for receptor trimerization, could also achieve tight binding to CD40 with receptor-binding elements of low surface areas (for example, small peptides)[20,21]. Although the CD40L-CD40 interaction has not been determined at the atomic level, a model of the complex built using the X-ray structure of CD40L and a homology model of CD40 (ref. 22) has provided the basis for the structure-based design of trivalent ligands (**Fig. 1a**). Both rigid, flat macrocyclic (D,L-α-hexapeptide and β^3-tripeptide) and flexible branched C_3-symmetric scaffolds have been considered as core structures to distribute receptor-binding elements with geometry and distances that could match those of the CD40L homotrimer (**Fig. 1b**). Five 'hot spot' residues in CD40L (namely, Lys143, Tyr145, Tyr146 (in the AA″ loop), Arg203 (in the DE loop) and Gln220 (in the F strand)) have been previously identified using a combination of molecular modeling and site-directed mutagenesis[22,23]. Mutations of these CD40L surface residues markedly affect binding to CD40. On the basis of these considerations, the small CD40-interacting

[1]UPR 9021 CNRS, Immunologie et Chimie Thérapeutiques, Institut de Biologie Moléculaire et Cellulaire, 15 rue René Descartes, F-67084 Strasbourg Cedex, France. [2]Laboratoire d'Immunologie Expérimentale (CP 615), Faculté de Médecine, Université Libre de Bruxelles, 808 Route de Lennik, 1070 Brussels, Belgium. [3]Department of Biochemistry, University of Lausanne, Ch. des Boveresses 155, CH-1066 Epalinges. [4]Leiden University Medical Center, Department of Immunohaematology and Blood Transfusion, Albinusdreef 2, E3-Q, Postbox 9600, 2300 RC, Leiden, The Netherlands. [5]Present address: Institute of Biological Science and Technology, Beijing Jiaotong University, 3 Shang Yuan Cun, Haidian District, 100044 Beijing, China. Correspondence should be addressed to G.G. (G.Guichard@ibmc.u-strasbg.fr) or S.F. (s.fournel@ibmc.u-strasbg.fr).

Received 7 July; accepted 17 October; published online 6 November 2005; doi:10.1038/nchembio746

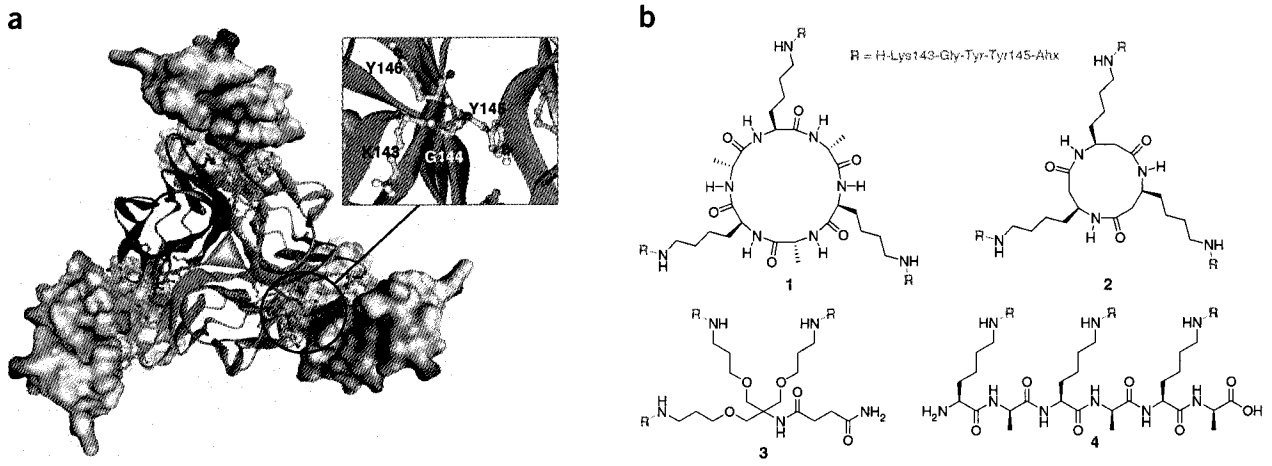

Figure 1 Synthetic C_3-symmetric CD40L mimetics. (**a**) Model of the 3:3 complex between CD40 (surface representation) and CD40L (ribbon) viewed down the C_3 axis[22] and schematic representation of the structure-based approach to the design of CD40L homotrimer mimetics. The distance between the center of the CD40L homotrimer and the CD40 binding surface is ~21 Å. Box shows a magnified view of the polar CD40-binding surface and the hot spot region Lys143–Tyr146 selected as the CD40 binding motif. (**b**) Trimeric compounds **1**–**4** were synthesized by fragment coupling of the fully protected Boc-Lys(Boc)-Gly-Tyr(O*t*Bu)-Tyr(O*t*Bu)-Ahx-OH pentapeptide to the corresponding cores in solution as described for **1** in the **Supplementary Methods**. Boc, *t*-butoxycarbonyl; O*t*Bu: *t*-butyl ether.

region Lys143-Gly-Tyr-Tyr146 of CD40L was selected as a CD40-binding motif and tethered via an amino hexanoic acid (Ahx) residue spacer to the central core structures to give compounds **1**–**3** (**Fig. 1b**).

To determine whether the resulting trimeric ligands interact with CD40, we performed a series of surface plasmon resonance (SPR) experiments using a recombinant human CD40-mouse immunoglobulin (hCD40:mIg) immobilized on the sensor chip via an anti-mouse Fc or 5C3 an anti-human CD40 monoclonal antibody (anti-hCD40 mAb; **Fig. 2** and **Supplementary Fig. 1** online). We mixed a fixed amount of recombinant human soluble CD40L tethered to a mouse CD8 tail (hCD40L:CD8) with increasing concentrations of synthetic molecules, and we then performed inhibition SPR by injecting those samples over the sensor surface. Compounds with the CD40 binding motif appended to a macrocyclic core (namely, **1** and **2**) competed with binding of hCD40L:CD8 to CD40 in a concentration-dependent manner with a median inhibitory

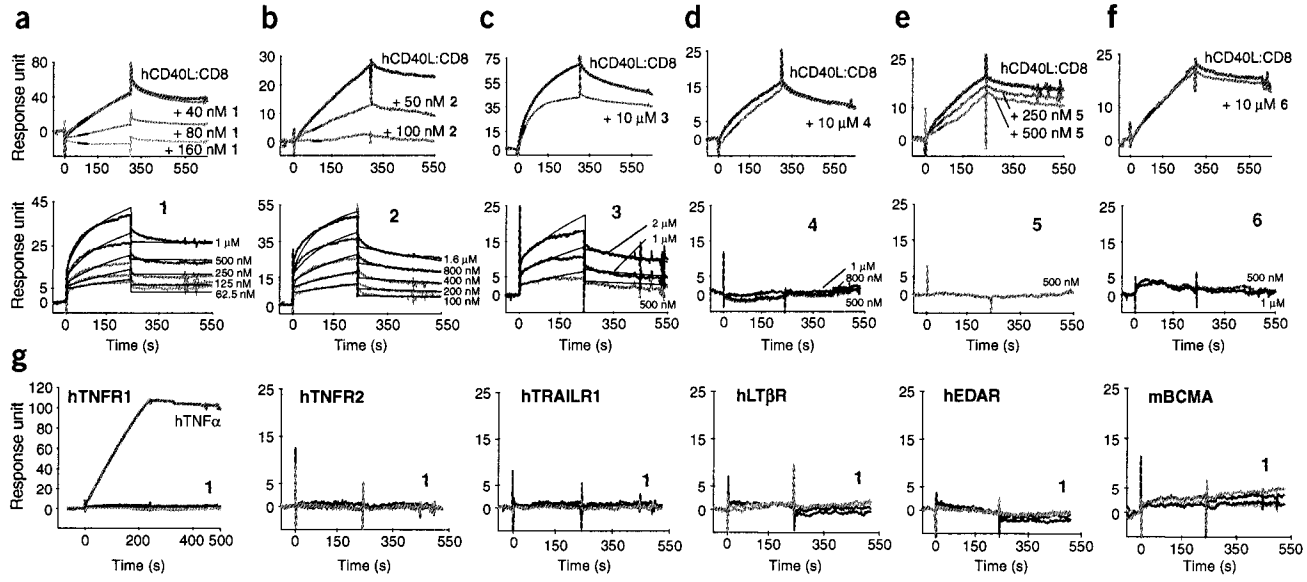

Figure 2 SPR experiments using hCD40:mIg. (**a**–**f**) Upper row shows inhibition of CD40-binding by SPR. Ligands **1**–**6** were tested for their capacity to inhibit the binding of soluble hCD40L:CD8 to CD40. The tendency of **5** to aggregate under SPR conditions prevented analyses of SPR data for concentrations >500 nM. Thick lines on the inhibition sensorgrams correspond to sections of the linear part of the kinetics (v_0) relevant to calculations of the percentage inhibition. Lower row illustrates direct binding to CD40, as shown by SPR. The binding data for **1** and **2** were fitted using a trivalent binding model (**Supplementary Table 1**). (**g**) Compound **1** (125 nM, 250 nM, 500 nM, 1 μM) did not bind to a subset of TNFR family members (~1,000 RU), as shown by SPR. As a control, binding of TNFα to TNFR1 is shown in the leftmost panel.

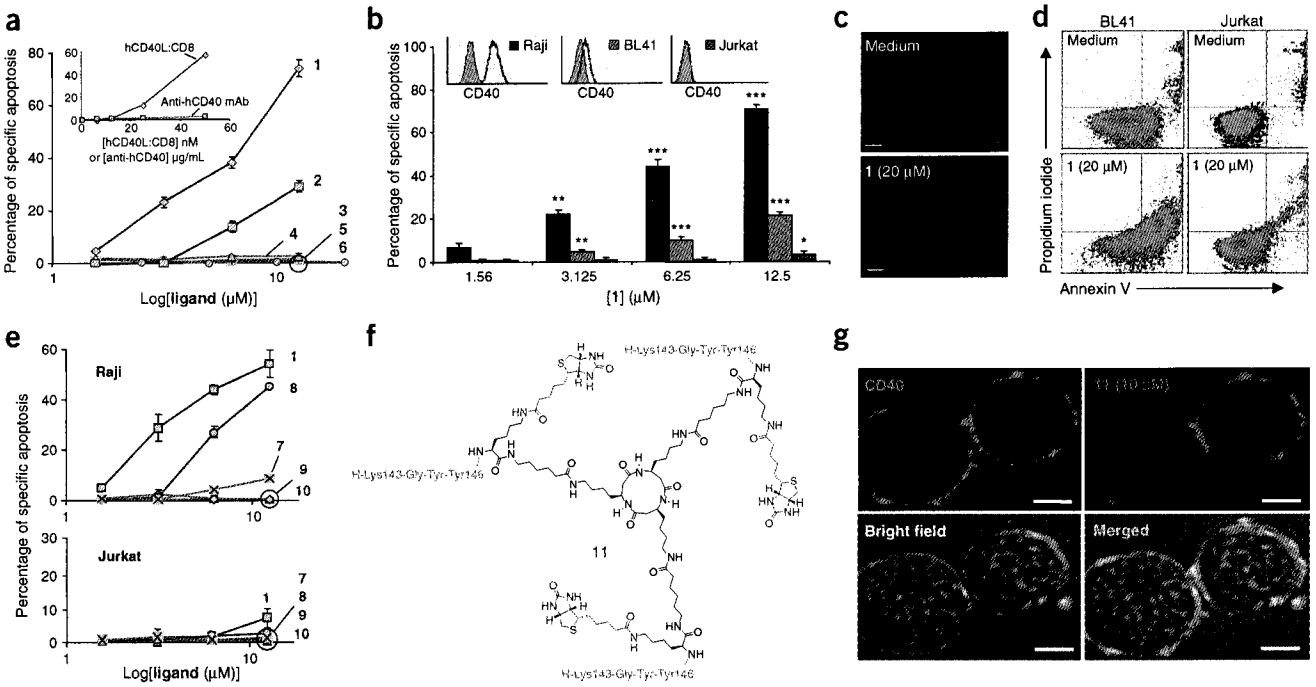

Figure 3 CD40L mimetics induce apoptosis of Burkitt lymphoma cells and colocalize with endogenous CD40. (**a**,**b**) Induction of apoptosis studied by the decrease of $\Delta\psi_m$, as detected by a reduction of $DiOC_6(3)$ dye uptake. (**a**) Effect of **1**–**6** on Raji cells. hCD40L:CD8 and anti-hCD40 mAb 5C3 are shown in inset. (**b**) Effect of **1** on cell lines expressing various levels of CD40. Results are expressed as the average (± s.e.m.) of three independent experiments. $^*P > 0.01$; ** $0.01 > P > 0.005$; *** $P < 0.005$ (Student's *t*-test). Insets show relative cell number as a function of CD40 expression (as measured by mean fluorescence intensity (MFI)). (**c**) Characteristic nucleus fragmentation of apoptotic BL41 cells treated by **1** observed after DAPI staining using epifluorescence microscopy. (**d**) Detection of phosphatidylserine externalization by flow cytometry after colabeling with annexin V-FITC and propidium iodide after treatment with **1**. (**e**) Scanning single–amino acid substitutions within the CD40 binding motif of **1**. Effect of **7** (K143G), **8** (G144A), **9** (Y145A), and **10** (Y146A) measured as in **a** and compared with **1**. (**f**) Structure of compound **11**, a biotinylated variant of **2**. (**g**) Analysis of colocalization of **11** and anti-CD40 mAb (5C3) by confocal microscopy on Raji cells. Scale bars, 5 µm. Pearson's correlation: $R_r = 0.47$; overlap coefficient: $R = 0.91$.

concentration (IC_{50}) of 78 nM and 50 nM, respectively (**Fig. 2a,b**). In contrast, **4**, a linear variant of **1** (**Fig. 2d**), the cyclic D,L-α-hexapeptide core structure of **1** (R = H, **5**; **Fig. 2e**) and the monomeric peptide H-Lys-Gly-Tyr-Tyr-Ahx-OH (**6**; **Fig. 2f**) did not inhibit CD40L binding and therefore served as valuable negative controls. Branched **3** only partially blocked binding of CD40L (20% inhibition at a concentration of 10 µM; **Fig. 2c**). We further investigated interaction of our synthetic molecules with CD40 by direct SPR binding experiments. Compounds **1**, **2** and, to a lesser extent, **3** bound to CD40 in this assay (**Fig. 2a–c** and **Supplementary Fig. 1**). Although the binding of the three molecules could be fitted to a simple monovalent binding model, analysis of SPR sensorgrams using a trivalent binding model gave a better fit for **1** and **2** with χ^2 values (which describe the closeness of the fit) of 1.34 and 0.97, respectively (**Supplementary Table 1** online). This is consistent with the rigid trimeric nature of the chemical CD40 ligands and the dense distribution of the receptor at the surface of the flexible dextran matrix, which could facilitate the formation of tetrameric complexes. The specificity of synthetic mimetics for CD40 is supported by the absence of binding of **1** to other TNFR family members (human TNFR1, TNFR2, LTβR, TRAILR1, EDAR and mouse BCMA, **Fig. 2g**).

To establish whether CD40L mimetics **1** and **2** display effector function(s), we used different cell-based assays with soluble CD40L as a positive control. The first test was based on the property of CD40-positive human Burkitt lymphoma cells to undergo apoptosis upon CD40 engagement[24]. Like hCD40L:CD8, but unlike anti-hCD40 mAb 5C3, compounds **1** and **2** induced a dose-dependent apoptosis of Burkitt lymphoma cells (maximal after 16 h of incubation) as measured by the decrease of the mitochondrial membrane potential ($\Delta\psi_m$; **Fig. 3a,b**), morphology criteria after DAPI staining (**Fig. 3c**), and detection of phosphatidylserine expression (by annexin V staining; **Fig. 3d**). The percentage of apoptosis correlated with CD40 expression (**Fig. 3b**). Neither control compounds **4**–**6**, which did not interact with CD40, nor branched **3**, induced apoptosis (**Fig. 3a**), indicating that the ligand architecture markedly influences both the CD40 binding capacity and downstream effector functions, and that distribution of the binding motif in a radial fashion is preferred. Furthermore, singly substituting alanine or glycine for each residue in the CD40 binding sequence in **1** established the importance of Lys143, Tyr145 and Tyr146 residues in both determining binding of **1** (**Supplementary Fig. 2** online) to CD40 and inducing apoptosis of B lymphoma cells (**Fig. 3e**).

To verify that CD40L mimetics target CD40 at the surface of lymphoma cells, we synthesized **11**, a biotinylated C_3-symmetric variant of **2** (**Fig. 3f**). Like **1** and **2**, compound **11** bound to CD40 in SPR experiments and induced Burkitt lymphoma cell apoptosis (**Supplementary Fig. 3** online). Using colocalization experiments with the anti-hCD40 mAb 5C3 (**Fig. 3g**) and flow cytometry staining (**Supplementary Fig. 3**), we found that compound **11** binds to CD40 at the surface of CD40-positive cells but was not detected at the surface of CD40-negative cells. Notably, binding of compound **11** was markedly reduced at 4 °C (**Supplementary Fig. 3**), suggesting that membrane fluidity is required for optimal CD40 binding.

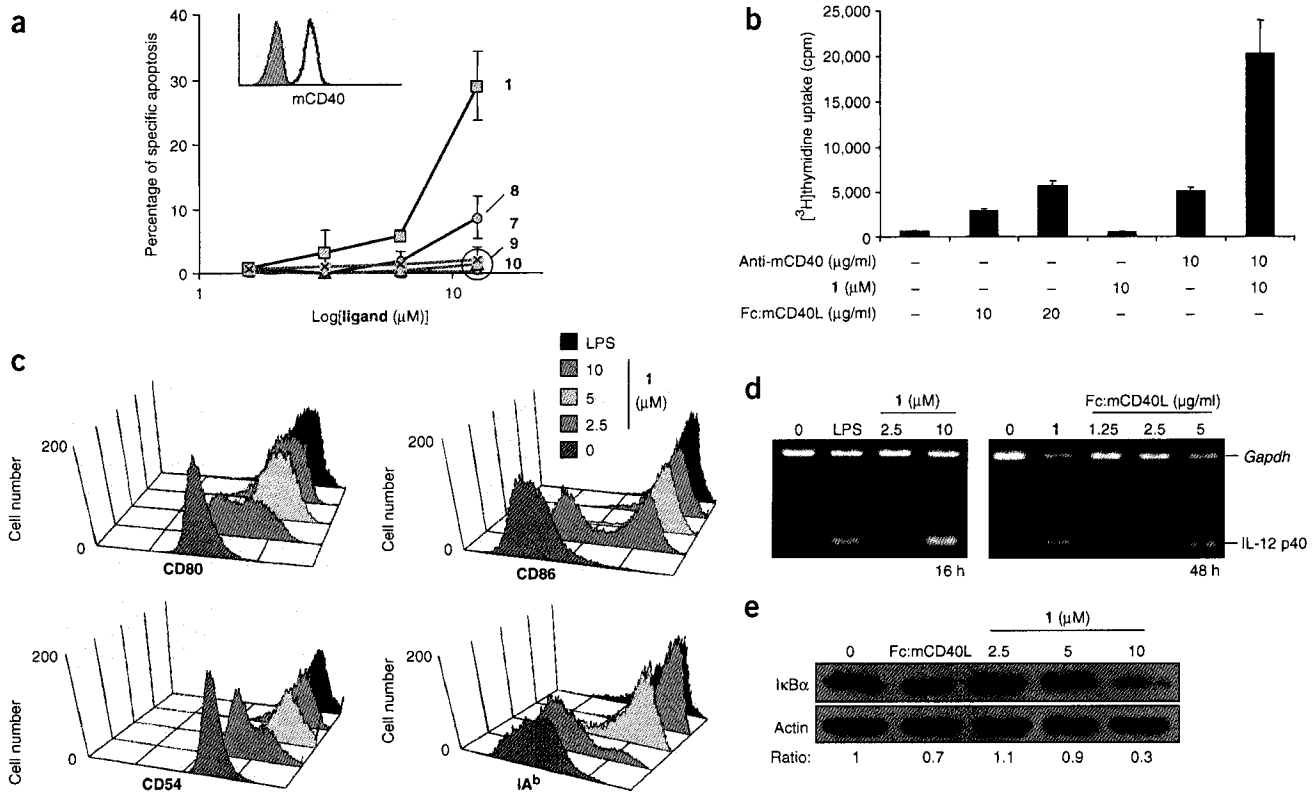

Figure 4 Effect of **1** on various mouse cells. (**a**) Induction of apoptosis of mouse A20 lymphoma cells after treatment with **1**, measured as in **Figure 3a**. Analogs **7–10** included as controls. Inset shows relative cell number as a function of CD40 expression (as measured by MFI). (**b**) Synergy by **1** of the proliferative response induced by an agonistic anti-mouse CD40 antibody. Results are expressed as average c.p.m. ± s.d. of two different experiments. (**c–e**) Compound **1** induces maturation of the mouse dendritic cell line D1 and activation of the NF-κB pathway. As a control, 10 μg ml^{-1} LPS was used. (**c**) Expression of maturation markers, as measured by flow cytometry after 48 h of treatment with **1**. (**d**) Comparative RT-PCR detection of IL-12 p40 mRNA in D1 cells, with mRNA expression of the housekeeping gene *Gapdh* as a control. (**e**) Analysis by immunoblotting of IκBα expression in D1 cells. As a control, actin expression was evaluated under the same conditions. Intensity ratio between IκBα and actin is shown below each lane.

Compound **1** also induced apoptosis of mouse CD40–expressing B lymphoma cells (**Fig. 4a**). Human and mouse CD40L sequences share 77% identity, and the sequence of the CD40-interacting loop region Lys143-Gly-Tyr-Tyr146 is conserved between both species. This result may suggest that ligands based on this conserved binding motif could also mimic mouse CD40L.

To study the effect of CD40L mimetics on nontransformed cells, purified splenic mouse B cells were treated with CD40L mimetics as well as with a mouse recombinant CD40L (Fc:mCD40L). Whereas Fc:mCD40L at high dose and anti-mouse CD40 mAb 3/23 induced B cell proliferation, compound **1** at 10 μM had no effect on B cell proliferation. However, in a manner analogous to soluble CD40L (ref. 25), **1** at 10 μM synergized the proliferation induced by the agonistic anti-mCD40 mAb 3/23 (**Fig. 4b**). These results underscore the difference between SPR binding data and cellular assays. On one hand, one can assume that the distribution of CD40 molecules at the surface of the chip significantly differs from that at the cell surface, both qualitatively (in terms of flexibility, accessibility and fluidity) and quantitatively (in terms of density). On the other hand, our findings are in agreement with a number of studies showing that receptor trimerization in the TNFR family is not always sufficient to induce effective signaling and that higher order oligomers are required[24–27]. Although synthetic ligands based on trimeric architectures probably bound CD40 on B cells by recruiting more than one receptor chain, they might fail to generate sufficient CD40 oligomerization to reach the activation threshold.

Finally, we investigated the capacity of CD40L mimetics to induce DC maturation by using the mouse DC line D1 which matures upon CD40 ligation[28]. Like Fc:mCD40L, compound **1** (5–10 μM) but not compounds **4–6**, induced upregulation of MHC and costimulatory molecule expression (**Fig. 4c** and **Supplementary Fig. 4** online) as well as production of interleukin (IL)-12, as visualized by IL-12 p40 mRNA (**Fig. 4d**) and protein (**Supplementary Fig. 4**) expression. At higher doses (>20 μM), maturation was accompanied by cell death. It is noteworthy that the maturation was not decreased in the presence of polymyxin B, an inhibitor of lipopolysaccharide (LPS) LPS activity, thus ruling out the possibility of a CD40-independent, LPS-mediated maturation of D1 cells (**Supplementary Fig. 4**). Moreover, compound **1** activated the NF-κB pathway[29] as shown by the increased degradation of the IκBα protein (**Fig. 4e**), suggesting that CD40L mimetics and natural CD40L use the same signaling pathway.

Our results indicate that relatively small (<3 kDa) synthetic trivalent architectures can mimic *in vitro* the effects of noncovalent signaling protein homotrimers and suggest the possibility of using small CD40 ligands to amplify immune responses *in vivo*. Extension of the approach to additional TNF members might prove useful to modulate TNFR functions in various pathological situations.

METHODS

CD40L mimetics. For details of preparation and characterization of **1** and **5** as well as alanine-substituted analogues **7–10**, see **Supplementary Methods** online and **Supplementary Figure 5** online. Trimeric ligands **1–4** were highly soluble in water (>20 mg ml^{-1}). For sample preparation, ligands were dissolved in water at a concentration of 1 mM before dilution to the indicated concentrations in appropriate buffer or medium.

SPR analysis. BIAcore 3000 (Biacore AB) was used to evaluate the binding of CD40L mimetics to CD40. Flow cells of a Biacore AB CM5 Sensor Chip (Research Grade, Biacore AB) were precoated with a rabbit polyclonal antibody directed against mouse immunoglobulin (RAM-Ig, Biacore AB) or with a goat antibody directed against human immunoglobulin (GAH-Ig, Jackson, ImmunoResearch Laboratories) using amine coupling at 30 μg ml^{-1} in 10 mM acetate buffer, pH 5.5, according to the manufacturer's protocol. The chip was then flushed with 1 M ethanolamine hydrochloride, pH 8.5 (Biacore AB), and 50 mM HCl to eliminate unbound antibody. Generally ~10,000 resonance units (RU) of RAM-Ig or GAH-Ig were obtained after immobilization. Biosensor assays were performed at 25 °C with HBS-EP buffer (10 mM HEPES, pH 7.4, containing 0.15 M NaCl, 3.4 mM EDTA and 0.005% (v/v) P20 surfactant (Biacore AB)) as running buffer. We captured soluble human CD40-mIg fusion protein (hCD40:mIg; Ancell Corporation), mouse anti-huCD40 antibody (Pharmingen), other TNFR:Fc fusion proteins, and LG11-2 (an IgG2a mouse monoclonal antibody directed against H2B histone used as irrelevant control) on individual flow cells at a flow rate of 5 μl min^{-1} and at a concentration allowing equivalent protein mass binding.

Binding of CD40L to CD40. hCD40L:CD8 (Ancell) was injected at a flow rate of 30 μl min^{-1} over the control channel and the CD40 channel for 5 min and was allowed to dissociate for an additional 5 min. The channels were regenerated for 30 s with 50 mM HCl. Control sensorgrams were subtracted from the CD40 sensorgrams and analyzed by BIAevaluation 4.1 with the 1:1 Langmuir binding model or a trivalent model[30].

Inhibition of CD40L binding to CD40. hCD40L:CD8 fusion protein was injected at 100 nM (**Fig. 2a,b,d–f**) or 200 nM (**Fig. 2c**) under the same conditions at a flow rate of 10 μl min^{-1} in the presence of various concentrations of CD40L mimetics. The IC_{50} was estimated from the decrease in the initial linear association phase.

Direct binding of the CD40L mimetics. CD40L mimetics were injected at different concentrations under the same conditions. The corrected sensorgrams were analyzed by BIAevaluation 4.1 with binding models as indicated in **Supplementary Table 1** online.

Measurement of apoptosis. Cell death was evaluated either by measurement of a decrease in mitochondrial transmembrane potential ($\Delta\psi_m$) associated with a reduction of the cationic dye $DiOC_6(3)$ uptake, as demonstrated by flow cytometry, or by detection of phosphatidylserine externalization by flow cytometry after colabeling with annexin V–FITC and propidium iodide (PI). Results are expressed as percentage of specific apoptosis according to the following formula: percentage specific apoptosis = ((percentage of apoptotic treated cells – percentage of apoptotic control cells) × 100)/(100 – percentage of apoptotic control cells). Full experimental procedures are provided in **Supplementary Methods**.

Cell culture and apoptosis induction. Burkitt lymphoma (BL41 and Raji), Jurkat human T lymphoma, and 3T6 murine fibroblasts were cultured in RPMI 1640 (Cambrex Bioscience) supplemented with 10% heat-decomplemented fetal bovine serum (FBS) and gentamicin (10 μg ml^{-1}). For apoptosis assays, cells (5×10^5 ml^{-1}) were incubated at 37 °C in 24-well plates at the indicated times and concentrations in presence of the various inducers. After incubation, cells were washed with PBS before measurement of apoptosis as described above.

Purification and culture of splenic B cells. Spleens were removed from 5- to 12-week-old BALB/c mice. Splenic B cells were prepared by positive selection using magnetic beads coated with anti-CD19 mAb (MACS, Milteny Biotech). This fraction contained more than 95% $B220^+$ cells. B cells (3×10^6 ml^{-1}) were then cultured in RPMI 1640 medium supplemented with 10% heat-decomplemented FBS, gentamicin (10 μg ml^{-1}), 25 mM HEPES and 10 μM β-mercaptoethanol in the presence of CD40L mimetics, or Fc:mCD40L and/or anti-mouse CD40 mAb (3/23). Cells were pulsed with $[^3H]$thymidine (1 μCi per well; ICN) during the last 20 h of culture, and $[^3H]$thymidine uptake was measured after 72 h using a Matrix 9600 direct β counter (Packard). The results are given as the arithmetic mean of thymidine uptake expressed as c.p.m.

Culture and maturation of D1 cells. D1 cells were cultured in nontreated plastic dishes in IMDM medium (Cambrex) supplemented with 10% heat-decomplemented FBS, penicillin (100 international units (IU) ml^{-1}), 10 μM β-mercaptoethanol, 2 mM L-glutamine and 30% (v/v) of supernatant of NIH/3T3 cells as a source of granulocyte-monocyte colony-stimulating factor (GM-CSF). For the maturation assay, 2×10^5 cells ml^{-1} were cultured for 48 h. Fresh medium containing the various inducers was then added. After various times of incubation, supernatants were collected to measure IL-12 production, and cells were washed with cold PBS and then harvested with 2 ml of PBS containing 2 mM EDTA. After centrifugation, cells were resuspended in cold PBS and analyzed for cell surface phenotyping by flow cytometry or were used for RT-PCR and western blotting analysis as described in **Supplementary Methods**.

Flow cytometry, confocal microscopy, western blot, RT-PCR and IL-12 measurement. Classical procedures were used. Full experimental procedures are provided in **Supplementary Methods**.

Note: Supplementary information is available on the Nature Chemical Biology website.

ACKNOWLEDGMENTS

We thank J.-P. Briand and S. Muller for support; J. Mutterer for assistance with confocal microscopy; N. Bonnefoy-Berard and M. Flacher for providing Burkitt lymphoma cells and M. Monestier for providing LG11-2 mAb. This work was supported by the Centre National de la Recherche Scientifique, the Ministère de la Recherche (ACI Jeunes Chercheurs), La Ligue contre le Cancer, Région Alsace and the Agence Nationale de Recherches contre le SIDA. S.W. was supported by a grant from the Ministère de la Recherche. W.S. was supported by the Ministère de la Recherche and the Fondation pour la Recherche Médicale. N.T. was supported by La Ligue Contre le Cancer.

AUTHOR CONTRIBUTION STATEMENT

S.F. and S.W. contributed equally to this work. W.S. and N.T. contributed equally to this work.

COMPETING INTERESTS STATEMENT

The authors declare that they have no competing financial interests.

Published online at http://www.nature.com/naturechemicalbiology/
Reprints and permissions information is available online at http://npg.nature.com/reprintsandpermissions/

1. van Kooten, C. & Banchereau, J. CD40–CD40 ligand. *J. Leukoc. Biol.* **67**, 1–17 (2000).
2. Diehl, L. *et al.* The role of CD40 in peripheral T cell tolerance and immunity. *J. Mol. Med.* **78**, 363–371 (2000).
3. Howard, L.M. *et al.* Mechanisms of immunotherapeutic intervention by anti-CD40L (CD154) antibody in an animal model of multiple sclerosis. *J. Clin. Invest.* **103**, 281–290 (1999).
4. Kirk, A.D. *et al.* Treatment with humanized monoclonal antibody against CD154 prevents acute renal allograft rejection in nonhuman primates. *Nat. Med.* **5**, 686–693 (1999).
5. Diehl, L. *et al.* CD40 activation *in vivo* overcomes peptide-induced peripheral cytotoxic T-lymphocyte tolerance and augments anti-tumor vaccine efficacy. *Nat. Med.* **5**, 774–779 (1999).
6. Sotomayor, E.M. *et al.* Conversion of tumor-specific CD4+ T-cell tolerance to T-cell priming through *in vivo* ligation of CD40. *Nat. Med.* **5**, 780–787 (1999).
7. Bodmer, J.-L., Schneider, P. & Tschopp, J. The molecular architecture of the TNF superfamily. *Trends Biochem. Sci.* **27**, 19–26 (2002).
8. Karpusas, M. *et al.* 2 Å crystal structure of an extracellular fragment of human CD40 ligand. *Structure* **3**, 1031–1039 (1995).
9. Schoenberger, S.P., Toes, R.E., van der Voort, E.I., Offringa, R. & Melief, C.J. T-cell help for cytotoxic T lymphocytes is mediated by CD40–CD40L interactions. *Nature* **393**, 480–483 (1998).
10. Bennett, S.R. *et al.* Help for cytotoxic-T-cell responses is mediated by CD40 signalling. *Nature* **393**, 478–480 (1998).
11. Cella, M. *et al.* Ligation of CD40 on dendritic cells triggers production of high levels of interleukin-12 and enhances T cell stimulatory capacity: T-T help via APC activation. *J. Exp. Med.* **184**, 747–752 (1996).

12. Chaussabel, D. *et al.* CD40 ligation prevents Trypanosoma cruzi infection through interleukin-12 upregulation. *Infect. Immun.* **67**, 1929–1934 (1999).
13. Edelmann, K.H. & Wilson, C.B. Role of CD28/CD80–86 and CD40/CD154 costimulatory interactions in host defense to primary herpes simplex virus infection. *J. Virol.* **75**, 612–621 (2001).
14. Heldin, C.-H. Dimerization of cell surface receptors in signal transduction. *Cell* **80**, 213–223 (1995).
15. Liu, Y. *et al.* Ligand-receptor binding revealed by the TNF family member TALL-1. *Nature* **423**, 49–56 (2003).
16. Hymowitz, S.G. *et al.* Structures of APRIL-receptor complexes: like BCMA, TACI employs only a single cysteine-rich domain for high affinity ligand binding. *J. Biol. Chem.* **280**, 7218–7227 (2005).
17. Wrighton, N.C. *et al.* Small peptides as potent mimetics of the protein hormone erythropoietin. *Science* **273**, 458–464 (1996).
18. Cwirla, S.E. *et al.* Peptide agonist of the thrombopoietin receptor as potent as the natural cytokine. *Science* **276**, 1696–1699 (1997).
19. Whitty, A. & Borysenko, C.W. Small molecule cytokine mimetics. *Chem. Biol.* **6**, R107–R118 (1999).
20. Mammen, M., Choi, S.-K. & Whitesides, G.M. Polyvalent interactions in biological systems: implications for design and use of multivalent ligands and inhibitors. *Angew. Chem. Int. Edn Engl.* **37**, 2754–2794 (1998).
21. Kiessling, L.L., Gestwicki, J.E. & Strong, L.E. Synthetic multivalent ligands in the exploration of cell-surface interactions. *Curr. Opin. Chem. Biol.* **4**, 696–703 (2000).
22. Singh, J. *et al.* The role of polar interactions in the molecular recognition of CD40L with its receptor CD40. *Protein Sci.* **7**, 1124–1135 (1998).
23. Bajorath, J. *et al.* Analysis of gp39/CD40 interactions using molecular models and site-directed mutagenesis. *Biochemistry* **34**, 9884–9892 (1995).
24. Tong, A.W. *et al.* CD40 ligand-induced apoptosis is Fas-independent in human multiple myeloma cells. *Leuk. Lymphoma* **36**, 543–558 (2000).
25. Pound, J.D. *et al.* Minimal cross-linking and epitope requirements for CD40-dependent suppression of apoptosis contrast with those for promotion of the cell cycle and homotypic adhesions in human B cells. *Int. Immunol.* **11**, 11–20 (1999).
26. Schneider, P. *et al.* Conversion of membrane-bound Fas (CD95) ligand to its soluble form is associated with downregulation of its proapoptotic activity and loss of liver toxicity. *J. Exp. Med.* **187**, 1205–1213 (1998).
27. Haswell, L.E., Glennie, M.J. & Al-Shamkhani, A. Analysis of the oligomeric requirement for signaling by CD40 using soluble multimeric forms of its ligand, CD154. *Eur. J. Immunol.* **31**, 3094–3100 (2001).
28. Schuurhuis, D.H. *et al.* Immature dendritic cells acquire CD8(+) cytotoxic T lymphocyte priming capacity upon activation by T helper cell-independent or -dependent stimuli. *J. Exp. Med.* **192**, 145–150 (2000).
29. O'Sullivan, B.J. & Thomas, R. CD40 ligation conditions dendritic cell antigen-presenting function through sustained activation of NF-kappaB. *J. Immunol.* **168**, 5491–5498 (2002).
30. Lortat-Jacob, H., Chouin, E., Cusack, S. & van Raaij, M.J. Kinetic analysis of adenovirus fiber binding to its receptor reveals an avidity mechanism for trimeric receptor-ligand interactions. *J. Biol. Chem.* **276**, 9009–9015 (2001).

THE JOURNAL OF IMMUNOLOGY

CUTTING EDGE

Cutting Edge: Small Molecule CD40 Ligand Mimetics Promote Control of Parasitemia and Enhance T Cells Producing IFN-γ during Experimental *Trypanosoma cruzi* Infection[1]

Mohammed Habib, Magali Noval Rivas,* Mustapha Chamekh,† Sébastien Wieckowski,‡ Weimin Sun,‡ Alberto Bianco,‡ Nathalie Trouche,‡ Olivier Chaloin,‡ Hélène Dumortier,‡ Michel Goldman,* Gilles Guichard,‡ Sylvie Fournel,[2‡] and Bernard Vray[2*]*

***Host resistance to* Trypanosoma cruzi *infection depends on a type 1 response characterized by a strong production of IL-12 and IFN-γ. Amplifying this response through CD40 triggering results in control of parasitemia. Two newly synthesized molecules (<3 kDa) mimicking trimeric CD40L (mini CD40Ls-1 and -2) bind to CD40, activate murine dendritic cells, and elicit IL-12 production. Wild-type but not CD40 knockout mice exhibited a sharp decrease of parasitemia and mortality when inoculated with* T. cruzi *mixed with miniCD40Ls. Moreover, the immunosuppression induced by* T. cruzi *infection was impaired in mice treated with miniCD40Ls, as shown by proliferation of splenic lymphocytes, percentage of $CD8^+$ T cells, and IFN-γ production. Mice surviving* T. cruzi *infection in the presence of miniCD40L-1 were immunized against a challenge infection. Our results indicate that CD40L mimetics are effective in vivo and promote the control of* T. cruzi *infection by overcoming the immunosuppression usually induced by the parasites. The Journal of Immunology,* 2007, 178: 6700–6704.**

Trypanosoma cruzi, Chagas' disease etiological agent, is a hemoflagellate parasitic protozoa that infects humans and other mammals where it multiplies as amastigotes within various cells. Human disease can be mimicked by experimental infection of BALB/c mice displaying an acute phase with parasitemia and mortality, followed by a chronic phase during which parasites become undetectable in peripheral blood while persisting in tissues and inducing pathological manifestations (1).

CD40L (or CD154) belongs to the TNF superfamily and is mainly expressed by activated $CD4^+$ T lymphocytes, whereas its cognate receptor CD40 is expressed by APC such as dendritic cells (DC).[3] CD40L-CD40 interaction plays a major role in immunity against intracellular pathogens such as *Leishmania amazonensis* and *T. cruzi* (2–4) by promoting an effective type 1 response. We have previously reported that 1) coinjection of CD40L-transfected 3T3 fibroblasts and *T. cruzi* trypomastigotes dramatically reduced both parasitemia and mortality of *T. cruzi*-infected mice through a cascade involving IL-12, IFN-γ, and NO (3), and 2) CD40L gene-transfected *T. cruzi* trypomastigotes induced very low parasitemia and no mortality when compared with the wild-type strain (Y strain) or to the Y strain transfected with the pTEX vector alone. Furthermore, the proliferative capacity and the secretion of IFN-γ were preserved in spleen cells (SC) from CD40L-infected mice compared with controls (4).

By taking advantage of the 3-fold symmetry of homotrimeric CD40L, we have recently designed small trivalent molecules (<3 kDa) that can bind to CD40 and reproduce similar functional properties of soluble CD40L (5). In this study, we have investigated whether these small molecules namely miniCD40Ls −1 and −2 (5) can induce a protective immune response against experimental *T. cruzi* infection in mice.

Materials and Methods

MiniCD40Ls

MiniCD40Ls −1 and −2 (C1 and C2) were designed as previously described (5) by attaching a short CD40-binding motif (Lys^{143}-Gly-Tyr-Tyr^{146}) to each arm of a trimeric C_3-symmetric circular peptide architecture cyclo(Lys-D-Ala)$_3$

*Laboratoire d'Immunologie Expérimentale and †Laboratoire de Bactériologie Moléculaire Faculté de Médecine, Université Libre de Bruxelles, Brussels, Belgium; and ‡Centre National de la Recherche Scientifique, Institut de Biologie Moléculaire et Cellulaire, Laboratoire d'Immunologie et Chimie Thérapeutiques, Strasbourg, France

Received for publication May 19, 2006. Accepted for publication April 2, 2007.

The costs of publication of this article were defrayed in part by the payment of page charges. This article must therefore be hereby marked *advertisement* in accordance with 18 U.S.C. Section 1734 solely to indicate this fact.

[1] This work was supported by grants from the Centre de Recherche Interuniversitaire en Vaccinologie (to M.H. and B.V.), by the Centre National de la Recherche Scientifique, the "Ministère de la Recherche" (Action Concertee Incitative "Jeunes Chercheurs") and "La Ligue contre le Cancer, Région Alsace" (to G.G., N.T., and S.F.). S.W. and W.S. were supported, respectively, by a grant from the "Ministère de la Recherche" and the "Fondation pour la Recherche Médicale."

[2] Address correspondence and reprint requests to Prof. Bernard Vray, Laboratoire d'Immunologie Expérimentale (CP 615), Faculté de Médecine, Université Libre de Bruxelles, 808 Route de Lennik, 1070 Brussels, Belgium; E-mail address: bvray@ulb.ac.be or Prof. Sylvie Fournel, Centre National de la Recherche Scientifique, Institut de Biologie Moléculaire et Cellulaire, Laboratoire d'Immunologie et Chimie Thérapeutiques, Strasbourg, France; E-mail address: S.Fournel@ibmc.u-strasbg.fr

[3] Abbreviations used in this paper: DC, dendritic cell; MPM, mouse peritoneal macrophage; SC, spleen cell.

for C1 and cyclo(β^3-HLys) for C2 via an appropriate spacer (amino hexanoic acid residue for C1 and C2). Compounds 3 and 4 (C3 and C4), which correspond, respectively, to the circular core of C1 and to the CD40-binding motif attached to the spacer, do not bind to CD40 and were used as controls.

T. cruzi *trypomastigotes, lysates, and mice infection*

Two strains (Tehuantepec strain and Y strain) were used (4). Trypomastigote lysate was obtained by six freeze/thaw cycles and then adjusted to 20 μg/ml (6, 7). BALB/c, C57BL/6, and C57BL/6 CD40 knockout mice were inoculated i.v. with 1×10^3 trypomastigotes/mouse (Tehuantepec strain) in 0.9% NaCl or mixed with C1, C2, C3, or C4 at the indicated concentrations. Mice (n = 5) inoculated with trypomastigotes (Tehuantepec strain) mixed with C1 at day 0 were inoculated with a different strain of *T. cruzi* (Y strain 1×10^3 trypomastigotes/mouse) at day 117. Parasitemia was monitored by counting the trypomastigotes in blood samples every week. Survival rates were determined daily.

Cytotoxicity of miniCD40Ls

The possible cytotoxicity of *miniCD40Ls* on parasite infectivity was tested by investigating the capacity of *T. cruzi* trypomastigotes incubated with C1, C2, C3, or C4 to infect Vero cells and mouse peritoneal macrophages (MPM) (4). Briefly, Vero cells (5×10^5 cells/well) and MPM (2×10^5 cells/well) were cultured in the presence of trypomastigotes (10:1, parasite:cell ratio), then incubated with C1, C2, C3, or C4 (200 μg/100 μl in 0.9% NaCl) for 8 h at 37°C. After 16 h, the cultures were washed to remove free parasites. For Vero cells, trypomastigotes released were counted on a Thoma chamber over 21 days. For MPM, cultures were fixed with methanol and stained with Giemsa. At least 200 MPM were microscopically counted to determine the percentage of infected cells and the mean of amastigotes per infected cell (4).

Immunophenotyping and intracellular detection of IFN-γ

SC were either labeled (8) directly or after stimulation with *T. cruzi* lysate (20 μg/ml) for 56 h at 37°C in the presence of brefeldin A (10 μg/ml; 3 h). FITC-conjugated anti-CD3ε chain for $CD3^+$, allophycocyanin-conjugated L3T4/RM4-5 for $CD4^+$, PerCP-conjugated Ly-2, 53-6.7 for $CD8^+$, and PE-conjugated anti-IFN-γ were from BD Pharmingen. Flow cytometry was performed using FACSCalibur (BD Biosciences).

SC cultures were cultured in the presence of *T. cruzi* lysate (20 μg/ml) for 96 h. Cells were pulsed with 2.5 μCi/well of tritiated thymidine (MP Biomedicals) during the last 16 h of culture (4). [^{3}H]Thymidine uptake was measured using an automated scintillation counter (Packard Microplate scintillation counter; Packard Instrument).

Culture and maturation of DC line D1 or bone marrow-derived DC

A total of 2×10^5 cells/ml was cultured for 24 h in fresh medium containing various inducers (9). Cells were harvested with PBS containing 2 mM EDTA and stained with anti-mouse PE-conjugated CD54, CD80, and CD86 and anti-mouse FITC-conjugated CD40 (BD Pharmingen). Cells were analyzed by flow cytometry with a FACSCalibur using the CellQuest 3.3 software (BD Biosciences). Data were processed with the WinMDI 2.8 freeware (J. Trotter; The Scripps Research Institute).

ELISA

IFN-γ measurement in SC supernatants was performed after 80 h of stimulation with *T. cruzi* lysates (7), according to the manufacturer's instructions (CytoSets; BioSource International). IL-12 secretion in D1 cell supernatants, after 48 h of stimulation, was evaluated by sandwich ELISA (5) using Ab from BD Pharmingen and polyvinyl plates (BD Falcon).

Statistical analysis

Data were compared using the Mann-Whitney U test. The survival analyses were obtained with Kaplan-Meier curves and Gehan's generalized Wilcoxon test.

Results and Discussion

MiniCD40Ls-1 and -2 decrease T. cruzi *infection and induce survival of inoculated mice*

To investigate the potential effects of trimeric molecules mimicking CD40L homotrimer, we inoculated BALB/c mice with trypomastigotes (Tehuantepec strain, 1×10^3 parasites/mouse) alone or mixed with C1 or C2 or with the control molecules C3 or C4. Inoculation in the presence of C1 or C2 (100 μg/mouse) induced a significant decrease in parasitemia at days 14, 21, 28, and 35 postinfection. Eighty percent of mice treated with C1 or C2 were still alive at day 42 postinfection in comparison with 20% in the absence of miniCD40L or in the presence of C3 or C4 (Fig. 1).

To investigate the possible cytotoxic effect of miniCD40Ls on trypomastigotes, Vero cells and MPM were incubated with trypomastigotes mixed with miniCD40Ls. In this setting, trypomastigote infection was not decreased (data not shown).

Interestingly, a second injection of C1, 7 days after the initial inoculation, improved the effect of the ligand (Table I). Trypomastigotes were injected (1×10^3 parasites/mouse) in the presence of 100, 10, or 1 μg/mouse C1. On day 7, a second injection using the same concentrations was performed. The maximal protective effect was obtained with 100 μg/mouse, but a significant decrease of parasitemia was already observed with 10 and 1 μg/mouse C1. These results indicate that C1 and C2 induce a protective immune response against *T. cruzi* infection. Furthermore, CD40-deficient mice inoculated with *T. cruzi* mixed with C1 (100 μg) exhibited very high parasitemia and succumbed to infection compared with wild-type mice (data not shown). This suggests that the protective capacity of miniCD40Ls peptides depends on CD40 interaction in vivo.

We have previously shown that both C1 and C2 bind to CD40 and display agonistic activity on immunocompetent cells (5). Therefore, one might hypothesize that an effective immune response against the parasite originates from activation of immunocompetent cells by miniCD40Ls at the onset of *T. cruzi* infection. Moreover, we have demonstrated that immune responses were more effective when a second injection of miniCD40Ls was administered on day 7 postinfection, demonstrating the importance of cellular recall for the induction of this effective immune response. Interestingly, live parasites have

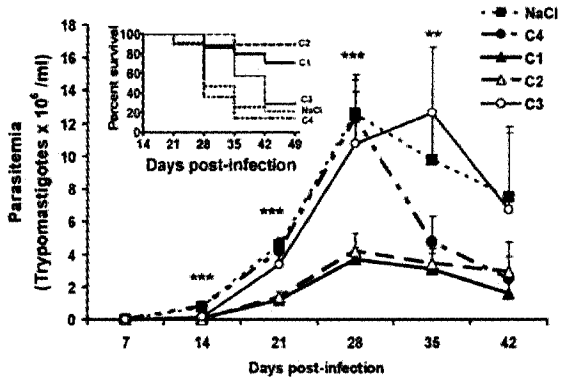

FIGURE 1. Inoculation with *T. cruzi* trypomastigotes mixed with C1 or C2 results in decreased parasitemia and mouse survival. Mice were inoculated i.v. with trypomastigotes (1×10^3/mouse) mixed with 100 μg in 100 μl of C1 (n = 34) or C2 (n = 8) or C3 (n = 7) or C4 (n = 28) or with NaCl 0.15 M (n = 41) at day 0. The numbers of trypomastigotes in blood, as well as the percentage of surviving mice (*insert*), were measured at various days postinfection. For parasitemia, the p values obtained with C1 or C2 vs C4 or NaCl were statistically significant; $p < 0.0009$ at days 14, 21, and 28 and C1 or C2 vs C3, $p < 0.01$ at days 14 and 28. For the mortality, statistically significant differences were obtained with C1 or C2 vs C4 or NaCl, $p < 0.0001$ and C1 or C2 vs C3, $p < 0.008$. No significant differences were obtained for C1 vs C2 or C4 or C3 vs NaCl both in parasitemia or mortality. Data are means of three independent or one representative experiments; *, $p < 0.05$, **, $p < 0.01$, and ***, $p < 0.001$.

Table I. *Efficacy of injection number and dose of C_1 on* T. cruzi *infection*[a]

MiniCD40L − 1 (μg) Day 0	Day 7	Parasitemia (×10⁶ parasites/ml) ± SEM Day 21	Day 28	Percent Survival
NaCl	NaCl	4.38 ± 0.37	11.2 ± 1.95	19
100	NaCl	1.20 ± 0.18	3.77 ± 0.72	66
100	100	0.36 ± 0.16	1.41 ± 0.70	86
10	10	1.00 ± 0.73	1.78 ± 1.12	40
1	1	5.24 ± 3.91	3.89 ± 1.95	40

[a]Mice (n = 12) were infected i.v. with *T. cruzi* trypomastigotes mixed with C1 (100 μg, 10 μg, and 1 μg/100 μl). A second i.v. injection of C1 (100 μg, 10 μg, and 1 μg/100 μl) was performed at day 7 postinfection. The control mice (n = 12) were infected with trypomastigotes in NaCl (0.9%) and reinjection of NaCl at day 7 postinfection. Significant differences were observed for both parasitemia and mortality at days 14, 21, and 28 postinfection (p = 0.0003). Improvement of parasite control occurred dose dependently and survival increased upon a second injection of C1. Significant differences as shown on days 21 and 28 postinfection for C1 (100 μg) vs NaCl ($p < 0.02$) and on day 21 postinfection for C1 (10 μg) vs NaCl ($p < 0.04$).

to be inoculated i.v. together with C1 (or C2) to trigger a protective immune response.

Inoculation of T. cruzi *in the presence of miniCD40Ls induces a "memory response"*

To investigate whether infection in the presence of miniCD40Ls could induce persistent protective immunity, we performed a challenge infection in surviving mice treated by C1 mixed with *T. cruzi* (Tehuantepec strain) with a different strain (Y strain). Whereas 100% of control mice died 20 days after inoculation, mice previously inoculated with C1 did not show significant parasitemia and survived (Fig. 2). These data show that *T. cruzi* inoculation in the presence of miniCD40Ls induces not only an effective immune response against *T. cruzi* but also the development of a "memory response" effective against infection by a different strain of *T. cruzi*.

The immunosuppression induced by T. cruzi *infection is impaired in mice treated with miniCD40Ls*

As for many other pathogens, the evolutionary adaptation of *T. cruzi* allows the parasite to evade the immune system and to induce dramatic immunodeficiency (6, 7, 10). We have previously reported a depletion of both $CD4^+$ and $CD8^+$ T cells at the peak of infection with *T. cruzi* that is believed to account for high parasitemia and mortality (7). To investigate whether treatment with miniCD40Ls could impair this immunosuppression, mice were sacrificed at days 21, 28, and 35 postinfection. SC were harvested, and the number of $CD4^+$ and $CD8^+$ T cells, as well as their IFN-γ production, was evaluated. As expected, in the absence of treatment, infection by *T. cruzi* was associated with a decrease in the percentage of splenic $CD4^+$ and $CD8^+$ T cells (Fig. 3, *A* and *B*). Although these cells displayed a transitory production of IFN-γ (Fig. 3, *C* and *D*), they were not able to induce an effective immune response. Treatment with C1 prevented the decrease of $CD8^+$ T cells at day 35 postinfection. Moreover, intra- and extracellular increases of IFN-γ was observed in C1-treated mice. This increase was particularly significant in the $CD8^+$ T cell population. Taken together, these results show that miniCD40Ls significantly induce an immune response. However, to investigate whether this response was directed against *T. cruzi*, SC were cultured in the presence of *T. cruzi* lysate. In this condition, proliferation and IFN-γ production was increased in SC from C1-treated mice (Fig. 3, *E* and *F*). These data suggest that miniCD40L treatment overcomes the immunosuppressive effect of *T. cruzi* by inducing a type 1 immune response that enhances $CD8^+$ T cell activation. Previous studies showed the pivotal role of $CD8^+$ T cells in protective immunity (11). Strong evidence pointed toward the important role of other immunocompetent cells such

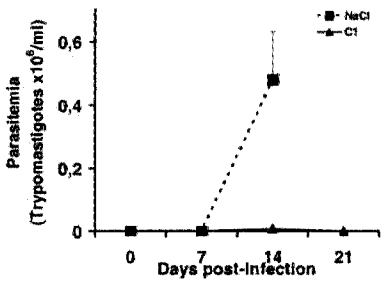

FIGURE 2. Inoculation of *T. cruzi* in the presence of miniCD40Ls induces a "memory response." Mice treated with C1 that survived to *T. cruzi* (Tehuantepec strain) inoculation were infected with a different strain of *T. cruzi* (Y strain). They all survived the challenge infection (no detectable parasitemia) while 100% of the control mice died at 20-day postinfection.

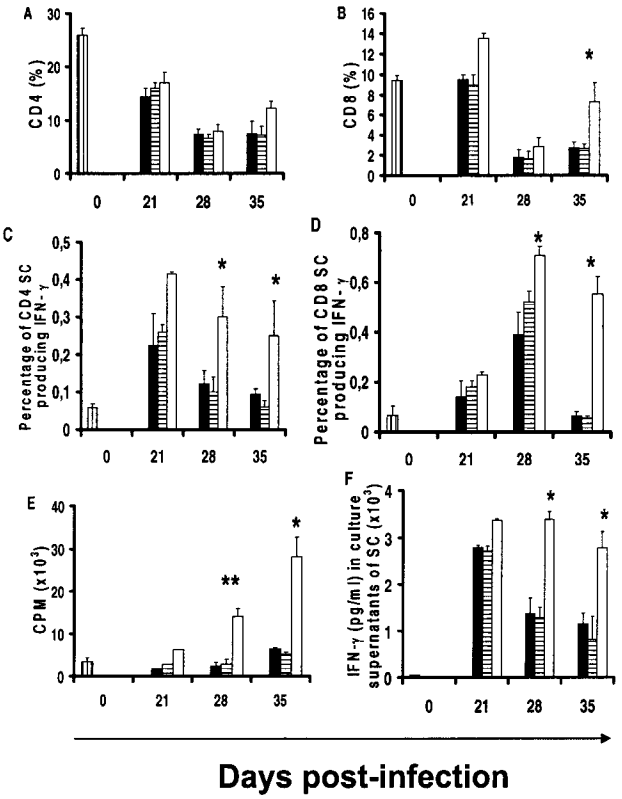

FIGURE 3. The immunosuppression induced by *T. cruzi* infection is impaired in mice treated with C1. Mice were infected at day 0 with *T. cruzi* in 0.15 M NaCl (■, n = 25) and mixed with C4 (▤, n = 22) or C1 (□, n = 18). Noninfected mice were used as controls (▥, n = 5). At days 0, 7, 28, and 35 postinfection, SC were harvested, and the percentage of $CD3^+CD4^+$ (*A*) and $CD3^+CD8^+$ (*B*) lymphocytes producing IFN-γ, as well as the percentage of $CD3^+CD4^+$ (*C*) and $CD3^+CD8^+$ lymphocytes (*D*), were evaluated by flow cytometry. A portion of the SC were also incubated with *T. cruzi* lysate (*E* and *F*), and the proliferative response (*E*; as cpm after [^{3}H]thymidine incorporation) and IFN-γ production (*F*; measured by ELISA) were evaluated after 96 h. Data are means ± SEM of two independent experiments; *, $p < 0.05$ and **, $p < 0.01$ (Mann-Whitney U test).

as $CD4^+$ and NK cells in immune protection against infection (12). Based on the protective capacity of miniCD40Ls peptides, one may speculate on the role of these potent immunocompetent cells through CD40-CD40L signaling.

MiniCD40Ls' effect on T. cruzi *infection can be mediated by DC maturation*

CD40L-induced $CD8^+$ T cell activation is mediated by DC maturation and IL-12 production (3, 13). Like soluble recombinant CD40L, C1 and C2 induced maturation of D1 cells, a DC line that matures upon CD40 ligation (14), as shown by both increased IL-12 production and up-regulation of CD80, CD86, CD54, and CD40 expression (Fig. 4). Similar effects were also observed with bone marrow-derived DC (data not shown).

Overall, these results are in line with two other reports establishing that CD40 ligation facilitates the control of *T. cruzi* infection through a cascade involving IL-12 and IFN-γ (3, 4). Early production of IL-12 during *T. cruzi* infection is critical in directing differentiation of Th precursors toward a Th1 phenotype that produces high levels of IFN-γ. Therefore, induction of DC maturation by miniCD40Ls could be responsible for high T $CD8^+$ IFN-γ production, which is important in the control of *T. cruzi* replication in acute infection.

Although cells exposed to live *T. cruzi* trypomastigotes produced IL-12, optimal induction of this cytokine by DC generally requires two signals (15, 16). The first signal originates from the parasite via activation of pattern recognition receptors such as members of the TLR family. Indeed, MyD88-deficient mice exhibited impaired production of proinflammatory cytokines and showed enhanced parasitemia and mortality upon challenge with trypomastigotes compared with wild-type mice.

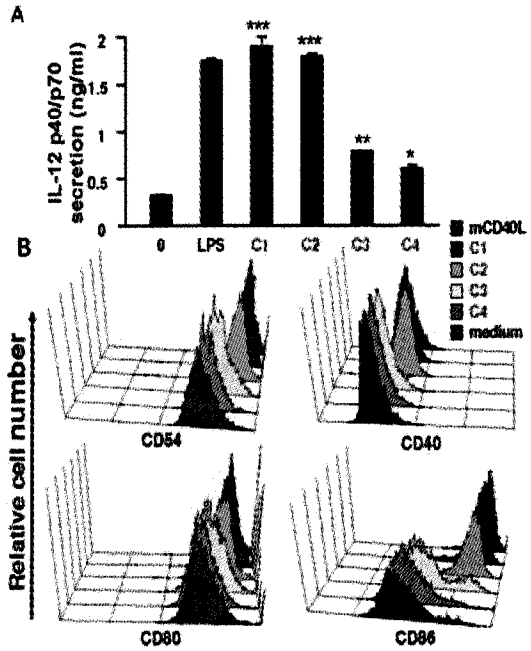

FIGURE 4. MiniCD40L-induced IL-12 production and DC maturation. *A*, IL-12p40/p70 secretion by D1 cells upon treatment with C1, C2, C3, and C4. LPS (10 $\mu g \cdot ml^{-1}$) served as a control; *, $p > 0.1$, **, $0.05 > p > 0.03$, and ***, $p < 0.02$. *B*, Increased expression of CD80, CD86, CD54, and CD40 in C1- and C2-treated D1 cells (mCD40L, soluble recombinant CD40L).

Several *T. cruzi* molecules known to stimulate the synthesis of proinflammatory cytokines by macrophages have been shown recently to function as TLR2 (GPI anchors) (17) or TLR4 (glycoinositolphospholipid) agonists (18). The second signal required for IL-12 production by DC involves CD40 triggering (19). This article suggests that miniCD40Ls induce a persistent immune response by providing this second signal at an early stage after *T. cruzi* inoculation. This is the first demonstration that rationally designed CD40L mimetics such as C1 and C2 are effective in vivo. Recent data showed that TLR agonists synergize with CD40L for DC activation, IL-12 production, and $CD8^+$ T cell expansion (20). This might provide a rationale for the use of miniCD40Ls in combination with TLR2 or TLR4 ligands purified from the parasite or with other TLR agonists such as imidazoquinolines (TLR7 and TLR8), unmethylated oligonucleotides (TLR9), or poly(deoxyinosinic-deoxycytidylic acid) (TLR3). Studies aimed at determining the effects of concomitant delivery of miniCD40Ls and such TLR agonists on protective immunity against intracellular pathogens are currently under investigation.

Acknowledgments

We acknowledge the help of A. Le Moine and J. Johnson (Institute for Medical Immunology, Gosselies, Belgium), J.-P. Briand, J. Hoebeke, and S. Muller (Unité Propre de Recherche 9021 Centre National de la Recherche Scientifique, Institut de Biologie Moléculaire et Cellulaire, Strasbourg, France), and C. Decaestecker, M. Libin, and I. Mazza (Université Libre de Bruxelles, Brussels, Belgium).

Disclosures

The authors have no financial conflict of interest.

References

1. Prata, A. 2001. Clinical and epidemiological aspects of Chagas disease. *Lancet Infect. Dis.* 1: 92–100.
2. Grewal, I. S., P. Borrow, E. G. Pamer, M. B. Oldstone, and R. A. Flavell. 1997. The CD40-CD154 system in anti-infective host defense. *Curr. Opin. Immunol.* 9: 491–497.
3. Chaussabel, D., F. Jacobs, J. de Jonge, M. de Veerman, Y. Carlier, K. Thielemans, M. Goldman, and B. Vray. 1999. CD40 ligation prevents *Trypanosoma cruzi* infection through interleukin-12 upregulation. *Infect. Immun.* 67: 1929–1934.
4. Chamekh, M., V. Vercruysse, M. Habib, M. Lorent, M. Goldman, A. Allaoui, and B. Vray. 2005. Transfection of *Trypanosoma cruzi* with host CD40L results in improved control of parasite infection. *Infect. Immun.* 73: 6552–6561.
5. Fournel, S., S. Wieskowski, W. Sun, N. Trouche, H. Dumortier, A. Bianco, O. Chaloin, M. Habib, J.-C. Peter, J.-P. Brian, et al. 2005. C_3-symmetric peptide scaffolds are functional mimetics of trimeric CD40L. *Nat. Chem. Biol.* 1: 377–382.
6. Van Overtvelt, L., M. Andrieu, V. Verhasselt, F. Connan, J. Choppin, V. Vercruysse, M. Goldman, A. Hosmalin, and B. Vray. 2002. *Trypanosoma cruzi* down-regulates lipopolysaccharide-induced MHC class I on human dendritic cells and impairs antigen presentation to specific $CD8^+$ T lymphocytes. *Int. Immunol.* 14: 1135–1144.
7. Chaussabel, D., B. Pajak, V. Vercruysse, C. Bisseye, V. Garze, M. Habib, M. Goldman, M. Moser, and B. Vray. 2003. Alteration of migration and maturation of dendritic cells and T cell depletion in the course of experimental *Trypanosoma cruzi* infection. *Lab Invest.* 83: 1373–1382.
8. Cobbold, P. S., R. Castejon, E. Adams, D. Zelenika, L. Graca, S. Humm, and H. Waldmann. 2004. Induction of *foxP3*$^+$ regulatory T cells in the periphery of T cell receptor transgenic mice tolerized to transplants. *J. Immunol.* 172: 6003–6010.
9. Lutz, M. B., N. Kukutsch, A. L. Ogilvie, S. Rossner, F. Koch, N. Romani, and G. Schuler. 1999. An advanced culture method for generating large quantities of highly pure dendritic cells from mouse bone marrow. *J. Immunol. Methods* 223: 77–92.
10. Abrahamsohn, I. A., and R. L. Coffman. 1995. Cytokine and nitric oxide regulation of the immunosuppression in *Trypanosoma cruzi* infection. *J. Immunol.* 155: 3955–3963.
11. Tarleton, R. L. 1990. Depletion of $CD8^+$ T cells increases susceptibility and reverses vaccine-induced immunity in mice infected with *Trypanosoma cruzi*. *J. Immunol.* 144: 717–724.
12. Vitelli-Avelar, D. M., R. Sathler-Avelar, R. L. Massara, J. D. Borges, P. S. Lage, M. Lana, A. Teixeira-Carvalho, J. C. Dias, S. M. Eloi-Santos, and O. A. Martins-Filho. 2006. Are increased frequency of macrophage-like and natural killer (NK) cells, together with high levels of NKT and $CD4^+CD25^{high}$ T cells balancing activated $CD8^+$ T cells, the key to control Chagas' disease morbidity? *Clin. Exp. Immunol.* 145: 81–92.

13. Cella, M., D. Scheidegger, K. Palmer-Lehmann, P. Lane, A. Lanzavecchia, and G. Alber. 1996. Ligation of CD40 on dendritic cells triggers production of high levels of interleukin-12 and enhances T cell stimulatory capacity: T-T help via APC activation. *J. Exp. Med.* 184: 747–752.

14. Schuurhuis, D. H., S. Laban, R. E. Toes, P. Ricciardi-Castagnoli, M. J. Kleijmeer, E. I. van der Voort, D. Rea, R. Offringa, H. J. Geuze, C. J. Melief, and F. Ossendorp. 2000. Immature dendritic cells acquire $CD8^+$ cytotoxic T lymphocyte priming capacity upon activation by T helper cell-independent or -dependent stimuli. *J. Exp. Med.* 192: 145–150.

15. Snijders, A., P. Kalinski, C. M. Hilkens, and M. L. Kapsenberg. 1998. High-level IL-12 production by human dendritic cells requires two signals. *Int. Immunol.* 10: 1593–1598.

16. Schulz, O., A. D. Edwards, M. Schito, J. Aliberti, S. Manickasingham, A. Sher, and C. Reis e Sousa. 2000. CD40 triggering of heterodimeric IL-12 p70 production by dendritic cells in vivo requires a microbial priming signal. *Immunity* 13: 453–462.

17. Campos, M. A., I. C. Almeida, O. Takeuchi, S. Akira, E. P. Valente, D. O. Procopio, L. R. Travassos, J. A. Smith, D. T. Golenbock, and R. T. Gazzinelli. 2001. Activation of Toll-like receptor-2 by glycosylphosphatidylinositol anchors from a protozoan parasite. *J. Immunol.* 167: 416–423.

18. Oliveira, A. C., J. R. Peixoto, L. B. de Arruda, M. A. Campos, R. T. Gazzinelli, D. T. Golenbock, S. Akira, J. O. Previato, L. Mendonca-Previato, A. Nobrega, and M. Bellio. 2004. Expression of functional TLR4 confers proinflammatory responsiveness to *Trypanosoma cruzi* glycoinositolphospholipids and higher resistance to infection with *T. cruzi*. *J. Immunol.* 173: 5688–5696.

19. Macatonia, S. E., N. A. Hosken, M. Litton, P. Vieira, C. S. Hsieh, J. A. Culpepper, M. Wysocka, G. Trinchieri, K. M. Murphy, and A. O'Garra. 1995. Dendritic cells produce IL-12 and direct the development of Th1 cells from naive $CD4^+$ T cells. *J. Immunol.* 154: 5071–5079.

20. Ahonen, C. L., C. L. Doxsee, S. M. McGurran, T. R. Riter, W. F. Wade, R. J. Barth, J. P. Vasilakos, R. J. Noelle, and R. M. Kedl. 2004. Combined TLR and CD40 triggering induces potent $CD8^+$ T cell expansion with variable dependence on type I IFN. *J. Exp. Med.* 199: 775–784.

1: J Virol. 2004 May;78(10):5223-32.

Human immunodeficiency virus type 1 activates plasmacytoid dendritic cells and concomitantly induces the bystander maturation of myeloid dendritic cells.

Fonteneau JF, Larsson M, Beignon AS, McKenna K, Dasilva I, Amara A, Liu YJ, Lifson JD, Littman DR, Bhardwaj N.

Institut de Biologie, INSERM U463, Nantes, France.

In this study, we analyzed the phenotypic and physiological consequences of the interaction of plasmacytoid dendritic cells (pDCs) with human immunodeficiency virus type 1 (HIV-1). pDCs are one cellular target of HIV-1 and respond to the virus by producing alpha/beta interferon (IFN-alpha/beta) and chemokines. The outcome of this interaction, notably on the function of bystander myeloid DC (CD11c+ DCs), remains unclear. We therefore evaluated the effects of HIV-1 exposure on these two DC subsets under various conditions. Blood-purified pDCs and CD11c+ DCs were exposed in vitro to HIV-1, after which maturation markers, cytokine production, migratory capacity, and CD4 T-cell stimulatory capacity were analyzed. pDCs exposed to different strains of infectious or even chemically inactivated, nonreplicating HIV-1 strongly upregulated the expression of maturation markers, such as CD83 and functional CCR7, analogous to exposure to R-848, a synthetic agonist of toll-like receptor-7 and -8. In addition, HIV-1-activated pDCs produced cytokines (IFN-alpha and tumor necrosis factor alpha), migrated in response to CCL19 and, in coculture, matured CD11c+ DCs, which are not directly activated by HIV. pDCs also acquired the ability to stimulate naïve CD4+ T cells, albeit less efficiently than CD11c+ DCs. This HIV-1-induced maturation of both DC subsets may explain their disappearance from the blood of patients with high viral loads and may have important consequences on HIV-1 cellular transmission and HIV-1-specific T-cell responses.

PMID: 15113904 [PubMed - indexed for MEDLINE]

1: Blood. 2003 May 1;101(9):3520-6. Epub 2003 Jan 2.

Activation of influenza virus-specific CD4+ and CD8+ T cells: a new role for plasmacytoid dendritic cells in adaptive immunity.

Fonteneau JF, **Gilliet M**, **Larsson M**, **Dasilva I**, **Münz C**, **Liu YJ**, **Bhardwaj N**.

Laboratory of Molecular Neuro-Oncology, Rockefeller University, New York, NY, USA.

Plasmacytoid dendritic cells (pDCs) contribute to innate antiviral immune responses by producing type I interferons (IFNs) upon exposure to enveloped viruses. However, their role in adaptive immune responses, such as the initiation of antiviral T-cell responses, is not known. In this study, we examined interactions between blood pDCs and influenza virus with special attention to the capacity of pDCs to activate influenza-specific T cells. pDCs were compared with CD11c(+) DCs, the most potent antigen-presenting cells (APCs), for their capacity to activate T-cell responses. We found that like CD11c(+) DCs, pDCs mature following exposure to influenza virus, express CCR7, and produce proinflammatory chemokines, but differ in that they produce type I IFN and are resistant to the cytopathic effect of the infection. After influenza virus exposure, both DC types exhibited an equivalent efficiency to expand anti-influenza virus cytotoxic T lymphocytes (CTLs) and T helper 1 (TH1) CD4(+) T cells. Our results pinpoint a new role of pDCs in the induction of antiviral T-cell responses and suggest that these DCs play a prominent role in the adaptive immune response against viruses.

PMID: 12511409 [PubMed - indexed for MEDLINE]